

# **Implications of Molecular Signaling in Therapeutic Efficacy of Nanodrug Delivery Systems in Cancer Model**



**By**

**Muhammad Hamid Siddique**

Department of Biochemistry  
Faculty of Biological Sciences  
Quaid-i-Azam University  
Islamabad, Pakistan

# **Implications of Molecular Signaling in Therapeutic Efficacy of Nanodrug Delivery Systems in Cancer Model**



A thesis submitted in partial fulfillment of the requirements for the degree of

**Doctor of Philosophy**

in

**Biochemistry/Molecular Biology**

Submitted by

**Muhammad Hamid Siddique**

Department of Biochemistry

Faculty of Biological Sciences

Quaid-i-Azam University, Islamabad

2024

## **DECLARATION**

I affirm that the PhD thesis titled "**Implications of molecular signaling in therapeutic efficacy of nanodrug delivery systems in cancer model**" is my original work and has not been previously submitted for any degree at Quaid-i-Azam University or elsewhere. I acknowledge that the university reserves the right to revoke my PhD degree if it is discovered that this statement is untrue, even after my graduation.

Furthermore, I declare that the research presented in this study is solely my own, with no significant contributions from any other individual. Any assistance received from others has been duly acknowledged, and the entire thesis has been authored by me.

I am aware of the strict policy against plagiarism enforced by the Higher Education Commission (HEC) and Quaid-i-Azam University. Therefore, I attest that no part of my thesis has been plagiarized, and all referenced materials have been properly cited.

I acknowledge that if I am found guilty of formal plagiarism in this thesis, even after being awarded the PhD degree, the university reserves the right to revoke my degree. Additionally, the HEC and the university may publish my name on their websites alongside other students found to have submitted plagiarized work.

**Muhammad Hamid Siddique**

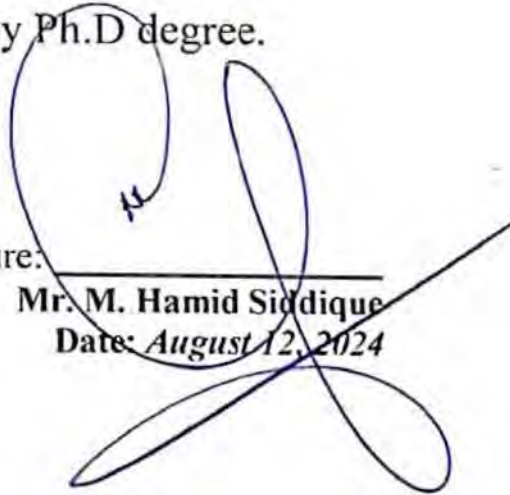
## Author's Declaration

I **Mr. Muhammad Hamid Siddique** hereby state that my PhD thesis, titled **"Implications of Molecular Signaling in Therapeutic Efficacy of Nanodrug Delivery Systems in Cancer Model"** is my own work and has not been submitted previously by me for taking any degree from Department of Biochemistry, Faculty of Biological Sciences, Quaid-i-Azam University, Islamabad, Pakistan.

Or anywhere else in the country/world.

At any time if my statement is found to be incorrect even after my graduation, the University has the right to withdraw my Ph.D degree.

Student/Author Signature:

  
Mr. M. Hamid Siddique

Date: August 12, 2024

## Plagiarism Undertaking

I solemnly declare that research work presented in the PhD thesis, titled **“Implications of Molecular Signaling in Therapeutic Efficacy of Nanodrug Delivery Systems in Cancer Model”** is solely my research work with no significant contribution from any other person. Small contribution/help wherever taken has been duly acknowledged and that complete thesis has been written by me.

I understand the zero-tolerance policy of the HEC and **Quaid-i-Azam University, Islamabad**, towards the plagiarism. Therefore, I as an Author of the above titled thesis declare that no portion of my thesis has been plagiarized and any material used as reference is properly referred/cited.

I undertake that if I am found guilty of any formal plagiarism in the above titled thesis even after award of PhD degree, the University reserves the right to withdraw/revoke my PhD degree and that HEC and the University has the right to publish my name on the HEC/University website on which names of students are placed who submitted plagiarized thesis.

Student/Author Signature: \_\_\_\_\_

**Mr. M. Hamid Siddique**

Date: *August 12, 2024*

# Certificate of Approval

This is to certify that the research work presented in this thesis, entitled: "**Implications of Molecular Signaling in Therapeutic Efficacy of Nanodrug Delivery Systems in Cancer Model**" was conducted by **Mr. Muhammad Hamid Siddique** under the supervision of Prof. Dr. Mariam Anees.

No part of this thesis has been submitted anywhere else for any other degree. This thesis is submitted to the Department of Biochemistry, Faculty of Biological Sciences, Quaid-i-Azam University, Islamabad, Pakistan in partial fulfillment of the requirements for the **Degree of Doctor of Philosophy** in the field of Biochemistry from Department of Biochemistry, Faculty of Biological Sciences, Quaid-i-Azam University, Islamabad, Pakistan.

**Mr. Muhammad Hamid Siddique**

Signature: \_\_\_\_\_

## **Examination Committee:**

### **1. External Examiner:**

**Dr. M. Sheeraz Ahmad**  
Associate Professor  
Department of Biochemistry  
PMAS Arid Agriculture University, Rawalpindi

Signature: \_\_\_\_\_

### **2. External Examiner:**

**Dr. Shaheen Shahzad**  
Assistant Professor  
Department of Bioinformatics & Biotechnology  
International Islamic University, Islamabad

Signature: \_\_\_\_\_

### **3. Supervisor:**

**Prof. Dr. Mariam Anees**

Signature: \_\_\_\_\_

### **4. Chairperson:**

**Prof. Dr. Iram Murtaza**

Signature: \_\_\_\_\_

**Dated:**

**12-08-2024**

---

1.11.6. TRAIL-NF- $\kappa$ B association.....	38
1.12. Wnt signaling pathway.....	38
1.12.1. Canonical signaling cascade .....	40
1.12.2. Non-canonical signaling cascade .....	41
1.13. HIF1-alpha signaling pathway .....	42
1.13.1. Dysregulation in HIF1-alpha pathway causing AML .....	44
1.14. Aims and Objectives .....	46
Chapter 2:.....	48
2.1. Introduction.....	49
2.2. Materials and Methods.....	51
2.2.1. Synthesis of MSNPs.....	51
2.2.2. Characterization of nanoparticles.....	53
2.2.3. Drug loading.....	54
2.2.4. Molecular docking studies .....	55
2.2.5. Cytotoxicity assay .....	55
2.2.6. <i>In vitro</i> bioassays.....	56
2.2.7. <i>In vivo</i> bioassays .....	56
2.2.8. Experiment design and <i>Sprague dawley</i> model .....	57
2.2.9. Morphological analysis .....	58
2.2.10. Blood profiling.....	58
2.2.11. mRNA extraction .....	59
2.2.12. cDNA synthesis.....	59
2.2.13. RT PCR expression analysis .....	59
2.2.14. Statistical analysis .....	61
2.3. Results.....	61
2.3.1. Characterization of MSNPs and drug loading .....	61
2.3.2. Nanomedicine demonstrating robust affinity with the TRAIL-DR5 complex.....	64
2.3.3. Docking studies.....	65
2.3.4. Nanomedicine and c-FLIP interactions.....	66
2.3.5. Antioxidant potential of nanomedicine.....	67
2.3.6. Biological efficacy of the nanomedicine.....	68
2.3.7. Relative organ weights .....	70
2.3.8. Blood parameters .....	71
2.3.9. Serum enzymatic levels .....	73

---

---

## Table of Contents

List of Figures .....	v
List of Tables .....	vii
List of Abbreviations .....	viii
Acknowledgements.....	x
Abstract.....	xi
Chapter 1: Introduction.....	1
1.1. Cancer .....	2
1.2. Levels of cancer progression .....	3
1.3. Hallmarks of cancer .....	3
1.4. Causes of cancer .....	4
1.5. Leukemia – blood cancer .....	5
1.6. Acute myeloid leukemia (AML).....	7
1.7. Occurrence and diagnosis of AML .....	9
1.8. Risk factors associated with AML .....	11
1.8.1. Role of benzene in AML induction.....	12
1.9. Treatment of AML.....	14
1.9.1. Chemotherapy .....	14
1.9.2. Nano technological advances in treatment of AML .....	18
1.9.3. Naturopathy.....	22
1.9.4. Synthetic organometallic compounds .....	26
1.10. TRAIL signaling pathway.....	29
1.10.1. TRAIL receptors .....	30
1.10.2. TRAIL signaling .....	31
1.10.2.1. The extrinsic pathway .....	31
1.10.2.2. The intrinsic pathway mediated by the mitochondria .....	32
1.10.3. Regulation of TRAIL pathway.....	34
1.11 NF- $\kappa$ B .....	35
1.11.1. NF- $\kappa$ B proteins.....	35
1.11.2. NF- $\kappa$ B inhibitors .....	36
1.11.3. Classical pathway of NF- $\kappa$ B .....	36
1.11.4. Alternative pathway of NF- $\kappa$ B.....	36
1.11.5. NF- $\kappa$ B activation.....	37



---

2.3.10. STMN1 genetic marker expression.....	74
2.3.11. Tumor suppressor gene p53 gets upregulated by nanomedicine.....	74
2.3.12. Nanomedicine regulates glycolysis in leukemic rats .....	74
2.3.13. mTOR pathway regulation by nanomedicine .....	74
2.3.14. Nanomedicine inhibits the NF-kappa B pathway .....	75
2.3.15. Regulation of TRAIL pathway by CcNPs .....	77
2.4. Discussion.....	78
Chapter 3:.....	87
3.1. Introduction.....	88
3.2. Materials & Methods .....	90
3.2.1. Materials.....	90
3.2.2. Characterization of CuET using XRD, SEM and EDX analysis .....	90
3.2.3. Molecular docking studies .....	90
3.2.4. Cytotoxicity assay .....	90
3.2.5. <i>In vitro</i> bioassays.....	90
3.2.6. <i>In vivo</i> bioassays .....	91
3.2.7. Development of AML model and experimental strategy.....	91
3.2.8. Morphological evaluation and tissue histology.....	92
3.2.9. Blood profiling and biochemical studies.....	92
3.2.10. Real time PCR analysis.....	92
3.2.11. Flow cytometry for apoptosis measurement .....	97
3.2.12. Statistical analysis .....	97
3.3. Results.....	97
3.3.1. Synthesis of CuET NPs.....	97
3.3.2. Characterization of CuET using XRD, SEM and EDX analysis .....	97
3.3.3. CD33 shows strong interaction with hyaluronic acid .....	100
3.3.4. Relative organ weights .....	101
3.3.5. Restoration of normal morphology and hematological profile .....	102
3.3.6. Notable antioxidant potential of CuET .....	105
3.3.7. Enhanced biological potential of CuET .....	105
3.3.8. Recovery of hepatic enzymes and serum uric acid levels.....	107
3.3.9. Dysregulation in STMN1 and S1009A genetic expression .....	108
3.3.10. Upregulation of negative regulators in canonical Wnt signaling pathway.....	108
3.3.11. Downregulation of HIF-1 $\alpha$ pathway pro-survival signaling markers .....	110

---

---

3.3.12. The AnnexinV/PI apoptosis assay .....	112
3.3.13. CD4 viability assay .....	112
3.4. Discussion .....	113
Chapter 4:.....	118
4.1. Introduction.....	119
4.2. Materials & Methods .....	121
4.2.1. Materials.....	121
4.2.2. Synthesis of NiET NPs.....	121
4.2.3. Characterization of NiET NPs.....	121
4.2.4. Cytotoxicity assay .....	122
4.2.5. <i>In vitro</i> bioassays.....	123
4.2.6. <i>In vivo</i> bioassays .....	123
4.2.7. Development of AML model and experimental strategy.....	124
4.2.8. Morphological evaluation and tissue histology.....	125
4.2.9. Blood profiling and biochemical studies.....	125
4.2.10. Real time PCR analysis.....	126
4.2.11. Flow cytometry for apoptosis measurement .....	129
4.2.12. Statistical analysis .....	129
4.3. Results.....	129
4.3.1. Characterization of NiET using DLS, XRD, SEM and EDX analysis.....	129
4.3.2. Relative organ weight recovery in treatment groups.....	132
4.3.3. Restoring the morphology and hematological profile.....	133
4.3.4. NiET's notable antioxidant potential.....	136
4.3.5. NiET's enhanced biological potential in rat model .....	136
4.3.6. Recovery of hepatic enzymes and serum uric acid levels.....	137
4.3.7. AML induction confirmation .....	138
4.3.8. The canonical Wnt signaling pathway .....	139
4.3.9. Downregulation of HIF-1 $\alpha$ pathway pro-survival signaling markers .....	141
4.3.10. The AnnexinV/PI apoptosis test.....	143
4.3.11. The CD4 viability test .....	144
4.4. Discussion.....	144
Conclusion .....	149
References.....	153

---

---

## List of Figures

Figure 1.1: Flow diagram of cancer progression .....	3
Figure 1.2: Hallmarks of cancer.....	4
Figure 1.3: Acute myeloid leukemia.....	8
Figure 1.4: Mechanism of benzene action .....	13
Figure 1.5: Graphical representation of chemotherapy.....	15
Figure 1.6: Structure and mechanism of action of doxorubicin.....	17
Figure 1.7: Conventional chemotherapy vs nanotherapy.....	18
Figure 1.8: Structure of caffeine .....	24
Figure 1.9: Mechanism of caffeine action .....	25
Figure 1.10: Five TRAIL receptors along with structures .....	31
Figure 1.11: Apoptosis signaling pathways including extrinsic and intrinsic cascades.....	32
Figure 1.12: NF- $\kappa$ B activation underlying mechanism.....	37
Figure 1.13: Wnt signaling pathway (canonical and non-canonical pathways).....	39
Figure 1.14: HIF1 alpha pathway signaling cascade .....	43
Figure 2.1: Study design and experimental strategy .....	51
Figure 2.2: Steps involved in the synthesis of mesoporous silica nanoparticles.....	52
Figure 2.3: Mesoporous silica nanoparticles (chemical synthesis).....	53
Figure 2.4: Techniques used for characterization of nanoparticles.....	54
Figure 2.5: The SEM images of mesoporous silica nanoparticles .....	62
Figure 2.6: The X-ray diffraction analysis of MSNPs .....	62
Figure 2.7: FTIR analysis of MSNPs.....	63
Figure 2.8: The absorbance spectra obtained through UV/Vis Spectroscopy.....	64
Figure 2.9: Molecular docking between CcNPs and TRAIL-DR5 complex .....	65
Figure 2.10: Molecular docking between CcNPs and NF $\kappa$ B-p52/RelB/DNA complex.....	66
Figure 2.11: Molecular docking between CcNPs and cFLIP-DISC complex.....	67
Figure 2.12: The assessment of antioxidant potential using TAC, TRP and DPPH assays.....	68
Figure 2.13: Biological potential analysis using various bioassays .....	69
Figure 2.14: Comparing the mean + SEM relative organ weights.....	70
Figure 2.15: Morphological evaluation of blood cells .....	71
Figure 2.16: Blood parameters of different experimental groups .....	72
Figure 2.17: Enzymatic biomarkers analysis using LFT and RFT .....	73
Figure 2.18: Genetic biomarkers analysis using qPCR.....	76

---

Figure 2.19: Relative genetic expression of TRAIL biomarkers .....	78
Figure 3.1: The dynamic light spectrum analysis confirming size of CuET Nps .....	98
Figure 3.2: The XRD pattern of copper diethyldithiocarbamate .....	98
Figure 3.3: Scanning electron microscopy of CuET .....	99
Figure 3.4: Energy dispersive spectroscopic image.....	99
Figure 3.5: CD33 protein's binding site docked with the hyaluronic acid .....	101
Figure 3.6: Restoration of mean relative organ weights. ....	102
Figure 3.7: Morphological analysis of blood and bone marrow cells.....	103
Figure 3.8: Blood parameters of different experimental groups. ....	104
Figure 3.9: Antioxidant potential analysis using TAC, TRP and DPPH assays .....	105
Figure 3.10: Biological potential analysis via various bioassays.....	106
Figure 3.11: Levels of hepatic and renal biomarkers.....	107
Figure 3.12: Gene expression analysis using qPCR .....	111
Figure 3.13: FACS analysis using propidium iodide and annexin V dye.....	112
Figure 4.1: The dynamic light spectrum analysis .....	130
Figure 4.2: The XRD pattern of Nickel diethyldithiocarbamate.....	131
Figure 4.3: Scanning electron microscopy of NiET .....	131
Figure 4.4: Energy dispersive spectroscopic image.....	132
Figure 4.5: Restoration of relative A) liver, B) heart and C) kidney weights.....	133
Figure 4.6: Morphological analysis of blood and bone marrow cells.....	134
Figure 4.7: Evaluation of heamotological parameters after dosage administration .....	135
Figure 4.8: Antioxidant potential analysis using TRP, TAC and DPPH .....	136
Figure 4.9: Biological potential analysis via various bioassays.....	137
Figure 4.10: Evaluation of levels of hepatic and renal biomarkers via LFT and RFT.....	138
Figure 4.11: Genetic expression analysis of Wnt pathway components using qPCR.....	140
Figure 4.12: Genetic expression analysis of HIF 1 $\alpha$ components using qPCR .....	142
Figure 4.13: FACS analysis using propidium iodide and annexin V dye.....	143
Figure 4.14: FACS analysis using CD4 antibody. ....	144

---

---

## List of Tables

Table 1.1: Types and causes of leukemia .....	6
Table 2.1: Chemicals involved in synthesis, loading and coating of MSNPs.....	52
Table 2.2: Dosage regime for brine shrimp assay.....	56
Table 2.3: Dosing and mode of administration of drugs among different groups. ....	58
Table 2.4: Primers for qPCR-based RNA expression analysis .....	60
Table 2.5: List of reagents used in qPCR.....	61
Table 3.1: Materials for RNA extraction .....	93
Table 3.2: Reagents required for cDNA synthesis mixture .....	93
Table 3.3: The reagents and their quantities used for conventional PCR .....	94
Table 3.4. List of primers used in qPCR.....	95
Table 3.5: The reagents used for qRT-PCR.....	96
Table 3.6: Individual elements and their percentages in copper dithiocarbamate .....	100
Table 4.1: Prerequisites for brine shrimp assay .....	122
Table 4.2: Requirements for total antioxidant capacity assay.....	123
Table 4.3: Requirements for DPPH assay.....	123
Table 4.4: List of primers used in qPCR.....	128
Table 4.5: Individual elements and their percentages in Nickel dithiocarbamate .....	132

## List of Abbreviations

ABS	Absorbance
ALL	Acute Lymphoblastic Leukemia
ALP	Alkaline Phosphatase
ALT	Alanine Amino transferase
AML	Acute Myeloid Leukemia
AST	Aspartate Aminotransferase
CcNPs	Caffeine coated Nanoparticles
CLL	Chronic Lymphoblastic Leukemia
CML	Chronic Myeloid Leukemia
CuET	Copper Diethyldithiocarbamate
DISC	Death Inducing Signaling Complex
DMSO	Dimethyl Sulfoxide
DNA	Deoxyribo Nucleic Acid
DOXO	Doxorubicin
DR4	Death Receptor 4
DR5	Death Receptor 5
DTC	Diethyldithiocarbamate
EDTA	Ethylene Diamine Tetra Acetic Acid
EDX	Energy-Dispersive X-ray Analysis
FADD	Fas-Associated Death Domain
FIT	Ferrocene Incorporated Thiourea
FLICE	FADD-Like Interleukin-1 $\beta$ -Converting Enzyme
FLIP <sub>L</sub>	FLICE-Like Inhibitory Protein (long form)
FTIR	Fourier Transform Infra-Red Spectroscopy
HB	Hemoglobin
HA	Hyaluronic acid
IAPs	Inhibitors of Apoptotic Proteins
IKB	Inhibitor of Kappa B
IRB	Institutional Review Board
MSNPs	Mesoporous Silica Nanoparticles
NF- $\kappa$ B	Nuclear Factor Kappa-light-chain enhancer of activated B cell
NiET	Nickel Diethyldithiocarbamates

PBS	Phosphate Buffer Saline
PTEN	Phosphatase and Tensin Homolog
RBCs	Red Blood Cells
ROS	Reactive Oxygen Species
TNF	Tumor Necrosis Factor
TRADD	TNF Receptor-Associated Death Domain
TRAIL	Tumor Necrosis Factor-Related Apoptosis-Inducing Ligand
VEGF	Vascular Endothelial Growth Factor
WBCs	White Blood Cells
XRD	X-Ray Diffraction

## Acknowledgements

I am grateful to **Prof. Dr. Iram Murtaza**, Chairperson of the Department of Biochemistry, and **Prof. Dr. Sarwat Jahan**, Dean of the Faculty of Biological Sciences, Quaid-i-Azam University, Islamabad, Pakistan, for providing me with all the available resources and research facilities.

I would want to express my gratitude to my charismatic, charming, kind, and encouraging mentor and supervisor, **Prof. Dr. Mariam Anees**, at Department of Biochemistry, Quaid-i-Azam University, Islamabad. I am grateful to her for her ongoing support and concerned supervision and for giving me the required support to complete my work on time. Thank you so much, ma'am.

I am also grateful to **Prof. Dr. Zia-Ur-Rehman** from the Department of Chemistry at Quaid-i-Azam University, Islamabad for providing synthetic chemicals for my research. I am also grateful to **Dr. Ibrar Ahmed** for extending research facilities and resources in Alpha Genomics, Islamabad, Pakistan.

I would also like to thank my loving family, including my father, **Mr. Muhammad Siddique**, my Ammi, my brothers **Umor Bhai**, **Zain-ul-Abadin**, my sister **Ms. Humeyra Siddique** and my devoted wife **Dr. Aliya Hamid** for believing in me and constantly supporting me. I also feel blessed to have my beloved son **Mr. Abdullah Hamid** and lovely nephews **Mr. Hussain Umor**, **Mr. Ahmed Umor** on my side throughout this struggle.

I'd want to express my gratitude to my esteemed senior, **Dr. Sidra Bukhari**, for constantly supporting and guiding me through difficult times. I am also grateful to my colleagues Inam Ullah Khan, Usama Sabir, Omiya Ayub, Kaveeta Kumari, Zia ul Nissa, Wajeeha Waheed, Asiya Essa, and Ayesha Ali Khan for their assistance, kindness, guidance, and support throughout. May they be blessed with good fortune and success in their future efforts.

I am grateful to every staff member of the Department of Biochemistry's office, particularly Mr. Tariq, Mr. Fayyaz, Mr. Shehzad, Mr. Saeed, and others, for their assistance and guidance. I would also like to offer my heartfelt gratitude to everyone who helped and supported this achievement, whether directly or indirectly.

---



## Abstract

Acute Myeloid Leukemia (AML) presents significant clinical challenges due to its heterogeneous molecular profile and the limitations of traditional chemotherapy, which often result in inadequate efficacy and high toxicity. This research has been conducted to address these issues by exploring the potential of nanomedicines, combined with doxorubicin, to enhance therapeutic outcomes and reduce adverse effects in AML treatment. .

This multidisciplinary study explores the combined efficacy of three different test compounds — caffeine-coated nanoparticles (CcNPs), copper diethyldithiocarbamate (CuET) nanoparticles, and nickel diethyldithiocarbamate (NiET) nanoparticles — as adjuncts to doxorubicin in the treatment of AML. Our research unfolds the anti-leukemic properties of these nanoparticles using a variety of investigative methodologies, including *in silico*, *in vitro*, and *in vivo* assays. *In silico* docking studies act as a foundational scaffold, revealing the molecular complexities of nanoparticle interactions with critical cellular targets. Complementing these computational efforts are *in vitro* antioxidant assays, which provide insight into the nanoparticles' potential for modulating oxidative stress—an important aspect in AML pathogenesis. *In vivo* experimentation with AML rat models demonstrates the profound impact of nanoparticles, particularly when combined with doxorubicin.

Our findings suggest that CcNP, CuET and NiET nanoparticles, when combined with doxorubicin, could be viable transformative therapeutic approaches in AML. These nanomedicines especially CcNPs act as potent inducers of the TRAIL-DR5 complex while also inhibiting the NF- $\kappa$ B p52/RelB/DNA complex. This dual action suggests their potential for reshaping the AML treatment landscape by targeting specific molecular pathways involved in leukemia progression. Moreover, their ability to modulate specific molecular pathways, improve treatment efficacy, and potential mitigation of the risks associated with conventional chemotherapies is a hallmark of their potential.

Notably, the combination therapies have a significant impact on key leukemic genetic markers, specifically the downregulation of STMN1 and S1009A expressions, as well as

the restoration of aberrant Wnt and HIF-1 alpha pathway gene expressions. The potent efficacy of these combination therapies is further supported by Annexin V/PI based apoptosis detection and CD4 viability tests, which highlight their significant potential against leukemic cells owing to enhanced intermolecular interaction of test compounds with CD33+ myeloid cells.

This study heralds a new era in AML therapeutics, urging further clinical investigation to confirm their efficacy and safety profiles. The tantalizing prospect of these nanomedicines redefining AML treatment paradigms signals a promising path towards more effective, targeted, and less toxic therapies, highlighting a transformative phase in the fight against this aggressive hematological malignancy.

The work presented here has resulted in the following manuscripts:

- **Siddique MH**, Bukhari S, Khan IU, Essa A, Ali Z, Sabir U, Ayoub O, Saadia H, Yaseen M, Sultan A, Murtaza I, Kerr PG, Bhat MA, Anees M. *In silico, in vitro, and in vivo* evaluation of caffeine-coated nanoparticles as a promising therapeutic avenue for AML through NF-Kappa B and TRAIL pathways modulation. *Pharmaceuticals* (2023) 16 (12), 1742 (Published).
- **Siddique MH**, Bukhari S, Sabir U, Khan I, Waheed W, Yaseen M, Sultan A, Murtaza I, Kerr P, Rehman ZU, Anees M. *In silico, in vitro, and in vivo* analysis of copper-diethyldithiocarbamate nanoparticles and doxorubicin: a novel combination strategy against AML (under review).
- **Siddique MH**, Bukhari S, Sabir U, Khan I, Waheed W, Yaseen M, Sultan A, Murtaza I, Kerr P, Rehman ZU, Anees M. Exploring the Synergistic Therapeutic Potential of Ni-Diethyldithiocarbamate Nanoparticles with Doxorubicin in Acute Myeloid Leukemia (in preparation).

# Chapter 1: Introduction

## 1. Introduction

### 1.1. Cancer

Cancer continues to be a severe worldwide health concern, with yearly incidence expected to reach a staggering 23.6 million by 2030. Cancer initiation is characterized by deregulation of cellular survival pathways, which exceeds normal thresholds of proliferation, ultimately leading to uncontrolled tumor formation (Hanahan & Weinberg, 2011).

The delicate orchestration of cellular growth and division in physiological situations is rigorously managed by the exact release and interaction of growth factors. These components are essential for maintaining cellular homeostasis and a healthy tissue environment. This delicate balance, however, is disrupted within cancer cells. Cellular pathways that typically maintain this fine-tuned control are disrupted, resulting in an environment that is out of sync with the body's natural checks and balances (Terzibasitazzi *et al.*, 2017).

This alteration supports the uncontrolled multiplication and survival of malignant cells. Furthermore, these disrupted cells cause mutations in nearby healthy cells, resulting in an increase in the release of growth factors inside the cellular niche. This never-ending cycle promotes cancer cell growth and metastasis, continuing disease progression and has devastating impact on the affected individual (Chang *et al.*, 2008).

The complex interaction of disturbed cellular pathways, growth factor accumulation, and changes in survival protein receptor levels creates a hostile milieu that promotes cancer cell proliferation and spread. Understanding these numerous molecular complexities is critical in designing tailored treatment strategies to restore balance and halt the uncontrolled course of this dreadful disease (Sawyers *et al.*, 2013).

## 1.2. Levels of cancer progression

Cancer is caused by a sequence of genetic alterations in cells that cause them to transform from normal to malignant. It begins with excessive cell growth, known as hyperplasia. The nucleus (the cell's control center) then gets bigger in comparison to the cell's body, indicating a shift to a dysplastic condition.

As the process progresses, these cells undergo additional transformation, obtaining the capacity to penetrate neighboring tissues and blood vessels. Figure 1.1 depicts these steps, showing how cells progress from basic alterations to becoming invasive and capable of spreading (Mayengbam *et al.*, 2021).



*Figure 1.1: Flow diagram of cancer progression*

## 1.3. Hallmarks of cancer

Cancer hallmarks are key biological characteristics gained during cancer development that serve as the foundation for comprehending the intricacies of metastatic cancers. These characteristics include cancer cells' capacity to fight apoptosis (cell death), establish replicative immortality, prolong cell survival signaling, avoid growth-suppressive signals, improve angiogenesis, and activate invasive activity (Hanahan & Weinberg, 2011).

These abilities are the result of a slew of mutations that promote genetic diversity and genomic changes inside cancer cells. Over the last decade, advances in cancer research have resulted in the inclusion of four new hallmarks to this list: reprogramming of energy metabolism, tumor-promoting inflammation, genomic instability, and immune evasion. These new additions have broadened our understanding of cancer's complexities, giving a more complete framework for elucidating the mechanisms behind tumor growth and progression (Hanahan & Weinberg, 2011).

This updated collection of hallmarks provides a critical foundation for investigating innovative therapeutic options in cancer treatment. By defining these essential skills, researchers may develop creative techniques to target these unique characteristics, possibly altering the landscape of cancer therapy and management.



*Figure 1.2: Hallmarks of Cancer (Hanahan & Weinberg, 2011)*

#### 1.4. Causes of Cancer

Cancer is a multidimensional illness caused by a complex interplay of several variables rather than a single mutation. It is still extremely difficult to identify a single cause of cancer beginning and progression. Cancer has traditionally been viewed as the result of genomic modifications happening inside transformed cells, which are frequently characterized by mutations in the DNA of normal cells (Vogelstein & Kinzler, 2004). These mutations are often caused by exposure to various mutagens or carcinogens, such as environmental causes, radiation, food ingredients, or chemical agents (Allen *et al.*, 1957).

These agents' mutations disturb the delicate process of DNA replication, resulting in an accumulation of genetic abnormalities that support cancer growth. Furthermore, some of

these mutations have inheritable features, which perpetuate a proclivity for heightened genetic abnormalities, increasing the likelihood of cancer incidence (Anand *et al.*, 2008)

Cancer etiology is difficult because it is multiple, with a plethora of genetic, environmental, and lifestyle factors interacting to orchestrate the delicate cellular alterations that drive cancer growth. Despite advances in understanding the role of mutations in cancer causation, the holistic picture of cancer causation remains opaque, demanding ongoing research efforts to uncover its complex origins (Feinberg, 2004).

### **1.5. Leukemia – blood cancer**

Leukemia, popularly known as blood cancer, stands as a complex and varied category of hematologic malignancies defined by the uncontrolled growth of aberrant white blood cells (leukocytes) within the bone marrow and peripheral circulation. This illness comprises a spectrum of diseases, each differentiated by specific clinical, pathological, and molecular aspects. The fundamental classification of leukemia rests on the differentiation lineage of the aberrant leukemic cells and their development pace, leading to its wide categorization into acute and chronic types (Lowenberg *et al.*, 1999).

Acute leukemias emerge as quickly advancing disorders, distinguished by the rapid growth of immature or undifferentiated cells, referred to as blasts, inside the bone marrow. These blasts fail to develop into functional blood cells, consequently entering the circulation and interfering with normal hematopoiesis. Acute leukemias are further subclassified into two basic types: acute lymphoblastic leukemia (ALL) and acute myeloid leukemia (AML), dependent upon the cell lineage affected—lymphoid or myeloid, respectively (Rose-Inman & Kuehl, 2017).

Conversely, chronic leukemias advance at a slower pace, characterized by the excessive buildup of mature yet abnormal leukocytes. Chronic myeloid leukemia (CML) and chronic lymphocytic leukemia (CLL) represent the primary subtypes within the spectrum of chronic leukemias, Chronic Myeloid Leukemia (CML) is characterized by a distinctive genetic abnormality known as the Philadelphia chromosome. This aberration arises from a reciprocal translocation event between chromosomes 9 and 22, leading to the fusion of two genes: BCR (Breakpoint Cluster Region) and ABL (Abelson). The resulting fusion gene,



BCR-ABL, is considered a hallmark feature of CML, playing a pivotal role in both the diagnosis and treatment of the disease.

The BCR-ABL fusion gene encodes for a constitutively active tyrosine kinase enzyme, which drives uncontrolled proliferation and survival of myeloid cells. This dysregulated signaling pathway is central to the pathogenesis of CML, contributing to the expansion of malignant myeloid progenitor cells characteristic of the disease.

Importantly, the detection of the BCR-ABL fusion gene is a key diagnostic criterion for CML, as its presence confirms the diagnosis of the disease. Furthermore, targeting the BCR-ABL fusion protein with tyrosine kinase inhibitors (TKIs), such as imatinib, has revolutionized the treatment landscape for CML. TKIs specifically inhibit the activity of the BCR-ABL tyrosine kinase, leading to suppression of leukemic cell proliferation and induction of apoptosis, thereby achieving significant clinical responses and improving patient outcomes.

In contrast, CLL includes the growth of aberrant B-lymphocytes, frequently demonstrating a somewhat indolent course and mostly affecting elderly persons (Pui & Evans, 1998).

**Table 1.1: Types and causes of leukemia**

No.	Types of Leukemia	Causes and Symptoms	References
1.	Acute lymphocytic leukemia (ALL)	<ol style="list-style-type: none"> <li>Genetic abnormalities in hematopoietic stem cells (HSCs).</li> <li>Activation of certain genes by chromosomal translocation</li> <li>Bone and joint pain</li> </ol>	(Armstrong & Look, 2005)
2.	Chronic lymphocytic leukemia (CLL)	<ol style="list-style-type: none"> <li>Homogenous disease of immature B-Cells.</li> <li>Defective apoptosis.</li> <li>Inability to elicit immune response.</li> <li>Most prevalent form i.e. 36%.</li> <li>Night sweats, Easy bruising and bleeding</li> </ol>	(Chiorazzi, Rai <i>et al.</i> , 2005)

3.	Acute myeloid leukemia (AML)	<ol style="list-style-type: none"> <li>1. Genetic alteration and malfunctioning of HSCs leading to clonal hematopoietic irregularity i.e. AML.</li> <li>2. Distortion of rational differentiation.</li> <li>3. Unrestrained growth of blast cells (Called immature leukemic cells).</li> <li>4. Fever, fatigue, hemorrhage, bone-pain and CNS malfunctioning.</li> </ol>	(Lowenberg <i>et al.</i> , 1999)
4.	Chronic myeloid leukemia (CML)	<ol style="list-style-type: none"> <li>1. Philadelphia chromosome translocation (BCR-ABL fusion gene)</li> <li>2. Genetic predisposition</li> <li>3. Ionizing radiation exposure</li> <li>4. Fatigue and weakness</li> <li>5. Unexplained weight loss</li> <li>6. Enlarged spleen and liver</li> </ol>	(Chiorazzi, Rai <i>et al.</i> , 2005)

Further sub-classification within each subtype is based on different cytogenetic, molecular, and immunophenotypic markers, enhancing diagnosis accuracy and assisting in prognostication and therapy planning. The identification of these distinct subtypes and their underlying molecular fingerprints has paved the way for customized therapy options, boosting treatment efficacy and patient outcomes in leukemia care. Continued breakthroughs in our understanding of the molecular processes and genetic foundations of leukemia subtypes remain crucial in improving diagnostic techniques and supporting the development of targeted treatments tailored to specific patient profiles.

### 1.6. Acute Myeloid Leukemia (AML)

Acute Myeloid Leukemia (AML) is commonly known as blood cancer which originates in bone marrow. The excessive proliferation of bone marrow cells result in the appearance of blast cells in bloodstream, which fail to differentiate into fully functional blood cells. Consequently, the normal process of blood cell formation is disrupted, leading to impaired bone marrow function.

The disturbance in bone marrow function manifests as a reduction in the synthesis of various types of blood cells. This includes a decline in the production of red blood cells, which are essential for oxygen transport, platelets, which play a critical role in blood clotting, and fully mature white blood cells, which are integral components of the immune system's defense mechanisms.

AML is a very variable illness, defined primarily on genetic and cytogenetic abnormalities, which greatly impact prognosis and treatment response. The WHO categorization system categorizes AML into various subtypes characterized by particular genetic mutations, chromosomal abnormalities, and variations in gene expression patterns. Mutations typically related with AML include FLT3, NPM1, CEBPA, and IDH1/2, among others (Döhner *et al.*, 2017).

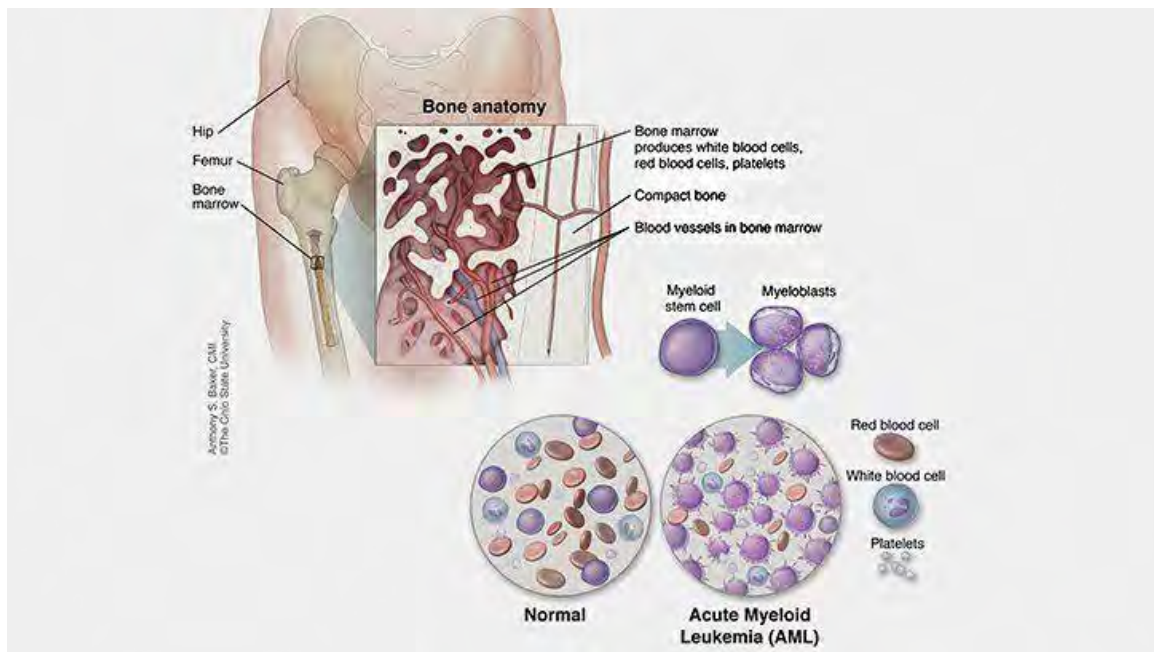


**Figure 1.3: Acute myeloid leukemia (Rubnitz *et al.*, 2008)**

Clinical signs of AML may include symptoms such as weariness, weakness, increased susceptibility to infections owing to neutropenia, easy bruising or bleeding arising from thrombocytopenia, and anemia due to diminished red blood cell formation. Diagnosis comprises blood testing, bone marrow aspiration, and genetic analysis to identify particular mutations, advise prognosis, and personalize treatment regimens (Döhner *et al.*, 2017).

Treatment for AML often comprises of chemotherapy aimed at inducing remission by targeting leukemic cells. Consolidation therapy, which may involve further chemotherapy or stem cell transplantation, tries to avoid disease recurrence. Hematopoietic stem cell transplantation (HSCT) serves as a potential curative alternative, particularly for individuals at high risk of recurrence or with refractory illness. The decision for HSCT depends on parameters such as patient age, comorbidities, and genetic risk stratification (Döhner *et al.*, 2017).

Advancements in molecular profiling and targeted treatments have altered AML therapy paradigms. Targeted medicines, such as tyrosine kinase inhibitors (e.g., midostaurin for FLT3 mutations) and inhibitors of mutant IDH1/2 enzymes, have shown success in particular AML subgroups, enabling more focused and perhaps less toxic therapy alternatives (Perl *et al.*, 2017).

Despite these breakthroughs, obstacles exist in treating recurrent or refractory illness, avoiding treatment-related toxicities, and establishing sustained responses in older or medically unfit patients. Ongoing research endeavors focus on identifying novel therapeutic targets, developing immunotherapies, refining risk stratification, and exploring combination therapies to improve outcomes and enhance the quality of life for individuals affected by AML (Perl *et al.*, 2017).

### **1.7. Occurrence and diagnosis of AML**

The frequency of AML fluctuates with age, exhibiting a propensity for older individuals, and it accounts for a considerable fraction of adult leukemias (Arber *et al.*, 2016). There are numerous techniques to detect AML, however the most frequent one is by blood testing. These tests are used to determine morphology of myeloblasts, peripheral blood cells and bone marrow cells as they are altered in leukemia. These morphological alterations include lower cytoplasmic content, higher nucleus to cytoplasm ratio and distortion in nuclear shape which are the features of immature blast cells.

If in blood, 30% or more cells display such shape of blast cells, then it is recognized as AML. AML is split into 9 additional kinds according to differentiation in blast cells morphology (Bennett *et al.*, 1976). Several staining processes may be adopted for such

morphological research but the most recommended one is Giemsa staining. Alteration in hepatic (ALT, ALP & AST) and renal biomarkers in serum of patients, owing to hepatic cytotoxicity by benzene, might also be one of the measures to detect AML (Dere & Ari, 2009).

Though, it is identified by a series of clinical assessments and laboratory testing, patients generally arrive with symptoms such as tiredness, infections, bleeding tendencies, and anemia, which require prompt medical screening. Blood tests, including complete blood count (CBC) and peripheral blood smears, typically indicate aberrant leukocyte counts, reduced red blood cells, and decreased platelets, indicating bone marrow failure.

Confirmation of AML diagnosis relies on bone marrow aspiration and biopsy. This process comprises taking samples from the bone marrow to examine cellular shape, calculate blast percentages, and perform immunophenotyping to detect particular markers expressed on leukemic cells. Additionally, cytogenetic and molecular investigations are critical for detecting genetic abnormalities and mutations that impact prognosis and guide therapy options. Mutations commonly found in acute myeloid leukemia (AML), including FLT3 play crucial roles in several aspects of the disease. They serve as important markers for assessing the risk profile of the patient, helping clinicians determine the prognosis and tailor treatment strategies accordingly. Additionally, these mutations provide valuable insights into the underlying molecular mechanisms driving AML pathogenesis. Understanding the presence and significance of these mutations allows for more personalized and targeted therapeutic approaches, ultimately improving patient outcomes. (Arber *et al.*, 2016).

Advanced diagnostic technologies, such as next-generation sequencing and multiparameter flow cytometry, provide more insight into the genetic landscape and immunophenotypic components of AML, allowing for more accurate subtyping and tailored treatment regimens. Early and accurate detection of AML is crucial for initiating fast and appropriate treatment. Induction chemotherapy regimens are widely used to promote remission, followed by consolidation therapy to prevent sickness recurrence. Furthermore, identifying specific genetic mutations allows for the use of targeted therapies such as tyrosine kinase

inhibitors or inhibitors of mutant enzymes, providing more tailored and potentially effective treatment options for select AML subgroups (DiNardo *et al.*, 2019)

Continuous advances in diagnostic techniques and molecular profiling continue to refine our understanding of AML pathogenesis, allowing for more precise diagnosis, risk stratification, and the development of novel therapeutic strategies aimed at improving outcomes for people living with this complex disease (Arber *et al.*, 2016).

### **1.8. Risk factors associated with AML**

Risk factors are components that increase the likelihood of getting a certain disease, and serve as critical markers for early identification. It is critical to understand that not everyone with these risk factors will acquire the disease (Belson *et al.*, 2007). Several risk factors for Acute Myeloid Leukemia (AML) have been identified:

1. Tobacco use
2. Age: Individuals aged 65 and older account for approximately 60% of AML cases.
3. Gender disparity: Males have a greater incidence of AML than females.
4. Prior chemotherapy or radiation therapy for other malignancies, notwithstanding the possibility of acquiring AML. The advantages of these medicines in cancer therapy exceed the hazards.
5. Myeloproliferative neoplasms (MPNs): Chronic bone marrow and blood illnesses, notably myelofibrosis, which can proceed to AML.
6. Myelodysplastic syndrome (MDS): A disorder characterized by insufficient generation of healthy blood cells, which results in AML transformation in 10% to 20% of patients.
7. Genetic predisposition: Certain genetic problems increase the risk of AML e.g. Down syndrome
8. Prolonged exposure to benzene, which is often present in the petroleum sector.

9. Family history: People who have a family history of AML, such as a parent, sibling, or child with the disease, are more likely to develop the condition.

Understanding and recognizing these risk factors is crucial for proactive disease management and individualized healthcare treatments for those who may be at increased risk of developing AML (Schmid *et al.*, 2012).

### **1.8.1. Role of benzene in AML induction**

Benzene, a common industrial chemical found in gasoline, solvents, and plastics, has been identified as a strong carcinogen. The link between benzene exposure and AML has been well established in epidemiological research and occupational exposure evaluations (Natelson, 2007).

The detrimental impact of benzene on DNA integrity within bone marrow cells, notably hematopoietic stem cells and progenitor cells essential for blood cell formation, is a significant factor in AML development. Chronic exposure to benzene and its metabolites instigates genetic mutations, chromosomal aberrations, and DNA damage in these cells. Consequently, this disturbance disrupts their normal physiological functions, fostering uncontrolled cell growth and eventually paving the way for malignant transformation, thus contributing to the pathogenesis of AML (Shallis *et al.*, 2021).

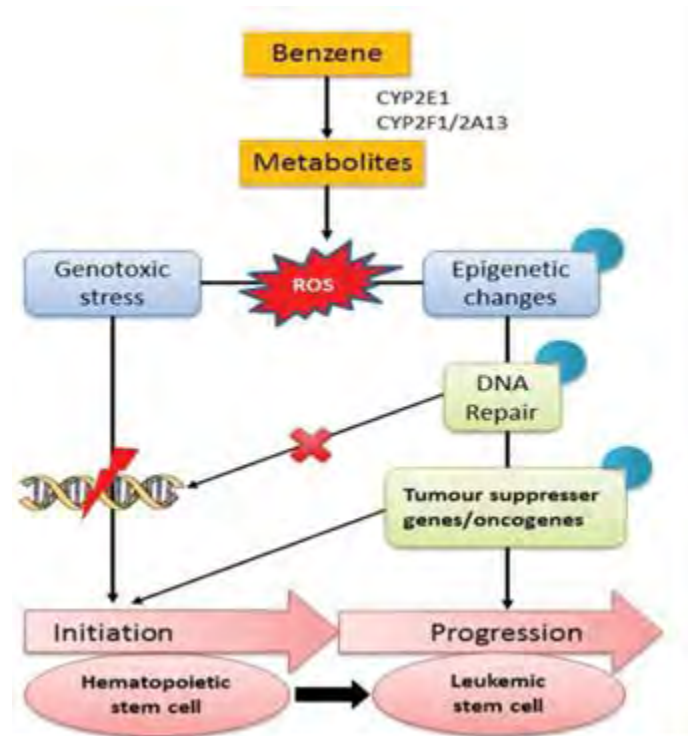


*Figure 1.4: Mechanism of benzene action (Kolachana et al., 1993)*

Benzene metabolites like benzene oxide and reactive intermediates like 1,4-benzoquinone have been linked to DNA adduct production and oxidative stress in bone marrow cells. These pathways can cause oncogene activation, tumor suppressor gene inhibition, and interference with cellular repair systems, ultimately leading to the onset of leukemogenesis and progression to AML

Furthermore, benzene's effect on the bone marrow microenvironment and hematopoietic niches may contribute to leukemic transformation by interrupting normal hematopoiesis and encouraging an environment permissive to leukemic cell growth.

It is crucial to emphasize that, while benzene exposure is an established risk factor for AML, not all people who are exposed to it will acquire the condition. The likelihood of developing AML is determined by a number of factors, including exposure length and severity, individual's vulnerability, and genetic predisposition.

Regulatory initiatives and occupational safety standards targeted at decreasing benzene exposure in industrial settings have played a critical role in lowering the frequency of



benzene-induced AML. Comprehensive risk assessment, monitoring, and adherence to safety standards are still required to reduce the possible health concerns associated with benzene exposure (Snyder, 2002b).

### **1.9. Treatment of AML**

Chemotherapy, radiation therapy, surgery, hormone therapy, and immunotherapy are all examples of traditional cancer treatments. Gene and stem cell transplantation is especially utilized to treat acute myeloid leukemia in order to enhance and extend patients' lives by a few years (Shaffer *et al.*, 2012).

Several chemotherapeutic anti-cancer drugs are employed in chemotherapy to kill cancer cells and prevent their growth. However, these chemotherapeutic drugs are costly and have several negative effects on nearby normal cells because of their inability to distinguish between malignant and normal cells (Burnett, 2005). As a result, in addition to the intended therapeutic impact, chemotherapy can trigger immunogenic cell death. Chemotherapy side effects include hair loss, tiredness, vomiting, nausea, and diarrhea. Despite this, chemotherapy is most commonly used to treat AML in adults aged 18 to 60 years. Anticancer medications are being utilized in conjunction with naturopathy to treat AML for increased efficacy (Burnett & Knapper, 2007).

With increasing age, recurrence-free survival becomes less likely. AML needs targeted therapy that targets molecules involved in deregulating cellular functions and sustaining leukemic state, such as tyrosine kinase over-expression, increased angiogenesis, and drug resistance (Bruserud *et al.*, 2001).

Leukemia recurrence can also develop after therapy due to persistent leukemic cells. This is known as minimum residual disease. Patients are given "Trisenox" in such circumstances. In HL60 cell line, a combined treatment of Etomoxir, Arsenic Trioxide, and Trisenox caused apoptosis. Arsenic trioxide inhibits the AKT and ERK pathways while having no harmful effects on normal cells (Roboz, 2011).

#### **1.9.1. Chemotherapy**

Chemotherapy remains a cornerstone therapeutic approach for managing this aggressive malignancy. Chemotherapy's primary objective in AML is to promote remission by

---

eliminating leukemic cells and restoring normal bone marrow function (Dombret & Itzykson, 2017).

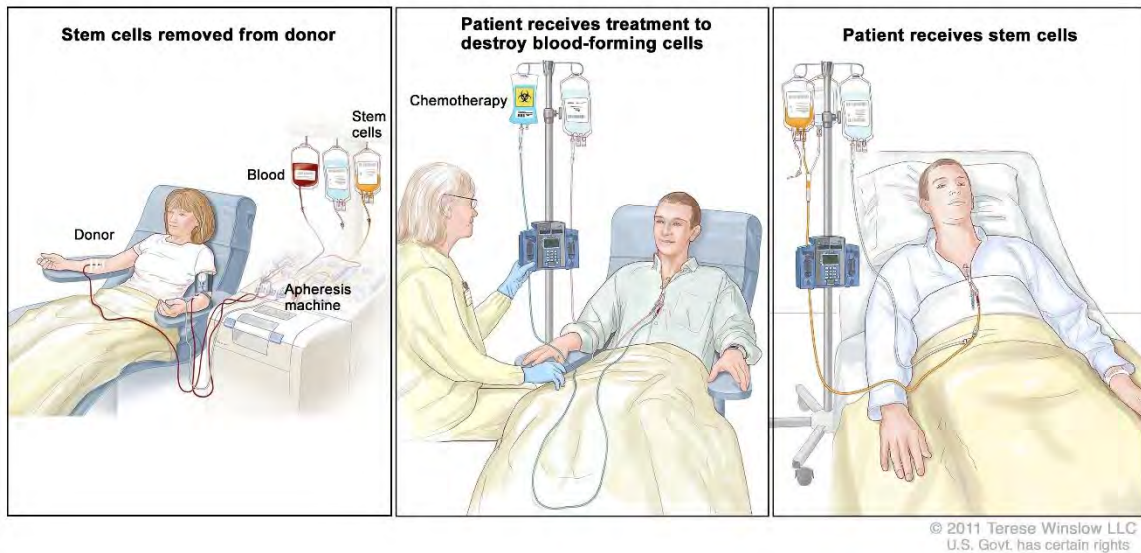


**Figure 1.5: Graphical representation of chemotherapy in AML patients (Dombret & Itzykson, 2017)**

In AML treatment, chemotherapeutic drugs such as cytarabine (ara-C) and anthracyclines such as daunorubicin or idarubicin are widely employed. By removing the majority of leukemia cells from the bone marrow, this intense first therapy tries to achieve full remission. Consolidation treatment, a following phase of chemotherapy, lowers leftover leukemic cells further to avoid return of illness.

Combination chemotherapy regimens tailored to the patient's age, overall health, and particular genetic or molecular features of the leukemia cells are frequently used in AML treatment. Chemotherapy medication selection and dose may differ depending on risk assessment, AML subtype, and individual patient characteristics (Yeung & Radich, 2017).

While chemotherapy might induce remission, it can also bring adverse effects such as bone marrow suppression (leading to anemia, neutropenia, and thrombocytopenia), nausea, vomiting, hair loss, and increased susceptibility to infections. To control these side effects and maintain blood cell counts throughout therapy, supportive care techniques like as growth factor support and transfusions are frequently used (Büchner *et al.*, 1985).

Following chemotherapy, stem cell transplantation (SCT) may be recommended for certain people, particularly those at high risk of recurrence or with specific genetic alterations. SCT entails replacing the patient's damaged bone marrow with healthy stem cells, either from a matched donor (allogeneic SCT) or from the patient (autologous SCT) (Yeung & Radich, 2017).

Novel chemotherapeutic medicines, combination therapies, and targeted agents are being investigated in order to enhance outcomes, decrease treatment-related toxicities, and adopt treatments based on individual AML cell characteristics (Büchner *et al.*, 1985).

The ultimate goal of chemotherapy in AML is to establish long-term remission and enhance overall survival while reducing treatment-related problems, emphasizing continuous efforts to optimize and tailor treatment options for this illness.

#### **1.9.1.1. Doxorubicin**

Doxorubicin, an anthracycline-class chemotherapy medicine, is widely used in the treatment of different malignancies, including leukemias such as AML and ALL (Chen, *et al.*, 2013).

Doxorubicin's action potential is based on its capacity to intercalate DNA, impede DNA and RNA synthesis, and induce DNA damage by creating free radicals via interaction with topoisomerase II. In rapidly developing cancer cells, including leukemia cells, these activities eventually result in cell cycle arrest and death (Kweon *et al.*, 2010).

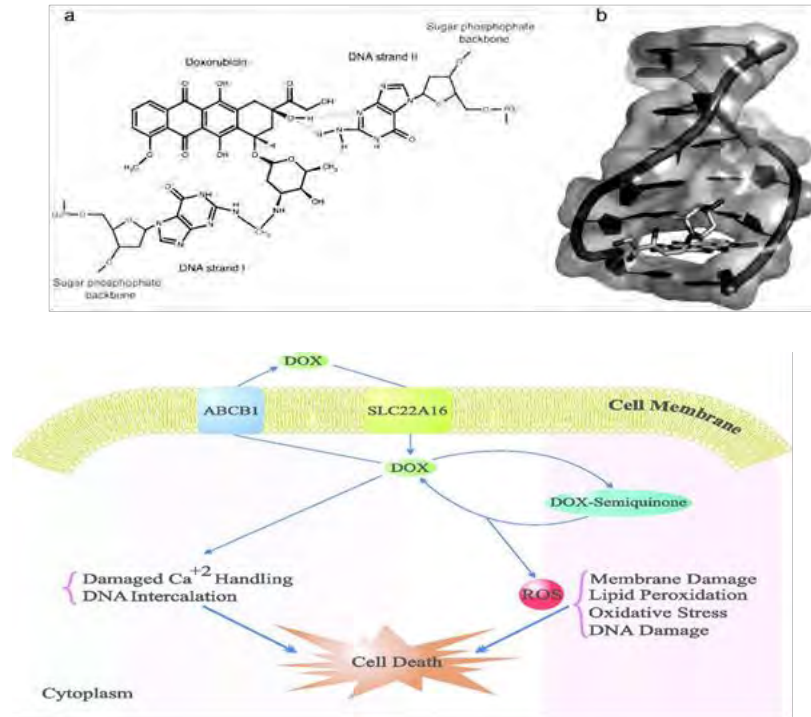


**Figure 1.6: Mechanism of action of doxorubicin (Xu et al. 2013)**

While doxorubicin is effective in treating cancer, it can also lead to several adverse effects. These include bone marrow suppression, resulting in conditions such as anemia. Additionally, patients may experience nausea, vomiting, and hair loss. There is also a risk of cardiotoxicity, particularly with higher cumulative doses of the drug. Doxorubicin use in leukemia therapy is frequently modified based on a variety of parameters, including the precise kind and stage of leukemia, the patient's overall health, and individual treatment response. Through innovative drug delivery technologies, combination therapy, and dose changes, researchers continue to look for ways to improve doxorubicin's effectiveness while minimizing its side effects (Wunderlich *et al.*, 2013).

To summarize, doxorubicin remains a cornerstone in leukemia treatment, playing an important role in inducing remission and improving survival outcomes for people with specific kinds of leukemia. Its usage, however, necessitates careful evaluation of its possible adverse effects as well as the overall treatment approach in combination with other medicines.

### 1.9.2. Nano technological advances in treatment of AML

Nanotechnology holds the promise of transforming drug delivery approaches, enhancing therapeutic efficacy, and mitigating off-target adverse effects commonly linked with conventional chemotherapy in managing AML. (Chen *et al.*, 2019).

Nanotechnology-based techniques entail the creation and application of nanoscale materials such as nanoparticles, liposomes, and micelles to deliver therapeutic medicines to leukemia cells while protecting healthy tissues. These nano-sized carriers can be designed to contain chemotherapeutic medicines, nucleic acids, or targeted agents, enabling precise administration and controlled release at the leukemic cells' point of origin (Fahrner, 2005)

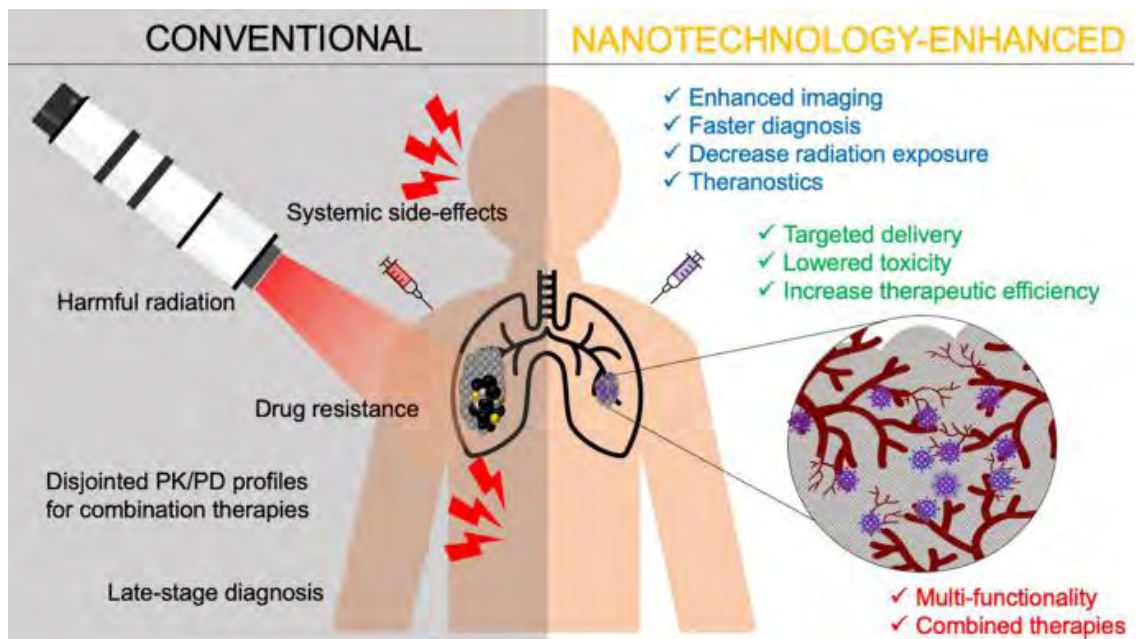


*Figure 1.7: Comparison between conventional chemotherapy and nanotherapy (Chen et al., 2019)*

Nanocarriers have various benefits in the context of AML treatment (Houshmand *et al.*, 2020):

1. Tailored medication administration: Nanoparticles can be functionalized with ligands or antibodies that identify and bind to receptors overexpressed on AML

cells, allowing for tailored medication administration while minimizing systemic toxicity.

2. Increased medication solubility and stability: Encapsulating chemotherapeutic drugs in nanoparticles improves their solubility, stability, and bioavailability, resulting in improved medication delivery to leukemia cells.

3. Less side effects: By delivering medications directly to leukemia cells, nanocarriers reduce exposure to healthy tissues, decreasing off-target effects and lowering systemic toxicity that is commonly associated with traditional chemotherapy.

4. Overcoming drug resistance: Nanotechnology-based techniques can aid in the elimination of drug resistance mechanisms seen in AML cells, potentially increasing the efficacy of treatment drugs.

Nanomedicine research for AML includes the creation of innovative nanoparticle formulations, such as liposomal cytarabine and daunorubicin, with the goal of increasing medication delivery and treatment results. Furthermore, nanocarriers loaded with targeted medicines, gene treatments, or immunotherapeutic agents are being investigated to improve treatment effectiveness. (Sauvage *et al.*, 2016)

While nanotechnology-based therapeutics show promise, there are still obstacles to overcome, such as improving nanoparticle design, guaranteeing biocompatibility and safety, and converting these novel techniques from preclinical to clinical applications.

Nanotechnology breakthroughs have the potential to revolutionize AML therapy by delivering more effective, tailored, and less toxic therapeutic choices, eventually aiming to enhance patient outcomes and quality of life (Deshantri *et al.*, 2018).

#### **1.9.2.1. Use of drug delivery system with natural compounds**

The use of nanotechnology in Drug Delivery Systems (DDS) in conjunction with natural chemicals provides an exciting new frontier in the treatment of AML. By integrating natural substances into nanocarriers, researchers hope to improve their transport, potency, and selectivity against leukemia cells (Kingsley *et al.*, 2006).

Some natural chemicals produced from plants, fungus, marine creatures, or other natural sources have intrinsic medicinal qualities, such as anti-leukemic capabilities. However, their therapeutic applicability is frequently hampered by issues such as poor solubility, fast degradation, and low bioavailability (Jiang *et al.*, 2007).

By encapsulating these natural substances into nano-sized carriers such as liposomes, polymeric nanoparticles, or micelles, nanotechnology provides a solution. This encapsulation improves natural component stability, solubility, and targeted administration to leukemia cells, overcoming their intrinsic limitations (Fang, 2006).

Several natural substances, including curcumin, resveratrol, quercetin, and different plant-derived extracts, have been shown in preclinical tests to have anti-leukemic effects. When these drugs are combined with nano DDS, they display better pharmacokinetics and increased accumulation within leukemia cells, possibly increasing their therapeutic effectiveness against AML.

The following are the benefits of employing nano DDS in conjunction with natural chemicals to treat AML (Hu *et al.*, 2021):

1. Targeted delivery: Nanocarriers can be customized to transport natural substances selectively to leukemia cells, limiting exposure to healthy tissues and lowering systemic adverse effects.
2. Increased stability: Encapsulating natural substances into nanoparticles shields them from degradation, increasing their stability and bioavailability.
3. Synergistic benefits: By co-delivering several natural substances or combining them with traditional anti-leukemic medications, nano-formulations might promote combination therapy, potentially leading to synergistic benefits and overcoming drug resistance.
4. Lower toxicity: Precise delivery to leukemia cells can reduce the needed dosage of natural substances, lowering toxicity and boosting therapeutic index.

While preclinical investigations have yielded encouraging findings, further research is required to improve nano DDS formulations, assess their safety profiles, and confirm their

usefulness in clinical settings. Scalability, regulatory concerns, and long-term stability are all issues that must be addressed for effective translation to clinical applications (Mintz & Leblanc, 2021).

Overall, the combination of nanotechnology and natural chemicals in DDS has enormous promise for revolutionizing AML therapy by providing a unique and focused therapeutic strategy with the goal of improving patient outcomes.

### **1.9.2.2. Use of synthetic nanoparticles against AML**

Many clinically approved nanoparticle formulations are used to treat various cancers at different stages. Interestingly, all but one of these systems (Abraxane) are liposomal systems encapsulating an anticancer drug. The first approved cancer nanomedicine was Doxil, a polyethylene glycol (PEG) functionalized liposomal doxorubicin, approved by the FDA in 1995. Soon after, other liposomal formulations, such as liposomal daunorubicin (DaunoXome), liposomal vincristine (Marqibo), and most recently, liposomal irinotecan (Onivyde), received FDA approval (Beals, 2018).

These man-made nanoparticles, often composed of polymers, metals (such as gold or silver), silica, or carbon-based nanomaterials, can be precisely tailored and functionalized to deliver therapeutic payloads to leukemia cells while sparing healthy tissues ( Smith, *et al.*, 2015). They can be tailored in several ways:

1. **Size and Shape:** The size and shape of nanoparticles can be controlled to optimize cellular uptake, circulation time, and bio-distribution. Smaller nanoparticles typically have better penetration into tissues, while the shape can influence cellular uptake mechanisms.
2. **Surface Chemistry:** The surface of nanoparticles can be modified to enhance stability, biocompatibility, and target specificity. This can involve adding various chemical groups or coatings to the nanoparticle surface.



3. Drug Loading: Nanoparticles can be engineered to encapsulate or conjugate therapeutic agents, ensuring controlled release and protecting the drug from premature degradation.

Approaches to functionalize nanoparticles include:

1. Ligand Attachment: Attaching ligands (such as antibodies, peptides, or small molecules) to the surface of nanoparticles can target specific receptors on leukemia cells, enhancing selectivity and uptake by the target cells.

2. Polyethylene Glycol (PEG): Adding PEG to the surface of nanoparticles can improve their circulation time by reducing opsonization and clearance by the immune system, as well as increasing solubility and stability.

3. Surface Coatings: Applying biocompatible coatings such as proteins, lipids, or synthetic polymers can improve the biocompatibility and reduce the immunogenicity of nanoparticles.

4. Magnetic Functionalization: Incorporating magnetic materials allows for the external control of nanoparticle movement and drug release using magnetic fields, which can target nanoparticles to specific sites within the body (Deshayes & Gref, 2014).

By employing these tailoring and functionalization strategies, nanoparticles can be designed to effectively deliver drugs to leukemia cells while minimizing impact on healthy tissues (Gao & Zhang, 2015).

### **1.9.3. Naturopathy**

Naturopathy, a holistic approach to healthcare that stresses natural cures and self-healing processes, provides supportive techniques that may supplement traditional AML therapies. While naturopathy is not a replacement for regular medical care, it can be used as a complementary therapy to improve general well-being and quality of life for those undergoing AML treatment (Calgarotto *et al.*, 2021).

Some naturopathic techniques that may be beneficial in the treatment of AML include:

1. Nutritional and dietary support: Naturopathic practitioners frequently highlight the need of a well-balanced diet rich in minerals, antioxidants, and phytochemicals. Dietary changes may be made to improve immunological function, decrease inflammation, and improve general health during and after AML therapy.
2. Herbal medicine: Naturopaths may offer some herbal supplements or plant extracts for alleged immune-boosting or anti-inflammatory effects. However, these supplements should be used carefully since they may interact with conventional medications or influence blood coagulation, necessitating constant monitoring and contact with healthcare specialists.
3. Lifestyle adjustments: Naturopathy frequently encourages lifestyle adjustments such as stress reduction strategies (e.g., meditation, yoga), regular physical activity, and appropriate sleep, all of which can help with general health and well-being throughout AML therapy.
4. Mind-body therapies: Acupuncture, massage therapy, and mindfulness-based practices may help with treatment-related side effects such as pain, exhaustion, and mental distress.
5. Nutritional supplements: Naturopathic practitioners may advise patients to take certain vitamins, minerals, or supplements to address nutritional deficiencies that may arise during AML therapy. However, it is critical to discuss these supplements with your healthcare professional to avoid any drug interactions or unwanted effects.

Individuals receiving AML therapy must speak freely with their healthcare team, including naturopathic practitioners, in order to provide integrated care and avoid any conflicts between naturopathic therapies and conventional treatments. Furthermore, naturopathic treatments should be utilized with, rather than in place of, traditional medical therapy, and their efficacy and safety in the context of AML should be extensively verified via clinical research (Roy *et al.*, 2017).

The incorporation of naturopathy into a comprehensive care plan can provide supportive measures to improve the general well-being and quality of life of those dealing with AML treatment problems.

### 1.9.3.1.Caffeine

Caffeine, a frequently ingested psychoactive ingredient present in a variety of drinks, has sparked interest because of its possible influence on cancer cells, including leukemia. Its methods of action include adenosine receptor antagonism and inhibition of specific enzymes such as phosphodiesterase, altering cellular signaling pathways that govern proliferation, apoptosis, and DNA repair processes in cancer cells (Amirizadeh *et al.*, 2023).

While some in vitro studies have suggested that caffeine may affect cancer cells by causing cell cycle arrest, promoting programmed cell death (apoptosis), or altering DNA repair mechanisms, the specific implications of caffeine in AML treatment are unclear and warrant further investigation (Gibbs *et al.*, 2015).

Research on caffeine's effect on AML cells or its possible involvement in AML treatment is sparse and frequently inconclusive. Because of the complexity of cancer cells and the heterogeneity in their responses to caffeine, thorough investigations, including preclinical models and clinical trials, are required to determine caffeine's effectiveness, safety, and possible therapeutic advantages for AML.

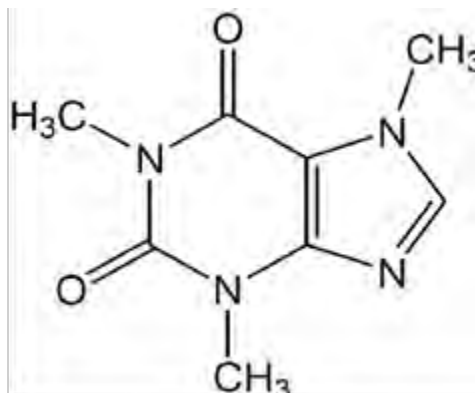


*Figure 1.8: Structure of Caffeine (Kolachana, et al., 1993)*

Furthermore, translating caffeine's effects reported in laboratory investigations to clinical applications necessitates a number of factors. Caffeine's practicality as an adjuvant therapy for AML requires careful consideration of factors such as caffeine concentration, length of exposure, possible interactions with other drugs or therapies used in AML therapy, and individual patient variability (Karalexi *et al.*, 2019).

Patients receiving AML therapy should seek medical advice before making any dietary modifications, including caffeine usage. Understanding the interaction between caffeine and AML cells necessitates extensive scientific research to evaluate its potential as a therapeutic adjuvant or find any contraindications in leukemia therapy.

In conclusion, while fascinating discoveries in laboratory settings suggest that caffeine has an effect on cancer cells, notably via modifying cellular pathways involved in cancer growth, its specific involvement in AML therapy remains unknown. Extensive scientific research and clinical trials are required to determine caffeine's therapeutic significance, safety, and optimal use in the context of AML care (Ugai *et al.*, 2018).

### 1.9.3.2. Mode of Action of Caffeine

For decades, studies have been done to dissect the mechanisms of action of caffeine. Out of several known mechanisms, the most projecting one is show in figure 1.9.

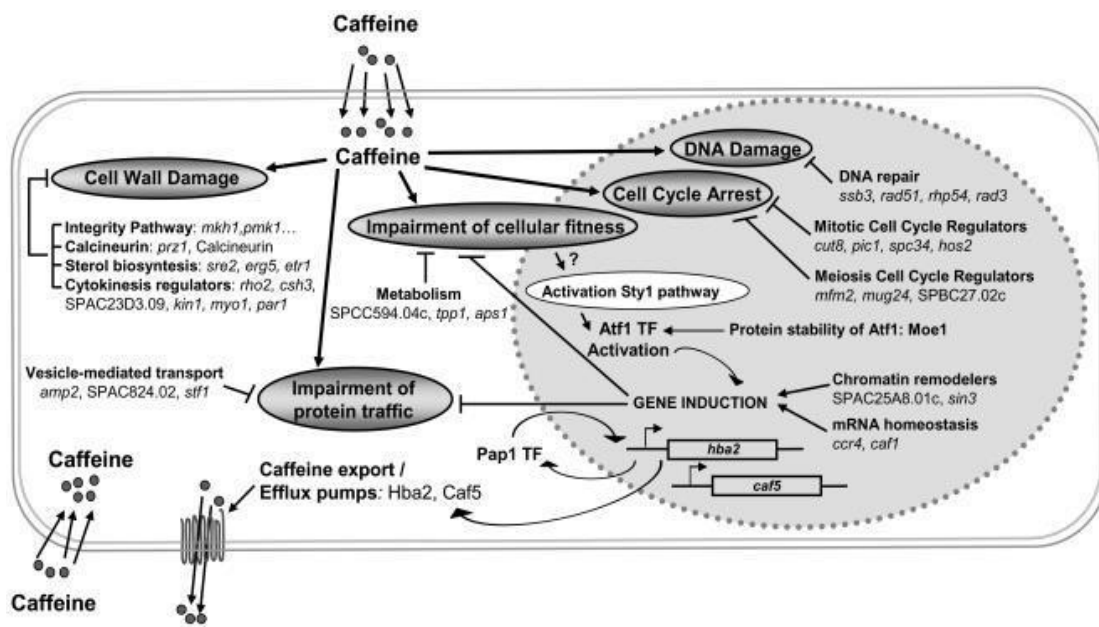


Figure 1.9: Mechanism of Caffeine Action (Deshayes & Gref)

Caffeine is said to reversibly disrupt the connection of adenosine with its receptor, preventing the onset of sleepiness and other effects generated by adenosine in the human body. Caffeine stimulates several other parts of our autonomic nervous system as well. Caffeine stimulates efflux pumps, the baseline levels of which are controlled by the transcription factor Pap1, to execute detoxifying functions (Hidalgo *et al.*, 2009).

Caffeine does not activate the Pap1 transcription factor; instead, it shuttles between the cytoplasm and the nucleus, regulating the expression of around fifty genes. Caffeine has a number of harmful consequences, as well as interference in cellular processes such as protein trafficking and general fitness impairment, cell wall destruction, cell cycle arrest, and DNA damage.

#### **1.9.4. Synthetic organometallic compounds**

The prospective uses of synthetic organometallic compounds against Acute Myeloid Leukemia (AML) have piqued the interest of cancer researchers. These complexes, which comprise metal atoms linked to carbon atoms in organic molecules, have a wide range of chemical configurations and may be tailored to target certain biological pathways or cellular processes related to cancer (Ong & Gasser, 2020).

Some synthesized organometallic compounds have shown promising anticancer effects in preclinical trials against AML. These complexes can be programmed to engage selectively with biomolecular targets within leukemia cells, possibly interfering with vital biological activities or signaling pathways important for cancer cell survival and proliferation (Sabnis, 2021).

Several ways for developing organometallic compounds for AML therapy have been investigated:

1. Targeted drug delivery: Organometallic compounds can be integrated into nanoparticles or carrier systems, allowing for precise drug delivery to AML cells. This method tries to increase medication accumulation within leukemia cells while decreasing off-target effects on healthy cells.

2. DNA binding and damage: Certain organometallic complexes can bind with DNA, producing DNA damage or interfering with replication and transcription processes, causing apoptosis or cell cycle arrest in leukemia cells.

3. Redox modulation: Certain complexes exhibit redox activity, disrupting cellular redox balance. Increased ROS levels cause oxidative stress, leading to damage of biological molecules within leukemia cells, ultimately triggering their demise.

4. Cellular process inhibition: Organometallic compounds can interfere with certain enzymatic pathways or molecular targets required for AML cell survival and proliferation, affecting key cellular processes.

While these synthetic complexes show promise in preclinical AML models, clinical translation will necessitate a thorough examination of their pharmacokinetics, safety profiles, and effectiveness in human trials. Understanding the underlying mechanisms of action, identifying possible resistance mechanisms, and improving delivery systems are also crucial for their successful use in AML treatment (Hemmati *et al.*, 2020).

Synthetic organometallic complexes research against AML is still ongoing, with the goal of developing novel and tailored therapeutic methods that may complement or augment current leukemia therapies.

#### **1.9.4.1. Copper diethyldithiocarbamate**

Copper diethyldithiocarbamate (CuET) has arisen as a molecule of interest in cancer research, particularly for its potential usefulness against leukemia such as AML. CuET is a synthetic compound comprising of copper ions coupled with diethyldithiocarbamate ligands that shows a variety of biological actions making it a candidate for anticancer treatment ( Peng *et al.*, 2020).

Preclinical research investigating CuET's impact on leukemia, especially AML, has yielded encouraging results (Meng *et al.*, 2024):

1. Anti-proliferative effects: CuET has shown in laboratory conditions decrease in growth of leukemia cells, particularly AML cells. This suppression might be

attributable to the effect it has on critical cellular processes involved in cell growth and division.

2. Induction of apoptosis: CuET has been found to promote programmed cell death (apoptosis) in leukemia cells. It has the potential to activate apoptotic pathways inside AML cells, resulting in their selective elimination.

3. Cellular process disruption: CuET's mode of action includes interfering with particular cellular processes required for leukemia cell survival and multiplication. It has the potential to disrupt critical pathways or biomolecular targets required for AML cell survival.

4. Antioxidant qualities: A research study suggests that CuET has antioxidant qualities, which may help to modulate oxidative stress levels in leukemia cells (Ref of research). This alteration of cellular redox balance may have an effect on the viability of AML cells.

While these findings in laboratory models are encouraging, clinical translation of CuET for AML therapy requires more research. The difficulties will be in determining its pharmacokinetics, toxicity profiles, and effectiveness in clinical studies. Furthermore, for its potential therapeutic application, improving its distribution, evaluating potential adverse effects, and finding resistance mechanisms are critical tasks.

CuET's potential as an anticancer agent against AML highlights continuing research efforts focused at researching novel chemicals and their processes in order to produce more effective and tailored leukemia therapeutics. However, rigorous clinical testing is required to establish its safety, effectiveness, and acceptability for inclusion in leukemia therapy regimens (Skrott & Cvek, 2012).

#### **1.9.4.2. Nickel diethyldithiocarbamate**

Nickel diethyldithiocarbamate (NiET) is a synthetic compound that has been researched for its possible usefulness in cancer, especially leukemia. NiET is composed of nickel ions that are coupled with diethyldithiocarbamate ligands and shows a variety of biological actions that have provoked the curiosity of cancer researchers (Madhusudanan *et al.*, 1975).

In laboratory settings, studies on NiET's impact on leukemia, especially AML, have revealed the following results:

1. Anti-proliferative effects: In experimental settings, NiET inhibited the growth of leukemia cells, including AML cells. This suppression might be related to its effect on cellular pathways required for cell growth and division.
2. Induction of apoptosis: NiET has the ability to induce programmed cell death (apoptosis) in leukemia cells. This characteristic may activate pathways that lead to the selective destruction of AML cells.
3. Cellular process disruption: NiET's method of action may entail interfering with critical cellular processes required for leukemia cell survival and proliferation. It might target particular pathways or biomolecular targets involved in the survival of AML cells.
4. Oxidative stress modulation: According to several research studies, NiET has antioxidant characteristics that may modify oxidative stress levels in leukemia cells. This adjustment may have an effect on the viability of AML cells (Cvek *et al.*, 2008).

Despite these promising outcomes in laboratory models, the translation of NiET for AML treatment requires additional research. Understanding its pharmacokinetics, safety profiles, potential adverse effects, and effectiveness in clinical trials are critical stages toward its potential medicinal use (Zidan, 2001).

NiET, like any new chemical, would require extensive clinical testing to confirm its safety, efficacy, and applicability as a potential candidate for AML therapy. Ongoing research is being conducted to determine the full therapeutic potential and usefulness of NiET and comparable chemicals in the treatment of leukemia (Cvek *et al.*, 2008).

### **1.10. TRAIL signaling pathway**

TNF-related apoptosis-inducing ligand (TRAIL) initiates apoptosis, a programmed cell death process, which selectively targets and eliminates mutated cells. This unique attribute makes TRAIL a highly promising candidate for cancer therapy. Its capacity to induce



apoptosis specifically in tumour cells, while sparing normal cells, highlights its substantial clinical significance. TRAIL's selective action against cancer cells offers a potential avenue for effective and targeted cancer treatment with reduced toxicity to healthy tissues. (Almasan & Ashkenazi, 2003).

### **1.10.1 TRAIL receptors**

In humans, there are five receptors for TNF-related apoptosis-inducing ligand (TRAIL). Among these, DR4 (also known as TRAIL-R1) and DR5 (TRAIL-R2) are categorized as death receptors. These receptors are membrane-bound and play pivotal roles in transmitting signals that lead to cellular apoptosis upon binding with TRAIL. On the other hand, DcR1 (TRAIL-R3) and DcR2 (TRAIL-R4) are classified as decoy receptors. Despite their similarity in structure to DR4 and DR5, these receptors lack functional death domains, rendering them incapable of inducing apoptosis. Instead, they act as decoys, competitively binding to TRAIL without triggering apoptosis, thereby modulating the cellular response to TRAIL signalling (Griffith *et al.*, 1999).

Additionally, Osteoprotegerin (OPG) is another soluble receptor that binds to TRAIL. However, unlike the membrane-bound receptors, OPG is not anchored to the cell membrane. Furthermore, OPG does not transmit signals for cellular apoptosis like DR4 and DR5. Instead, it acts as a soluble decoy receptor, sequestering TRAIL and inhibiting its apoptotic effects. This diversity in TRAIL receptors provides a sophisticated regulatory mechanism for controlling cellular responses to TRAIL signalling, thereby influencing cell fate decisions such as apoptosis. Understanding the roles and interactions of these receptors is crucial for elucidating the intricate mechanisms underlying TRAIL-mediated apoptosis and for developing targeted therapeutic strategies for cancer treatment. (Griffith *et al.*, 1999).

DcR1 does not have death domain while DcR2 has a truncated death domain, so both are unable to transmit signals for apoptosis. At body temperature, osteoprotegerin has low affinity for TRAIL. Therefore, it is also unable to transmit any apoptotic signal (Wang & El-Deiry, 2003)

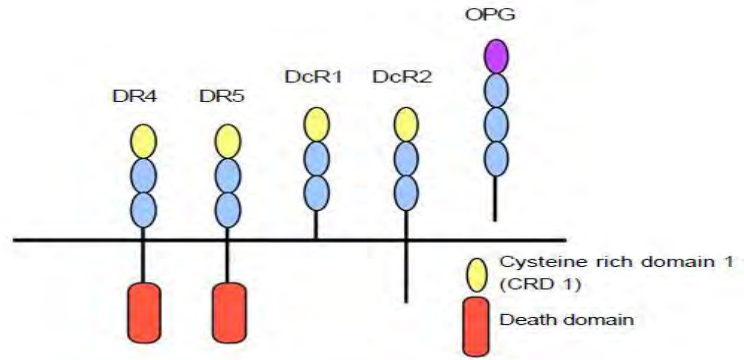


**Figure 1.10: Five TRAIL receptors showing different domains(Kimberley & Screaton, 2004).**

### 1.10.2. TRAIL signaling

Cells initiate the process of apoptosis through extracellular signals, so called “death factors”, or through internal factors such as oxidative stress or DNA damage. The pathway initiated by extracellular factors is known as extrinsic pathway and the pathway activated by internal factors is known as intrinsic pathway (Kim *et al.*, 2005)

#### 1.10.2.1 The extrinsic pathway

Within the extrinsic pathway, TRAIL interacts with transmembrane death receptors like DR4 or DR5, initiating receptor oligomerization. This process induces a conformational shift in the receptors, facilitating signal transduction into the cell. The structural changes in these receptors enable the exposure of specific regions known as death domains. These exposed domains serve as docking sites for intracellular adaptor proteins, including FADD (Fas-associated death domain protein) and TRADD (TNF receptor-associated death domain protein). Once bound to the death domains of the receptors, these adaptor proteins initiate downstream signalling cascades that ultimately lead to apoptotic cell death. This intricate process highlights the crucial role of receptor conformational changes in facilitating the transmission of apoptotic signals within the cell (Ganten *et al.*, 2004)

These adaptor proteins function as carriers to transfer the signal from death receptors to caspases. These adaptor proteins recruit molecules of procaspase 8 and 10. These procaspases are inactive and become activated by self-cleavage. The combination of the death ligand, death receptor, adaptor, and initiator caspase forms a complex referred to as the death-inducing signalling complex (DISC). DISC assembly triggers the activation of

caspase 8, which in turn activates effector caspases 3, 6, and 7, ultimately leading to apoptosis. Caspase 8 and caspase 10 are categorized as initiator caspases, initiating a cascade of caspase activation where one activated caspase triggers the activation of others known as executioner or effector caspases (caspases 3, 6, and 7). This cascade ultimately cleaves specific protein targets within the cell, culminating in apoptosis. The apoptotic process can be hindered by FLIP<sub>L</sub>, an inhibitor of apoptosis. FLICE-like inhibitory protein (FLIP<sub>L</sub>) inhibits the activation of caspase 8 by impeding DISC assembly (He, *et al.*, 2004).

### 1.10.2.2 The intrinsic pathway

Internal signals originating from within the cell, such as DNA damage, aberrant cell cycle regulation, and oxidative stress, can activate the intrinsic pathway of apoptosis. This occurs through the involvement of the Bcl-2 family of proteins, which operate at the outer mitochondrial membrane. Consisting of approximately 25 members, each Bcl-2 protein contains at least one Bcl-2 homology (BH) domain crucial for mediating protein-protein interactions. Within this family, one subset of Bcl-2 proteins promotes apoptosis, while another subset inhibits it. These distinct groups, characterized by opposing functions, regulate apoptosis within the cell (Elumalai *et al.*, 2012).

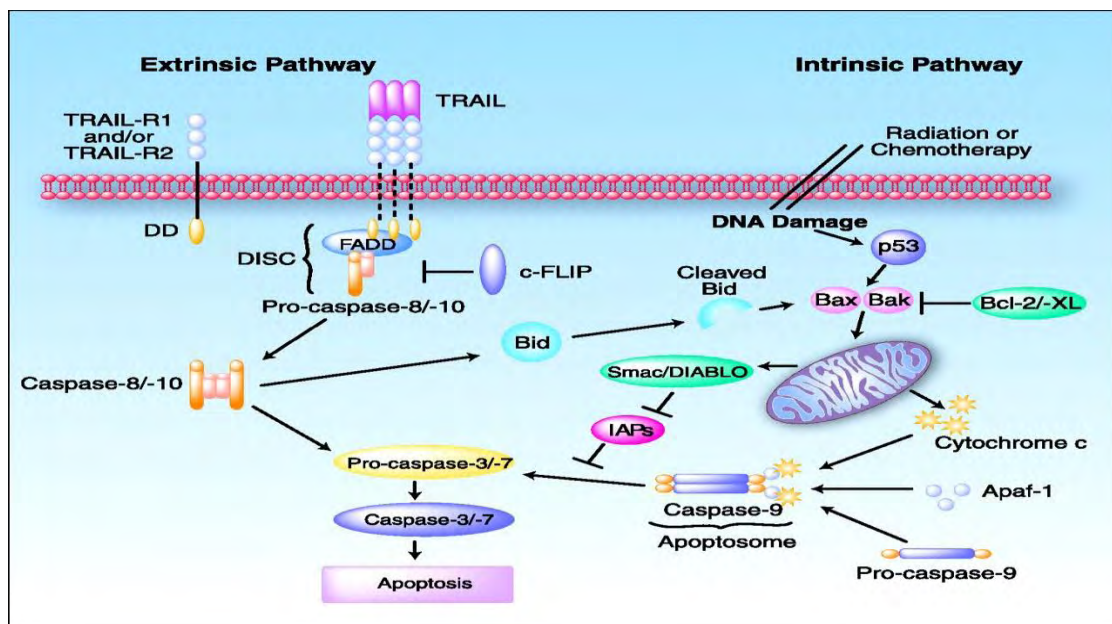


**Figure 1.11: Extrinsic and intrinsic apoptosis signalling pathways**

(Johnstone *et al.*, 2008)

Upon receiving an apoptotic signal, Bid and Bim become activated and subsequently bind to Bax, activating it in the process. This interaction induces a conformational alteration in Bax, prompting its translocation from the cytoplasm to the outer mitochondrial membrane. This change in the mitochondrial membrane structure leads to the formation of channels, thereby augmenting the permeability of the outer mitochondrial membrane. Following the activation of the intrinsic apoptotic pathway, cytochrome-c and SMAC (Second Mitochondria-Derived Activator of Caspases) or DIABLO (Direct Inhibitor of Apoptosis-Binding protein with Low pI) are released from the mitochondria into the cytoplasm. Cytochrome-c then interacts with Apaf-1, an essential cofactor required for the activation of procaspase 9, forming a complex known as the apoptosome. This wheel-like heptameric structure serves as a platform for the recruitment and activation of procaspase 9. Once procaspase 9 is activated within the apoptosome, it initiates a cascade of proteolytic events that culminate in the execution phase of apoptosis, ultimately leading to programmed cell death. This sequence of events underscores the critical role of the apoptosome in coordinating the activation of downstream caspases and regulating the apoptotic process (Song *et al.*, 2003).

Bcl-2/Bcl-XL proteins hinder this translocation process, thereby exerting an anti-apoptotic function. Upon the release of Smac/DIABLO from the mitochondria, caspase 9 activation is initiated, subsequently leading to the cleavage of caspase-3. Diablo diminishes the inhibitory effect of IAPs (Inhibitor of Apoptotic Proteins), facilitating the progression towards apoptosis (Wang & El-Deiry, 2003). In the intrinsic pathway of apoptosis, the aggregation of procaspases triggers the activation of caspase 9, which acts as an initiator caspase. Once activated, caspase 9 initiates a cascade of events by cleaving and activating effector caspases such as caspases 3, 6, and 7. These effector caspases play pivotal roles in executing the process of apoptosis by cleaving various cellular substrates, ultimately leading to cell death. Therefore, caspase 9 serves as a central regulator in the intrinsic pathway of apoptosis, orchestrating the activation of downstream effectors and ensuring the orderly progression of the apoptotic process.

### 1.10.3. Regulation of TRAIL pathway

Tumour cells have evolved various strategies to evade the host's immune responses, allowing them to proliferate and survive. One such mechanism involves alterations in the expression or functionality of death receptors, which are crucial for triggering apoptosis in cancer cells. Tumour cells may acquire mutations that render these receptors ineffective or downregulate their expression, thereby escaping death signals delivered by the immune system. These mechanisms collectively contribute to TRAIL resistance, limiting the effectiveness of the host's immune surveillance mechanisms, particularly those mediated by cytotoxic T cells. By evading apoptosis and immune recognition, tumour cells can evade destruction by the immune system and continue to proliferate unchecked. Understanding these escape mechanisms is crucial for developing strategies to overcome TRAIL resistance and enhance the effectiveness of immunotherapy in cancer treatment. ( Kim & Lee, 2007).

The regulation of TRAIL involves various proteins within the pathway. Inhibitors of Apoptotic Proteins (IAPs) and Smac/DIABLO are particularly pivotal in modulating the apoptosis process (Verhagen *et al.*, 2000). IAPs function to suppress apoptosis by impeding the activation of effector caspase-3 or caspase-7. Additionally, they inhibit the intrinsic pathway by directly blocking caspase-9 activation ( Wang & El-Deiry, 2003).

Activation of the intrinsic pathway of apoptosis leads to the release of Smac/DIABLO, a critical regulator that counteracts the inhibitory effects of inhibitor of apoptosis proteins (IAPs) on caspase activation. By binding to IAPs, Smac/DIABLO disrupts their interaction with caspases, particularly caspase-3 and caspase-7, which are essential for the execution of apoptosis. This disruption effectively removes the blockade imposed by IAPs, allowing caspases to proceed with their apoptotic functions and ultimately promoting programmed cell death. Thus, the binding of Smac/DIABLO to IAPs represents a key regulatory step in apoptosis, ensuring the efficient elimination of unwanted or damaged cells (Deng, *et al.*, 2002).

Bcl-2 and Bcl-XL function as anti-apoptotic proteins by impeding the activity of Bax and Bak, acting as terminators that disrupt the apoptotic cascade. Likewise, FLIP<sub>L</sub>, another anti-apoptotic factor, impedes the activation of initiator caspases by binding to the Death-

Inducing Signalling Complex (DISC). Despite its structural resemblance to caspase-8 and caspase-10, FLIP<sub>L</sub> lacks protease functionality. Therefore, its association with the DISC precludes the activation of initiator caspases, thereby obstructing the initiation of apoptosis. (El-Gazzar *et al.*, 2010)

TRAIL exhibits a strong affinity for binding with receptors DcR1 and DcR2. However, these receptors lack the ability to transmit an apoptotic signal due to the absence of a death domain in DcR1 and a truncated death domain in DcR2. Consequently, overexpression of these receptors serves as a protective mechanism against TRAIL-induced apoptosis. Moreover, studies have revealed that cancer cells often display elevated expression levels of these decoy receptors compared to normal cells, providing another mechanism for tumour cells to evade apoptosis (Hersey & Zhang, 2001).

### **1.11. NF- $\kappa$ B**

NF- $\kappa$ B is a transcription factor and acts as an initiator of inflammatory responses. It is activated by several types of cells, such as cancer cells, macrophages and number of target cells of inflammation. In addition to inflammation, NF- $\kappa$ B has many effects that lead to tumorigenesis i.e., apoptosis inhibition, metastasis and angiogenesis. Many human cancers activate NF- $\kappa$ B gene, including breast and prostate cancers, myeloma and acute lymphocytic leukaemia through different pathways (Baeuerle & Henkel, 1994)

#### **1.11.1 Classification of NF- $\kappa$ B proteins**

NF- $\kappa$ B belongs to a family of transcription factors that exist in homo- or heterodimeric form. NF- $\kappa$ B proteins are divided into two types:

- p65 (Rel-A), Rel-B and Rel-C have a transactivation domain for interaction with transcriptional machinery. These proteins are produced in mature forms.
- p105/p50 or NF- $\kappa$ B1 and p100/p52 or NF- $\kappa$ B2 are produced in their inactive form. DNA binding domain is present in these proteins, but lack a transactivation domain. They contain ankyrin repeats on C-terminal. They are activated by proteosomal degradation of Ankyrin repeats and converted into mature proteins. Among these five, p65 and p50 proteins are present most abundantly in the cell (Serasanambati & Chilakapati, 2016)

### **1.11.2 NF- $\kappa$ B inhibitors**

Normally NF- $\kappa$ B dimers remain transcriptionally inactive. In inactive form, they are sequestered to cytoplasm because of interaction with I $\kappa$ Bs (Inhibitors of NF- $\kappa$ B). The I $\kappa$ Bs belong to protein family that contain ankyrin repeats at C-terminal. These repeats bind with NF- $\kappa$ B. I $\kappa$ Bs undergo proteasomal degradation, upon phosphorylation of conserved serine domains by I $\kappa$ B kinases (IKKs). When I $\kappa$ Bs are degraded, NF- $\kappa$ B is free to move from cytoplasm to the nucleus. In nucleus, NF- $\kappa$ B transcribes target genes. NF- $\kappa$ B transcribes more than 200 genes to produce diverse effects. Many important genes regulated by NF- $\kappa$ B include BCL-2, cyclin D1, MMP-9, IL-6, IL-8 and VEGF (Zinatizadeh *et al.*, 2021).

### **1.11.3 Classical pathway of NF- $\kappa$ B**

Classical pathway is also known as canonical pathway. Dimers of NF- $\kappa$ B complex comprises of either Rel-A or Rel-C, along with p50. Dimers exist in inactive form due to their interaction with I $\kappa$ B proteins in the cytoplasm. Classical pathway is normally initiated by TNF family. Dimers are activated, when IKK complex consisting of IKK $\beta$ , IKK $\alpha$  and NEMO phosphorylates serine residues of I $\kappa$ B. When I $\kappa$ B are phosphorylated, they are ubiquitinated and proteasomal degradation occurs. Subsequently, NF- $\kappa$ B is free and moves from cytoplasm to nucleus and functions as a transcription factor (Moynagh, 2005).

### **1.11.4 Alternative pathway of NF- $\kappa$ B**

In alternative pathway, also known as non-canonical pathway, NF- $\kappa$ B is activated by viral infections, pro-inflammatory cytokines, radiations and other stimuli. In this case, the dimers consist of Rel-B and p100). In this pathway, the complex IKK $\alpha$  along with NIK is mainly activated, which then phosphorylates p100 that results in its conversion into mature form (p52). After converting to activated form, NF- $\kappa$ B complex is translocated to nucleus for transcription of genes (Senftleben *et al.*, 2001; Greten & Karin, 2004).

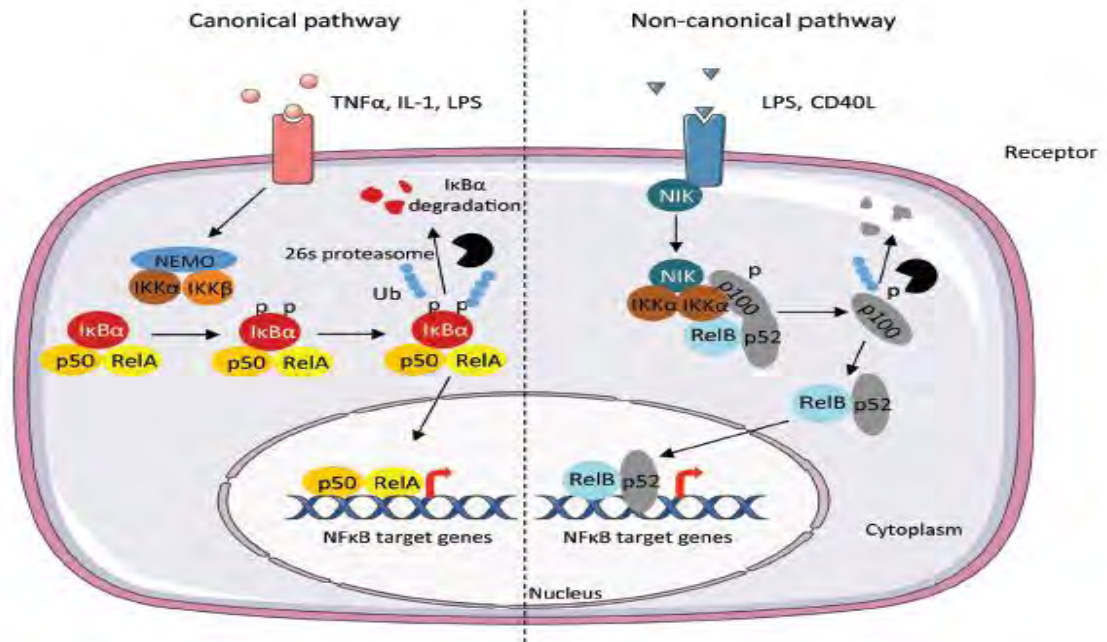


**Figure 1.12: Classical (canonical) and alternative (non-canonical) pathways leading to NF- $\kappa$ B activation (Hariharan *et al.*, 2021)**

### 1.11.5 NF- $\kappa$ B activation

The process of cellular activation involves the initiation of signalling cascades triggered by a variety of molecules, including cytokines, growth factors, and tyrosine kinases. These molecules bind to their respective receptors on the cell surface, initiating intracellular signalling pathways that ultimately lead to cellular responses. In particular, NF- $\kappa$ B, a transcription factor known for its role in regulating immune and inflammatory responses, can be activated by the increased expression of certain receptors. For example, the epidermal growth factor receptor (EGFR), insulin-like growth factor receptor (IGFR), and tumour necrosis factor receptor (TNFR) are known to stimulate NF- $\kappa$ B activation when their expression levels are elevated (Kreuz *et al.*, 2001)..

Overall, the activation of NF- $\kappa$ B by receptors such as EGFR, IGFR, and TNFR highlights the interconnectedness of signalling pathways in regulating cellular responses to various extracellular stimuli. In cancerous cells, molecular modifications affect the activation and regulation of NF- $\kappa$ B. In such case, NF- $\kappa$ B becomes permanently activated leading to unregulated expression of the genes under the control of NF- $\kappa$ B. Some of these genes are



involved in cell cycle control, apoptosis evasion and migration. So, variations due to any of the pathways result in changes in NF- $\kappa$ B regulation consequently contributing to cancer progression showing a clear association between NF- $\kappa$ B and cancer propagation (Senftleben & Karin, 2002). The NF- $\kappa$ B pathway is only marginally affected by TRAIL. The adaptors Rip and TRAF2 are necessary for TRAIL to activate NF- $\kappa$ B (Liang, *et al.*, 2004)

#### **1.11.6 TRAIL-NF- $\kappa$ B association**

NF- $\kappa$ B transcribes number of genes which are involved in inhibition of apoptosis in TRAIL pathway. NF- $\kappa$ B activates those genes that obstruct the apoptosis pathway e.g., Bcl-XL, cellular inhibitor of apoptosis (c-IAP), FLIP<sub>L</sub>, etc. FLIP<sub>L</sub> is an inhibitory protein that binds to the DISC and inhibits the activation of caspase-8. Thus, high FLIP<sub>L</sub> expression results in the inhibition of caspase-8 activation. FLIP<sub>L</sub> is upregulated in many tumours (Kreuz *et al.*, 2001).

NF- $\kappa$ B also activates the expression of the IAPs and some anti-apoptotic proteins of Bcl-2 family. The TRAIL induced apoptosis is suppressed by IAPs as they directly inhibit the effector caspases, whereas the Bcl-2 family proteins that are anti-apoptotic, antagonize the role of the pro-apoptotic protein Bcl-XL (Wang *et al.*, 1998).

#### **1.12. Wnt signaling pathway**

The Wnt signaling system is a critical biochemical mechanism that affects embryonic development, tissue homeostasis, and adult physiological activities. Dysregulation of the Wnt pathway has been linked to a variety of cancers, including colorectal cancer, breast cancer, and leukemia (Huelsenken & Behrens, 2002) .

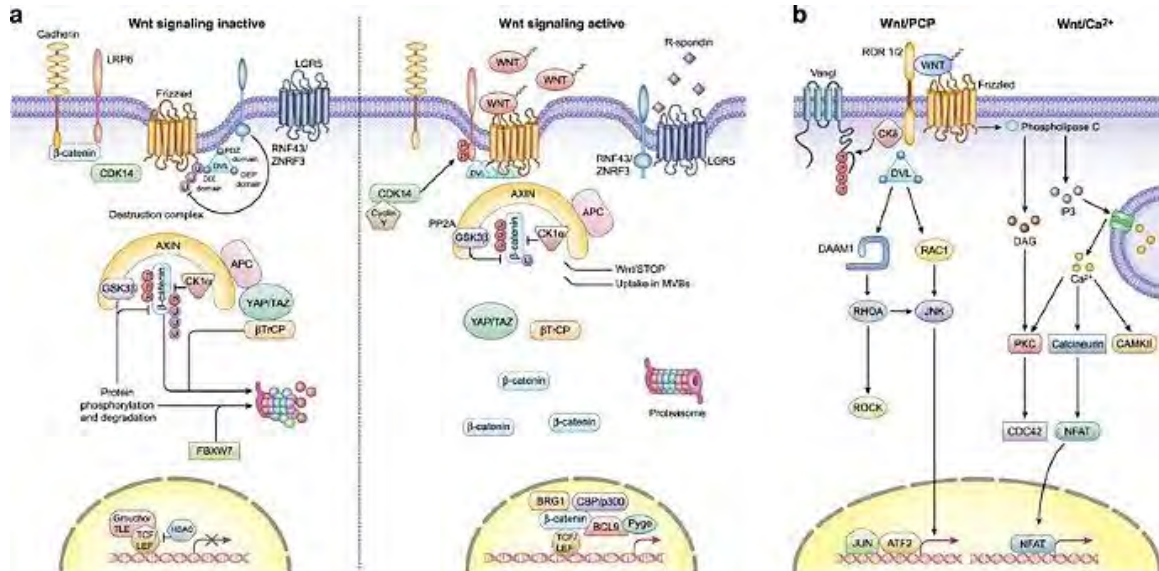


**Figure 1.13: Wnt signaling pathway including a) canonical and b) non-canonical signaling cascades (Deshayes & Gref)**

Wnt ligands interact with cell surface receptors (frizzled and LRP5/6 co-receptors), as well as downstream signaling molecules such as disheveled (DVL) proteins, axin, glycogen synthase kinase 3 beta (GSK-3), and  $\beta$ -catenin. The Wnt signaling pathway in cancer is summarized below (Seidensticker & Behrens, 2000):

1. Wnt signaling activation: In the absence of Wnt ligands, a protein complex composed of Axin, APC, GSK-3, and  $\beta$ -catenin promotes phosphorylation and subsequent ubiquitination of  $\beta$ -catenin. Wnt ligand binding to Frizzled receptors and LRP5/6 co-receptors, on the other hand, suppresses the destruction complex, resulting in the stability and accumulation of  $\beta$ -catenin in the cytoplasm.
2. Nuclear  $\beta$ -catenin translocation: Accumulated  $\beta$ -catenin translocate into the nucleus, where it interacts with TCF/LEF transcription factors, resulting in the activation of Wnt target genes involved in cell proliferation, survival, and differentiation.
3. Role in carcinogenesis: Aberrant Wnt pathway activation, commonly caused by mutations in critical system components like as APC,  $\beta$ -catenin, or Axin, can result

in excessive  $\beta$ -catenin accumulation and constitutive activation of Wnt target genes. This dysregulated signaling has been linked to uncontrolled cell proliferation, apoptosis inhibition, and tumor growth in a variety of malignancies.

4. Therapeutic consequences: Potential cancer therapeutics are based on targeting Wnt pathway components such as  $\beta$ -catenin, Wnt ligands, or downstream effectors. However, because of the Wnt pathway's intricacy and crucial involvement in normal cellular activities, therapeutic approaches targeting this system must be carefully planned to minimize deleterious effects on healthy tissues.

Understanding how the Wnt signaling pathway is regulated and dysregulated in cancer is critical for creating targeted therapeutics that disrupt oncogenic Wnt signaling while protecting normal cellular activities. Ongoing studies are being conducted to investigate the therapeutic potential of Wnt pathway modulators in various cancer types.

#### **1.12.1. Canonical signaling cascade**

The canonical Wnt signaling system regulates several biological functions, including embryonic development, tissue homeostasis, and cell fate determination. The canonical Wnt signaling pathway is as follows (Moon, 2005):

1. Binding of Wnt ligands: Wnt proteins, a class of secreted glycoproteins, bind to cell surface receptors to activate the pathway. Wnt ligands interact with Frizzled (FZD) receptors and co-receptors of low-density lipoprotein receptor-related proteins 5 and 6 (LRP5/6).
2. Activation of intracellular signaling cascades: When the Frizzled-LRP5/6 complex binds to a Wnt ligand, it experiences conformational changes that activate intracellular signaling cascades. This activation prevents the  $\beta$ -catenin destruction complex from phosphorylating  $\beta$ -catenin for degradation.
3.  $\beta$ -catenin stabilization and accumulation: In the absence of Wnt signaling, the destruction complex continually degrades cytoplasmic  $\beta$ -catenin, preventing its accumulation. Wnt activation, on the other hand, disturbs the destruction complex, resulting in the stability and cytoplasmic accumulation of  $\beta$ -catenin.

4. Nuclear  $\beta$ -catenin translocation: Stabilized  $\beta$ -catenin translocate into the nucleus and interacts with T-cell factor/lymphoid enhancer factor (TCF/LEF) transcription factors. This interaction results in the formation of a transcriptional complex that regulates the expression of Wnt target genes, including those involved in cell proliferation, survival, and differentiation.
5. Cellular responses: Wnt target gene activation mediated by the  $\beta$ -catenin/TCF/LEF complex regulates a wide range of cellular processes, including embryonic patterning, stem cell maintenance, tissue regeneration, and cell fate determination.
6. Dysregulation in disease: Dysregulation or mutations affecting critical components of the canonical Wnt pathway, such as APC (adenomatous polyposis coli),  $\beta$ -catenin, or Axin, can result in abnormal Wnt signaling activation. This dysregulation is linked to a number of illnesses, including cancer, where hyper activation of the system promotes uncontrolled cell proliferation and tumor growth.

Understanding the complicated processes of the canonical Wnt signaling pathway is critical for determining its functions in normal physiology and disease situations. Wnt signaling dysregulation is linked to a variety of malignancies, making it an appealing target for therapeutic approaches targeted at reducing aberrant pathway activity while retaining its fundamental physiological activities.

### **1.12.2. Non-canonical signaling cascade**

Non-canonical Wnt signaling pathways are branches of Wnt signaling that differ from the well-studied canonical route. While the canonical Wnt pathway is primarily involved in  $\beta$ -catenin-mediated transcriptional activation, non-canonical routes typically govern different physiological activities such as cell polarity, migration, and cytoskeletal reorganization. The following are two types of non-canonical Wnt signaling pathways (Duchartre, *et al.*, 2016):

1. Wnt/PCP (Planar Cell Polarity) signaling pathway: The Wnt/PCP pathway regulates cell polarity, cytoskeletal dynamics, and tissue morphogenesis through the activation of Frizzled receptors and specific intracellular signaling molecules

such as Disheveled (Dvl), Van Gogh (Vangl), and Prickle. Wnt/PCP pathway activation results in cytoskeletal rearrangements, changes in cell shape, and directional cell movements, particularly during processes such as gastrulation during embryonic development.

2. Wnt/Ca<sup>2+</sup> (Calcium) pathway: In response to Wnt ligand binding, the Wnt/Ca<sup>2+</sup> pathway activates intracellular signaling via Frizzled receptors, resulting in the activation of proteins such as Protein Kinase C (PKC) and Calcium/Calmodulin-dependent protein kinase II (CaMKII).

These non-canonical Wnt pathways differ from the canonical system in that they are not controlled by  $\beta$ -catenin-mediated transcriptional regulation. While the canonical route is well-known for its function in cell fate determination and proliferation, non-canonical Wnt signaling is involved in tissue morphogenesis, cell motility, and cytoskeletal architecture.

Non-canonical Wnt signaling dysregulation has been linked to a variety of developmental problems and illnesses, including cancer metastasis and neurodevelopmental defects. Understanding the complex interaction between canonical and non-canonical Wnt signaling pathways is critical for determining their roles in normal physiology and disease pathogenesis, possibly opening the door to targeted therapeutic approaches in a variety of pathological diseases (Deshayes & Gref, 2023).

### **1.13. HIF1-alpha signaling pathway**

The Hypoxia-Inducible Factor 1 alpha (HIF-1 $\alpha$ ) signaling pathway is a critical regulatory mechanism that orchestrates cellular responses to oxygen deficiency (hypoxia). It is crucial in adapting cells to low oxygen circumstances by modulating the expression of genes involved in a variety of physiological processes such as angiogenesis, metabolism, cell survival, and erythropoiesis (Poon *et al.*, 2009; Deshayes & Gref, 2023).

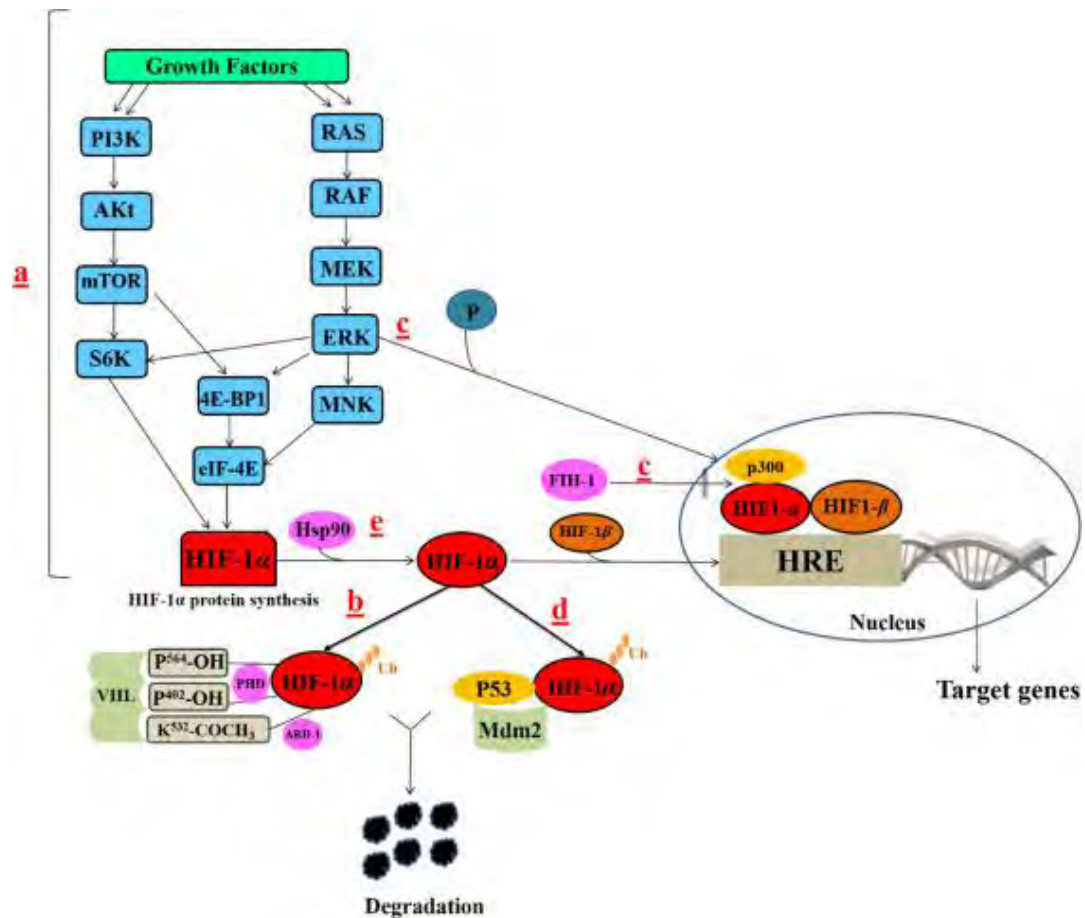


*Figure 1.14: HIF1 alpha pathway signaling cascade (Deshayes & Gref)*

Here is a summary of the HIF-1 signaling pathway:

1. HIF-1 control: Under normoxic (normal oxygen) circumstances, the proteasome in the cytoplasm constantly synthesizes and degrades HIF-1 $\alpha$  via oxygen-dependent prolyl hydroxylation. HIF-1 $\alpha$  is marked for identification by the von Hippel-Lindau tumor suppressor protein (VHL), which leads to ubiquitination and destruction.
2. Under hypoxic conditions (low oxygen levels), the rate of prolyl hydroxylation lowers due to decreased oxygen availability. As a result, HIF-1 $\alpha$  is not destroyed effectively and accumulates in the cytoplasm.
3. HIF-1 transport and activation: Accumulated HIF-1 translocates to the nucleus, where it forms a heterodimeric complex with HIF-1 $\beta$  (Aryl hydrocarbon receptor

nuclear translocator - ARNT). The HIF-1 $\alpha$ /HIF-1 $\beta$  complex binds to hypoxia response elements (Wunderlich et al.) in target gene promoters, triggering transcription of numerous genes involved in hypoxia adaptation.

4. Target gene expression: HIF-1 $\alpha$  controls the expression of several genes involved in cellular adaptation to hypoxia, including VEGF, erythropoietin (de Castro et al.), glucose transporters (GLUTs), glycolytic enzymes, and genes implicated in angiogenesis and death.

5. The activation of HIF-1 $\alpha$  target genes causes adaptive responses such as increased angiogenesis (the development of new blood vessels), better oxygen delivery, changed metabolism to favor glycolysis, and improved cell survival under low oxygen circumstances.

6. Disease role: Dysregulation of the HIF-1 $\alpha$  pathway has been linked to a variety of illnesses, including cancer, ischemia diseases, and metabolic disorders. Abnormal HIF-1 $\alpha$  activation increases tumor development, angiogenesis, metastasis, and resistance to treatment in cancer.

Understanding the HIF-1 $\alpha$  signaling pathway and its function in cellular adaptation to hypoxia sheds light on its participation in physiological responses and illnesses, pointing to possible therapeutic targets for ailments impacted by oxygen levels and tissue oxygenation.

### **1.13.1. Dysregulation in Hif1-alpha pathway causing AML**

Dysregulation of the HIF-1 $\alpha$  pathway can contribute to the etiology and progression of AML. The dysregulation usually includes abnormal HIF-1 $\alpha$  stabilization or activation, which results in altered cellular responses to hypoxia and influences different facets of leukemogenesis. Here's how dysregulation expresses itself in AML (Maxwell *et al.*, 2001):

1. Increased HIF-1 stabilization: AML cells are frequently found in a hypoxic bone marrow microenvironment. Even under normoxic settings, leukemic cells adapt to hypoxia by stabilizing HIF-1 $\alpha$ , resulting in its accumulation. This dysregulated stabilization might be caused by mutations, changes in oxygen-sensing systems, or abnormalities in signaling pathways.

2. Changes in gene expression: Abnormal HIF-1 $\alpha$  activation affects the transcriptional profile of AML cells. This abnormal activation causes the overexpression of genes involved in cell survival, angiogenesis (such as VEGF), glycolytic enzymes, and other factors that promote tumor development and cell death resistance.
3. Effect on cell survival and metabolism: HIF-1 $\alpha$  dysregulation in AML cells contributes to cellular metabolic rewiring, favoring glycolysis even in oxygen-rich environments (the warburg effect). This metabolic change meets the energy needs of rapidly proliferating leukemic cells while also providing a survival advantage.
4. Angiogenesis and impacts on tumor microenvironment: HIF-1 $\alpha$  dysregulation promotes angiogenesis by upregulating pro-angiogenic factors, allowing the development of new blood vessels that keep leukemic cells alive in the bone marrow niche. It also has an impact on the tumor microenvironment by regulating immune responses and interactions with stromal cells.
5. Clinical implications: The dysregulated HIF-1 $\alpha$  pathway in AML might be a therapeutic target. In order to disrupt the pro-survival and pro-growth signals supplied by the hypoxic bone marrow niche, efforts are being made to reduce or alter HIF-1 $\alpha$  activity in leukemic cells.

Understanding the dysregulation of the HIF-1 pathway in AML provides insights into the mechanisms underlying leukemogenesis and offers potential avenues for targeted therapies aimed at disrupting leukemic cells' adaptive responses to hypoxia, potentially slowing disease progression and improving treatment outcomes.



### 1.14. Aims and Objectives

The aim of this study was to advance therapeutic options for Acute Myeloid Leukemia by developing targeted drug delivery system using different metal compounds. The specific objectives are given below:

*Objective 1: Synthesis of caffeine-coated nanoparticles*

- Synthesize and characterize caffeine-coated nanoparticles to serve as a potential drug carrier system.
- Evaluate the biological properties and stability of the synthesized nanoparticles.

*Objective 2: Design and synthesis of metal complexes-based nanoparticles*

- Develop and characterize metal complexes-based nanoparticles intended for anti-leukemic therapy.
- Optimize the formulation to ensure stability and controlled drug release properties.

*Objective 3: Molecular docking analysis*

- Identify binding efficacy of surface ligands with active sites of target proteins
- Assessment of potential interaction/ inter-molecular forces between ligand and pro-apoptotic complexes.

*Objective 4: In vitro evaluation of Nano drugs in multiple combinations*

- Evaluation of anti-oxidant potential of synthetic and natural Nano drugs at multiple concentrations.
- Optimize the various dosage regimes for *in vivo* administration via IC50 values analysis

*Objective 5: Examination of anti-leukemic potential*

- Assess the cytotoxicity and anti-leukemic efficacy of caffeine-coated nanoparticles against AML in *Sprague Dawley* rat model.

- Determine the selectivity and targeting efficiency of the DDS in delivering caffeine to AML cells and study its effect on various molecular pathways via different molecular biology techniques.

*Objective 6: Evaluation of combined therapy effects*

- Investigate the synergistic or additive effects of combining chemotherapy with the developed nanomedicine.
- Assess the combinatorial therapy's impact on AML cell viability, apoptosis, and therapeutic efficacy compared to individual treatments.

*Objective 7: Examination of biological potential of various treatment regimes*

- Evaluation of anti-coagulant, anti-depressant and analgesic potentials in multiple combinations

## **Chapter 2: Caffeine coated nanoparticles**

### **Exploring Therapeutic Potential of Caffeine-Coated Nanoparticles in AML Treatment**

## 2.1. Introduction

Cancer encompasses a range of diseases characterized by uncontrolled cell growth and infiltration into surrounding tissues. Its complexity arises from genetic, environmental, and lifestyle factors triggering abnormal proliferation, leading to malignant tumors or tissue disruption. This research aims to uncover critical mechanisms driving cancer development, aiding the development of targeted treatments and prevention strategies. (Hanahan & Weinberg, 2011). Leukemia, a form of cancer, originates from the malignant transformation of bone marrow hematopoietic cells, leading to abnormal and excessive proliferation of white blood cells known as leukocytes (Sahu *et al.*, 2011). Henceforth, this condition precipitates an augmented presence of immature white blood cells within the circulatory system, juxtaposed with a diminished synthesis of mature erythrocytes, The diagnosis of AML is confirmed clinically when hematological analysis reveals the presence of blast cells, accounting for 30% or more of the cell morphology (Bennett *et al.*, 1976). Conventional approaches for treating AML encompass chemotherapy, radiation, surgery, hormone therapy, and immunotherapy.

However, while chemotherapy aims for therapeutic effects, it can inadvertently trigger immunogenic cell death. Although natural compounds like paclitaxel and vincristine have been extensively utilized in clinical studies as anticancer agents, chemotherapy often faces limitations such as dose-related toxicities and the emergence of drug resistance. Nano-delivery systems offer a promising avenue by enabling precise targeting and direct delivery of pharmaceuticals to malignant sites, enhancing drug permeability and intracellular accumulation for more effective anticancer treatments (Paul & Jindal, 2017).

Doxorubicin, a widely recognized anti-leukemic medication, induces cell death in aberrant cells by intercalating with DNA bases and triggering the generation of reactive oxygen species (ROS) (Tacar *et al.*, 2013). The cytotoxic action of doxorubicin hinges on the formation of ROS, a crucial aspect contributing to its effectiveness in cancer therapy. Nevertheless, the non-specific nature of TRAIL can result in a range of undesired side effects, such as hair loss, fatigue, vomiting, nausea, and diarrhea (Partridge *et al.*, 2001). Hence, it is vital to replace these medications with natural compounds known for their potent anticancer properties.

Caffeine exerts a robust stimulatory effect on the human central nervous system. Caffeine's action involves stimulating efflux through pumps regulated by the Pap1 transcription factor, thereby aiding detoxification processes. Although caffeine is acknowledged for its anticancer properties, its short half-life limits its preference as a medication (Monteiro *et al.*, 2019). Studies indicate that caffeine disrupts DNA repair pathways within cancer cells, heightening their susceptibility to cell death. Additionally, it disrupts the cell cycle progression of cancer cells, inducing cell cycle arrest and impeding their uncontrolled division (Calvo *et al.*, 2009).

Nanotechnology is an increasingly promising field in therapeutics, and the integration of caffeine into nanoparticles shows potential as an effective approach for drug delivery (Sinha *et al.*, 2006). In medicine, the utilization of nanotechnology is rapidly evolving to enhance drug absorption and targeted delivery, notably through mesoporous silica nanoparticles (MSNPs). These nanoparticles offer precise control over medication distribution to specific areas within the body (Monteiro *et al.*, 2019).

In response to the distinctive attributes of caffeine and MSNPs, we developed caffeine-coated nanoparticles (CcNPs) as a novel nanomedicine. Our investigation aimed to assess the effectiveness of these CcNPs against benzene-induced AML in rat model, employing a comprehensive approach encompassing *in silico*, *in vitro*, and *in vivo* studies. These studies focus on evaluating various anti-cancer markers to ascertain the therapeutic potential of CcNPs. Throughout our analysis, we conducted hematologic profiling to gauge changes in blood components, examining how CcNPs influenced crucial parameters indicative of AML progression and treatment response.

Moreover, our investigations delved into the underlying pathways affected by CcNPs, utilizing pathway analysis to elucidate the mechanisms through which these nanoparticles exerted their therapeutic effects against AML. The collective findings from these diverse analyses consistently supported the efficacy of CcNPs as a promising treatment modality for benzene-induced AML, showcasing their potential through multiple layers of evidence across *in silico*, *in vitro*, and *in vivo* studies.

## 2.2. Materials and Methods

All molecular assays (*in vitro* and *in vivo*) along with synthesis of nanomedicine were performed under standard conditions, with optimized protocols. Various tools, materials and molecular biology techniques were utilized to obtain desired results. This study was also approved by Institutional Review Board (IRB) of Quaid-i-Azam University, Islamabad.

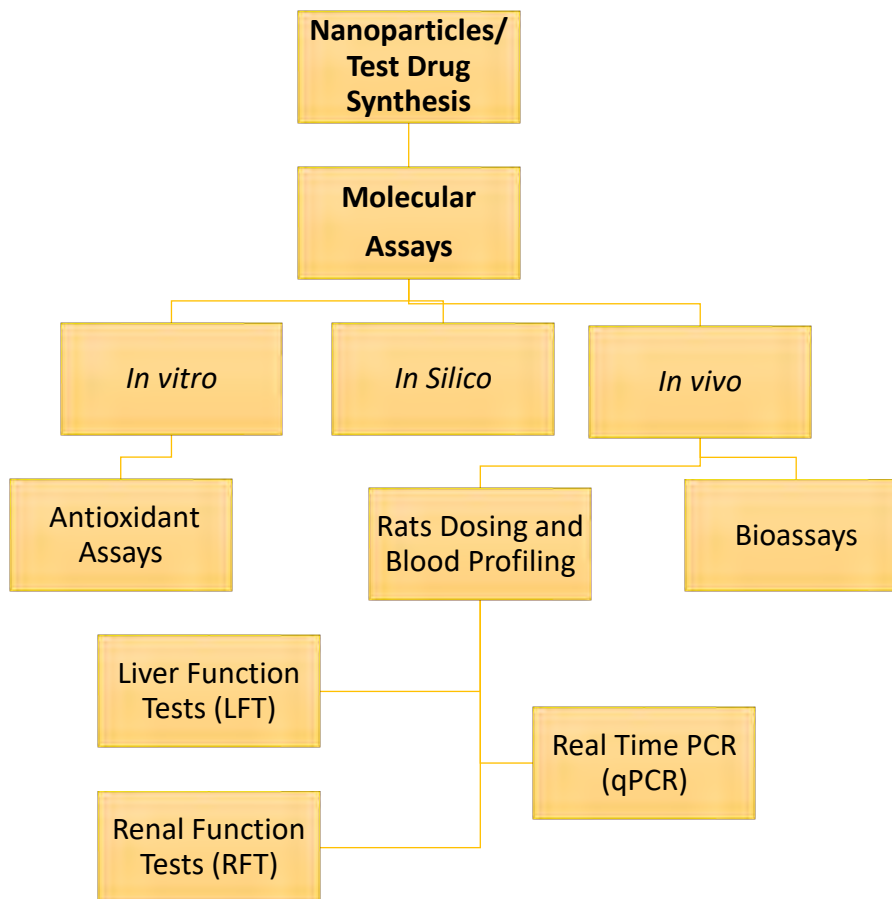


*Figure 2.1: Study design*

### 2.2.1. Synthesis of MSNPs

Mesoporous silica nanoparticles were generated employing a chemical synthesis method as described earlier (Wu *et al.*, 2013).

**Table 2.1: Chemicals involved in synthesis, loading and coating of mesoporous silica nanoparticles (MSNPs).**

No.	Chemical Name	Chemical Formula	Function
1.	Ammonia solution (29%)	NH <sub>4</sub> OH	Used to maintain PH
2.	CTAB (Cetyl trimethyl ammonium bromide)	C <sub>19</sub> H <sub>42</sub> BrN	Surfactant
3.	TEOS (Tetra methyl ortho silicate)	SiC <sub>8</sub> H <sub>20</sub> O <sub>4</sub>	Silica precursor
4.	DMSO (dimethyl sulfoxide)	C <sub>2</sub> H <sub>6</sub> OS	Solvent
5.	Polyethylene glycol (PEG)	C <sub>2n</sub> H <sub>4n+2</sub> O <sub>n+1</sub>	Polymer compound for coating of nanoparticles

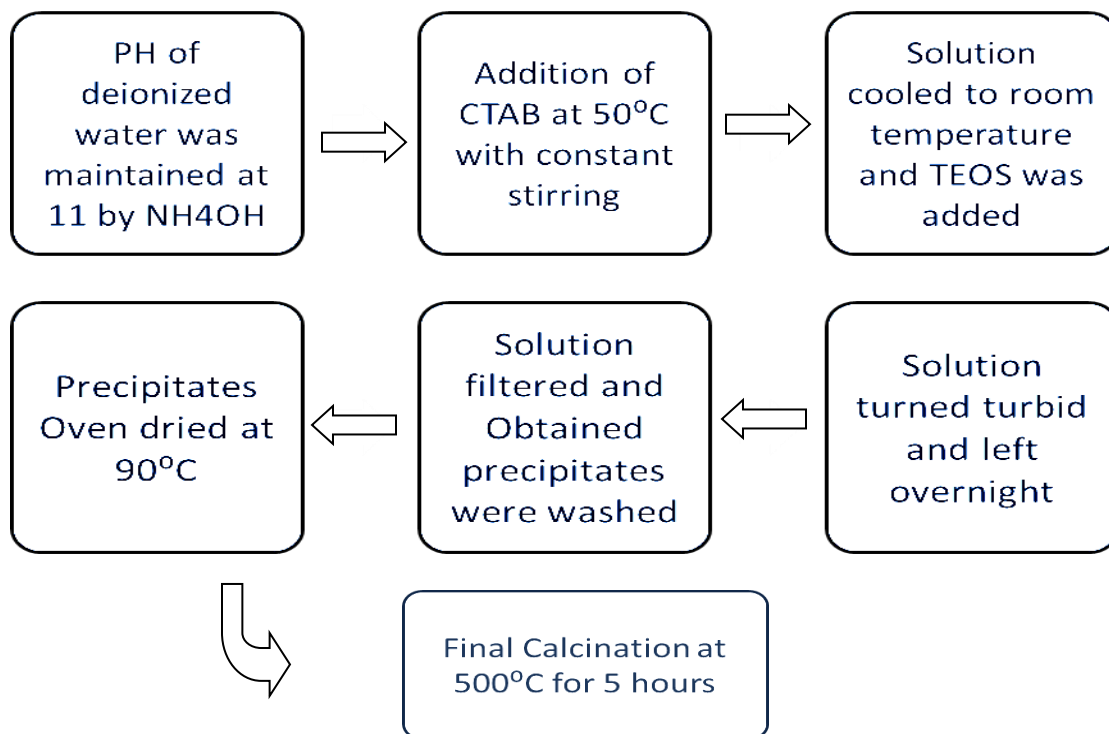


**Figure 2.2: Steps involved in the synthesis of mesoporous silica nanoparticles.**

Deionized water (442mL) was adjusted to pH 11 using 29% ammonium hydroxide. Then, heated to 323.15K (50°C), 0.279 g of cetyltrimethylammonium bromide (CTAB) was added with continuous stirring, maintaining pH at 10.3. After cooling, 1.394mL of tetramethyl orthosilicate (TMOS) was added with stirring, resulting in turbidity within 2 minutes. The solution was stirred overnight, filtered, washed with deionized water, and dried at 363.15K (90°C). The material was calcined at 773.15K (500°C) for 5 hours, producing a white product that was finely milled. To remove the CTAB template, the dry powder was refluxed in methanol (100mL) with strong HCl (1mL) for 24 hours at 323.15K (50°C).

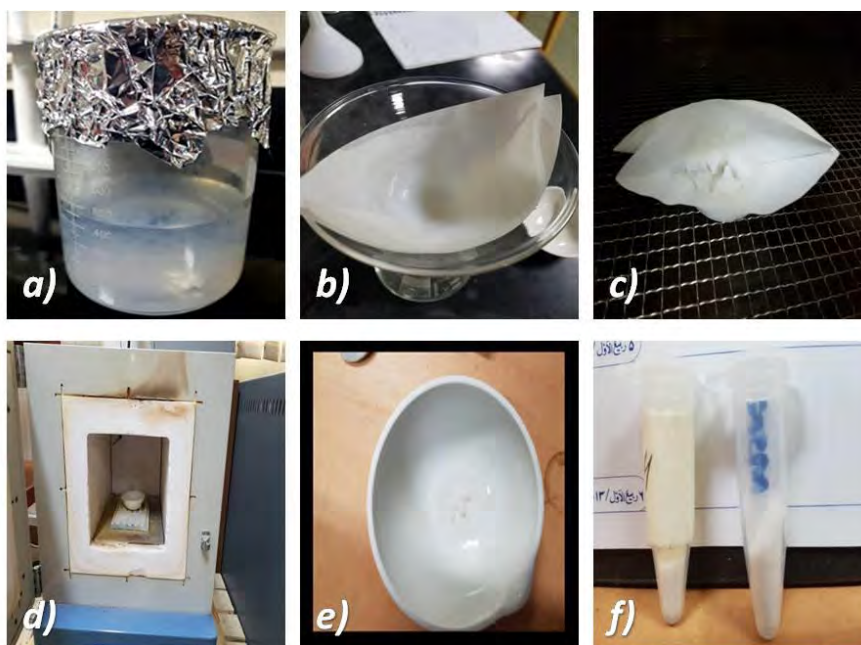


**Figure 2.3:** a) Turbid solution b) Filtered MSNPs c) Overnight drying of MSNPs d) Calcination e) Calcined MSNPs f) Final ground form of mesoporous silica nanoparticles

### 2.2.2. Characterization techniques

Multiple characterization techniques were utilized to examine size and nature of nanomedicine including SEM, FTIR, XRD, UV/Vis spectroscopy and DLS using already published protocols.



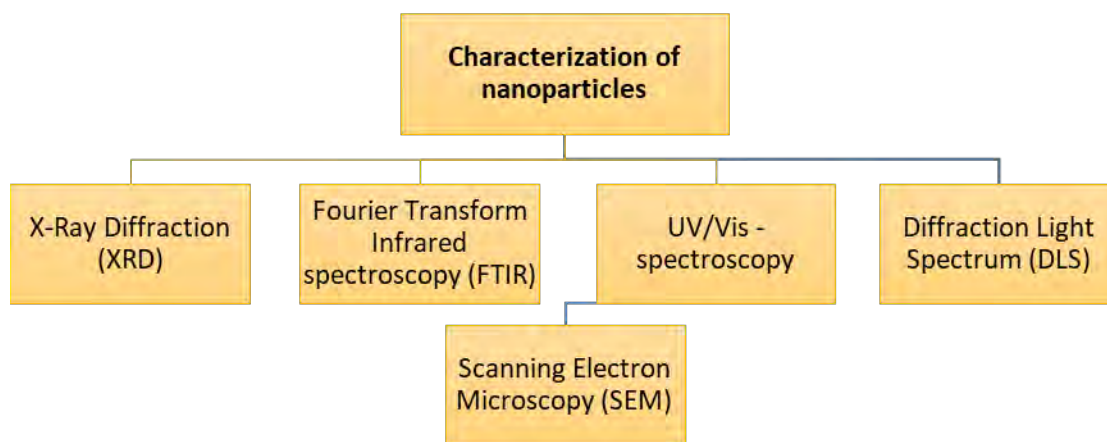


*Figure 2.4: Techniques used for characterization of nanoparticles.*

### 2.2.3. Loading of caffeine over MSNPs

For this purpose, caffeine (0.583g) was dissolved in normal saline (35mL) followed by sonication upto 3 hours, and addition of MSNPs (145.75mg) with overnight stirring. A modified approach based on the aforementioned method was employed to determine the percentage of medication loaded into the nanocarrier (J. Wang *et al.*, 2015). 1mL sample underwent centrifugation at 10,000 rpm for 10 minutes. Subsequently, UV-Vis spectra were captured at 209 nm.

Encapsulation efficiency =  $W2 - W3 / W2 \times 100$ ; Drug Loading =  $W1/W2 \times 100$ .

The composition of the weights (W1, W2, and W3) suggests that W1 represents the weight of caffeine in the nanomedicine, W2 represents the total weight of the nanomedicine, and W3 represents the weight of the extract that remained in the supernatant after centrifugation.

To increase the bioavailability of the nanomedicine, a polymer solution was created by blending 0.006g of Polyethylene glycol (PEG) with 4mL of DMSO (Nakamura *et al.*, 2012). The procedure entailed sonication of the mixture until complete dissolution of PEG was attained. Moreover, the polymer solution was combined with the silica nanoparticles loaded with caffeine, resulting in a total volume of 35mL. The mixture was then subjected to continuous stirring for a duration of two hours (Vojoudi *et al.*, 2018).

#### 2.2.4. In silico analysis

Nanomedicine (ligand) was docked into the active sites of pro-apoptotic markers (such as the cFLIP-DISC complex and TRAIL-DR5 complex) as well as anti-proliferative markers (like the NF- $\kappa$ B-p52/Rel B/DNA complex) using PyRx v.0.8 (<https://pyrx.sourceforge.io>). This molecular docking software facilitated the exploration of potential interactions and binding affinities between the nanomedicine and these specific biomolecular targets (Kondapuram *et al.*, 2021) via Autodock Vina (Trott & Olson, 2010). The ligand's energy was minimized through Autodock, aligning the resulting protein-ligand interactions with the values projected by quantum chemistry simulations. This process aimed to refine and optimize the molecular configuration of the ligand within the protein's active sites, correlating the computational predictions with the actual observed interactions (Mirzaei *et al.*, 2015). This study scrutinized the binding affinity values, serving as indicators of the interaction strength between the ligand and the targeted proteins. Furthermore, BIOVIA Discovery Studio was employed to visualize both two-dimensional (2D) and three-dimensional (3D) interactions of amino acid residues. This software facilitated the comprehensive examination and graphical representation of how the ligand interacts with specific amino acids within the protein structures in both two and three dimensions (Studio, 2015).

#### 2.2.5. Cytotoxicity assay

In this experiment, brine shrimp eggs were hatched in a sea salt solution to conduct a dosage assessment for the medication. Table 2.2 exhibits the count of fifteen brine shrimps observed under a microscope and subsequently placed in various repeated dilutions for a duration of 24 hours. Each concentration underwent replication three times, and a control was maintained using distilled water. The probit approach was employed to compute the lethal concentration that induces a 50% mortality rate ( $LC_{50}$ ) following 24 hours of exposure (Rath *et al.*, 2011).

**Table 2.2: Brine shrimp assay**

	<b>Drug</b>	<b>Conc. 1</b>	<b>Conc. 2</b>	<b>Conc. 3</b>	<b>Conc. 4</b>
<b>1.</b>	Caffeine	33.4mg/mL	16.7mg/mL	8.35 mg/mL	4.175mg/mL
<b>2.</b>	Doxorubicin	2.1mg/mL	1.05mg/mL	0.525mg/mL	0.2625mg/mL
<b>3.</b>	Caffeine + Doxorubicin	16.7mg/500uL + 1.05mg/500uL	8.32mg/500uL + 0.525mg/500uL	4.18mg/500uL + 0.26mg/500uL	2.09mg/500uL + 0.13mg/500uL

### 2.2.6. *In vitro* bioassays

The assessment of antioxidant potential involved the utilization of various assays, with the total antioxidant capacity determined specifically using phosphomolybdenum method (Phatak *et al.*, 2015). Similarly, the total reducing power and DPPH assay were conducted according to the procedures outlined by Moein and colleagues (Moein *et al.*, 2012).

### 2.2.7. *In vivo* bioassays

The evaluation of pain-relief efficacy across various treatment regimens was conducted using the hot plate assay (Yamamoto *et al.*, 2002). The anti-coagulant assay, assessing the clotting time of blood in the absence of external substances, was also conducted (Samuelson *et al.*, 2017). Each group of mice was administered an intraperitoneal dose, and the initial readings were taken immediately post-treatment. The mice's tails were sterilized with ethanol, before a 1-2 mm section of the tail tip was excised using sterile scissors. A drop of blood was gently squeezed from the tail onto a clean microscope slide. Using a toothpick, the blood was swirled in circular motions until fibrin threads formed, and the time taken for coagulation was measured using a stopwatch. Three hours post-dosage, another reading was obtained, and the results were analyzed. The negative control utilized DMSO (0.1%), while the positive control employed aspirin (1mg/kg). Additionally, the assessment of antidepressant activity was conducted using the standardized tail suspension method established by Zhou and colleagues (Xu *et al.*, 2014).

### 2.2.8. Experiment design and Sprague Dawley model

This study received ethical approval from the Institutional Review Board of Quaid-i-Azam University, as confirmed by approval letter No. #BEC-FBS-QAU2020-221. Forty female Sprague Dawley rats, obtained from the National Institute of Health, were used in the study (Bobinihi, Osuntokun, & Onwudiwe) which were allocated into eight groups to receive distinct treatments: 1) control (normal saline); 2) benzene alone; 3) doxorubicin + benzene; 4) caffeine + benzene; 5) MSNPs + benzene; 6) CcNPs + benzene; 7) caffeine + doxorubicin + benzene; 8) CcNPs + doxorubicin + benzene. The rats were housed at Quaid-i-Azam University's Primate Facility, maintained on a 12-hour light/dark cycle, and provided ad libitum access to water and rat meal following a seven-day acclimation period.

Benzene and normal saline were combined in a 1:3 ratio to form an injection solution. This benzene solution (200  $\mu$ L) was injected into the tail veins of rats in groups 2-8 on alternate days over a 14-day period to induce leukemia, which was subsequently confirmed. Doxorubicin, obtained from Actavis, Italy, was prepared as a stock solution of 3.75 mg/1.8mL. Following the 14 intravenous benzene doses, rats in groups 3, 7, and 8 received doxorubicin (0.625 mg/0.3mL) on alternate days for three weeks.

A caffeine stock solution (Cat. No. C0750-5G) was created by combining caffeine (0.583g) with normal saline (35mL). Upon confirmation of leukemia induction, rats in groups 4 and 7 received the caffeine stock solution (0.3mL/rat) intravenously for three consecutive weeks (8mg/kg). Caffeine-coated Nanoparticles (CcNPs) were administered intraperitoneally (0.3mL/rat) to rats in groups 6 and 8 on alternate days for three weeks. All compounds administered, except for MSNPs (group 5) and CcNPs (groups 6 & 8), were free medications, including caffeine and doxorubicin.

**Table 2.3: Dosing and mode of administration of drugs among different groups.**

No.	Groups	No. of Rats	Dosage Regime	Mode of Administration
1.	Normal/ Control	3	0.9% saline (200 uL)	<i>intravenous</i>
2.	Benzene	3	0.2mL for 2 weeks regularly.	<i>intravenous</i>
3.	Caffeine	3	0.3mL for 3 weeks regularly.	<i>intravenous</i>
4.	Doxorubicin	3	0.3mL for 3 weeks alternatively.	<i>intravenous</i>
5.	MSNPs	3	0.3mL for 3 weeks regularly.	<i>intravenous</i>
6.	Caffeine + MSNPs	3	0.3mL for 3 weeks regularly.	<i>intravenous</i>
7.	Caffeine + Doxorubicin	3	0.3mL for 3 weeks regularly/ alternatively.	<i>intravenous</i>
8.	Caffeine + MSNPs + Doxorubicin	3	0.3mL for 3 weeks regularly/ alternatively.	<i>intravenous</i>

Following the completion of their respective treatment schedules, all rats were euthanized and dissected following the protocols outlined in the Guide for the Care and Use of Laboratory Animals (Care & Animals, 1986).

### 2.2.9. Morphological analysis

After the dissections, blood samples were used to prepare blood smears on slides. These smears were air-dried and then stained with Giemsa dye by applying it drop by drop onto the slides. The slides were left to stain for a duration of 10 minutes. Following staining, the slides were rinsed with tap water to remove excess dye and air-dried once again. Finally, the dried slides were examined under a microscope for morphological analysis (Sathpathi *et al.*, 2014).

### 2.2.10. Blood profiling

The blood complete picture (CP) was obtained via an automated Z3 hematology analyzer at the Islamabad Diagnostic Centre (IDC) in Islamabad, Pakistan, evaluating various

parameters. For biochemical studies, a Micro Lab 300 auto-analyzer (Merk) was employed. Biochemical analysis kits, specifically AMP diagnostic kits, facilitated the assessment of parameters including alkaline phosphatase (Malovichko et al.), alanine aminotransferase (ALT), aspartate aminotransferase (AST), and creatinine.

#### **2.2.11. mRNA extraction**

mRNA extraction from liver tissue involved utilizing 10 mg of frozen tissue samples homogenized in 1 mL of TRIzol reagent (Sigma-Aldrich Cat No. 136426-54-5). Following this, the material underwent processing in accordance with the methodology outlined by Chomczynski and colleagues for subsequent relative expression measurement using Real-Time PCR (Chomczynski, 2010). The extracted RNA was quantified using NanoDrop spectrophotometry and subsequently subjected to 1% agarose gel electrophoresis to ensure its quality and integrity.

#### **2.2.12. cDNA synthesis**

The acquired mRNAs were used to create complementary DNA (cDNA) with the Vivantis kit (cDSK01-050). To confirm the cDNA synthesis, traditional PCR was carried out following the manufacturer's protocol to assess the annealing temperatures of selected primers and validate cDNA quality. The target transcript was then amplified via PCR by combining reaction components in 200  $\mu$ L PCR tubes (Axygen, USA). After PCR, the resulting amplified product was observed on a 2% agarose gel containing ethidium bromide (Stellwagen, 1998).

#### **2.2.13. RT PCR expression analysis**

BioMolecular Sciences (BMS) MIC qPCR was utilized to conduct relative expression analysis and quantify the amplified cDNA. This method employs Biotium EvaGreen® Master mix, a non-specific binding dye. Various genes were screened for relative gene expression analysis, including:

**Table 2.4: Primers for qPCR-based RNA expression analysis**

No	Primers Name	Primer Sequence (5' – 3')
1.	B-Actin	(F-CTCACGGTGTGCCAAAATG, R-GCCTTGATCCTTTGGTTATTTCG)
2.	STMN1	(F-TTGCCAGTGGATTGTGTAGAG, R-TTCTTTTGATCGAGGGCTGAG)
3.	P53	(F-GAAATGGTGAATAAGGACTTGCC, R-TCAACTTCCCATCAGCATC)
4.	GAPDH	(F-ACGGAGTCTGACCTGATGTAG, R-CACCTGTCGCTCTCATGTAC)
5.	mTOR	(F-TGAAATGCCACCTTCTACC, R-AAGTGTCCTGAAAGTGAAG)
6.	REL-A	(F-ACCTGCCCTCTTCAACTTTAC, R-CACGGTCTCCAGCATTAGTATC)
7.	REL-B	(F-CAGCCTTCTCATCTCTTCATCC, R-GTGATTTTGTCTCTGCTTGG)
8.	DR5	(F-GGTGGATATGTCTGGGTTGAG, R-AGGGAGAAAATCAAGTCGTGC)
9.	cFLIP	(F-TTTGGCTCTTCAGGGATGC, R-CACCGCTCTTCAGGGTATAC)
10.	TRAIL	(F-CTCGCGTTATTTGAAGCCTG, R-TCGCAGATGAAATAGGGCTG)
11.	Cyt c	(F-TCAAGGGAGTCTGGAACATTG, R-GCTTCCCAACTTTTGTAACCG)

The fold change in gene expression of the samples was determined using the Pfaffl method, a widely used technique for analyzing relative gene expression in quantitative PCR experiments (Deshayes & Gref, 2023).

**Table 2.5: RT-PCR reagents**

Sr. No.	Reagents	Quantity
1	cDNA	5 $\mu$ L
2	Forward Primer	1 $\mu$ L
3	Reverse Primer	1 $\mu$ L
4	Eva Green Master Mix	2 $\mu$ L
5	RNase free H <sub>2</sub> O	1 $\mu$ L
Total Reaction Volume		10 $\mu$ L

For calculating relative expression in real-time PCR using the pairwise fixed reallocation randomization test, the Relative Expression Software Tool (REST-384, version 2) was utilized.

#### 2.2.14. Statistical analysis

Descriptive statistics were generated using GraphPad Prism software (version 5.01), presenting the results as mean  $\pm$  standard error of the mean (Khwaja et al.). Statistical significance was assessed, considering p-values below 0.05 as statistically significant, denoted as (\*), p-values below 0.01 as (\*\*), and those below 0.001 as (\*\*\*). Group comparisons were performed using one-way analysis of variance (Hendrych *et al.*, 2010).

### 2.3. Results

#### 2.3.1. Characterization of MSNPs

Scanning electron microscope images display spherical structures of MSNPs that are uniformly distributed, with an average diameter measuring 120 nanometers (figure 2.5).



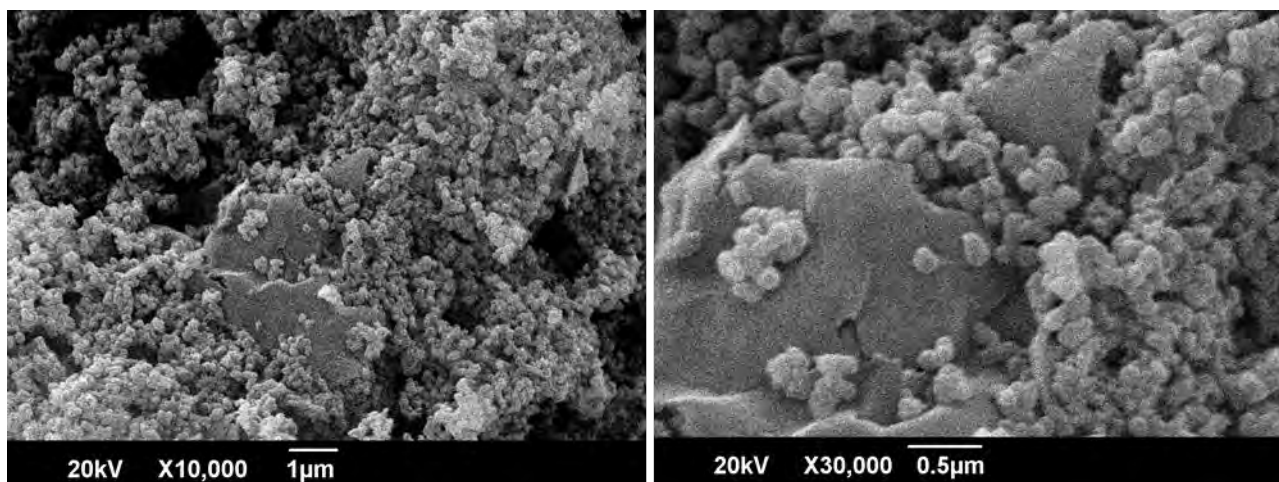


*Figure 2.5: The SEM images of mesoporous silica nanoparticles*

The presence and formation of MSNPs were confirmed by analyzing the X-ray diffraction pattern. A distinct diffraction peak was observed at  $2\theta = 29.18$ , which corresponds to MSNPs with a calculated diameter of 118.18 nanometers. This peak serves as evidence of the crystalline structure of the MSNPs, confirming their successful synthesis (figure 2.6).

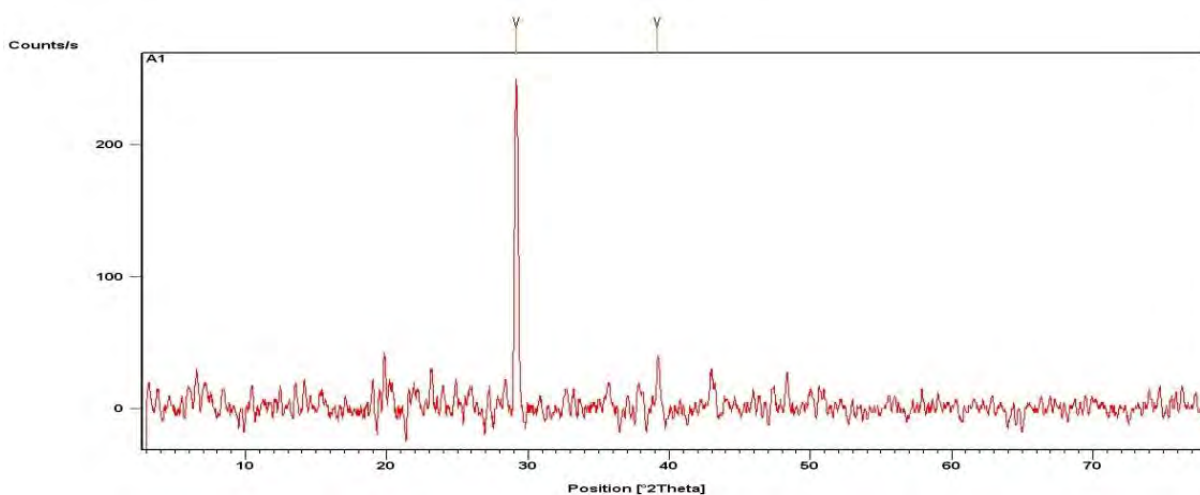


*Figure 2.6: The X-ray diffraction analysis of MSNPs*

FTIR spectroscopy demonstrated characteristic peaks in the nanomedicine, resembling those of caffeine. These findings suggest the presence of caffeine coating on the nanomedicine, as illustrated in figure 2.7.

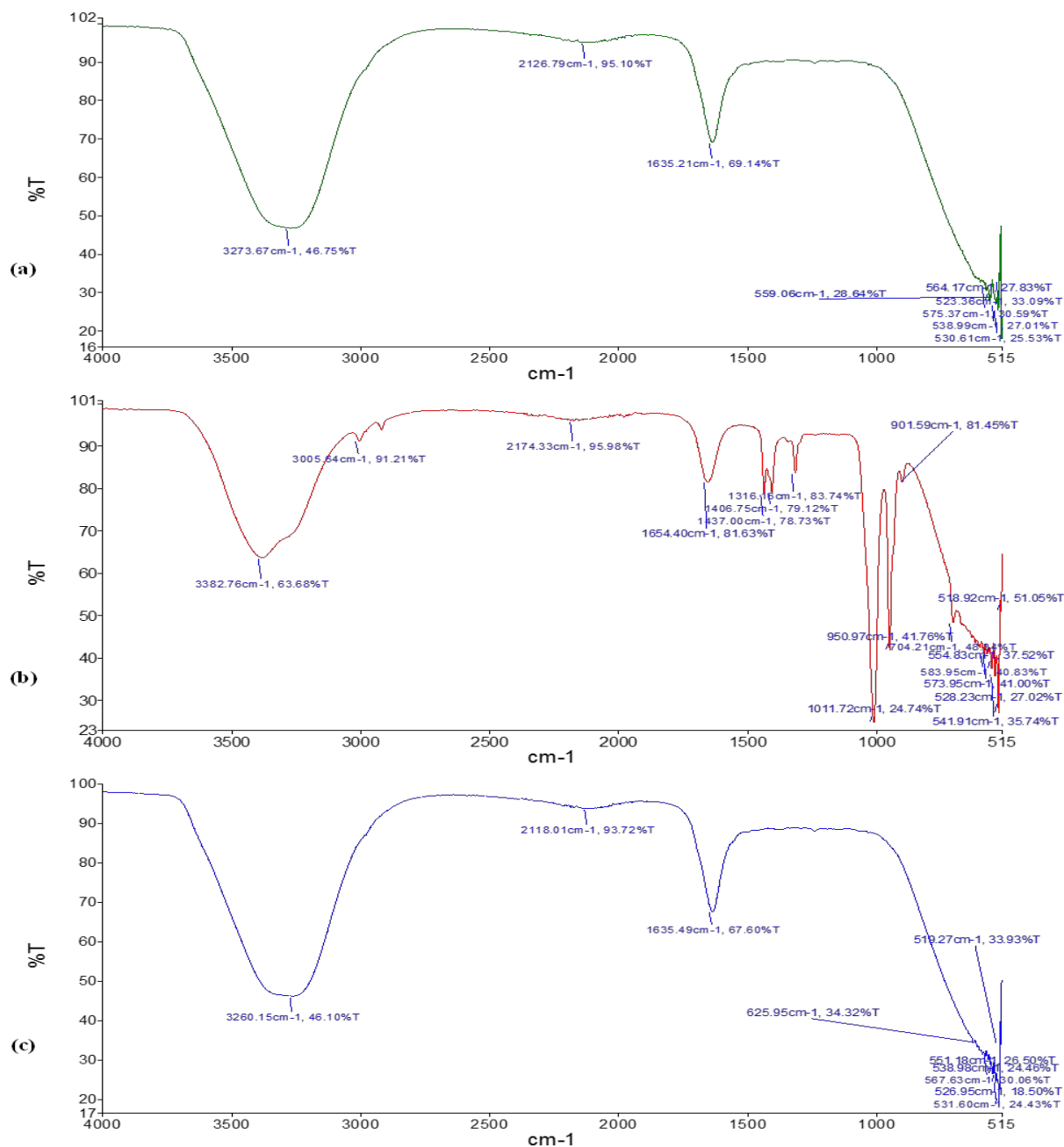


**Figure 2.7: FTIR analysis of (a) caffeine (b) MSNPs and (c) nanomedicine**

The absorption patterns observed using UV-Vis spectroscopy for caffeine, nanomedicine, and MSNPs validate the successful attachment of caffeine onto nanoparticles. This attachment exhibits a loading efficiency of 28%. This technique essentially helps in confirming the presence and quantity of caffeine integrated into the nanoparticles, which

is crucial for understanding their interaction and potential applications in various fields. (Figure 2.8).

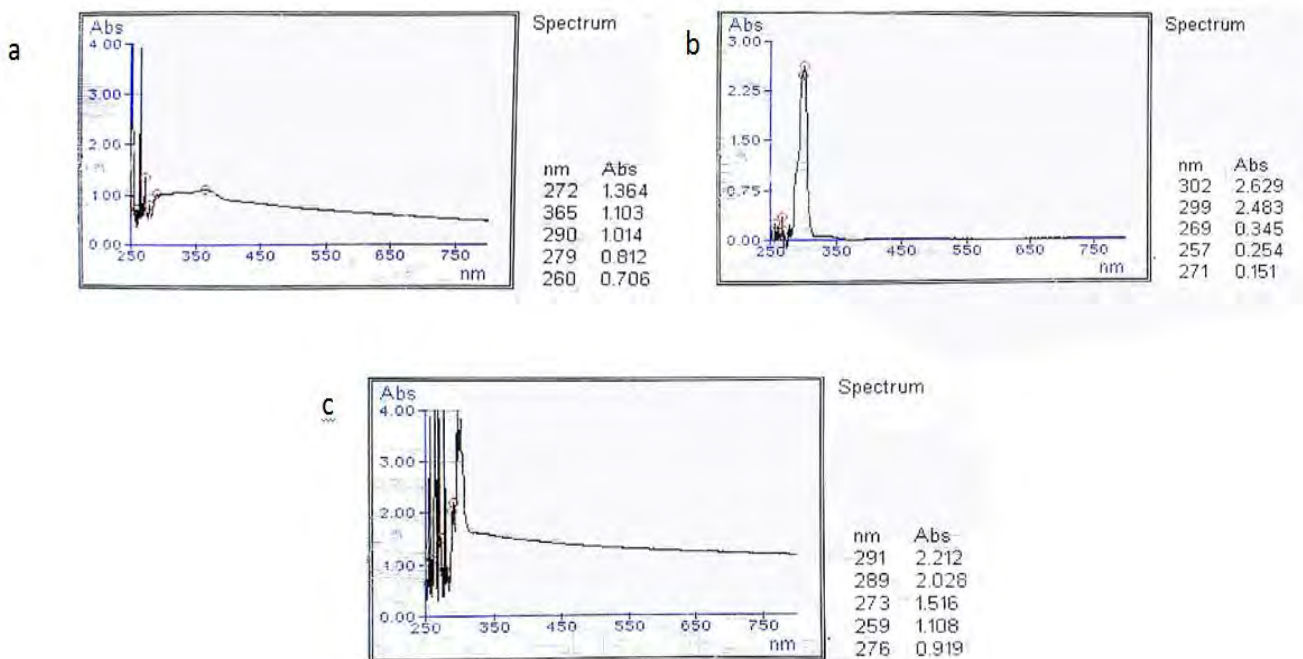


**Figure 2.8:** The absorbance spectra obtained through UV/Vis Spectroscopy for a) MSNPs, b) caffeine, and c) nanomedicine

### 2.3.2. Nanomedicine demonstrating robust affinity with the pro-apoptotic TRAIL-DR5 complex

The TRAIL-DR5 protein's binding site was subjected to molecular docking analysis employing caffeine in nanomedicine form as the ligand (PDB:1du3), depicted in figure 2.9. The PyRx tool computed the binding affinity of the most favorable confirmation, yielding a robust -6.8 kcal/mol with an RMSD of 0.00, implying a close alignment between the docked and experimental structures. This investigation, using BIOVIA Discovery Studio, unveiled several critical interactions: prominent hydrogen bonds formed between the ligand and the receptor's ASN228 amino acid. Moreover, four carbon-hydrogen bonds involving ASN228, SER229, and TYR240 were identified. Additionally, two pi-sulfur interactions with CYS230 were noted.

Hydrophobic interactions proved significant, comprising two pi-pi stacked and two pi-pi T-Shaped interactions with TYR240, alongside a pi-alkyl interaction with ARG227. Notably, Van der Waals interactions pervaded multiple amino acid residues, contributing substantially to the ligand-receptor stabilization and specificity. This comprehensive analysis aids in comprehending the molecular basis of the caffeine-TRAIL-DR5 binding interaction, essential in designing potent nanomedicines or pharmaceutical agents targeting this protein.

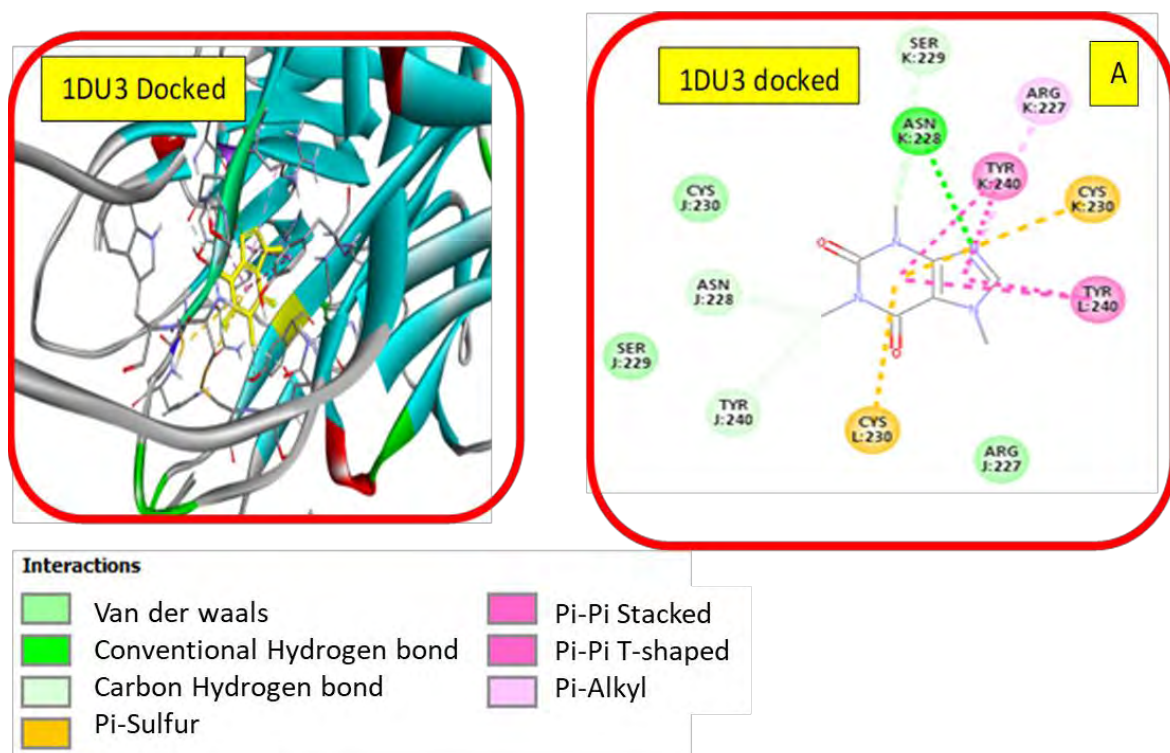


**Figure 2.9: Molecular docking between CcNPs and TRAIL-DR5 complex (PDB:1du3)**

### 2.3.3. Docking analysis of NF- $\kappa$ B p52/RelB/DNA complex

Caffeine's binding affinity for the NF- $\kappa$ B p52/RelB/DNA complex protein binding site was assessed to be -5.6 kcal/mol, with an RMSD of 0.00, indicating a remarkable binding efficiency and interaction, as depicted in figure 2.10. Further investigations using BIOVIA Discovery Studio (version 2021) on this conformation unveiled a spectrum of interactions, encompassing Van der Waals forces, hydrophobic bonds, and hydrogen bonds. Notably, a

significant interaction was observed with the amino acid ARG:119, emphasizing its involvement in the binding.

These docking experiments assert the nanomedicine's capacity to bind to both pro-apoptotic and anti-proliferative complexes. Importantly, these findings have been substantiated through *in vitro* and *in vivo* validations, consolidating the nanomedicine's efficacy in engaging with and modulating these critical protein complexes.

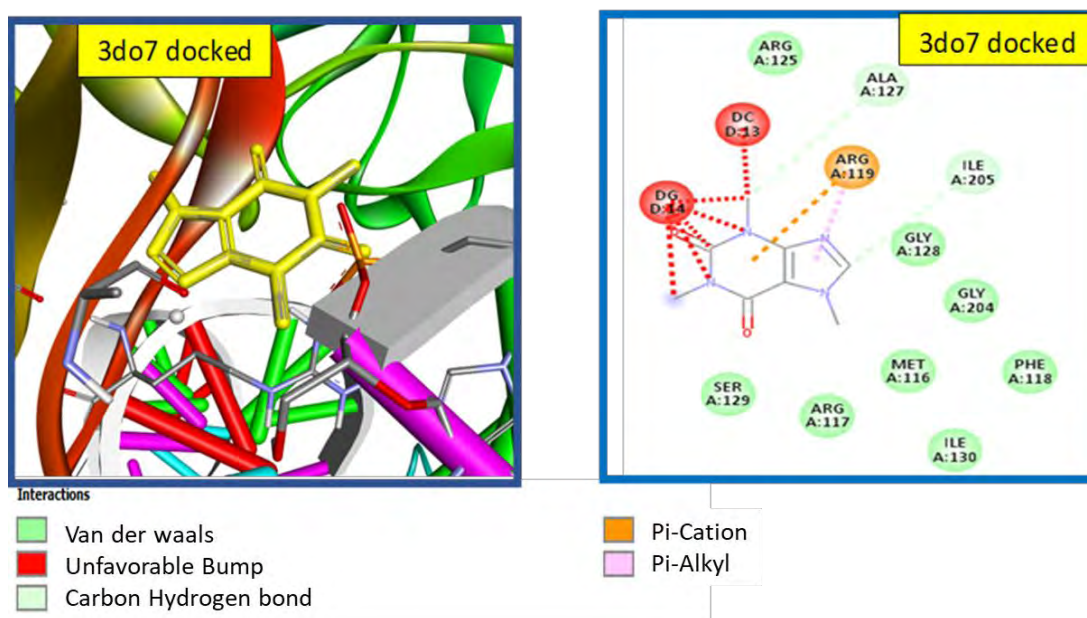


**Figure 2.10: Molecular docking between CcNPs and NFκB-p52/RelB/DNA complex (pdb:3do7)**

#### 2.3.4. Docking analysis with c-FLIP

In figure 2.11, the ligand was precisely docked within the active site of c-FLIP (PDB: 7dee). The computed binding affinity recorded -5.3, coupled with an RMSD of 0.00, indicating a strong interaction between the ligand and the protein structure. Analysis revealed the presence of carbon-hydrogen bonds, traditional hydrogen bonds, along with notable Van der Waals interactions involving specific amino acid residues within the active site. These interactions underscore the ligand's engagement and stabilization within the c-FLIP protein structure.

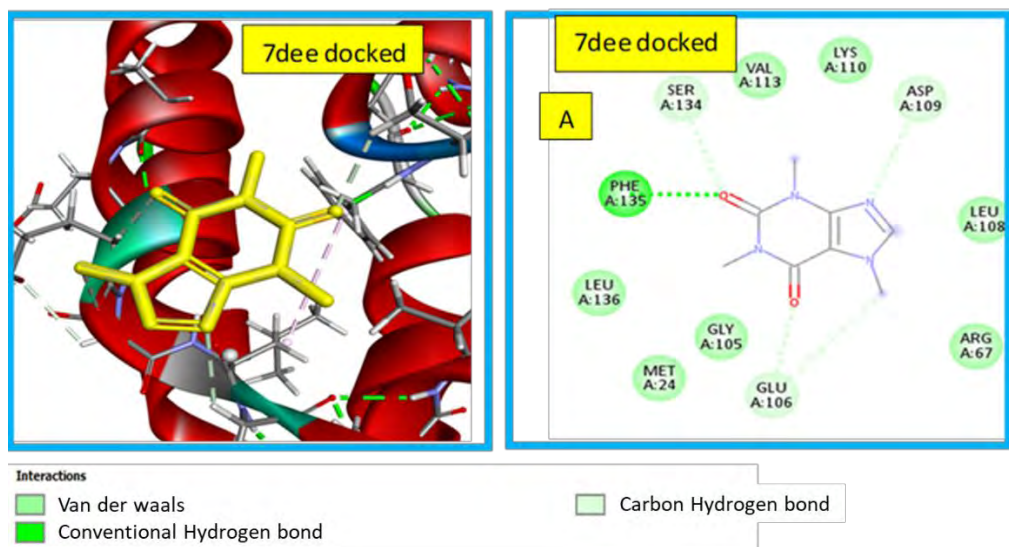


**Figure 2.11: Molecular docking between CcNPs and cFLIP-DISC complex (pdb:7dee)**

### 2.3.5. Antioxidant potential of caffeine

Across all treatment regimens, the comprehensive assessment of reducing potential exhibited a substantial ( $p < 0.001$ ) increase in the overall reducing action. Specifically, when caffeine was administered in the form of nanomedicine, there was a notable elevation ( $p < 0.05$ ) in its reduction potential, as depicted in figure 2.12A.

Moreover, a consistent pattern was observed in the total antioxidant capacity test. The administration of caffeine as nanomedicine demonstrated a considerable enhancement, exhibiting a 16.5% increase ( $p < 0.001$ ) in antioxidant activity compared to caffeine administered solely as medication (Figure 2.12B).

The findings from the DPPH assay further support this trend, revealing a significant 24.8% surge ( $p < 0.05$ ) in caffeine's antioxidant capacity when delivered in the form of nanomedicine, as illustrated in Figure 2.12C. These results collectively highlight the pronounced improvement in antioxidant efficacy when caffeine is utilized as a nanomedicine formulation, suggesting its potential for enhanced therapeutic benefits.

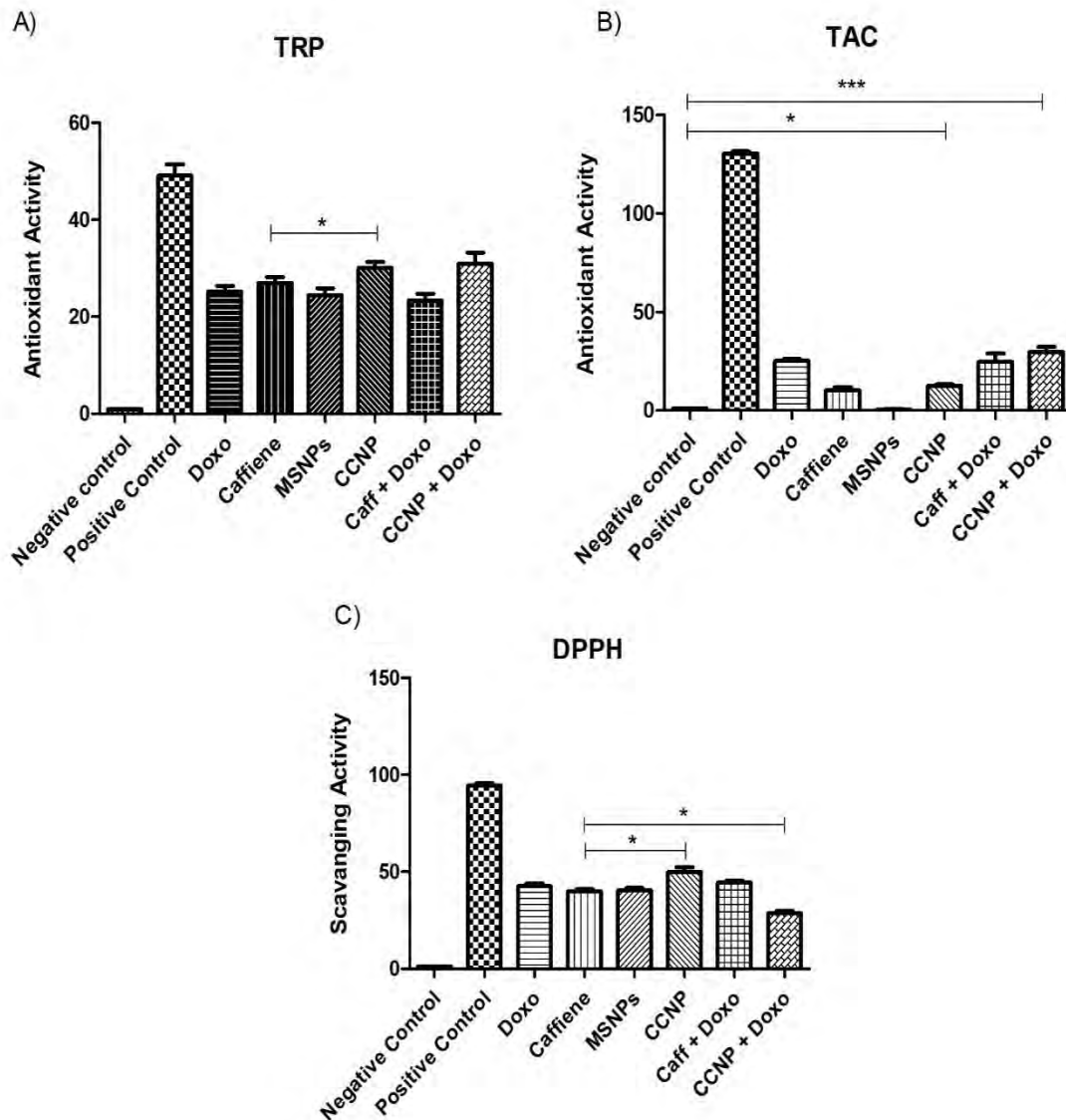


**Figure 2.12: Antioxidant potential analysis of different treatment groups (n=3) using A) TRP B) TAC and C) DPPH assays**

### 2.3.6. Biological efficacy of the nanomedicine

In the brine shrimp experiment (Figure 2.13A), the combination of nanomedicine with chemotherapy notably diminished cytotoxicity levels ( $p < 0.01$ ). Additionally, in comparison to doxorubicin alone, the combined treatment remarkably enhanced the antidepressant (15.3%), analgesic (88%), and anti-coagulation properties (16%) of the

nanomedicine ( $p < 0.001$ ). These results underscore the substantial bio efficacy of the nanomedicine in Sprague Dawley rat model, as depicted in figures 2.13B-D.

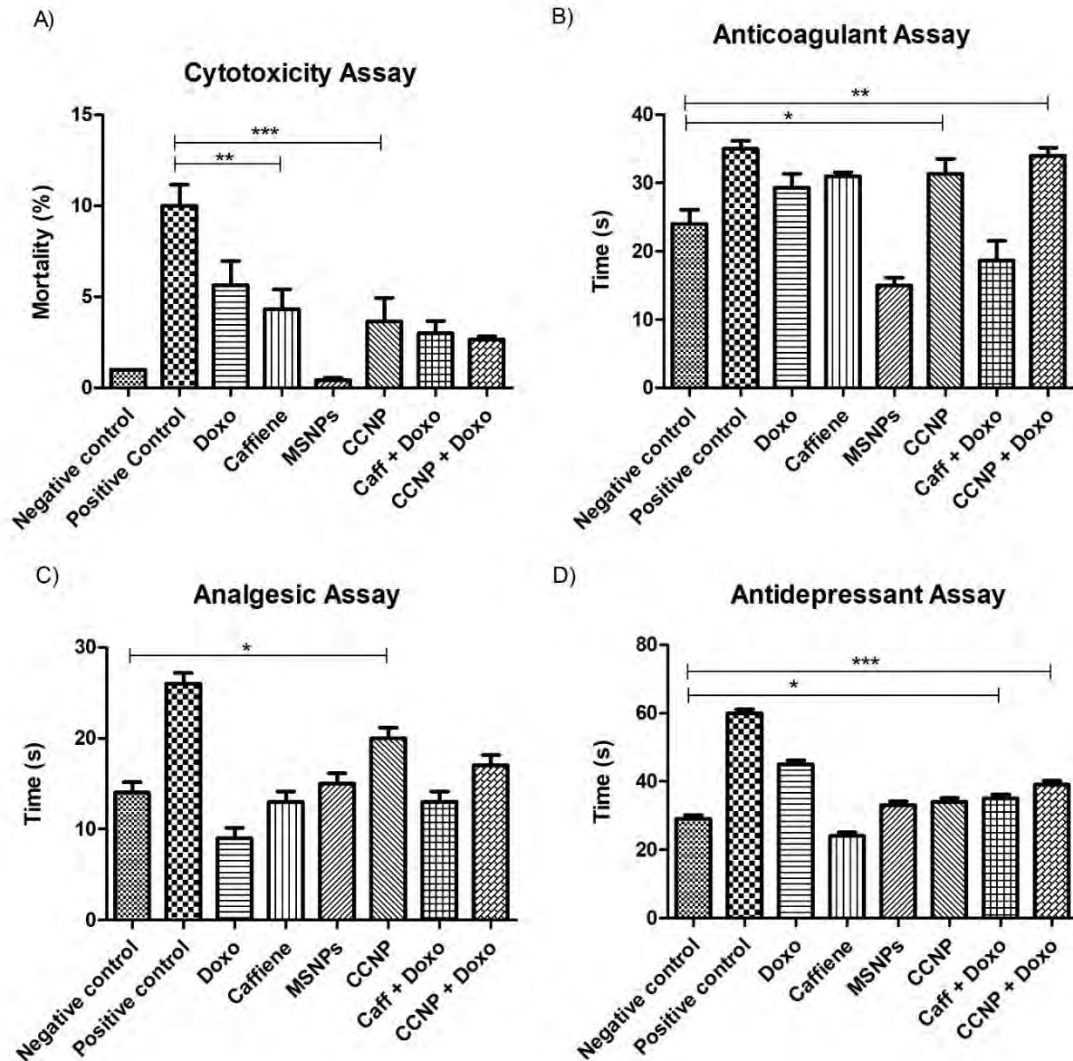


**Figure 2.13: Evaluation of biological potential using A) brine shrimp assay B) anti-depressant assay C) anti-coagulant assay and D) analgesic assay in animal model (n=3)**



### 2.3.7. Relative organs weight analysis

In the benzene-treated groups (Figure 2.14A-C), there were significant increase observed in the weights of the liver ( $p < 0.05$ ), heart ( $p < 0.001$ ), and kidney ( $p < 0.05$ ). Subsequent therapy with nanomedicine (CcNPs) led to a notable decrease ( $p < 0.05$ ) in organ weights, effectively restoring them to levels comparable to those in the control group. Interestingly, other therapies also showed similar effects on organ weight reduction.

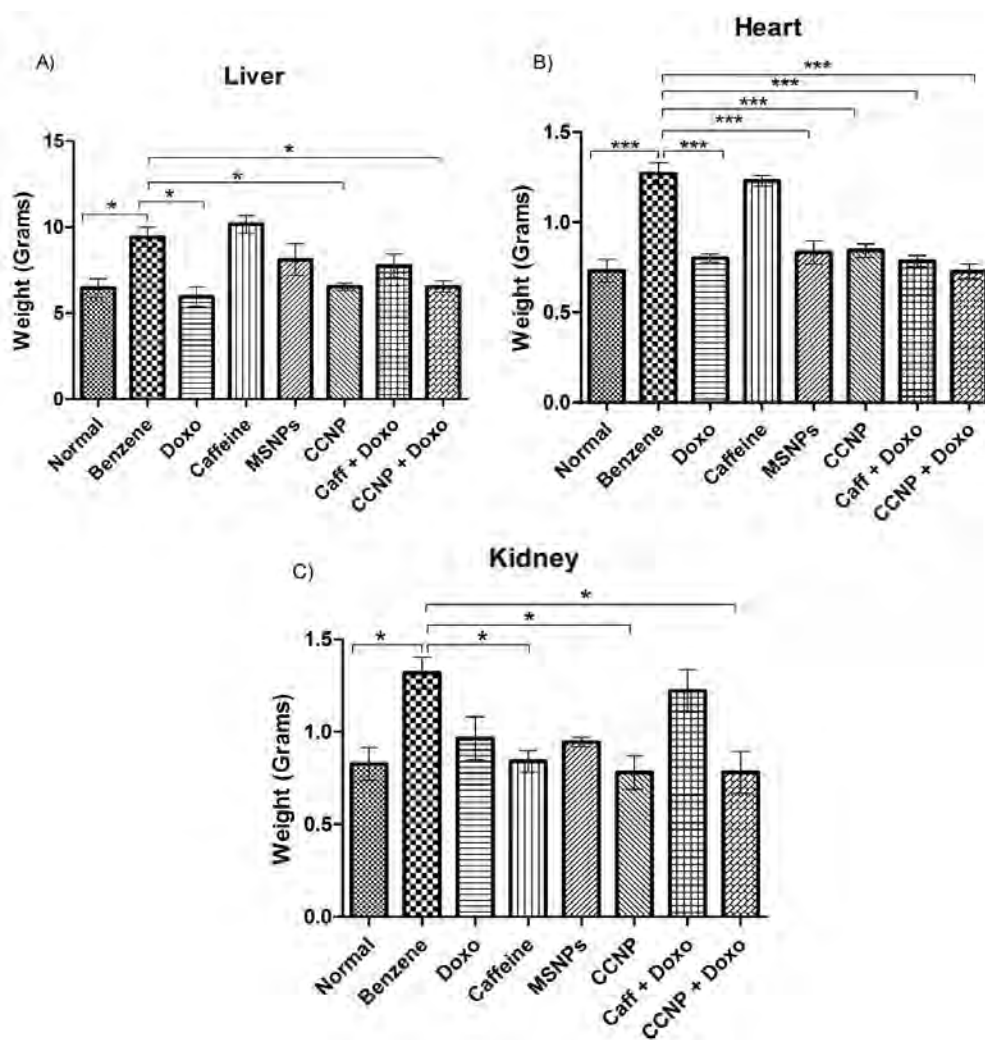


**Figure 2.14:** Comparing the mean + SEM relative organ weights of the liver (A), heart (B), and kidney (C) in rat model ( $n=3$ ).

### 2.3.8. Blood parameters analysis

Morphological examination revealed that benzene-treated leukemic rats exhibit erythrocytosis and the appearance of leukoblasts. The nanomedicine treatment restored cell morphology, with treated groups displaying normalcy (Figure 2.15).

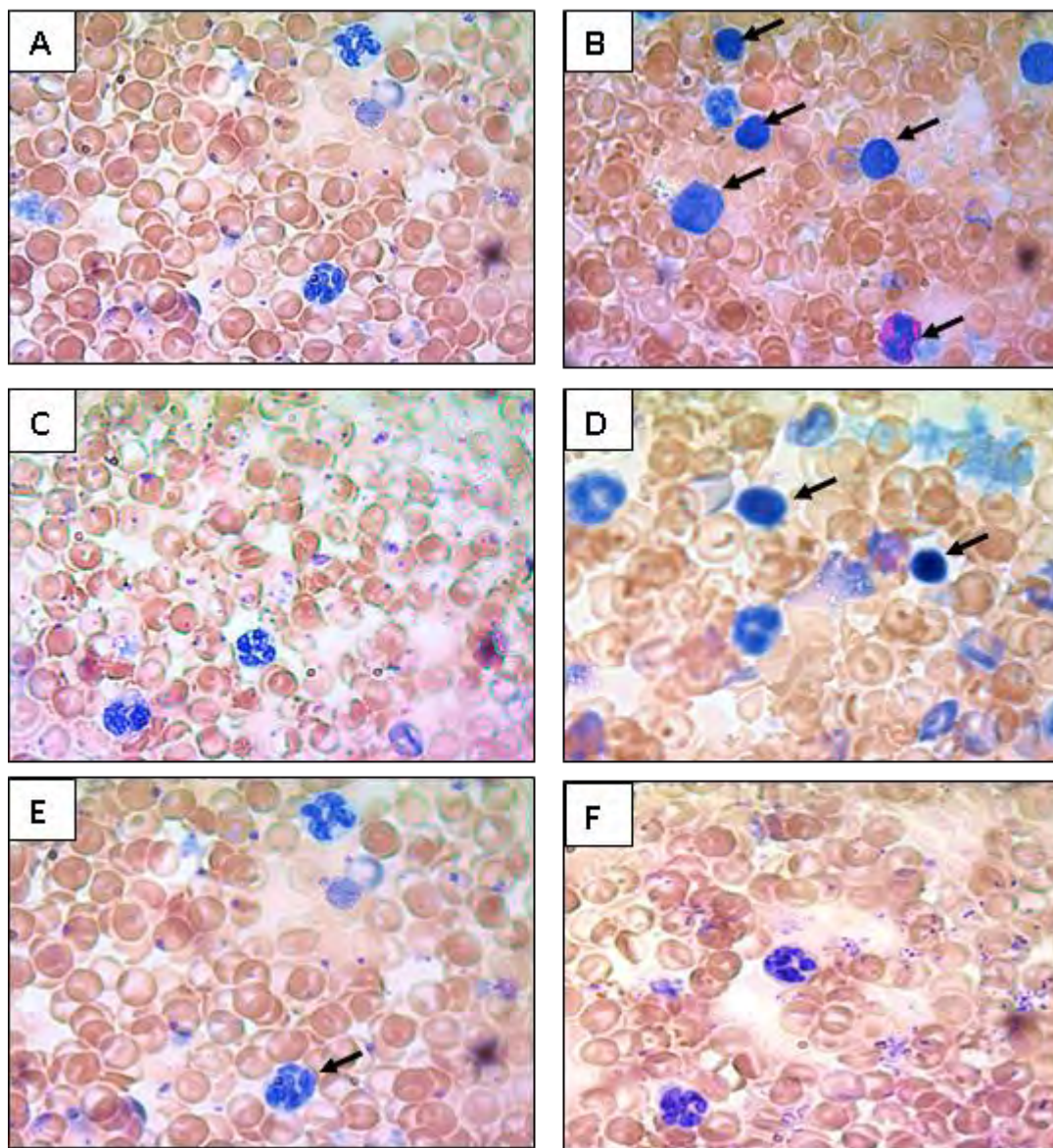


**Figure 2.15:** The morphology of blood cells in the normal (A) leukemic (B) doxorubicin (C), caffeine-treated (D), caffeine + doxo (E) CcNPs + doxo treated rat tissue (n=3) samples.

Analysis of the entire blood count in rats treated with benzene revealed a considerable increase in the total number of white blood cells and a notable decrease in red blood cells

( $p < 0.05$ ). Combinational treatment seemed to be more effective than nanomedicine alone when it comes to WBCs, particularly when nanomedicine is combined with doxorubicin (Figure 2.16A). Monocytes, eosinophils, neutrophils, and lymphocytes exhibited aberrant proliferation in leukemic rats and were favorably modulated by nanomedicine but the observed effect lacked statistical significance. Red blood cell (RBC) counts, however, significantly rebound to their normal levels after nanomedicine treatment (Figure 2.16B). Hemoglobin levels were dropped in the leukemic group ( $p < 0.05$ ), but the treatment had no considerable impact on hemoglobin levels. The platelet counts decreased considerably ( $p < 0.001$ ) upon leukemia induction and significantly increased ( $p < 0.05$ ) among the treated rats with varied degrees of effectiveness (Figures 2.16C-D).

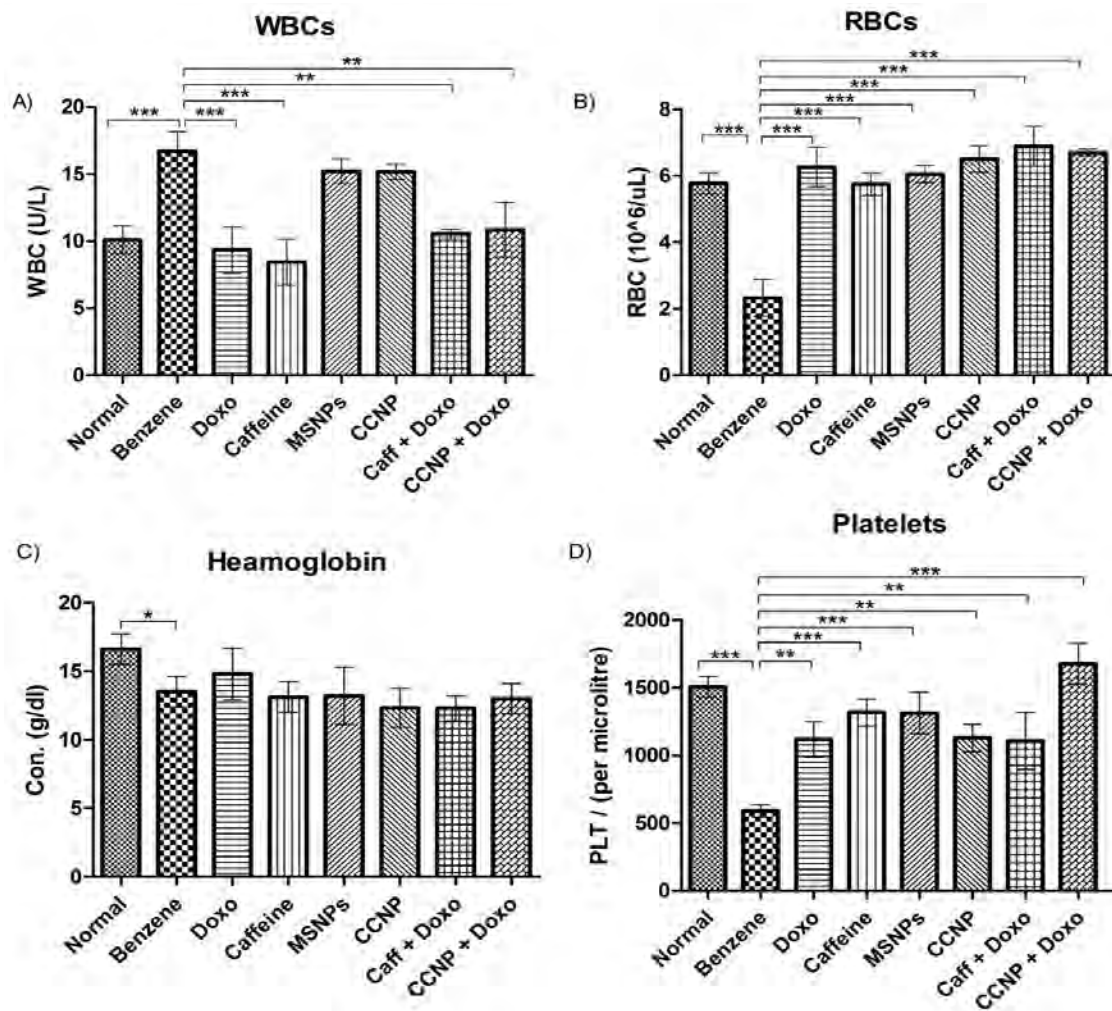


Figure 2.16: Blood parameters of different experimental groups ( $n=3$ )

### 2.3.9. Serum enzymatic analysis

Hepatic biomarkers indicated lower ( $p < 0.001$ ) ALP levels and raised ( $p < 0.001$ ) ALT and AST levels in benzene-treated rats, which were reverted to normal following nanomedicine administration. Following nanomedicine treatment, ALP levels dramatically rose ( $p < 0.001$ ), and ALT and AST levels significantly reduced ( $p < 0.001$ ). Other therapeutic regimens produced promising results with varied efficacy (Figure 2.17A-C). The treatment of nanomedicine effectively recovered ( $p < 0.01$ ) the normal creatinine levels, which were drastically raised ( $p < 0.05$ ) in benzene-treated rats. The combination therapeutic regimens improved renal function substantially (Figure 2.17D).

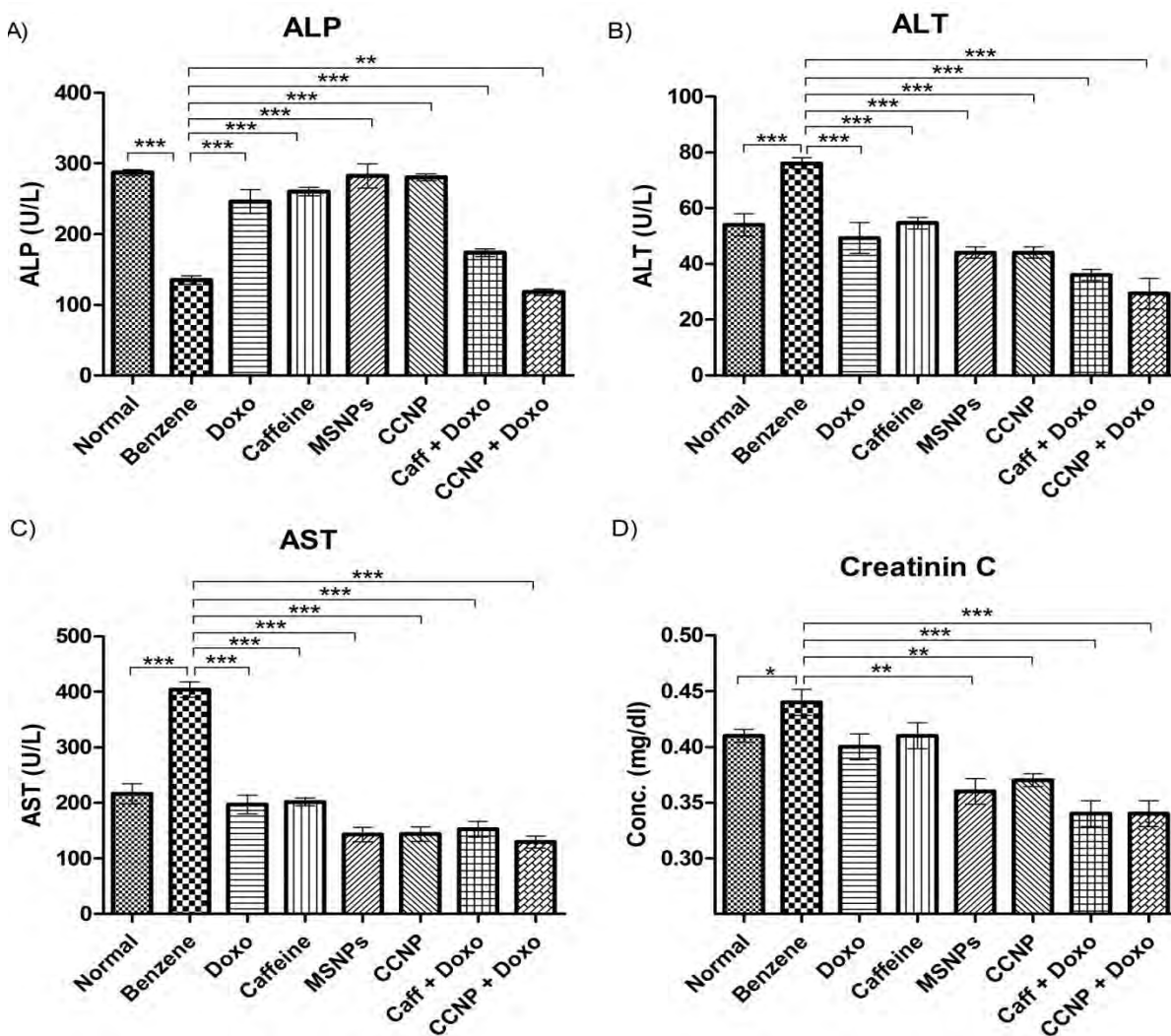


Figure 2.17: Levels of hepatic and renal biomarkers among various experimental groups ( $n=3$ ).

### **2.3.10. STMN1 expression analysis**

AML is distinguished by STMN1 overexpression, which acts as a genetic marker for the illness. STMN1 expression was significantly increased in the benzene-treated group ( $p < 0.001$ ), indicating AML induction. Treatment with the nanomedicine, on the other hand, resulted in a substantial decrease in STMN1 expression ( $p < 0.001$ ) (Fig 2.18A).

### **2.3.11. Tumor suppressor gene p53 expression analysis**

The genome's guardian, p53, mainly works as a tumor suppressor gene, and its expression is regularly modified during the initiation of cancer. The normal genetic expression of p53 is restored following nanomedicine treatment ( $p < 0.001$ ), but it was decreased after AML development in our leukemic rat model (Figure 2.18B).

### **2.3.12. Nanomedicine regulates glycolysis in leukemic rats**

GAPDH serves as a molecular biomarker of cellular energy production, playing a pivotal role as an enzyme in the sixth phase of glycolysis. After benzene injections, a significant increase in GAPDH genetic expression was observed, indicating heightened energy production and cellular proliferation. Conversely, treatment with the nanomedicine led to a notable reduction in GAPDH expression ( $p < 0.001$ ). Additionally, combinations involving caffeine, doxorubicin, and other drugs also demonstrated beneficial effects. (Figure 2.18C).

### **2.3.13. mTOR pathway regulation by nanomedicine**

The mTOR protein kinase, a serine/threonine kinase, plays a pivotal role in regulating transcription, cell growth, proliferation, and survival. Benzene induction markedly elevates the expression of mTOR, whereas nanomedicine delivery significantly reduces it ( $p < 0.001$ ). Additionally, as depicted in Figure 2.18D, other combinations also demonstrate substantial efficacy ( $p < 0.001$ ).

#### **2.3.14. Nanomedicine inhibits the NF-kappa B pathway, resulting in anti-proliferative effects**

The NF-kappa B pathway is known to play a pivotal role in governing somatic cell proliferation, particularly in acute myeloid leukemia (AML). In experiments conducted on leukemic rats, a pronounced upregulation of the expression of NF-kappa B pathway genetic markers, namely Rel-A and Rel-B, was observed, suggesting heightened proliferation activity. However, when these rats were treated with nanomedicine, either as a standalone treatment or in conjunction with doxorubicin, a noteworthy decrease in Rel-A expression was observed ( $p < 0.001$ ). This reduction signifies a significant inhibitory effect on the aberrant proliferation associated with AML, highlighting the potential therapeutic efficacy of the nanomedicine in targeting the NF-kappa B pathway in leukemia treatment. Moreover, both doxorubicin and the nanomedicine, either alone or combined, led to a substantial decrease in Rel-B expression ( $p < 0.001$ ), suggesting suppression of the non-canonical pathway (Figure 2.18E-F).

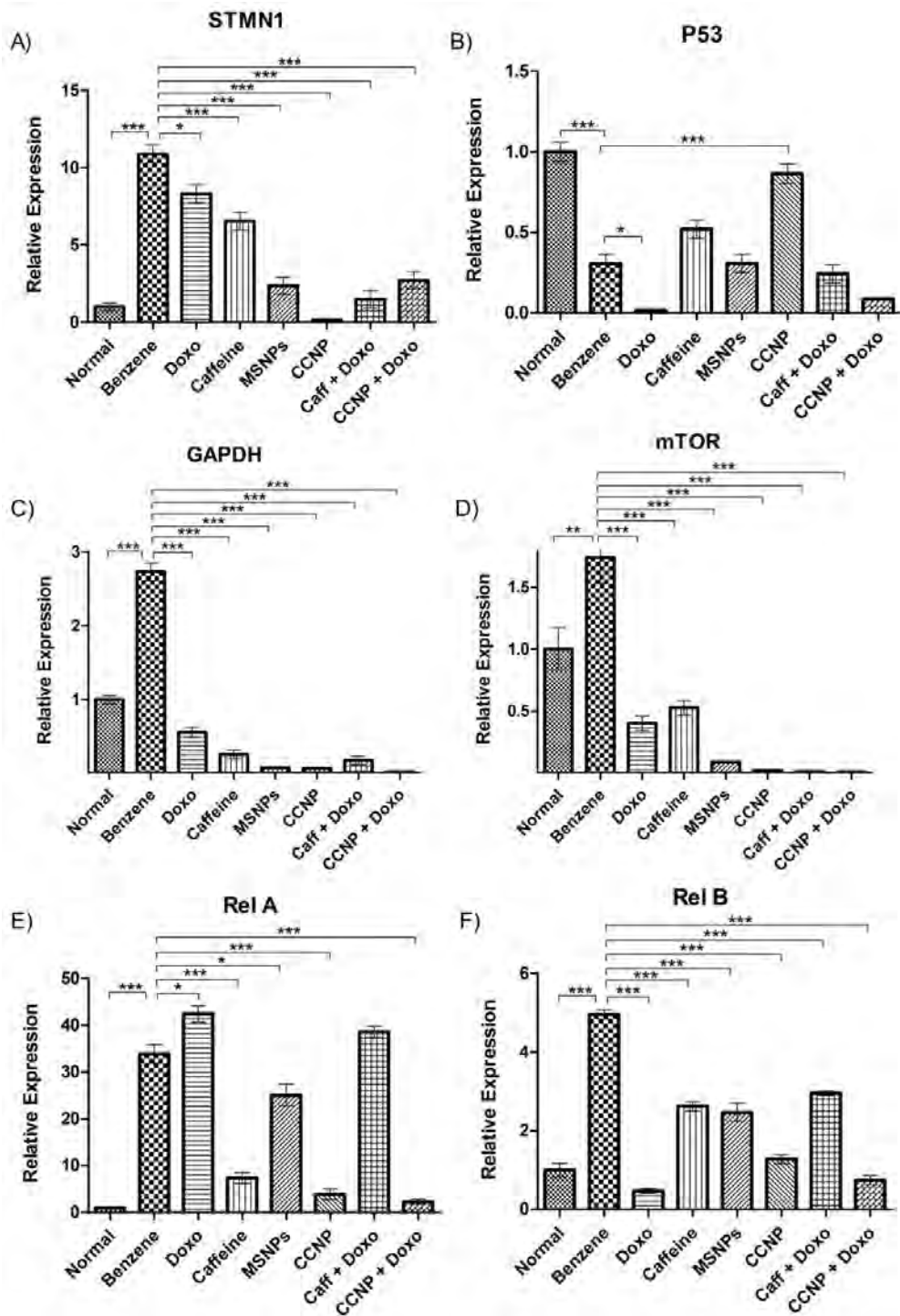


*Figure 2.18: Genetic expression analysis of molecular markers among various experimental groups (n=3).*

### **2.3.15. Regulation of TRAIL pathway by CcNPs**

Benzene impacts specific cellular proteins involved in controlling cell death processes through the extrinsic TNF-related apoptosis-inducing ligand (TRAIL) pathway. In our model, it reduced the expression of the death receptor 5 (DR5) and increased the presence of the inhibitory protein FLIP as shown in figure 2.19A-B. However, CcNPs effectively countered these effects caused by benzene exposure. CcNPs not only restored the expression of DR5 significantly but also synergistically amplified its levels when combined with classical chemotherapy (Figure 2.19C).

Moreover, CcNPs potentially inhibited apoptosis by reducing the levels of the anti-apoptotic protein cFLIP. Benzene induced an increase in the TRAIL ligand expression, which was normalized back to original levels when treated with the nanomedicine. Benzene exposure led to elevated levels of cytochrome c in leukemic cells. Different medication protocols, including the use of nanomedicine, effectively restored these levels as shown in figure 2.19D.

The nanomedicine did not alter much the expression patterns of caspases 3, 7, 8, and 9, which are pro-apoptotic proteins of the extrinsic pathway.



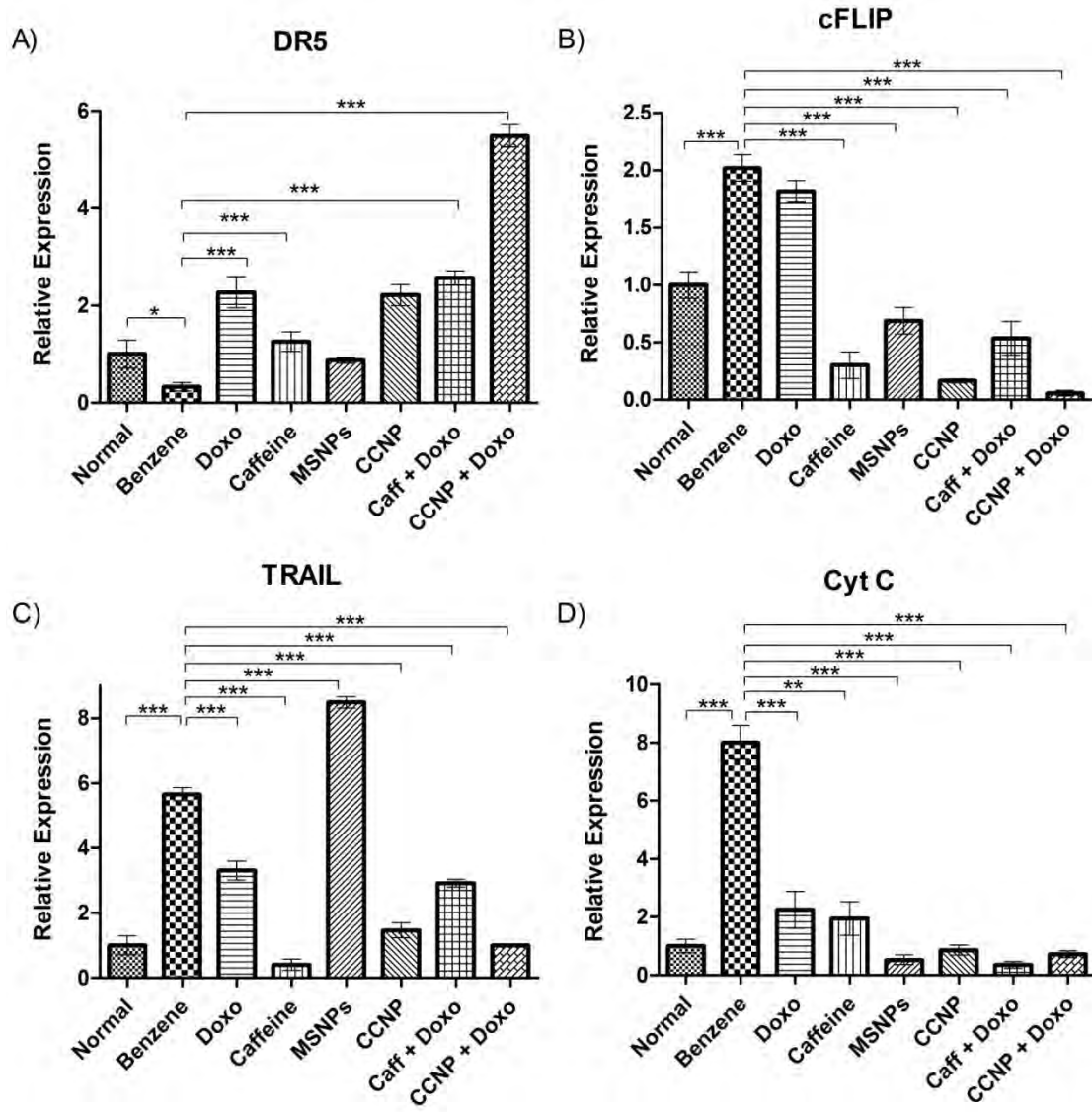


**Figure 2.19: Relative gene expression of TRAIL pathway components in different experimental groups (n=3).**

## 2.4. Discussion

Nanoparticles are extensively utilized for drug delivery due to their ability to mitigate unintended side effects by effectively traversing both blood-brain and cell membrane barriers. This capability enables them to overcome the main challenge of delivering drugs to specific sites within the body (Zhang *et al.*, 2010).

Scanning electron microscopy (SEM) corroborated the hollow spherical morphology of mesoporous silica nanoparticles (MSNP), providing additional insights into particle size.

Additionally, X-ray diffraction (XRD) data corroborated the findings, confirming both the size and shape of the particles, which aligns with previously published data (Ferreira *et al.*, 2015). The observed peaks in the MSNP spectra corroborated the existence of SiO<sub>2</sub> (silicon dioxide), providing further support that aligns with previous findings reported in studies (Jiao *et al.*, 2012). The results obtained from both FTIR (Fourier-transform infrared) and UV analyses were consistent, indicating the successful deposition or coating of caffeine onto the surface of the MSNPs. This congruence in outcomes from these analyses serves as confirmation of the caffeine coating on the nanoparticles (Nandiyanto *et al.*, 2009).

Through *in silico* simulations, the investigation focused on understanding how nanomedicine interacts with the active sites of specific proteins or complexes. This exploration was prompted by the detection of caffeine on the outer surface of the nanomedicine particles in the FTIR results. In the study, the interactions between caffeine (identified on the surface of the nanomedicine) and active site residues were examined, utilizing caffeine as a substrate. Prior studies have asserted that quinacrine (QC), a known substrate, induces cellular death by modifying both the TRAIL-DR5 complex and the intrinsic mitochondrial route (Das *et al.*, 2017). QC and caffeine were compared in terms of their binding affinity and interactions. The binding affinity values were measured at -6.5 for QC and -6.8 for caffeine, indicating slightly higher affinity for caffeine. Caffeine displayed multiple hydrogen bonds with the active site of the target complex, surpassing the number observed for QC interactions (Das *et al.*, 2017).

Furthermore, it was observed that QC attached to the edge of the protein complex, forming the QC-TRAIL-DR5 complex. Concurrently, caffeine also became integrated into the protein complex, resulting in the caffeine-TRAIL-DR5 complex. Caffeine exhibited robust hydrogen bonds with the TRAIL-DR5 complex, facilitated by its exposed hydrophilic ends. Additionally, Van der Waals contacts were observed due to caffeine's exposed non-polar ends (alkyl groups), while the ligand's aromatic rings induced pi-pi stacking and pi-pi T-shaped interactions. The extensive hydrogen bonding interactions suggested that caffeine serves as a promoter of the TRAIL-DR5 complex. The plethora of interactions between caffeine and proteins supports the proposition that the CcNP-TRAIL-DR5 complex is notably more stable than the QC-TRAIL-DR5 complex (Safa *et al.*, 2008).

The p52:RelB:κB DNA complex identifies the DNA backbone as asymmetrical, primarily due to its direct interaction with the protein via ARG 125. Previous *in vitro* binding experiments and cell-based reporter assays have demonstrated that the presence of Arginine 125 within the p52:RelB complex is essential for binding and the subsequent activation of transcription at certain κB sites, although this requirement is not universal across all such sites (Fusco *et al.*, 2009).

According to our docking studies, ARG 119 and ARG 125 display interactions with caffeine, leading to steric incompatibility with the DNA at the ligand's binding site. This interaction ultimately causes a hindrance that interferes with the binding of the DNA to the complex. Consequently, caffeine, when administered as nanomedicine, behaves as a competitive inhibitor, affirming the inhibitory action of the ligand. This inhibition effectively prevents the formation of the complex.

c-FLIP functions as a crucial regulator of apoptosis triggered by death ligands. This procaspase-8-like molecule plays a pivotal role by binding to FADD (Fas-associated death domain) and/or caspase-8 or -10, depending on the presence of specific ligands. By doing so, it effectively suppresses apoptosis initiated by various death-inducing factors such as TNF-α, Fas ligand (Fas-L), and TRAIL. This suppression halts the formation of the death-inducing signaling complex (Studio), consequently preventing the activation of the apoptotic cascade (Safa *et al.*, 2008). Recent studies have indicated that dapagliflozin induces apoptosis by decreasing the expression of cFLIP-L (cellular FLICE-like inhibitory protein - long isoform) and enhancing the instability of cFLIP-S (short isoform of cFLIP) in human kidney cancer. This study suggests that targeting of FLIP is crucial for countering evasion of apoptosis in human cancers (Jang *et al.*, 2022).

In our study, we conducted docking simulations of caffeine and dapagliflozin within the structure of c-FLIP, building upon the previous discovery. Despite dapagliflozin demonstrating a lower binding affinity (-6.5) compared to caffeine, the nature of interactions differed. Dapagliflozin engaged in Van der Waals' and pi-alkyl interactions, while caffeine established not only Van der Waals' interactions but also hydrogen bonds. Interestingly, caffeine's interaction pattern resembled that of procaspase-8, indicating its potential as an effective competitor of cFLIP. Subsequent relative expression analysis

---

confirmed caffeine's ability to down-regulate cFLIP, corroborating the anticipated impact based on its interactions within the c-FLIP structure.

The observed rise in organ weights documented in *in vivo* experiments could potentially be linked to the impact of benzene metabolites. These metabolites have a direct effect on these organs, leading to the generation of free radicals associated with hypertrophy, which might explain the observed increase (Rana & Verma, 2005). Nevertheless, the swift restoration of organ weights across all treatment protocols presents compelling evidence supporting the protective influence of nanomedicine against benzene-induced hypertrophy. This suggests that the use of nanomedicine significantly mitigates the effects caused by benzene on organ sizes.

Benzene metabolites, including phenol, catechol, and hydroquinone, are linked to the development of acute myeloid leukemia. Morphological examinations reveal that benzene induces erythrocytosis through these cytotoxic metabolites, leading to a reduction in the overall red blood cell count. Additionally, other abnormalities such as elevated levels of eosinophils and leukocytes are observed due to the effects of benzene metabolites (Smith *et al.*, 2011). Likewise, benzene induces various abnormalities in bone marrow cells, disrupting the normal development of leukocytes. This disruption leads to an overall increase in the white blood cell (WBC) count, resulting in higher levels of immature leukoblasts present in the blood of individuals affected by leukemia caused by benzene exposure (Greenwood *et al.*, 2006). In our investigation, consistent findings were observed.

Various medication regimens were successful in restoring a normal blood profile in leukemic rats by counteracting erythrocytosis, eosinophilia, and leukocytosis. These treatments effectively reversed the abnormal blood cell counts and restored them to typical levels (Smith *et al.*, 2011). Caffeine has the capability to trigger G2/M arrest, a phase within the cell cycle where the cells are halted before entering the mitotic phase. Additionally, caffeine has been reported to induce apoptosis, which is programmed cell death, specifically in leukemic cells (Ito *et al.*, 2003). The decrease in platelet levels observed in our study is likely a result of the harmful impact on bone marrow cells induced by the administration of benzene. However, notably, the use of nanomedicine as a

treatment significantly increased platelet counts by mitigating or reversing thrombocytopenia, the condition characterized by low platelet levels (Olsson *et al.*, 2005).

Benzene has been observed to disrupt the normal levels of ALP, ALT, and AST due to the production of reactive oxygen species (ROS) by its secondary metabolites. The liver, being one of the organs specifically affected by benzene toxicity, experiences alterations in these enzyme levels as a consequence of oxidative stress induced by benzene metabolites (Ito *et al.*, 2003) In benzene-induced leukemic rats, the observed decrease in ALP levels was attributed to the absence of detectable leukocyte alkaline phosphatase (LAP) mRNA, which is a characteristic finding in AML. This absence of LAP mRNA contributes to the reduction in ALP levels.

On the other hand, the rise in ALT levels in leukemic rats was potentially linked to the abnormal proliferation of liver cells. This abnormal proliferation might result in increased alanine transaminase activity, leading to elevated ALT levels in the blood (Farrow *et al.*, 1997). Similarly, the increase in AST concentration in the blood serum reflects hepatocytotoxicity and the damage caused to liver cells due to benzene exposure. Elevated AST levels often indicate liver injury induced by benzene.

Furthermore, the administration of benzene resulted in increased serum creatinine levels, which can serve as a predictor of acute kidney injury in leukemic rats. This elevation in creatinine levels suggests potential kidney damage caused by benzene exposure in these rats (Lahoti *et al.*, 2010). However, the abnormal levels of these hepatic enzymes (ALP, ALT, AST) and creatinine, indicative of liver and kidney damage, were notably restored to normal levels following treatment with our nanomedicine. This restoration could likely be attributed to reduced cytotoxicity and an increase in antioxidant potential conferred by the nanomedicine, effectively mitigating the detrimental effects induced by benzene exposure on the liver and kidneys.

Genetic expression analysis was conducted by homogenizing liver cells, considering the liver's significant role as the primary site for metabolizing various xenobiotic substances, such as benzene. In this analysis, STMN1, known for its notable overexpression in AML, exhibited elevated expression levels in leukemic rats exposed to benzene. This heightened expression of STMN1 serves as confirmation at the genetic level of the induction of

leukemia caused by benzene administration in these rats (Handschuh *et al.*, 2018). Treatment with CcNPs appeared to mitigate the impact of benzene by reducing STMN1 expression. This reduction in STMN1 expression potentially influences the function of actin and the dynamics of microtubules within cells. By decreasing STMN1 levels, CcNPs treatment likely contributes to altering the cellular dynamics regulated by these structural proteins, consequently minimizing the effects induced by benzene exposure (Wu *et al.*, 2014).

The loss of P53, a common tumor suppressor, is a frequent genetic alteration observed in various malignancies. In AML, increased P53 expression is often observed due to mutations and DNA damage induced by reactive oxygen species (ROS). Remarkably, our nanomedicine was able to restore aberrant P53 levels in leukemic rats. This correction is likely attributed to the nanomedicine's abilities, acting as both a pro-apoptotic agent and an antioxidant. Additionally, caffeine's known capability to inhibit lipid peroxidation caused by ROS might have contributed to this repair process (Devasagayam *et al.*, 1996).

The observed overexpression of GAPDH in the benzene-treated group could potentially be linked to an increase in glycolysis. Enhanced glycolysis is recognized as a hallmark of cancer, and increased expression of GAPDH might be associated with this metabolic shift, reflecting the altered energy metabolism characteristic of cancer cells (Hanahan & Weinberg, 2011; Ward & Thompson, 2012). However, the administration of our nanomedicine, along with other treatment regimens, resulted in the restoration of normal GAPDH expression levels. This normalization was likely achieved by restoring cellular energetics and restraining the excessive proliferation observed in transformed cells. The intervention of these treatments seems to have effectively counteracted the aberrant GAPDH expression, thereby contributing to the normalization of cellular metabolism and proliferation (Jiang *et al.*, 2011)

mTOR (mechanistic target of rapamycin), a pivotal signal transducer both within cells and in the extracellular environment, was found to be heightened in the benzene-treated groups. This protein plays a central role in governing several fundamental cellular processes including growth, proliferation, and cell survival. Additionally, mTOR is involved in regulating the growth of leukemic cells, facilitating tumor-associated angiogenesis, and

controlling the expression of vascular endothelial growth factor (Fruchon *et al.*, 2012). The heightened activity of the mTOR protein observed in this context may also link to its recognized capacity to recruit microRNAs, which subsequently silence apoptotic genes. This process contributes to the development or progression of leukemogenesis, as it suppresses the expression of genes involved in programmed cell death (Martelli *et al.*, 2011). The administration of our nanomedicine notably reduced the levels of mTOR, which might be attributed to its pro-apoptotic capabilities. This reduction in mTOR levels suggests that the nanomedicine likely influences cellular pathways associated with apoptosis.

Rel A and Rel B, both components of the NF-kappa B pathway, are known to support cell survival in AML. This is evidenced by the observed increase in their mRNA transcripts during leukemogenesis. Their heightened expression indicates their role in promoting cell survival within AML, suggesting their involvement in sustaining the disease by contributing to the survival and proliferation of leukemic cells (Xu *et al.*, 2014). Doxorubicin, known for its ability to induce apoptosis primarily through the production of reactive oxygen species, led to a reduction in Rel B levels. This decrease in Rel B expression could be linked to doxorubicin's apoptotic effects, indicating that the drug's mechanism of action involves the suppression or downregulation of Rel B within the NF-kappa B pathway (Tapia *et al.*, 2007). In the case of Rel A, doxorubicin-induced DNA damage activated the conventional NF-kappa B pathway, potentially contributing to doxorubicin resistance in leukemic cells. This might explain the observed high levels of Rel A expression in rats treated with doxorubicin.

However, our nanomedicine exhibited the ability to downregulate indicators of the NF-kappa B pathway, including Rel A and Rel B, both individually and in combination. This suggests that the nanomedicine possesses anti-proliferative and anti-tumor potential in leukemic rats. This effect is likely due to the properties of caffeine, which has demonstrated anti-survival and inhibitory effects against Rel A and Rel B. In the form of nanomedicine, these properties might be enhanced, as the mesoporous silica nanoparticles improve the bioavailability, stability, and half-life of the coated caffeine, as previously described (Szatkowska *et al.*, 2013).

In studying the role of apoptosis, the TRAIL pathway has been extensively investigated. The observed increase in the expression of the TRAIL ligand in benzene-treated rats is not unexpected, considering that numerous benzene derivatives are recognized for their involvement in TRAIL-mediated cell death. This elevation in TRAIL ligand expression aligns with the well-established association between benzene derivatives and the initiation of cell death through the TRAIL pathway (Ahn *et al.*, 2018). The overexpression of cFLIP functions to inhibit the activity of TRAIL in leukemic rats. This heightened expression of cFLIP serves to counteract or block the activity of TRAIL-induced apoptosis, effectively suppressing the cell death signals triggered by the TRAIL pathway in these leukemic rats (Sayers *et al.*, 2003).

FLIP shares homology with procaspase 8 and competes for binding with death-effector-domain of FADD molecule. High FLIP expression renders binding of procaspase 8 unlikely and thereby blocks the downstream activation of caspases and consequently inhibits apoptosis (Mérino *et al.*, 2006).

It seems that our nanomedicine acts as a potent regulator of the TRAIL pathway and an inducer of apoptosis. This is suggested by the considerable increase in the expression of the TRAIL ligand and the simultaneous decrease in cFLIP levels upon nanomedicine treatment. Furthermore, there was an enhancement observed in the expression of DR5, which supports the effectiveness of the nanomedicine in modulating the TRAIL pathway.

Notably, when the nanomedicine was used in combination with chemotherapy, there was an even greater elevation observed in DR5 expression levels. This indicates a potential mechanism of interaction between the nanomedicine and chemotherapy, suggesting a synergistic effect in enhancing DR5 expression, possibly through a cross-linking mechanism (Mérino *et al.*, 2006).

An increase in DR5 levels in response to treatment represents a crucial step towards TRAIL-induced apoptosis through extrinsic mechanisms. However, merely elevating the death receptors is insufficient to trigger apoptosis; their functional activation by forming trimers is also essential for inducing cell death. As we did not observe an increase in initiator or effector caspases, we suggest exploring the use of agonistic antibodies in future



---

studies to enhance the functional efficiency of death receptors in triggering apoptosis (El-Gazzar *et al.*, 2010).

Furthermore, the heightened cytochrome-c levels in leukemic rats indicate rapid production and release from mitochondria due to mitochondrial membrane breakdown and subsequent cell death. Nevertheless, treatment with various pharmacological regimens restored cytochrome-c levels to normal values, presumably attributed to their antioxidant and other protective properties, helping to mitigate the consequences of mitochondrial damage.

---

## **Chapter 3: CuET nanoparticles**

***In silico, in vitro, and in vivo* analysis of copper-diethyldithiocarbamate nanoparticles and doxorubicin: a novel combination strategy against AML**

### 3.1. Introduction

Leukemia is a group of clinical disorders characterized by the unregulated expansion of pluripotent bone marrow stem cells, which results in aberrant cellular proliferation and neoplasms (Ramdass *et al.*, 2013). Acute myeloid leukemia (AML) is the most common kind, resulting from the malignant transformation of early progenitor or hematopoietic stem cells (Khwaja *et al.*, 2016). Extrinsic factors that contribute to the formation of AML include infectious agents such as viruses, tobacco smoke, radiation, and chemicals such as benzene and polychlorinated biphenyls (Bhatia & Das, 2020). Benzene stands as the most prevalent causative agent for AML (McHale *et al.*, 2012). The primary metabolism of benzene occurs in the liver, where it is transformed into a variety of phenolic and opened-ring compounds, as well as various conjugates. All of these metabolites are harmful to bone marrow and hematopoietic stem cells (HSCs), where they cause redox reactions by creating reactive oxygen species, resulting in cellular genotoxicity. This eventually results in the creation of protein adducts, which change cellular progression and impair cellular processes, leading to the development of AML (Ross, 1996).

Several traditional chemotherapeutic drugs, including doxorubicin, are used to treat and manage AML. Doxorubicin, an anthracycline antibiotic, has been used for over three decades to treat a variety of malignancies, including both haematological and solid tumors (Chen *et al.*, 2013). So far, several modes of action for doxorubicin's cytostatic and cytotoxic properties have been hypothesized. These include 1) intercalating with DNA bases to inhibit macromolecule synthesis, 2) production of ROS, which leads to the initiation of DNA damage, 3) peroxidation of lipids, 4) disruption of strand separation of DNA and helicase activity, and 5) causing direct damage to DNA by inhibiting topoisomerase II. All of these ways of action eventually result in apoptotic cell death. However, doxorubicin not only targets cancer cells but also affects the body's normal developing cells, resulting in inevitable side effects such as double stranded DNA breaks and death in normal cells (Lu *et al.*, 2007).

This non-specific targeting of conventional therapy underlines the need for innovative therapeutic molecules with lower toxicity and greater efficacy than currently available conventional chemotherapeutic medicines (Castro *et al.*, 2019). To address this issue, the

use of targeted nanoparticles to administer chemotherapeutic agents in cancer therapy provides several benefits in terms of improving drug delivery and overcoming many of the issues associated with traditional chemotherapy (Nguyen, 2011). Nanoparticles have a unique ability to boost the intracellular accumulation of medicines or genes selectively within cancer cells, whether through passive or active targeting methods. This targeted delivery reduces toxicity in normal cells, providing a dual benefit of increased therapeutic efficacy in tumors while protecting the health of surrounding healthy tissues.

Organometallic compounds in the form of nanoparticles are useful in the creation of site-specific drug delivery systems in this respect (Bajracharya *et al.*, 2023). Copper-diethyldithiocarbamate (CuET) is an organometallic complex composed of copper as the core metal atom, coupled with amine-1-carbodithionic acid (a dithiocarbamate derivative) (Paun *et al.*, 2022). The capacity of the complex to chelate copper and its lipophilic characteristics are of importance in cancer treatment. Copper plays important functions in biological activities on its own, but when coupled to certain chemicals such as diethyldithiocarbamate, it can have deadly effects on cancer cells. This happens through a variety of ways, including the production of reactive oxygen species (ROS), which cause oxidative stress, cellular damage and apoptosis (Dumut *et al.*, 2021). Moreover, copper is involved in angiogenesis (the formation of new blood vessels), a critical process in tumor growth and metastasis. Chelation of copper by compounds like diethyldithiocarbamate can hinder angiogenesis, thereby impeding tumor progression (Ji *et al.*, 2023). Additionally, these complexes might interfere with specific signaling pathways crucial for cancer cell survival and proliferation (Huang *et al.*, 2021).

This study aimed to look at the anti-leukemic effectiveness of CuET in combination with doxorubicin, as well as the expression levels of biomarkers linked with the HIF-1 $\alpha$  and Wnt pathways in AML rat model.

## **3.2. Materials & Methods**

### **3.2.1. Materials**

Methanol, HCl , dimethyl sulfoxide (DMSO) , benzene , doxorubicin, TRIzol, cDNA synthesis Vivantis kit, EvaGreen® Master mix.

### **3.2.2. Characterization of CuET using XRD, SEM and EDX analysis**

CuET nanoparticles were characterized using XRD, SEM and EDX analysis using already published protocols respectively (Merroun *et al.*, 2003; Parmar *et al.*, 2012; Hua & Yu, 2019).

### **3.2.3 Molecular docking studies**

The docking of hyaluronic acid (ligand) present on the surface of coated CuET to the active site of CD33 AML marker was conducted with the help of PyRx (v.0.8; Kitware, Inc., NY, USA)(Kondapuram *et al.*, 2021) and Autodock (Vina v.1.2.5) (Trott & Olson, 2010). The findings of the protein-ligand interactions were consistent with the values predicted by quantum chemistry simulations, and Autodock was used to lower the ligand's energy (Mirzaei *et al.*, 2015). The binding affinity values were then analysed to assess various interactions.

### **3.2.4. Cytotoxicity Assay**

To ascertain the most effective dosage of CuET, brine shrimp assay was performed. In a sea salt solution, brine shrimp eggs were hatched. Following that, fifteen brine shrimp were methodically counted under a microscope and treated to several levels of dilution for 24 hours. Each concentration was reproduced three times using distilled water as a control to verify accuracy. Using the probit approach, the lethal concentration necessary to generate a 50% death rate (LC<sub>50</sub>) was estimated after 24 hours of exposure (Banti & Hadjidakou, 2021).

### **3.2.5. In Vitro Bioassays**

The evaluation of antioxidant capacity involved three different assays. The determination of total antioxidant capacity was carried out using the phosphomolybdenum method (Jamuna, Ramesh, Srinivasa, & Raghu, 2011), with minor adjustments to the procedure.

Similarly, the assessment of total reducing power and the DPPH assay were performed as per protocols previously outlined by Moein and colleagues (Moein *et al.*, 2008).

### **3.2.6. In Vivo Bioassays**

The assessment of the analgesic efficacy of various treatment regimes was assessed through the hot plate assay (Tita *et al.*, 2001). Likewise, the evaluation of anticoagulant activity, which determines the coagulation time of blood in the absence of any foreign substance, was carried out using already reported protocol (Samuelson *et al.*, 2017). Furthermore, the assessment of antidepressant activity was carried out using the conventional tail suspension method, as delineated by Zhou and colleagues (Zhou *et al.*, 2010).

### **3.2.7. Development of AML model and Experimental Strategy**

A cohort of twenty-five Sprague Dawley rats, aged five weeks and weighing between 150 to 180 grams, was sourced from the National Institute of Health in Islamabad. Ethical clearance for all experimental procedures was obtained from the Quaid-i-Azam University Institutional Review Board under letter No. #BEC-FBS-QAU2020-221. The rats were housed in pairs within laboratory cages constructed from polypropylene material, complete with stainless-steel lids, to ensure proper containment and ventilation throughout the duration of the study. Rats were fed standard rodent chow and water ad libitum at the Quaid-i-Azam University Primate Facility, which had identical photoperiods of 12 hours of light and 12 hours of darkness daily, an ambient temperature of  $298.15\text{K}$  ( $25^{\circ}\text{C}$ ) $\pm 2$ , and humidity of  $42\pm 5\%$ .

All rats ( $n = 25$ ) were divided into five equal groups of five rats each. The animals were allowed to acclimate for seven days.  $100\ \mu\text{L}$  of intravenous benzene was given to rats in groups 2, 3, 4, and 5 on alternate days for three weeks. Group 1 (Normal/control) received normal saline intravenously while all other groups were treated with benzene, as explained earlier, for the induction of AML. After AML induction, Group 2 (Benz) received no additional treatment. Rats in Group 3 (Benz + Doxo) received a normal dosage of doxorubicin ( $300\ \mu\text{L}$  of  $0.625\text{mg/mL}$ ) intravenously on alternate days for three weeks. Similarly,  $100\ \mu\text{L}$  of CuET ( $0.1\ \text{mg/mL}$  in  $0.1\%$  DMSO) was given intravenously to rats in Group 4 (Benz + CuET). Group 5 (Benz + CuET + Doxo) received both CuET and

doxorubicin intravenously on alternate days for three weeks after leukemia confirmation. All rats were dissected after their individual dosages were completed in accordance with the parameters outlined in the Guide for the Care and Use of Laboratory Animals (Care & Animals, 1986).

### **3.2.8. Morphological evaluation and tissue histology**

After dissection, blood and bone marrow smears were produced on glass slides and stained with Giemsa dye (10X) for morphological examinations. The glass slides containing streaks were air-dried for this purpose, and the dye was applied dropwise, allowing it to stain for 10 minutes. Before microscopy, the dyed slides were rinsed with tap water and air-dried again (Houwen, 2002). For tissue histology, liver, kidney, and heart tissue samples were removed and stored in 10% formalin for histological examination using Chan and colleagues' haematoxylin and eosin staining procedure (Chan, 2014).

### **3.2.9. Blood profiling and biochemical studies**

The blood complete picture (CP) was determined at RIUT, Islamabad, Pakistan, to assess total blood cell count along with other vital parameters. Biochemical diagnostic kits (LTA and AMP diagnostic kits) were used to assess alanine aminotransferase (ALT), aspartate aminotransferase (AST), and alkaline phosphatase (Malovichko *et al.*, 2004). Thermofisher Scientific's Amplex® Red Uric acid/ Uricase Assay kit was used to calculate uric acid levels. The lipid profile and lactate dehydrogenase levels were estimated using a Merk Micro Lab 300 auto-analyzer (Darmstadt, Germany).

### **3.2.10. Real time PCR analysis**

TRIzol reagent RNA extraction method was used to extract mRNA from bone marrow cells using protocol published by Chomczynski and co-workers (Chomczynski *et al.*, 2010). Nanodrop quantification on a NanoDrop™ 2000/2000c Spectrophotometer (Cat. No: ND-2000; MN, USA) and 1% agarose gel electrophoresis were conducted for quality assurance.

**Table 3.1: Materials for RNA extraction**

No.	Chemical Name	Quantity
1.	TRIZOL	1 mL/cycle
2.	Isopropanol	200 $\mu$ L /cycle
3.	Chloroform	200 $\mu$ L /cycle
4.	75% Ethanol	2 mL/cycle
5.	RNase Free Water	20 $\mu$ L /cycle

The acquired mRNAs were then used to generate cDNA using a Vivantis kit (cDSK01-050, Malaysia). Conventional PCR was used to validate the cDNA synthesis according to the manufacturer's recommendations. The required transcript was amplified by PCR by adding the reaction mixture's chemicals to 200L PCR tubes (Axygen, USA).

**Table 3.2: Reagents required for cDNA synthesis mixture**

No	Chemical Name	Amount/ Volume
1.	5X Reaction Buffer	4 $\mu$ L
2.	Revert Aid M-MuLV Reverse Transcriptase	(200 U / $\mu$ L) 1 $\mu$ L
3.	10mM dNTP mix	2 $\mu$ L
4.	RiboLock RNase Inhibitor	(20 / $\mu$ L) 1 $\mu$ L



**Table 3.3: Conventional PCR reagents**

No	Reagents	Quantity
1.	10X Taq Buffer with (NH <sub>4</sub> ) <sub>2</sub> SO <sub>4</sub>	2.5 μL
2.	MgCl <sub>2</sub> (25mM)	1.5 μL
3.	dNTPs (10mM)	0.5 μL
4.	Taq DNA polymerase (5U/ μL)	0.2 μL
5.	Forward Primer (0.4uM)	1 μL
6.	Reverse Primer (0.4uM)	1 μL
7.	cDNA Sample	1 μL
8.	Ultrapure DNase free distilled water	17.3 μL
<b>Total Reaction Volume</b>		<b>25 μL</b>

Bio Molecular Sciences (BMS) employed MIC qPCR for real-time PCR analysis of relative gene expression. The PCR reactions were conducted in a final volume of 10 μL. This volume comprised 2 μL of Syber green master mix, 1 μL each of reverse and forward primers, 5 μL of cDNA, and 1 μL of nuclease-free water. The amplification process began with an initial heat denaturation stage at 368.15K (95°C) for 15 minutes, followed by 40 cycles of denaturation at 368.15K (95°C) for 30 seconds, annealing at 333.15K (60°C) for 30 seconds, and extension at 345.15K (72°C) for 30 seconds.

Upon completion of the cycling program, a melting curve analysis was conducted. The melting curve was programmed to incrementally increase the temperature from 345.15K (72°C) to 368.15K (95°C), with each step raising the temperature by 273.15K (1°C). The software was configured to allow 118 seconds of pre-melt conditioning during the first step and 5 seconds for each subsequent step. This analysis aids in determining the specificity of the PCR products and identifying any nonspecific amplification or primer dimers. The housekeeping gene beta-actin was employed for relative genetic expression analysis. The following primer sequences were used for tested genes:

**Table 3.4: List of primers**

No	Primers Name	Primer Sequence (5' – 3')
1.	B-Actin	(F-CTCACGGTGTGCCCCAAAATG, R-GCCTTGATCCTTTGGTTATTTCG)
2.	STMN1	(F-TTGCCAGTGGATTGTGTAGAG, R-TTCTTTTGATCGAGGGCTGAG)
3.	S1009A	(F-GAAATGGTGAATAAGGACTTGCC, R-TCAACTTCCCATCAGCATC)
4.	Wnt	(F-ACGGAGTCTGACCTGATGTAG, R-CACCTGTCGCTCTCATGTAC)
5.	LRP6	(F-TGAAATGCCACCTTCTACC, R-AAGTGTCCTGAAAGTGAAG)
6.	GSK3 $\beta$	(F-ACCTGCCCTTCAACTTTAC, R-CACGGTCTCCAGCATTAGTATC)
7.	AXIN	(F-CAGCCTTCTCATCTCTTCATCC, R-GTGATTTTGCTCTGCTTGG)
8.	HIF1 $\alpha$	(F-GGTGGATATGTCTGGGTTGAG, R-AGGGAGAAAATCAAGTCGTGC)
9.	VHL	(F-TTTGGCTCTTCAGGGATGC, R-CACCGCTCTTTCAGGGTATAC)
10.	C-myc	(F-CTCGCGTTATTTGAAGCCTG, R-TCGCAGATGAAATAGGGCTG)
11.	Cox 2	(F-TCAAGGGAGTCTGGAACATTG, R-GCTTCCCAACTTTTGTAACCG)
12.	VEGF	(F-AAAGCCAGCACATAGGAGAG, R-ATTAAACCGGATTTCTTGCG)
13.	PTEN	(F-CCACAAACAGAACAAGATGCTC, R-CAAAGACTTCCATTTCCAC)

The fold change in gene expression of the samples was determined using the Pfaffl technique, a widely used method for analyzing quantitative real-time PCR data. This

technique takes into account the efficiency of amplification of the target gene and reference gene, allowing for accurate calculation of relative expression levels.

To calculate the relative expression in real-time PCR, the pair wise fixed reallocation randomization test was employed, utilizing the Relative Expression Software Tool (REST-384, version 2). This statistical approach enables robust comparison of gene expression levels between different experimental conditions while considering experimental variation and efficiency differences between PCR runs.

Following the analysis, a melt curve analysis was conducted to identify any non-specific amplification products. qPCR products exhibiting a single peak on the melt curve graph indicate the absence of primer dimers or non-specific amplification, confirming the specificity of the PCR reaction. This step ensures the reliability of the gene expression data obtained from the real-time PCR experiments.

*Table 3.5: The reagents used for qRT-PCR*

No.	Reagents	Quantity
1	Forward Primer	1 $\mu$ L
2	Reverse Primer	1 $\mu$ L
3	cDNA	5 $\mu$ L
4	Syber Green Master Mix	2 $\mu$ L
5	Nuclease free water	1 $\mu$ L
	<b>Total Volume</b>	<b>10 <math>\mu</math>L</b>

### 3.2.11. Flow cytometry for apoptosis measurement

Cold Bio Legends Cell Staining Buffer was used to wash the sample cells twice. Annexin V binding buffer was used to re-suspend the cells at a concentration of  $0.25-1 \times 10^7$  cells/mL for the apoptosis experiment. A cell suspension of 100uL was transferred to a 5mL test tube. It received 5uL of FITC Annexin V. The solution was then treated with 10uL of propidium iodide. The cells were gently vortexed at 298.15K (25°C) before being incubated in the dark for 15 minutes. Then 400uL of Annexin V binding buffer was added to each tube before being examined on the flow cytometer.

### 3.2.12 Statistical analysis

GraphPad Prism software (version 5.01) was used to construct descriptive statistics, which were presented as  $\pm$  standard error of the mean ( $\pm$ SEM). Statistical significance was assessed using a p-value threshold of  $< 0.05$  (\*),  $p < 0.01$  (\*\*), and  $p < 0.001$  (\*\*\*). For inter-group comparisons, one-way analysis of variance (Hendrych et al.) was used, followed by Tukey's post hoc test.

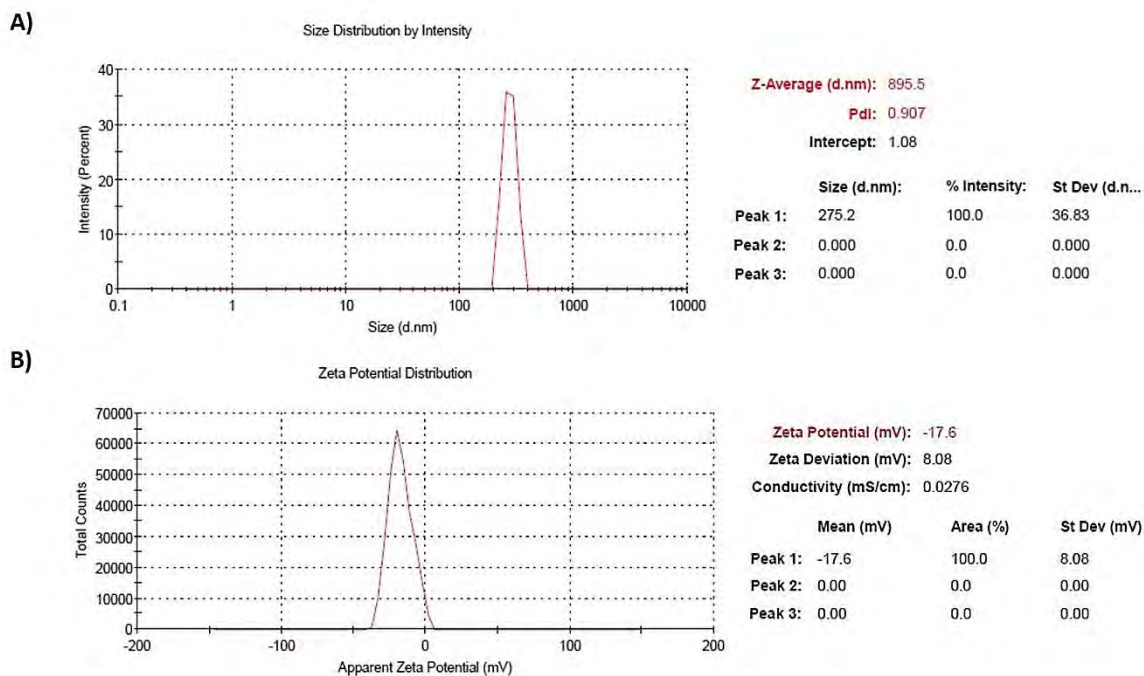
## 3.3. Results

### 3.3.1 Synthesis of CuET NPs

For this purpose, a mixture of diethyldithiocarbamate (DTC) and  $\text{CuCl}_2$  solutions was used. To synthesize CuET NPs, a 2mL (2mM) solution of  $\text{CuCl}_2$  was dropwise added to a 4mL (2 mM) solution of DTC (containing 0.4% PVP) and mixed for 5 minutes to prevent particles from clumping together. Then, the precipitate was collected by centrifugation (16,000 rpm for 15 min) and washed twice with water. The synthesized CuET were modified by adding an equivalent volume of HA (0.6 mg/mL), and stirring for 6 hours (Peng *et al.*, 2020)

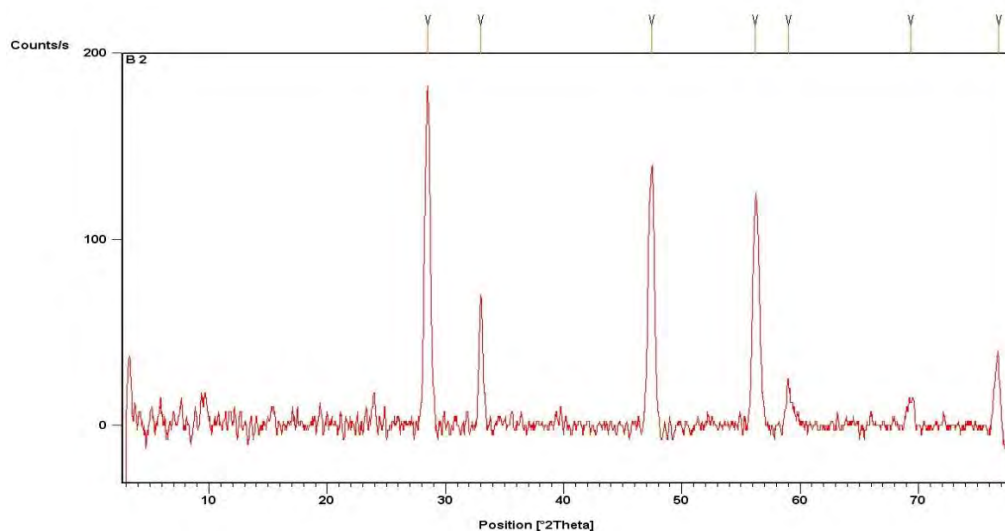
### 3.3.2. Characterization of CuET using XRD, SEM and EDX analysis

The dynamic size of CuET Nps was observed as  $\sim 275.2$  nm with population density index (PdI)  $\sim 0.907$ , while the surface charge expressed was  $-17.6$  mV due to surface coating of hyaluronic acid as in figure 3.1



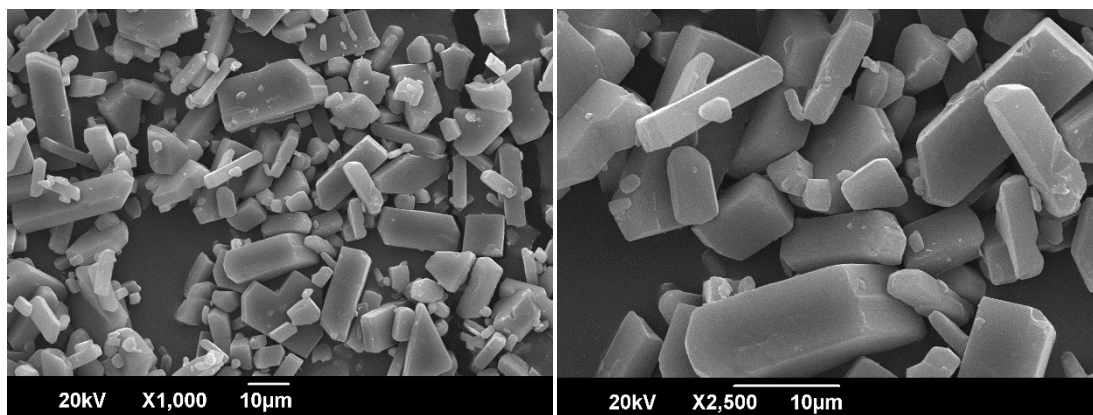
**Figure 3.1:** The dynamic light spectrum analysis confirming size of CuET

Figure 3.2 shows an XRD diffraction pattern with three major peaks at  $29^\circ$ ,  $34^\circ$ ,  $48^\circ$ , and  $67^\circ$  showing a square-planar structure of CuET crystal with overall pseudo-octahedral coordination geometry and particle size 280 nm.



**Figure 3.2:** The XRD pattern of CuET

SEM images clearly showed complex formation of metal atom with diethyldithiocarbamate complex as in figure 3.3.



*Figure 3.3: Scanning electron microscopy of CuET*

Whereas, energy-dispersive X-ray (EDX) analysis exhibited 6.7% copper, 14.4% sulphur, 5.1% oxygen, 7% nitrogen, and 66.9% carbon by weight as shown in figure 3.4 and table 3.6.

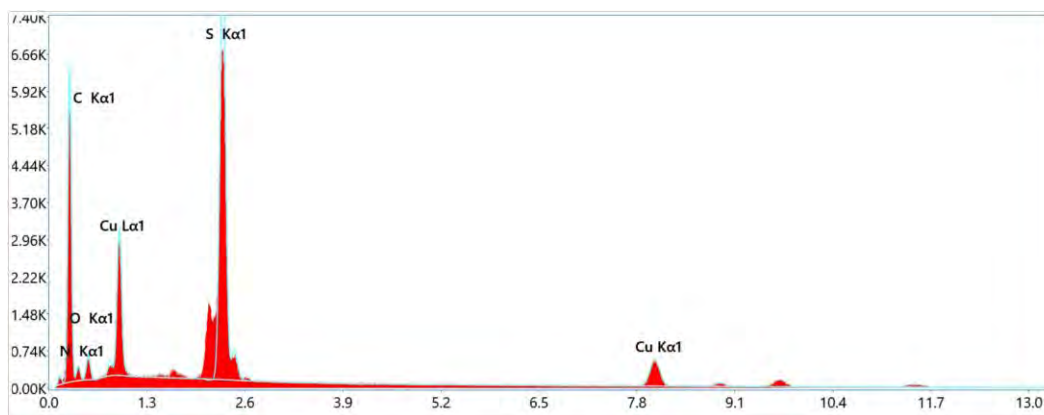


*Figure 3.4: Energy dispersive spectroscopic image of copper diethyldithiocarbamate*

**Table 3.6: Individual elements and their percentages by weight and atomic size in composition of CuET**

Element	Weight%	Atomic %
C	66.9	80.3
N	7.0	7.2
O	5.1	4.6
S	14.4	3.4
Cu	6.7	1.5

### 3.3.3 CD33 shows strong interaction with hyaluronic acid indicating enhanced CuET uptake by leukemic cells

The CD33 protein's binding site was docked with hyaluronic acid coated CuET, as illustrated in figure 3.5. Using PyRx, the binding affinity of the lowest value confirmation was determined to be -6.0, with an RMSD of 0.00. Further examination using BIOVIA Discovery Studio revealed the existence of hydrogen bonds and van der Waals interactions. Interestingly, typical hydrogen bond interactions are identified between the ligand and the receptor amino acid GLY A:69, showing improved absorption of CuET by CD33+ leukemic cells.

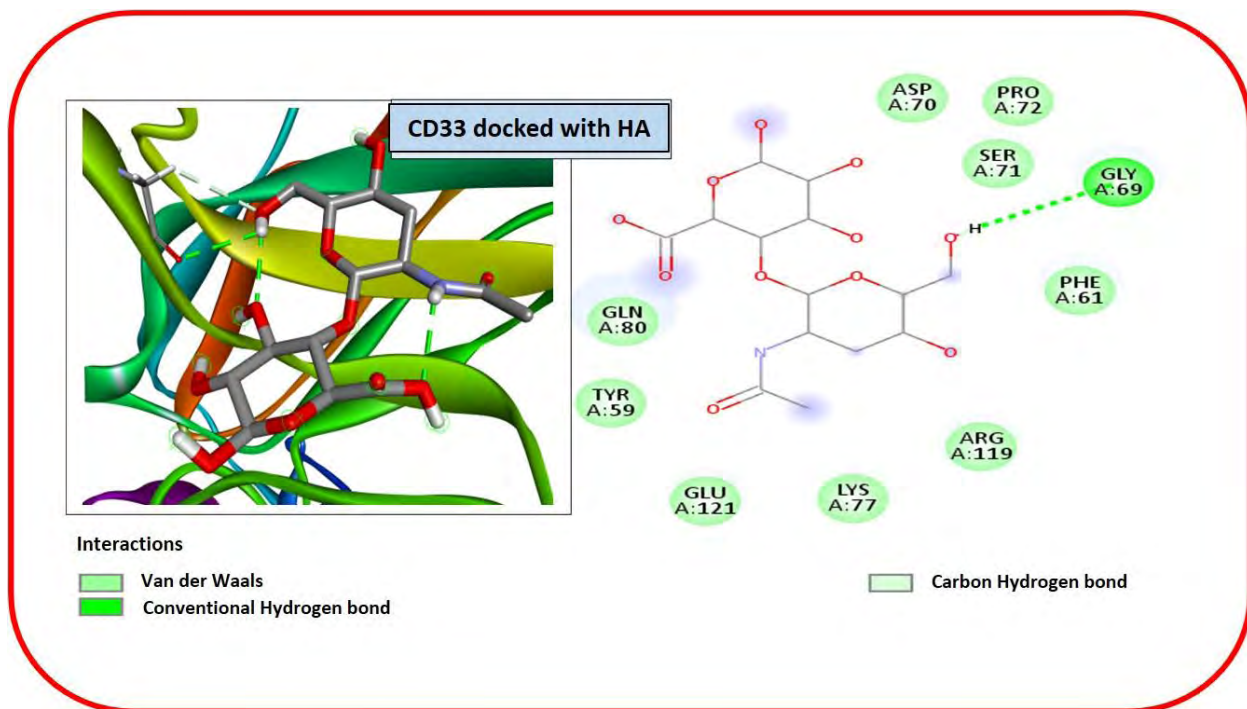


*Figure 3.5: CD33 protein's binding site docked with the hyaluronic acid coated over CuET through receptor amino acid GLY A:69 via hydrogen bonds*

### 3.3.4. Relative organs weight analysis

The relative organ weights of the essential organs liver, heart, and kidney were considerably raised in leukemic rats; however, following treatment, groups exhibited a fall in the weight of liver ( $p < 0.05$ ), heart ( $p < 0.01$ ), and kidney ( $p < 0.001$ ). Doxorubicin was shown to be more successful in restoring liver weight than CuET and combination regimens, however, for heart and kidney, combination therapy seemed to be extremely beneficial, demonstrating synergistic potential (figure 3.6).



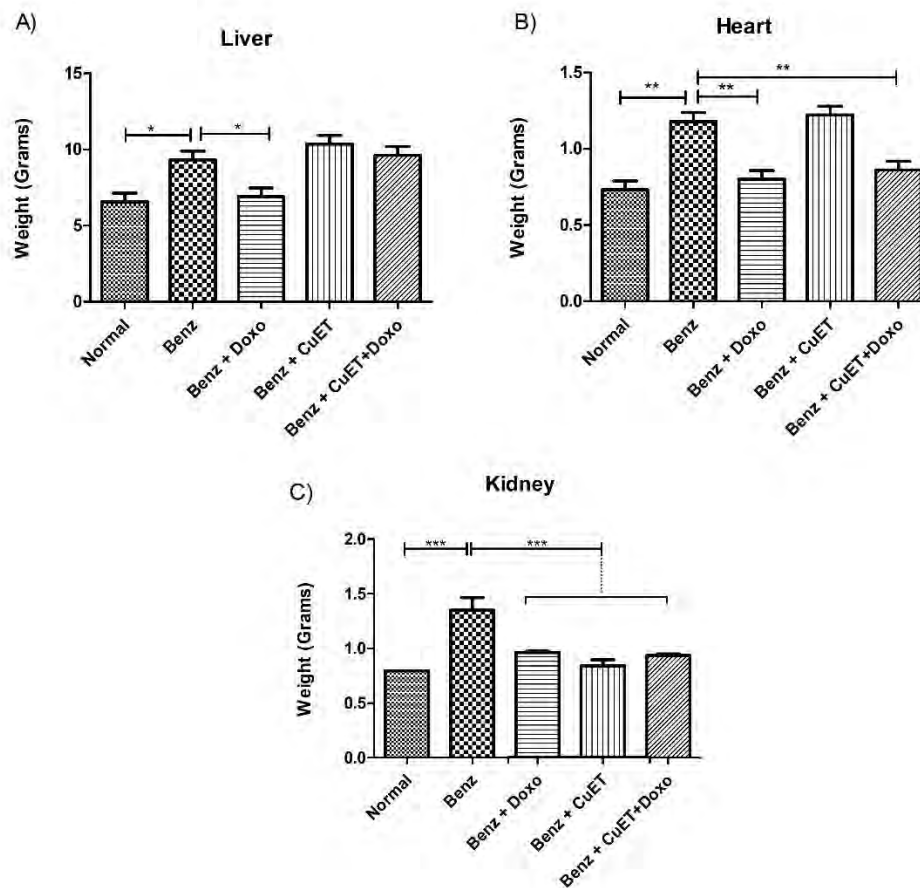


*Figure 3.6: Restoration of mean relative A) liver, B) heart and C) kidney weights after various treatments (n=3).*

### 3.3.5. Restoration of normal morphology and hematological profile

Morphological investigations of benzene-treated leukemic blood and bone marrow indicated erythrocytosis and the presence of leukoblasts. CuET therapy improved cell shape, resulting in intact red blood cells and a normal nucleus-to-cytoplasm ratio. Similarly, as shown by the arrows in figure 3.7, the abnormal morphology of leukoblasts in bone marrow samples was normalized following CuET injection.

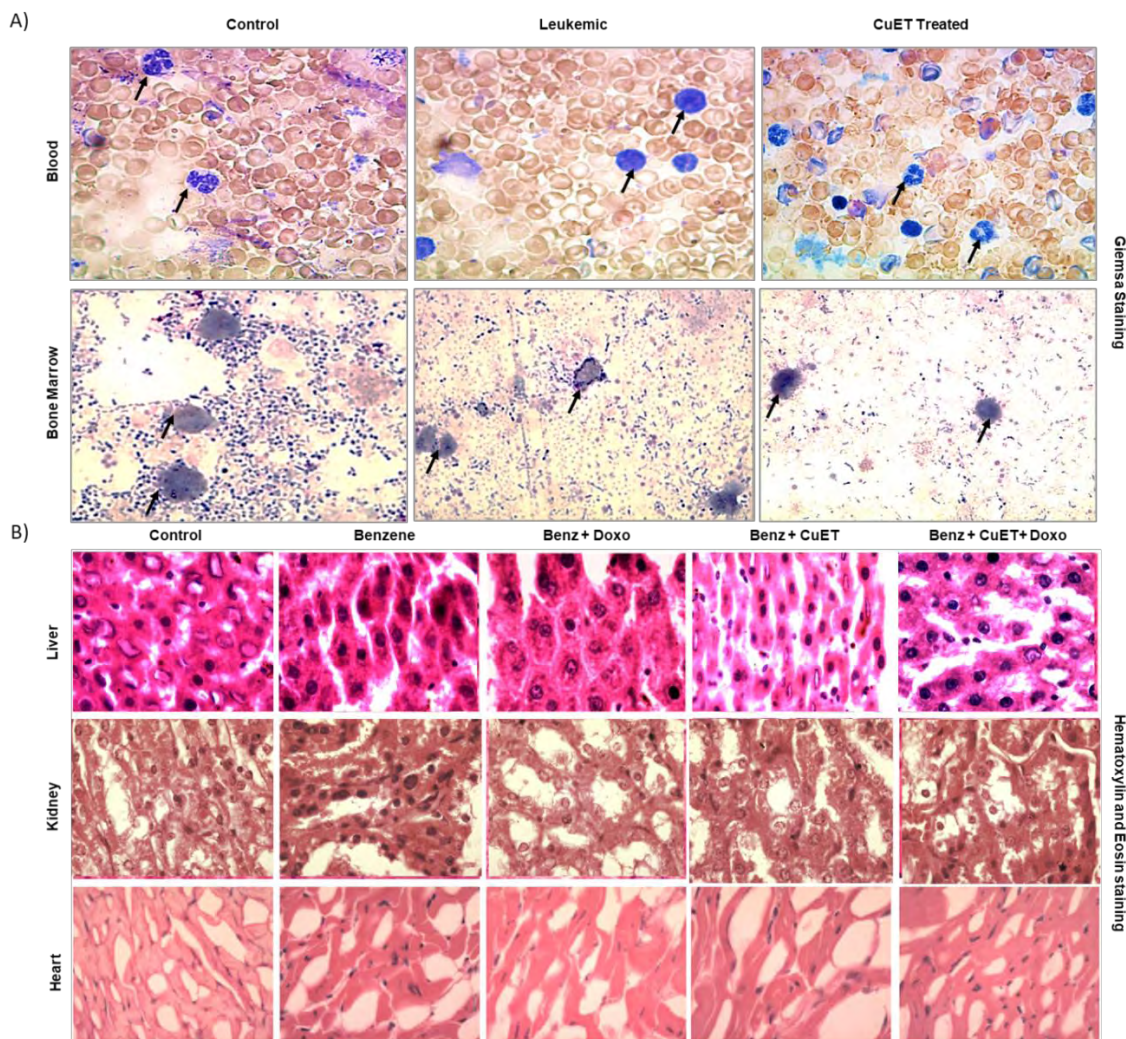


**Figure 3.7: Morphological analysis of (A) blood and bone marrow cells using giemsa staining dye (10X) and (B) liver, kidney and heart tissue samples using hematoxylin and eosin staining.**

In the benzene-treated rats, whole blood count analysis revealed an abnormal rise in total WBCs and neutrophils, as well as a significant decrease in RBCs, lymphocytes, hemoglobin, and platelets ( $p < 0.05$ ). This abnormal cell count was substantially recovered in leukemic rats after administration of CuET as free drug and in combination with doxorubicin. The combination therapy was more effective in recovering RBCs ( $p < 0.001$ ), lymphocytes ( $p < 0.01$ ), hemoglobin ( $p < 0.001$ ), and platelets count ( $p < 0.001$ ), however, standalone CuET treatment showed better reduction in WBCs ( $p < 0.001$ ) and neutrophils count ( $p < 0.001$ ) only as shown in figure 3.8A-F.

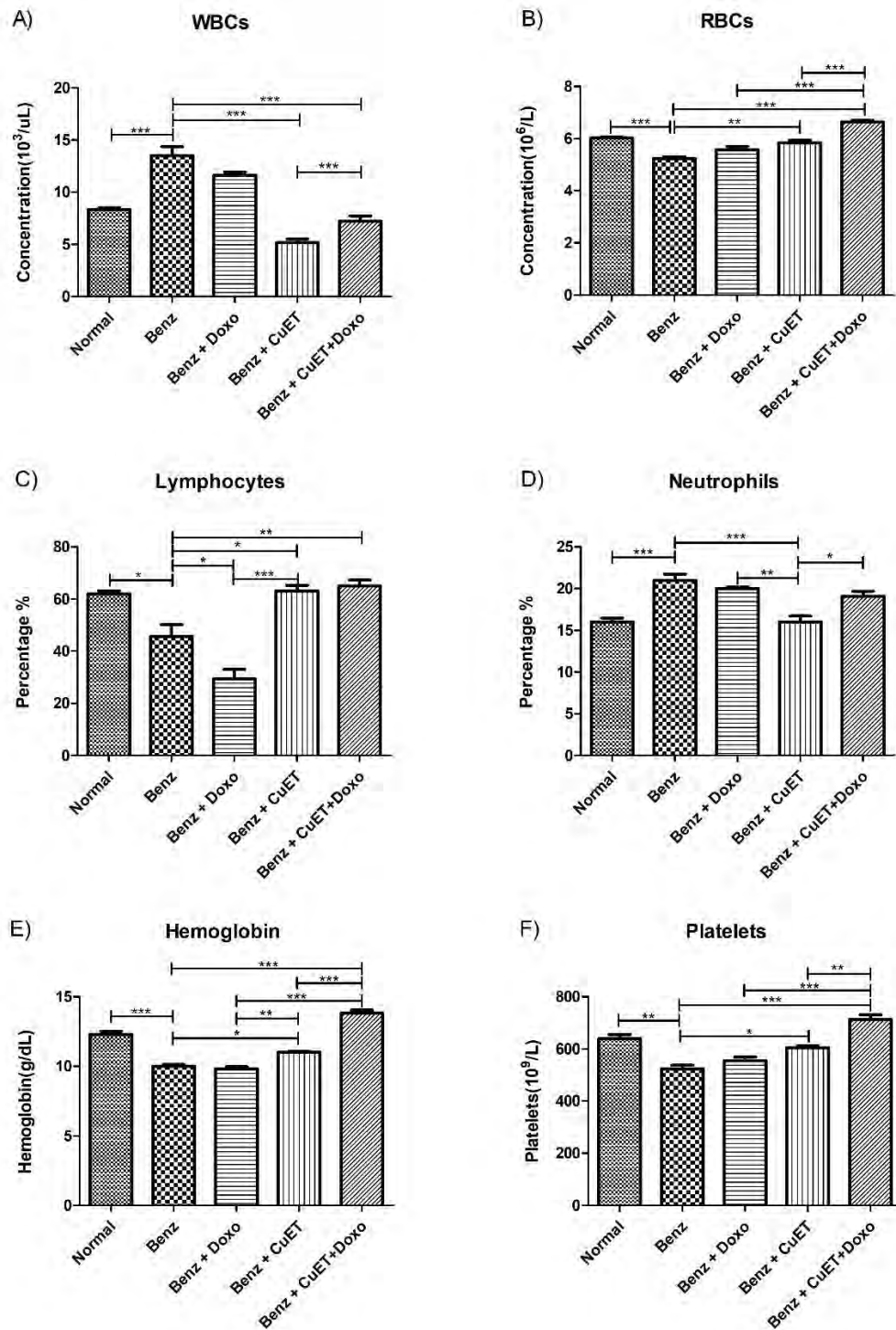
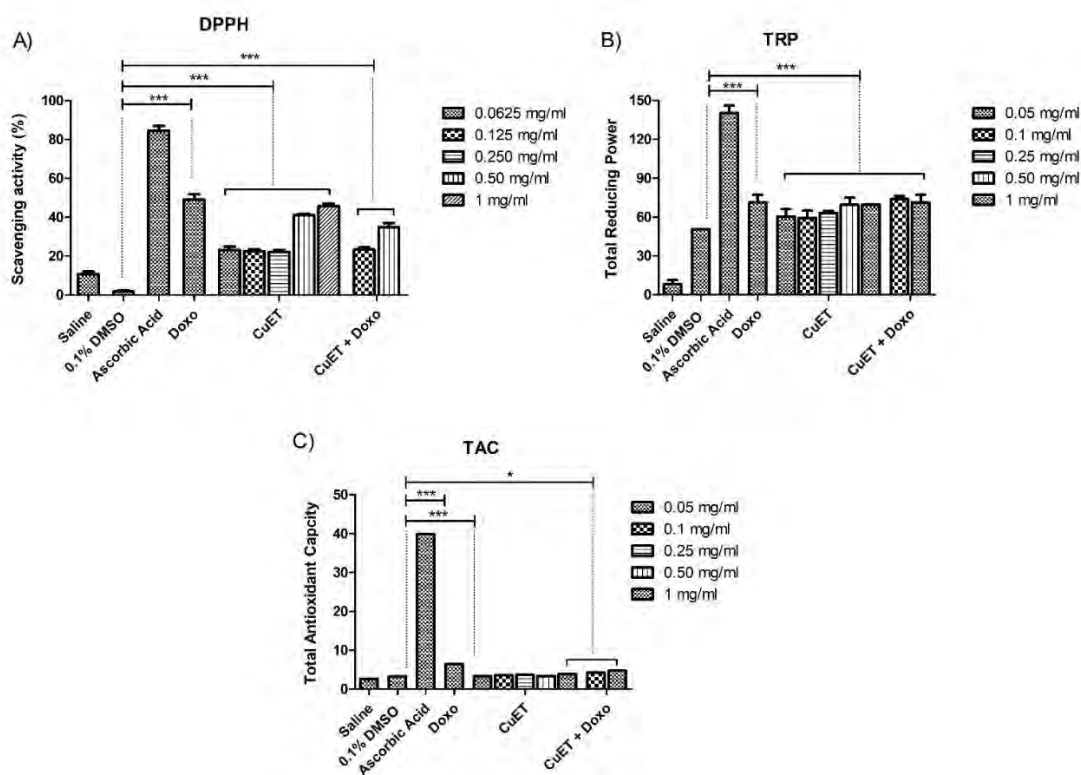


Figure 3.8: Evaluation of blood parameters of different experimental groups (n=3).

### 3.3.6. Notable antioxidant potential of CuET confirmed via DPPH, TRP and TAC assays

The DPPH assay exhibited significant ( $p < 0.001$ ) antioxidant potential of CuET at multiple concentrations, however, substantial increase was observed at 1mg/mL dilution (Figure 3.9A). Likewise, the total reducing potential assay exhibited significant ( $p < 0.001$ ) reducing activity at all dilutions. It was observed that the reducing potential of CuET increased substantially when administered at 1mg/mL concentration as shown in Figure 3.9B. The total antioxidant capacity assay also exhibited a similar pattern (Figure 3.9C).



**Figure 3.9: Antioxidant potential analysis of different treatment groups ( $n=3$ ) using A) DPPH B) TRP and C) TAC assays**

### 3.3.7. Enhanced biological potential of CuET

The results presented in Figure 3.10 highlight the significant impact of combining CuET with chemotherapy in various aspects of therapeutic efficacy. Firstly, the brine shrimp assay revealed a substantial reduction in cytotoxicity when CuET was administered

alongside chemotherapy, indicating a potentially safer and more tolerable treatment regimen. Furthermore, the combination therapy showed remarkable improvements in antidepressant, analgesic, and anti-coagulation effects compared to chemotherapy alone. This suggests that CuET may enhance the overall therapeutic outcomes of chemotherapy by providing additional benefits beyond its cytotoxic effects. These findings underscore the potential synergistic interactions between CuET and chemotherapy in mitigating depressive symptoms, alleviating pain, and preventing blood clot formation. Moreover, the use of fluoxetine, aspirin, and diclofenac acid as positive controls in the respective assays adds validity to the observed effects of CuET. By comparing CuET's efficacy with established pharmaceutical agents known to exert similar therapeutic effects, the study demonstrates the potential of CuET as a promising adjunct therapy in cancer treatment.

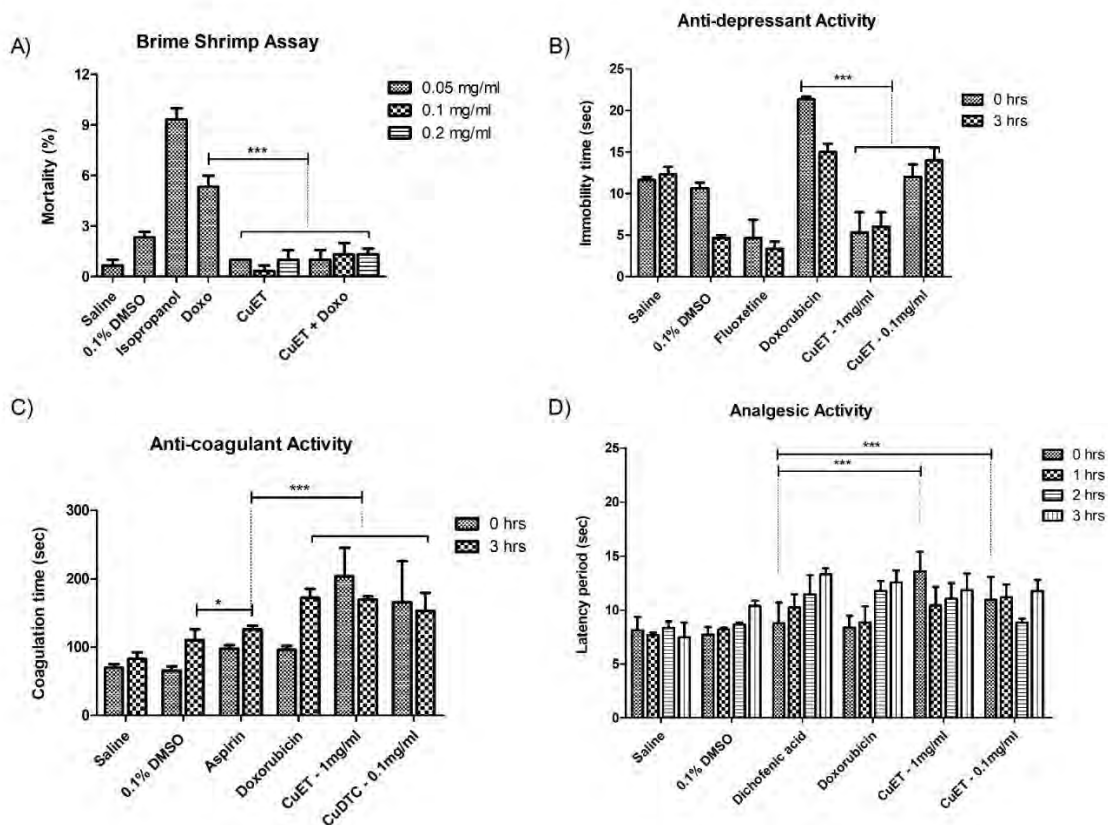


**Figure 3.10:** Evaluation of biological potential using A) brine shrimp assay B) anti-depressant assay C) anti-coagulant assay and D) analgesic assay in animal model (n=3).

### 3.3.8. Recovery of hepatic enzymes and serum uric acid levels

Hepatic biomarkers including ALT, AST and ALP showed significant ( $p < 0.001$ ) increase in their serum levels upon benzene treatment. However, both CuET and combination therapy expressed remarkable reduction ( $p < 0.001$ ) in serum levels of all three hepatic markers as shown in figure 3.11A-C. Likewise, significant increase in serum uric acid levels ( $p < 0.01$ ) was observed in leukemic rats which were reduced back to normal by CuET ( $p < 0.05$ ) and combination therapy ( $p < 0.01$ ) as indicated in figure 3.11D.

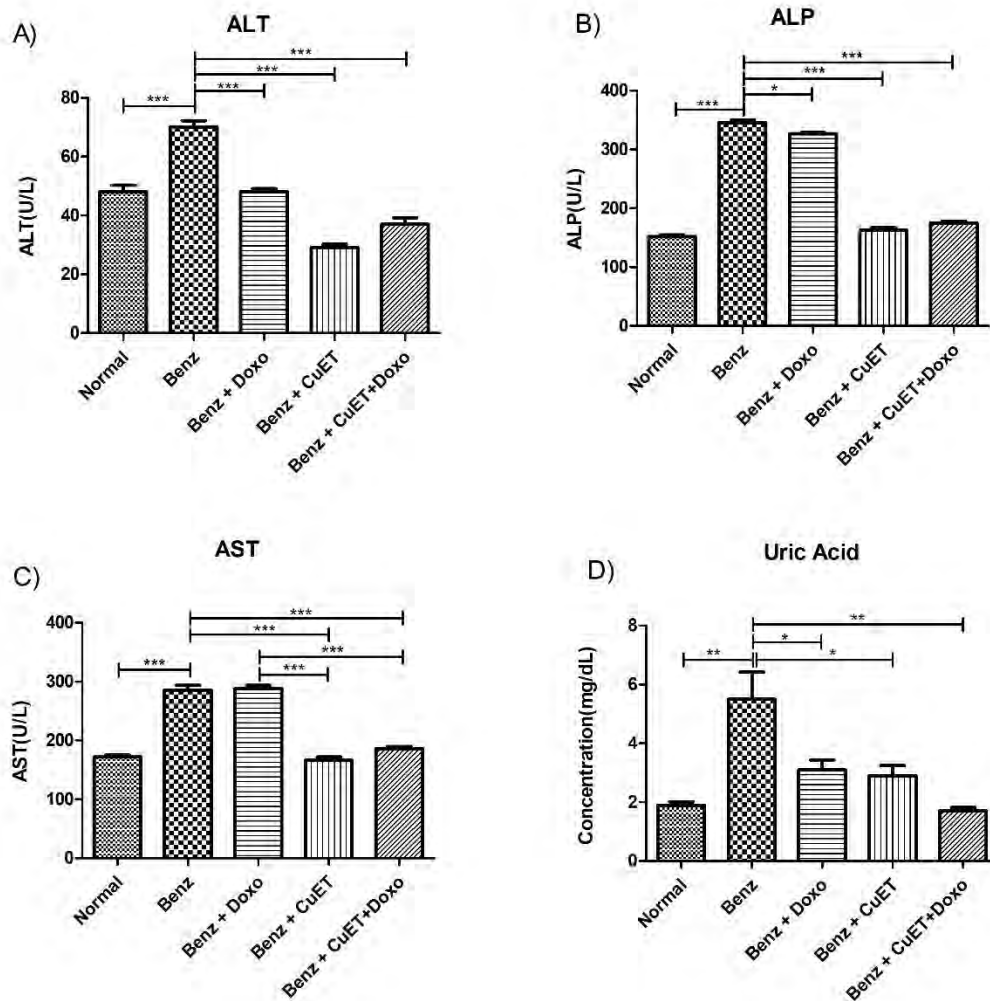


Figure 3.11: Levels of hepatic and renal biomarkers in different experimental groups (n=3).

### **3.3.9. Dysregulation in STMN1 and S1009A genetic expression confirms AML induction**

Significant increase ( $p < 0.05$ ) in STMN1 while decrease ( $p < 0.01$ ) in S1009A expression in benzene treatment group confirmed AML induction. Doxorubicin alone did not exhibit any noticeable recovery of STMN1 in leukemic rats however, CuET treatment significantly reduced ( $p < 0.001$ ) STMN1 and elevated ( $p < 0.001$ ) S1009A expressions. Combination regimen remained most effective in decreasing STMN1 expression ( $p < 0.001$ ) indicating the synergy as shown in figure 3.12A, B.

### **3.3.10. Upregulation of negative regulators in canonical Wnt signaling pathway**

The expression of Wnt significantly enhanced ( $p < 0.001$ ) in benzene treated group, while its negative regulators, GSK3 $\beta$  ( $p < 0.001$ ) and AXIN ( $p < 0.05$ ), reduced significantly in leukemic rats indicating stimulation of Wnt pathway which gives growth advantage to cancerous cells (Figure 3.12C-F). Combination of CuET and doxorubicin synergistically reduced the genetic expression of Wnt along with increasing GSK3 $\beta$  expression levels ( $p < 0.001$ ). However, individual drug treatment proved to be most effective in enhancing the expression of AXIN gene ( $p < 0.001$ ) depicting anti-proliferative potential of individual drugs.

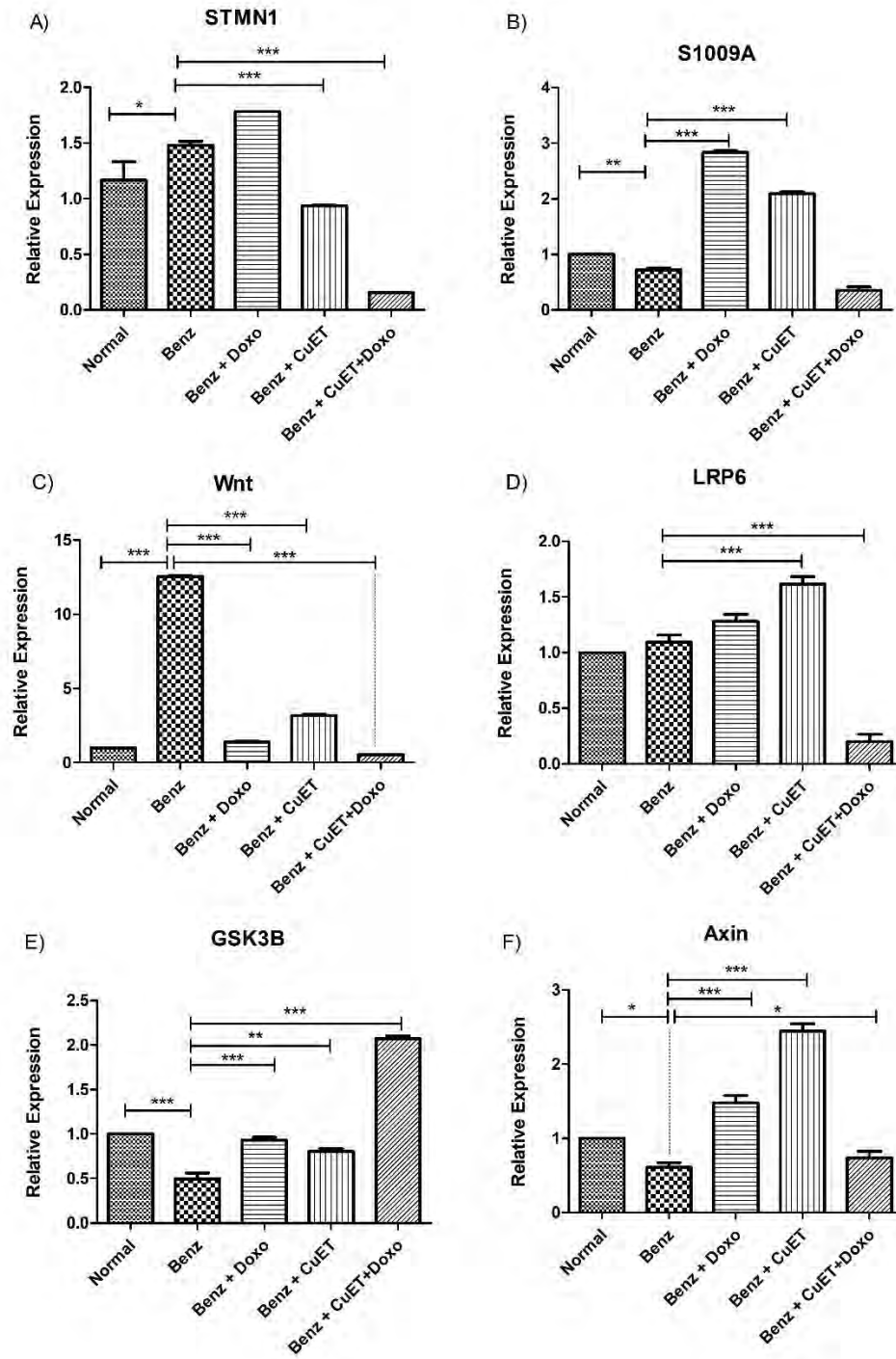


**Figure 3.12: Gene expression analysis of AML genetic markers and Wnt Pathway components in different experimental groups (n=3).**



**3.3.11. Downregulation of HIF-1 $\alpha$  pathway pro-survival signaling markers**

Combination therapy significantly reduced expression of HIF-1 $\alpha$  ( $p < 0.001$ ) and VEGF ( $p < 0.001$ ) however, standalone CuET treatment was more effective in increasing VHL ( $p < 0.001$ ) and PTEN expression ( $p < 0.001$ ) indicating promising effects of individual drug treatment in restoring expression of tumor suppressor genes. Cox-2 and c-Myc expression significantly increased ( $p < 0.001$ ) in benzene treated leukemic rats, however, both individual drug treatment and combination therapy significantly reduced expression of cox-2 ( $p < 0.001$ ) and c-myc expression ( $p < 0.001$ ) to various degrees as shown in figure 3.13A-F.

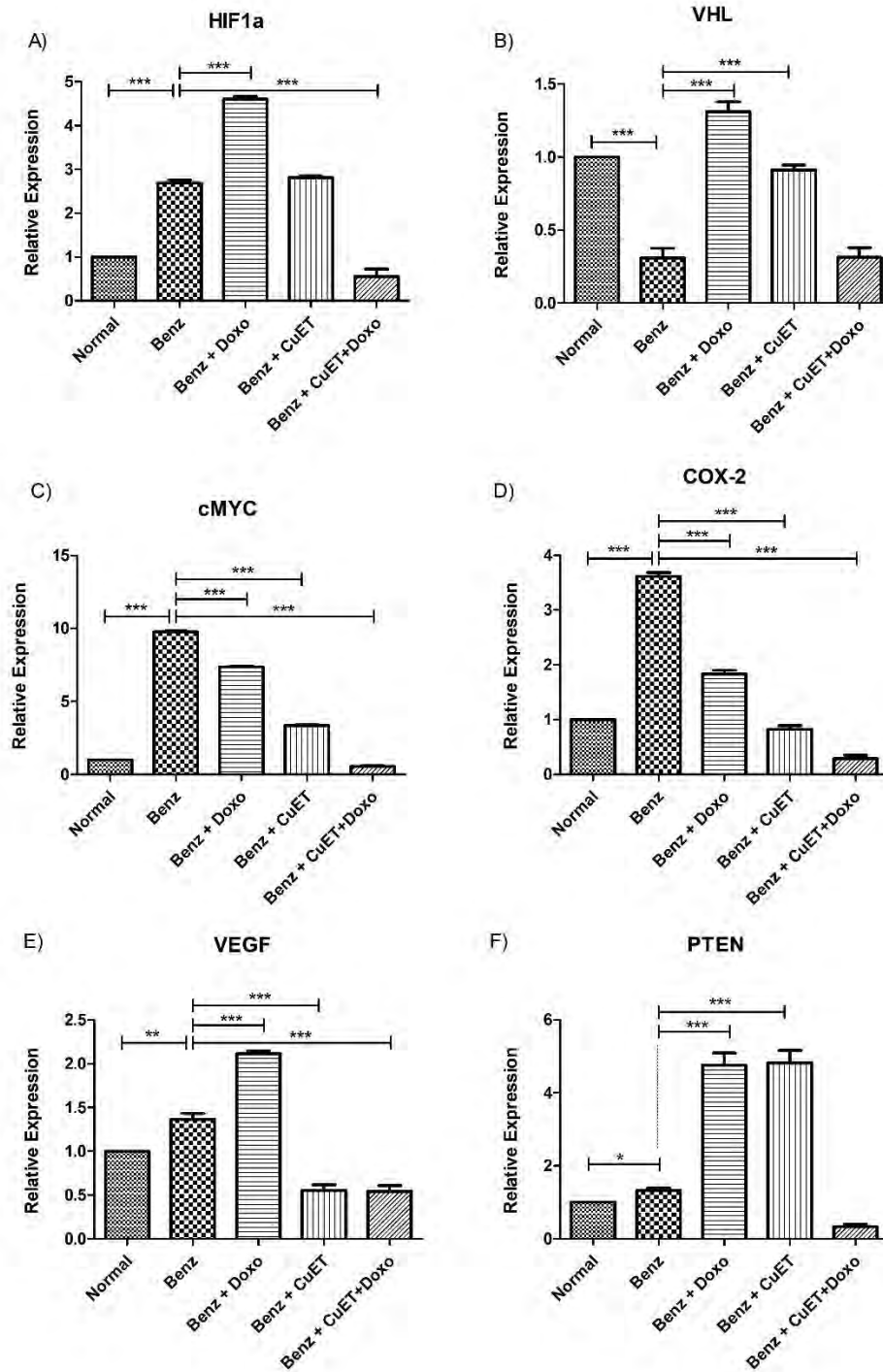


**Figure 3.13: Gene expression analysis of HIF 1 $\alpha$  pathway markers in different experimental groups (n=3)**

### 3.3.12. The AnnexinV/PI apoptosis assay demonstrated a powerful synergy in combination therapy

Flow cytometry analysis utilizing annexin V and propidium iodide dyes was employed to evaluate the apoptotic potential of the treatment regimes. The normal/control group displayed a basal apoptotic cell population of 2.47%, contrasted by a significant increase in leukemic rats i.e. 7.68% due to benzene-induced cell death (figure 3.14A, B). Doxorubicin treatment increased the apoptotic population to 14.45%, while CuET as a free drug induced 23.58% apoptosis in leukemic cells (figure 3.14C, D). However, the combination therapy exhibited a substantial enhancement in apoptotic cell population, escalating it to 66.82% in leukemic rats (as shown in figure 3.14E). This remarkable surge in apoptotic cells underscores the synergistic potential of the combined CuET and doxorubicin treatment regimen, presenting a compelling therapeutic advantage.

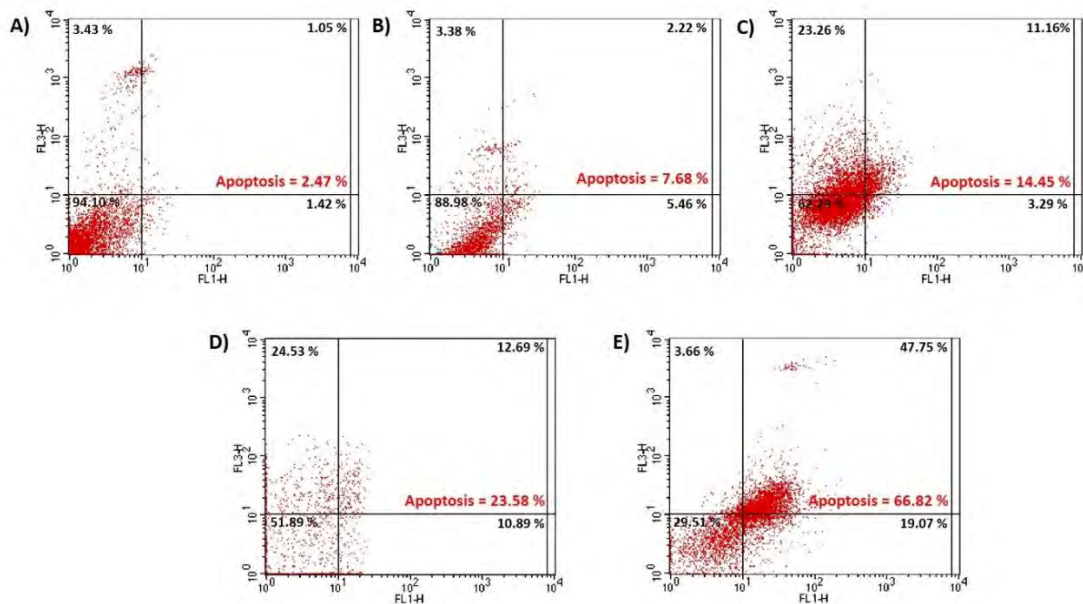


**Figure 3.14:** FACS analysis using propidium iodide and annexin V dye in (A) normal (B) benzene (C) doxorubicin (D) CuET and (E) CuET along with doxorubicin treated groups ( $n=3$ ).

### 3.3.13. CD4 viability assay exhibited optimum cell viability in combination treatment

Flow cytometry analysis using CD4 antibody demonstrated the immunomodulatory impact of combination therapy. The control group exhibited 30.95% CD4<sup>+</sup> cells population, which

significantly reduced to 7.67% in benzene-induced leukemic rats. However, doxorubicin increased CD4<sup>+</sup> population to 24.25%, whereas 18.89% CD4<sup>+</sup> population was observed in CuET treated group. Notably, the combination therapy effectively restored CD4<sup>+</sup> population to 32.85%, demonstrating its superior efficacy in reinstating viable cells population in leukemic rats (Figure 3.15A-E).

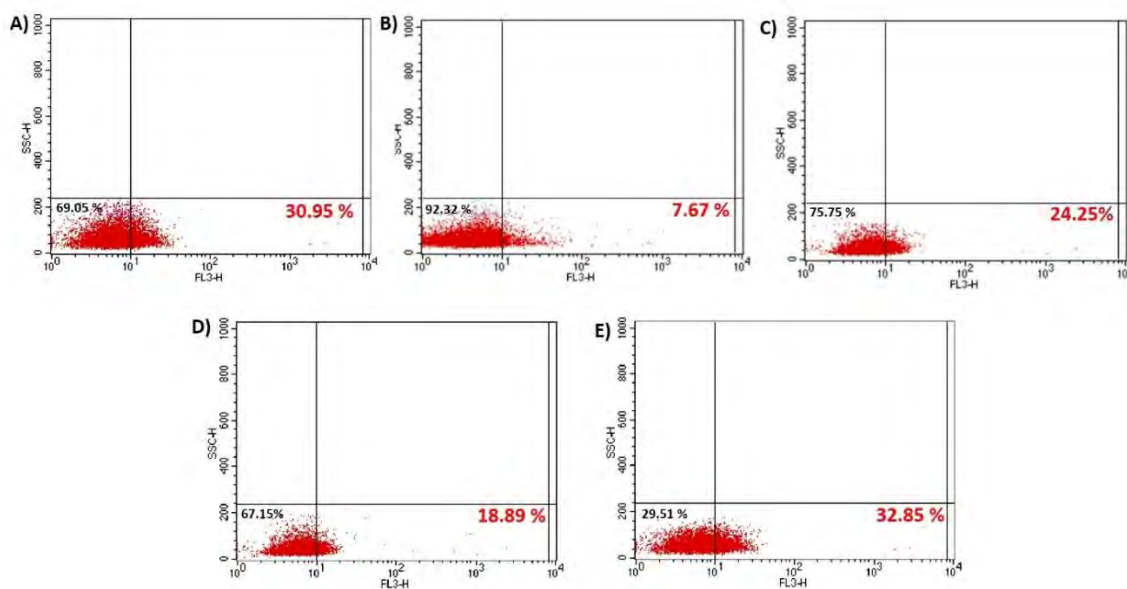


**Figure 3.15: FACS analysis using CD4 antibody in (A) normal (B) benzene (C) doxorubicin (D) CuET and (E) CuET along with doxorubicin treated groups (n=3).**

### 3.4. Discussion

Because of their ability to cross blood-brain and cell membranes, nanoparticles serve as very effective medication carriers, decreasing off-target adverse effects and enabling accurate, site-specific administration. (Luo *et al.*, 2020). The synthesis of CuET nanoparticles (NPs) involved a straightforward process facilitated by the coordination between dithiocarbamate (DTC) ligands and Cu<sup>2+</sup> ions under moderate conditions. The self-assembly of CuET NPs occurred spontaneously when the DTC/Cu<sup>2+</sup> molar ratio was maintained at 2:1, as each copper ion binds two DTC molecules to form the CuET complex. This specific stoichiometry ensured the efficient formation of stable nanoparticles with well-defined properties. The reported zeta potential of CuET NPs was found to be slightly positive, measured at approximately +1.73 mV. This positive charge can be attributed to the presence of Cu<sup>2+</sup> ions on the surface of the nanoparticles. The electrostatic interaction

between the positively charged  $\text{Cu}^{2+}$  ions and the surrounding solvent molecules or counter ions results in the overall positive zeta potential of the CuET NPs (Peng *et al.*, 2020). Such a positively charged surface enabled for the electrostatic binding of negative hyaluronic acid (HA) to generate modified CuET NPs, which gave the NPs target ability against leukemic cells that overexpressed CD33. This CuET coordination polymer can dissolve in the presence of acidic endo/lysosomes and intracellular GSH, resulting in fast drug release and anti-tumor activity. The CuET NPs demonstrated extremely robust and selective leukemic cell damage in flow cytometry due to their unique anti-tumor mechanism and surface HA alteration (Peng *et al.*, 2020). After intravenous administration, the nanoparticles can passively aggregate in bone marrow cells, inhibiting AML development at a medication dosage as low as 0.1 mg/kg. This concentration is justified as it is low enough to minimize systemic toxicity and adverse effects, while still being effective in targeting and delivering the therapeutic payload directly to the leukemia cells. The relevance of this dosage to clinical endpoints is significant, as achieving therapeutic efficacy at lower doses reduces the risk of side effects and improves the overall safety profile of the treatment. Scanning electron microscopy confirmed the pseudo-octahedral coordination geometry of CuET (Jin *et al.*, 2022). The EDX peaks confirmed the presence of Cu in CuET nanoparticles. Scanning electron microscopy was used in this investigation to validate the pseudo-octahedral coordination geometry of CuET. XRD measurements confirmed the particle size and shape, which corresponded to previously reported data (Peng *et al.*, 2020). The presence of Cu in CuET nanoparticles was verified by the EDX peaks.

The docking studies show that GLY A:69 is one of the key residues of CD33 that interacts with HA coated over CuET in AML cells. CD33 forms a conventional hydrogen bond with the HA, as well as carbon-hydrogen bonds and van der Waals interactions. This interaction leads to uptake of CuET and can affect the activation and differentiation of macrophages, monocytes, and dendritic cells, as well as the production of inflammatory cytokines such as IL-6 and IL-8 (Jin *et al.*, 2022). HA-CD33 interaction also have implications for the treatment of AML (Walter, 2020; Donelan *et al.*, 2022).

The observed increase in organ weight in our *in-vivo* trials is most likely due to benzene metabolites directly targeting these organs, causing free radical production and consequent

hypertrophy (Rana & Verma, 2005). The rapid recovery in organ weights by combination therapy, on the other hand, provides considerable evidence of CuET's preventive impact against benzene-induced hypertrophy.

Through its metabolites phenol, catechol, and hydroquinone, benzene causes acute myeloid leukemia. Morphological examination shows that benzene and its cytotoxic metabolites cause erythrocytosis, which contributes to a drop in total red blood cell count as well as other abnormalities such as eosinophilia and leukocytosis (Hallenbeck & Cunningham 1985; Smith *et al.*, 2011). Similarly, benzene-induced bone marrow cell mutations disturb normal leukocyte development, leading to an increase in total white blood cell count and an increase in the number of immature leukoblasts in the leukemic circulation (Greenwood *et al.*, 2006). The same conclusions were reached in this investigation. CuET alone and in combination considerably improved the blood profile of leukemic rats by decreasing erythrocytosis (Hallenbeck & Cunningham, 1985). The decline in platelet levels seen in our study is most likely owing to benzene's negative influence on bone marrow cells. Interestingly, the combo therapy significantly increased platelet counts by reducing thrombocytopenia, providing a possible option for combating this decrease (Olsson *et al.*, 2005). CuET works within tumor cells by strongly binding to nuclear protein localization-4 (NPL4), causing it to clump together. This interaction impairs the critical p97-NPL4-UFD1 pathway, causing ubiquitinated proteins to accumulate and preventing waste protein degradation. As a result, this chain of events leads to cell apoptosis (Peng *et al.*, 2020).

Benzene disrupts the normal levels of ALP, ALT, and AST by inducing reactive oxygen species (ROS) production through its secondary metabolites. Given that the liver is a primary target of benzene toxicity, this dysregulation occurs as a consequence of its impact on hepatic functions (Ito *et al.*, 2003). The increased levels of ALP and ALT were possibly a result of abnormal liver cell proliferation, subsequently leading to elevated alanine phosphatase and transaminase levels in leukemic rats (Farrow *et al.*, 1997; Islam *et al.*, 2020). Similarly, the elevation in blood serum AST concentration serves as an indicator of hepatocytotoxicity, reflecting the damage inflicted upon liver cells by benzene exposure. Benzene administration also led to increased serum creatinine levels, indicating an impending acute kidney injury in leukemic rats. Remarkably, our combination therapy

reversed these abnormal levels of hepatic enzymes and creatinine, owing to its reduced cytotoxicity and an enhanced antioxidant potential (Lahoti *et al.*, 2010).

Genetic expression analysis was performed by homogenizing bone marrow cells since AML originates in myeloid stems cells and CuET is reported to accumulate in bone marrow of leukemia patients. The increased expression of STMN1, one of the most prominently over-expressed genes in AML, was observed in benzene-administered leukemic rats. This elevation confirms leukemia induction, marking a genetic manifestation of the disease. (Handschuh *et al.*, 2018). Likewise, The decrease in S1009A expression in AML affirms its role in disease induction, signifying its crucial involvement in leukemia development and progression (Laouedj *et al.*, 2017). Treatment with CuET minimized the benzene effect by decreasing STMN1 and enhancing S1009A expression thereby potentially altering the actin function and microtubule dynamics of cells (Wu *et al.*, 2014).

In benzene induced AML rats, aberrant signaling leads to the upregulation of LRP6, possibly due to enhanced Wnt ligand expression. This upregulation activates Wnt signaling. Conversely, GSK3 $\beta$  and Axin, key components in the destruction complex that usually inhibit Wnt signaling, are downregulated which might result from various mechanisms, including mutations or altered expression patterns, disrupting the inhibitory function of the destruction complex (Zhan *et al.*, 2017). However, CuET synergistically reverses dysregulated Wnt signaling in leukemic cells by targeting key components of the pathway, when administered with doxorubicin. It intervenes by inhibiting the overactive LRP6 receptor and promoting the restoration of GSK3 $\beta$  and Axin expression. CuET's action inhibits aberrant Wnt signaling, thereby restoring the balance and mitigating the abnormal cell proliferation and survival observed in leukemic cells (Hendrych *et al.*, 2022). Hypoxic environment in AML triggers the stabilization and increased expression of HIF-1 $\alpha$ , promoting its transcriptional activity. Conversely, the downregulation of VHL (Von Hippel-Lindau) in AML contributes to HIF-1 $\alpha$  upregulation as VHL is responsible for targeting HIF-1 $\alpha$  for degradation under normal oxygen levels. The reduced expression or function of VHL leads to the accumulation of HIF-1 $\alpha$ , fostering an environment conducive to leukemic cell survival, proliferation, and angiogenesis within the hypoxic niche of the bone marrow in AML (Magliulo & Bernardi, 2018). Whereas, CuET as combination regime counteracts hypoxia-driven HIF-1 $\alpha$  upregulation by possibly inhibiting its

---

stabilization, promoting VHL-mediated degradation. This restoration of balanced HIF-1 $\alpha$  and VHL expression levels helps regulate the hypoxic responses, impeding aberrant survival and proliferation pathways in AML cells. Likewise, benzene exposure induces genetic mutations and epigenetic changes that promote the overexpression of c-myc, a critical regulator of cell proliferation. In contrast to this, CuET's action likely involves inhibiting factors, restoring a more balanced and controlled expression of this oncogene within AML cells (Tang *et al.*, 2021). Additionally, COX-2, an enzyme involved in inflammation and cell signaling, is upregulated, likely due to benzene-induced inflammatory responses (Carter *et al.*, 2019). CuET in combination with doxorubicin may exert its synergy on upstream regulators or signaling cascades influencing COX-2 expression, contributing to its restoration within AML cells. PTEN, a tumor suppressor gene, shows increased expression, potentially as a compensatory response to the heightened proliferation signaling induced by benzene exposure (Chen *et al.*, 2010).

In AnnexinV/PI assay, benzene exposure led to increased apoptosis, indicated by higher levels of Annexin V (marking early apoptosis) and Propidium Iodide (highlighting late apoptosis) as in earlier studies (Malovichko *et al.*, 2021). Doxorubicin intercalates into DNA, inhibiting topoisomerase II and leads to DNA damage. This DNA damage triggers cellular stress responses, activating apoptotic pathways resulting in enhanced apoptosis as observed in AV/PI assay (Fujiwara *et al.*, 2006). CuET also induces apoptosis in leukemic population probably by hindering survival pathways, but when combined with doxorubicin, the two compounds act synergistically. CuET's ability to sensitize the cells amplifies doxorubicin's apoptotic effect, leading to a greater induction of programmed cell death than both standalone treatments. The same synergy is observed in CD4 viability assay as when CuET treatment is applied, it potentially targets leukemic cells, allowing the combination therapy to spare normal/ healthy cells (Huang *et al.*, 2021). This selective targeting, coupled with the enhanced apoptotic potential of the combination, may result in a higher proportion of viable non-leukemic cells within the leukemic population compared to standalone treatments.



---

## **Chapter 4: NiET nanoparticles**

**Exploring the synergistic therapeutic potential of Ni-Diethyldithiocarbamate nanoparticles with doxorubicin in Acute Myeloid Leukemia**

#### 4.1. Introduction

Leukemia is a group of clinical disorders characterized by the unregulated expansion of pluripotent bone marrow stem cells, which results in aberrant cellular proliferation and neoplasms (Ramdass *et al.*, 2013). Among its many varieties, acute myeloid leukemia (AML) ranks as the prominent one, that develops from the malignant transformation of early progenitor or hematopoietic stem cells (Khwaja *et al.*, 2016). AML is caused by a variety of factors, including extrinsic ones such as infectious agents like viruses, tobacco smoke, radiations, and chemicals like benzene and polychlorinated biphenyls (Bhatia & Das, 2020). Among these, benzene is the most common causative factor for AML (McHale *et al.*, 2012). The liver is responsible for the primary metabolism of benzene, which is transformed into a variety of phenolic and opened-ring compounds, as well as various conjugates. All of these compounds are harmful to bone marrow and hematopoietic stem cells (HSCs), inducing redox reactions that produce reactive oxygen species, resulting in cellular genotoxicity. This eventually leads to the creation of protein adducts, which change cellular progression and impair cellular processes, resulting in the development of AML (Ross, 1996).

Several traditional chemotherapeutic drugs are employed, including doxorubicin, which is especially useful in treating and managing AML. Doxorubicin, classed under the anthracycline category of antibiotics, has been a cornerstone in treating numerous malignancies, encompassing both haematological and solid tumors, for over 30 years (Chen *et al.*, 2013). So far, numerous potential modes of action have been hypothesized for the cytostatic and cytotoxic properties of doxorubicin. These include 1) inhibiting macromolecule synthesis by intercalating with DNA bases, 2) producing ROS, which leads to the initiation of DNA damage, 3) lipid peroxidation, 4) disrupting DNA strand separation and helicase activity, and 5) causing direct DNA damage by inhibiting topoisomerase II. All of these ways of action eventually cause apoptotic cell death. Doxorubicin, however, not only targets cancer cells but also affects normal developing cells of the body, resulting in inevitable side effects such as double-stranded DNA breaks and death in normal cells (Lu *et al.*, 2007).

This non-specific targeting of conventional treatment stresses the necessity for the study and development of innovative therapeutic molecules that must display lower toxicity and greater effectiveness than presently available conventional chemotherapeutic medicines (Castro *et al.*, 2019). To address this issue, the use of targeted nanoparticles to deliver chemotherapeutic drugs in cancer treatment provides various benefits to increase drug delivery and overcome many issues associated with traditional chemotherapy (Nguyen, 2011). Nanoparticles, whether via passive or active targeting techniques, have a remarkable ability to boost the intracellular accumulation of medicines or genes, particularly inside cancer cells. This targeted delivery reduces toxicity in normal cells, providing a dual benefit of increased therapeutic effectiveness in tumors while protecting the health of surrounding healthy tissues (Suri *et al.*, 2007).

Organometallic compounds in the form of nanoparticles play an important role in the creation of site-specific drug delivery systems (Bajracharya *et al.*, 2023). Nickel-diethyldithiocarbamate (NiET) is an organometallic complex that consists of Nickel as a core metal atom, coupled with amine-1-carbodithionic acid (a derivative of dithiocarbamate) (Bobinihi *et al.*, 2018). The complex's capacity to chelate nickel, as well as its lipophilic character, are both interesting in cancer treatment.

Nickel serves important functions in biological activities, however, when combined with particular substances such as diethyldithiocarbamate, it may have lethal effects on cancer cells. This happens via several methods, including the formation of reactive oxygen species (ROS), which generate oxidative stress, resulting in cell damage and death. Compounds such as diethyldithiocarbamate (DTC) may attach to nickel ions via a process known as chelation (Huang *et al.*, 2021). This indicates that DTC may trap or bind to nickel ions, thereby lowering the amount of free nickel in the body.

When nickel ions are chelated by chemicals such as DTC, they may disrupt the process of angiogenesis. These substances inhibit the body's capacity to produce new blood vessels, hindering tumor development and spread by lowering nickel availability. This interference with angiogenesis is one manner in which nickel chelation by chemicals such as DTC may delay or prevent tumor growth (Cvek *et al.*, 2008). Additionally, these complexes might interfere with specific signalling pathways crucial for cancer cell survival and proliferation (Huang *et al.*, 2021).

The present study aims to evaluate the effectiveness of NiET in combination with doxorubicin against leukemia, as well as their impact on the relative expression of biomarkers related to the HIF-1 $\alpha$  and Wnt pathways in AML rat model.

## **4.2. Materials & Methods**

### **4.2.1 Materials**

Methanol, HCl, dimethyl sulfoxide (DMSO), benzene, doxorubicin, TRIzol, cDNA synthesis Vivantis kit, EvaGreen® Master mix.

### **4.2.2 Synthesis of NiET NPs**

Nickel-diethyldithiocarbamate complex was prepared by using synthesis protocol already published by Hogarth and coworkers (Hogarth, 2012). The synthesized NiET were then modified by adding an equivalent volume of hyaluronic acid (0.6 mg/mL), and stirring for 6 hours (Peng *et al.*, 2020).

### **4.2.3 Characterization of NiET NPs**

The characterization of NiET NPs involved several analytical techniques. Firstly, the particle diameter, zeta potential, and polydispersity index were determined using dynamic light scattering with a Zetasizer Nano ZS90 instrument manufactured by Malvern Instruments in the UK. This technique allows for the measurement of particle size and distribution in a liquid suspension based on the analysis of scattered light. Additionally, X-ray Diffraction Analysis was conducted using an X-ray spectrophotometer (Bucker D8 Advance, Karlsruhe, Germany) equipped with Cu-K $\alpha$  radiation ( $\lambda = 1.54^\circ \text{A}$ ), operating at 40 KV and 30 mA. This analysis provides valuable information about the crystalline structure of the nanoparticles.

To further confirm the size of the nanoparticles, the full width at half maximum (FWHM) obtained from the X-ray diffraction data was utilized in the Debye-Scherrer equation ( $D = 0.9\lambda/\beta\text{Cos}\theta$ ). This equation allows for the calculation of particle size based on the diffraction pattern observed. (Parmar *et al.*, 2012).

For morphological analysis, a small portion of NiET powder was securely attached to the stage of a scanning electron microscope (SEM) model LEO SUPRA 55 manufactured by Carl Zeiss AG in Oberkochen, Germany, using carbon tape. Images of the sample were then captured at an operating voltage of 12 keV, allowing for detailed examination of the surface morphology and structure of the NiET powder particles. (Hua & Yu, 2019). Energy-dispersive X-ray (EDX) analysis was conducted to ascertain the elemental composition of the synthesized NiET. This analytical technique provides valuable insights into the presence and distribution of different elements within the sample. By measuring the characteristic X-rays emitted when the sample is bombarded with high-energy electrons, EDX enables the identification and quantification of elements present in the material. (Merroun *et al.*, 2003).

#### 4.2.4 Cytotoxicity Assay

To ascertain the most effective dosage of NiET, brine shrimp assay was performed (Sarah *et al.*, 2017). Brine shrimp eggs were hatched in a sea salt solution. Following that, fifteen brine shrimp were methodically counted under a microscope and exposed to different degrees of dilution for 24 hours. To assure accuracy, each concentration was reproduced three times using pure water as a control. The probit method was used to compute the lethal concentration necessary to cause a 50% death rate (LC<sub>50</sub>) after 24 hours of exposure (Banti & Hadjidakou, 2021).

*Table 4.1: Prerequisites for brine shrimp assay*

No.	Materials	Quantity	Company name
1.	Brine shrimp eggs	As required	Ocean Star International, Inc
2.	Sea Salt	17g	-
3.	Distilled water	500mL	-

#### 4.2.5 *In vitro* bioassays

The evaluation of antioxidant capacity involved three different assays. The determination of total antioxidant capacity was carried out using the phosphomolybdenum method (Jamuna *et al.*, 2011), with minor adjustments to the procedure.

**Table 4.2: Requirements for total antioxidant capacity assay**

No.	Chemicals	Quantity
1.	(NH <sub>4</sub> ) <sub>2</sub> MoO <sub>4</sub>	0.247g
2.	NaH <sub>2</sub> PO <sub>4</sub>	1.679g
3.	H <sub>2</sub> SO <sub>4</sub>	1.63mL

Similarly, the assessment of total reducing power and the DPPH assay were conducted in accordance with the protocols previously outlined by Moein and colleagues (Moein *et al.*, 2008).

**Table 4.3: Requirements for DPPH assay**

No.	Chemicals	Quantity
1.	DPPH	96mg DPPH in 1000mL methanol
2.	Ascorbic acid	1mg/mL

#### 4.2.6. *In vivo* bioassays

The assessment of the analgesic efficacy of various treatment regimes was assessed through the hot plate assay (Tita *et al.*, 2001). Likewise, the evaluation of anticoagulant activity, which determines the coagulation time of blood in the absence of any foreign substance, was carried out using already reported protocol (Samuelson *et al.*, 2017). Furthermore, the assessment of antidepressant activity was carried out using the

conventional tail suspension method, as delineated by Zhou and colleagues (Zhou *et al.*, 2010).

#### **4.2.7. Development of AML model and experimental strategy**

The experimental setup involved the procurement of Sprague Dawley rats from the National Institute of Health in Islamabad. These rats were specifically selected for their suitability for experimental purposes and were of a standardized age range of five weeks, with weights ranging from 150 to 180 grams. The authorization for conducting all experimental procedures was obtained from the Institutional Review Board of Quaid-i-Azam University, as evidenced by letter No. #BEC-FBS-QAU2020-221.

Upon arrival, the rats were housed in pairs to ensure social interaction and minimize stress, utilizing laboratory cages constructed from polypropylene material with stainless-steel covers. This housing setup provided a controlled environment conducive to the well-being of the animals. The rats were provided with standard rodent chow and water ad libitum, ensuring their nutritional needs were met adequately. This provision of food and water was carried out at the Primate Facility of Quaid-i-Azam University, which adhered to standardized protocols for animal care and welfare. The rats were subjected to a consistent photoperiod consisting of 12 hours of light and 12 hours of darkness each day, maintaining a stable ambient temperature of  $298\text{K}(25^{\circ}\text{C})\pm 2$ . Additionally, the humidity levels were regulated to remain within the range of  $42\pm 5\%$ , further optimizing the environmental conditions for the rats' health and comfort.

All rats ( $n = 25$ ) were split into five equal groups (5 rats/ group). Animals were allowed to acclimate for a period of seven days.  $100\mu\text{L}$  of intravenous benzene was administered to rats group 2, 3, 4 & 5 at alternate days for three weeks. Group 1 (Normal) was given normal saline intravenously. Group 2 (Benz) was not treated further following onset of acute myeloid leukemia. After leukemia confirmation, standard dosage of doxorubicin ( $300\mu\text{L}$  of  $0.625\text{mg/mL}$ ) was intravenously administered to rats in Group 3 (Benz + Doxo) for three weeks on alternate days. Likewise,  $100\mu\text{L}$  of NiET ( $0.1\text{ mg/mL}$  in  $0.1\%$  DMSO) was delivered intravenously to Group 4 (Benz + NiET) rats. Whereas, both NiET and

doxorubicin were co-administered intravenously to Group 5 (Benz + NiET + Doxo) on alternate days for three weeks following leukemia confirmation. After finishing respective dosages, all rats were dissected according to the standards outlined in the Guide for the Care and Use of Laboratory Animals (Care & Animals, 1986).

#### **4.2.8. Morphological evaluation and tissue histology**

The preparation of blood and bone marrow smears for morphological studies involved several steps. After dissections, smears were created on glass slides. These slides were air-dried, and subsequently, Giemsa dye (10X) was applied drop by drop, allowing for a 10-minute staining period. Following staining, the slides were washed with tap water to remove excess dye and then air-dried once more in preparation for examination under a microscope (Houwen, 2002). For tissue histology analysis, samples from the liver, kidney, and heart were extracted and preserved in a 10% formalin solution. Histological examination was conducted using the haematoxylin and eosin staining protocol according to the method described by Chan and colleagues. This staining process involves the use of haematoxylin, a dye that stains cell nuclei blue, and eosin, a contrasting stain that colors other cellular components, allowing for detailed examination of tissue structures under a microscope (Chan *et al.*, 2014).

#### **4.2.9. Blood profiling and biochemical studies**

To assess the total blood cell count and various blood parameters, an automated Z3 hematology analyzer from Zybion Inc. Shenzhen, China, was utilized. This instrument provided comprehensive information on hemoglobin (HGB), platelets (PLT), red blood cells (RBC), white blood cells (WBC), and other essential blood parameters. For biochemical assays, the Microlab 300 auto analyzer from Merck was employed. Alanine aminotransferase (ALT), aspartate aminotransferase (AST), and alkaline phosphatase (Malovichko *et al.*) were measured using specific biochemical diagnostic kits, such as LTA and AMP diagnostic kits. Additionally, the Amplex® Red Uric acid/Uricase Assay kit from ThermoFisher Scientific was used to estimate uric acid levels. Moreover, the estimation of lipid profile and lactate dehydrogenase levels was performed using the Micro Lab 300 auto-analyzer from Merck, Germany. These various diagnostic kits and instruments



were employed to analyze different biochemical parameters and blood components in the study.

#### **4.2.10. Real time PCR analysis**

The TRIzol reagent RNA extraction method was employed to extract messenger RNA (mRNA) from the bone marrow cells. This method follows the protocol established and published by Chomczynski and colleagues. TRIzol reagent is a commonly used reagent in molecular biology for isolating RNA, DNA, and proteins from various biological samples, and the protocol developed by Chomczynski and co-workers provides standardized guidelines for RNA extraction using this reagent (Chomczynski *et al.*, 2010). For quality control measures, nanodrop quantification was conducted using the NanoDrop™ 2000/2000c spectrophotometer (Cat. No: ND-2000; MN, USA) to assess the concentration and purity of the extracted mRNAs. Additionally, 1% agarose gel electrophoresis was performed to further evaluate the quality of the extracted mRNAs.

Subsequently, the obtained mRNAs underwent cDNA synthesis using a Vivantis kit (cDSK01-050, Malaysia). To confirm the successful cDNA synthesis, a conventional PCR was carried out following the manufacturer's instructions. The PCR reaction mixture was prepared by mixing required reagents in 200µL PCR tubes (Axygen, USA).

Following PCR amplification, the resulting products were visualized on a 2% agarose gel stained with ethidium bromide. This visualization process enabled the confirmation of successful amplification of the desired transcript via PCR and allowed for the assessment of the size and purity of the amplified DNA fragments (Gleissner *et al.*, 2001). The size-specific amplicons were then confirmed.

For real-time PCR to determine relative gene expression, the MIC qPCR system from Bio Molecular Sciences (BMS) was utilized. The PCR amplification was conducted in a final volume of 10 µl, comprising 2 µl of Syber Green master mix, 1 µl each of reverse and forward primers, 5 µl of cDNA, and 1 µl of nuclease-free water.

The PCR (Polymerase Chain Reaction) cycling conditions were meticulously designed to ensure optimal amplification of the target DNA sequence. The process commenced with an initial heat denaturation stage at 368.15K (95°C), lasting for 15 minutes. This step facilitated the separation of the DNA double strands, providing single-stranded templates for subsequent amplification.

Following the initial denaturation, the PCR machine underwent 40 cycles, each consisting of three distinct temperature-controlled stages. The first stage involved denaturation at 368.15K (95°C) for 30 seconds, where the hydrogen bonds holding the DNA strands together were broken, allowing them to separate. Subsequently, the temperature was lowered to 333K (60°C) for 30 seconds, promoting the annealing of the primers to their complementary sequences on the target DNA. This annealing step ensured precise and specific binding of the primers, enabling the DNA polymerase to initiate replication. Finally, the temperature was raised to 345.15K (72°C) for 30 seconds, facilitating the extension of the primers by the DNA polymerase, resulting in the synthesis of new DNA strands.

Upon completion of the 40 cycles, a crucial step known as the melting curve analysis was conducted. This analysis involved gradually increasing the temperature from 345.15K to 368.15K, with each step incrementing by 274.15K (1°C). During this process, the DNA strands dissociated, and the fluorescence intensity was monitored. The melting curve provided valuable information about the DNA sequences present in the reaction mixture, enabling the detection of any nonspecific products or primer dimers. This analysis was crucial for ensuring the specificity and accuracy of the PCR amplification.

For the assessment of relative genetic expression, beta-actin served as the housekeeping gene. The primer sequences utilized for the tested genes were as follows:

#### 4.4: List of Primers

No	Primers Name	Primer Sequence (5' – 3')
1.	B-Actin	(F-CTCACGGTGTGGCCAAAATG, R-GCCTTGATCCTTTGGTTATTCG)
2.	STMN1	(F-TTGCCAGTGGATTGTGTAGAG, R-TTCTTTTGATCGAGGGCTGAG)
3.	S1009A	(F-GAAATGGTGAATAAGGACTTGCC, R-TCAACTTCCCATCAGCATC)
4.	Wnt	(F-ACGGAGTCTGACCTGATGTAG, R-CACCTGTCGCTCTCATGTAC)
5.	LRP6	(F-TGAAATGCCACCTTCTACC, R-AAGTGTCCTGAAAGTGAAG)
6.	GSK3 $\beta$	(F-ACCTGCCCTCTTCAACTTTAC, R-CACGGTCTCCAGCATTAGTATC)
7.	AXIN	(F-CAGCCTTCTCATCTCTTCATCC, R-GTGATTTTGTCTCTGCTTGG)
8.	HIF1 $\alpha$	(F-GGTGGATATGTCTGGGTTGAG, R-AGGGAGAAAATCAAGTCGTGC)
9.	VHL	(F-TTTGGCTCTTCAGGGATGC, R-CACCGCTCTTCAGGGTATAC)
10.	C-myc	(F-CTCGCGTTATTTGAAGCCTG, R-TCGCAGATGAAATAGGGCTG)
11.	Cox 2	(F-TCAAGGGAGTCTGGAACATTG, R-GCTTCCCAACTTTTGTAACCG)
12.	VEGF	(F-AAAGCCAGCACATAGGAGAG, R-ATTTAAACCGGGATTTCTTGCG)
13.	PTEN	(F-CCACAAACAGAACAAGATGCTC, R-CAAAGACTTCCATTTTCCAC)

Following the completion of PCR cycles, a melt curve analysis was conducted to identify any non-specific products. The qPCR products were displayed as a single peak on the melt

curve graph, indicating the absence of primer dimers or non-specific products. This analysis is crucial for verifying the specificity of the amplification and ensuring that the observed changes in gene expression are accurate and not influenced by unintended products.

#### **4.2.11. Flow cytometry for apoptosis measurement**

The procedure for the apoptosis assay involved several steps. Cells were washed twice with cold Bio Legends Cell Staining Buffer. For the apoptosis assay, cells were re-suspended in Annexin V binding buffer at a concentration of  $0.25-1 \times 10^7$  cells/mL. A 100 $\mu$ L cell suspension was transferred to a 5mL test tube. Then, 5  $\mu$ L of FITC Annexin V was added to the cell suspension. Subsequently, 10  $\mu$ L of propidium iodide solution was added. The cells were gently vortexed at 298.15K (25°C) and incubated in dark conditions for 15 minutes. Following the incubation period, 400 $\mu$ L of Annexin V binding buffer was added to each tube. The samples were then analyzed using a flow cytometer. This assay allowed for the detection and quantification of apoptotic cells using fluorescent markers such as FITC Annexin V and propidium iodide, which bind to specific cellular components indicative of apoptosis. The flow cytometer was utilized to analyze and interpret the obtained results.

#### **4.2.12. Statistical analysis**

Descriptive statistics were computed utilizing GraphPad Prism software (version 5.01), displaying the results in the format of  $\pm$  standard error of the mean ( $\pm$ SEM). Statistical significance was assessed with a significance threshold set at p-value  $< 0.05$  (\*),  $p < 0.01$  (\*\*), and  $p < 0.001$  (\*\*\*)).

For inter-group comparisons, one-way analysis of variance (Hendrych *et al.*, 2004) was employed, followed by Tukey's post hoc test. This statistical approach allowed for comprehensive comparisons among multiple groups, assessing the differences between individual groups.

### **4.3. Results**

#### **4.3.1 Characterization of NiET using DLS, XRD, SEM and EDX analysis**

---

The dynamic size of NiET Nps was observed as  $\sim 712.5$  nm with population density index (PdI)  $\sim 0.670$ , while the surface charge expressed was  $-12.7$  mV due to surface coating of hyaluronic acid as in figure 4.1.

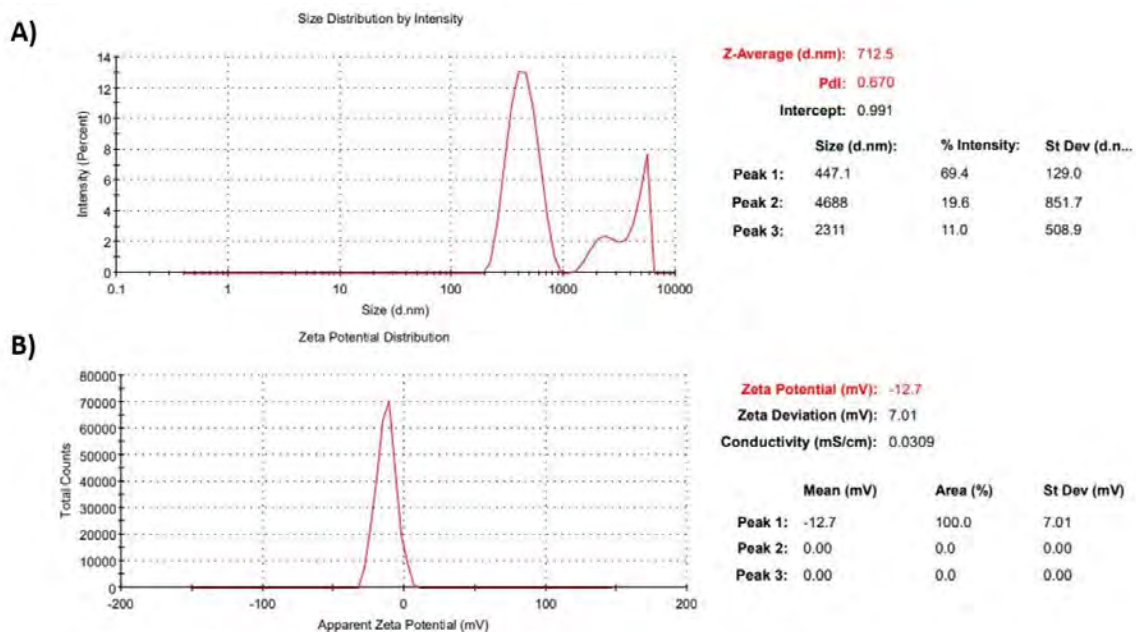


**Figure 4.1:** The dynamic light spectrum analysis confirming size of NiET Nps  $\sim 712.5$  nm with population density index (PdI)  $\sim 0.670$ , and surface charge  $-12.7$  mV

XRD diffraction pattern indicates three significant peaks at  $29^\circ$ ,  $34^\circ$ ,  $48^\circ$  and  $67^\circ$  indicating square-planar structure of NiET crystal with overall pseudo-octahedral coordination geometry with particle size  $\sim 715$  nm as shown in figure 4.2.

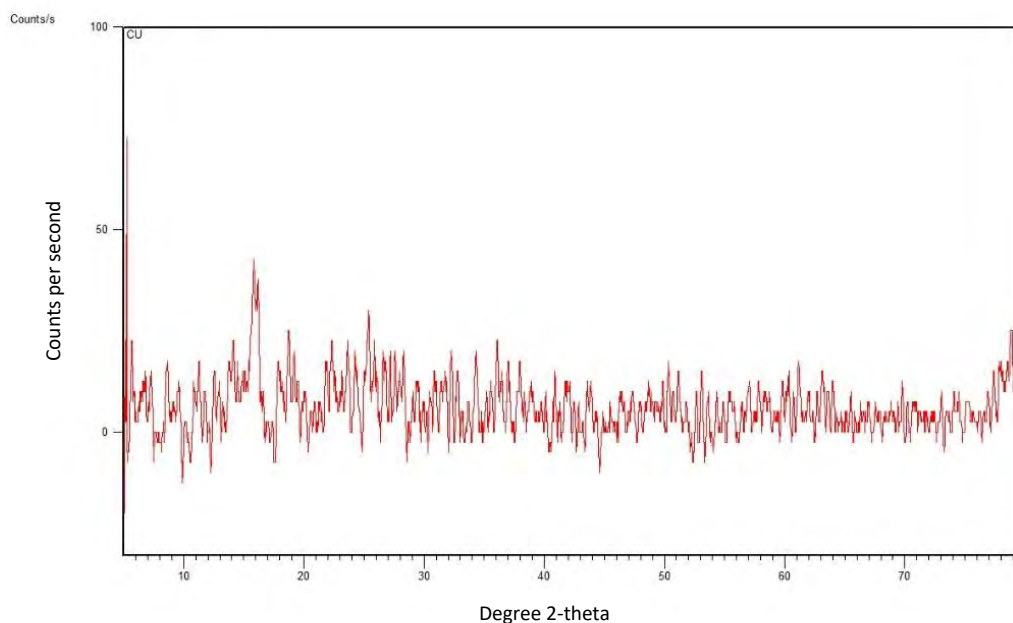


**Figure 4.2:** *The XRD pattern of Nickel diethyldithiocarbamate*

SEM images clearly showed complex formation of metal atom with diethyldithiocarbamate complex as in figure 4.3.

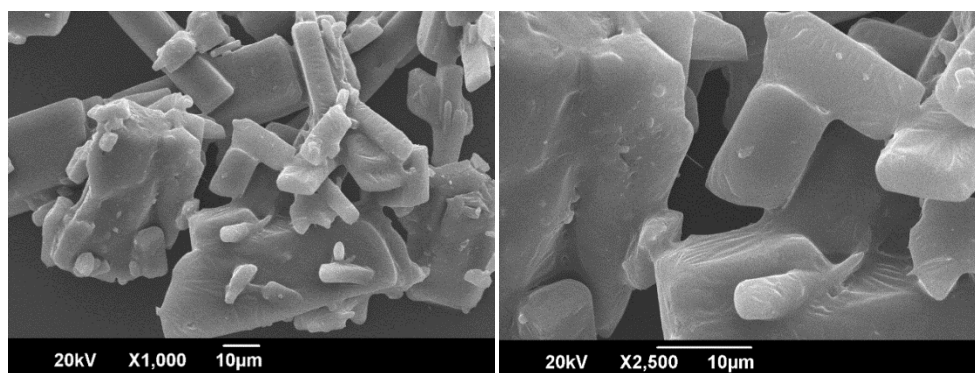


**Figure 4.3:** *Scanning electron microscopy of NiET with magnifications at 1000X and 2500X respectively*

Whereas, energy-dispersive X-ray (EDX) analysis exhibited 12.9% nickel, 32.1% sulphur, 1.8% oxygen, 9.4% nitrogen, and 43.8% carbon by weight as shown in figure 4.4 and table 4.5.

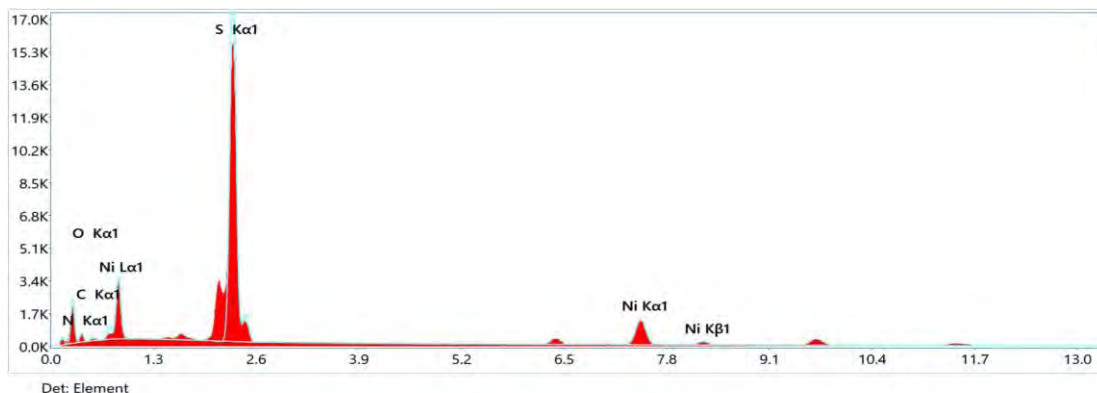


**Figure 4.4:** Energy dispersive spectroscopic image of Nickel diethyldithiocarbamate exhibiting individual elements in its composition via intensity under peaks.

**Table 4.5:** Individual elements and their percentages by weight and atomic size in composition of NiET

Element	Weight %	MDL	Atomic %	Error %
C	43.8	0.70	64.5	13.2
N	9.4	0.94	11.9	19.8
O	1.8	0.54	2.0	34.1
S	32.1	0.07	17.7	3.3
Ni	12.9	0.26	3.9	4.3

#### 4.3.2 Relative organ weight recovery in treatment groups

Relative organ weights of vital organs liver, heart and kidney were significantly increased in leukemic rats. Doxorubicin alone was found to be more effective than NiET and combination regimes in restoring liver, heart and kidney weights (Figure 4.5A-C)

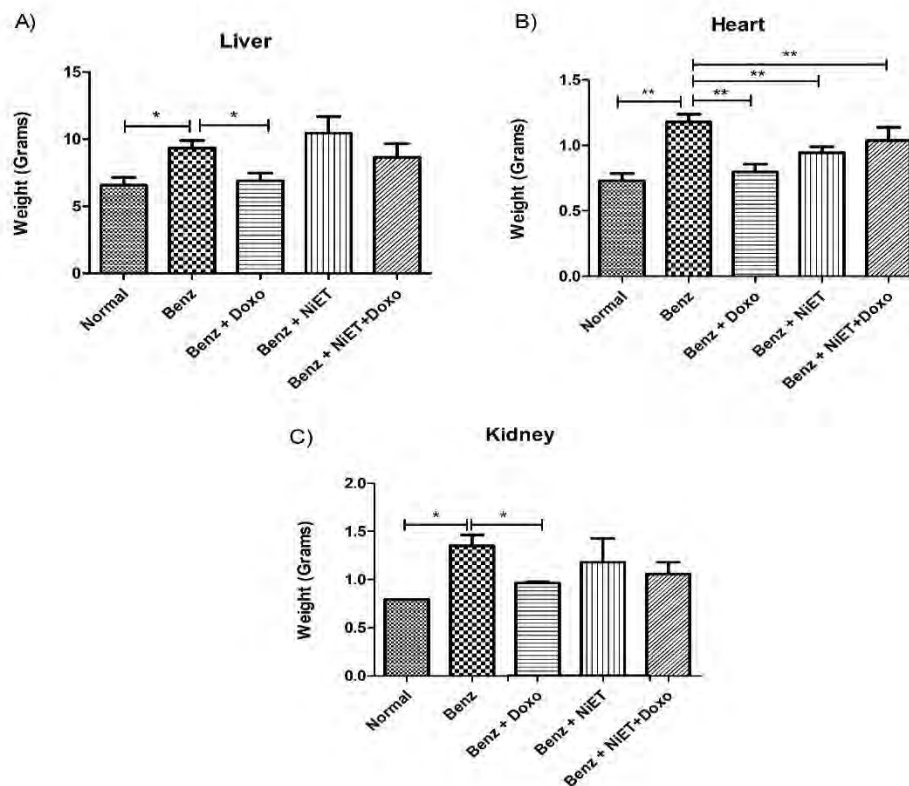


**Figure 4.5: Restoration of relative A) liver, B) heart and C) kidney weights of different treated groups ( $n=3$ )**

### 4.3.3 Restoring the morphology and hematological profile

Morphological examinations revealed erythrocytopenia and presence of myeloblasts in benzene-treated leukemic blood and bone marrow. The NiET treatment restored cell morphology, displaying intact red blood cells and a normal nucleus-to-cytoplasm ratio. Similarly, the aberrant shape of leukoblasts in bone marrow samples normalized after NiET administration, as indicated by arrows in figure 4.6.

In the benzene-treated rats, whole blood count analysis revealed an abnormal rise in total WBCs and neutrophils, as well as a significant decrease in RBCs, lymphocytes, hemoglobin, and platelets ( $p<0.05$ ). These abnormal cell counts were substantially recovered in leukemic rats after administration of NiET as free drug and in combination with doxorubicin. The combination therapy was more effective in recovering WBCs ( $p<0.001$ ), RBCs ( $p<0.01$ ), haemoglobin ( $p<0.01$ ), and platelets count ( $p<0.001$ ), however,



standalone NiET treatment showed better recovery in lymphocytes ( $p < 0.001$ ) and neutrophils count ( $p < 0.05$ ) only as shown in figure 4.7A-F.

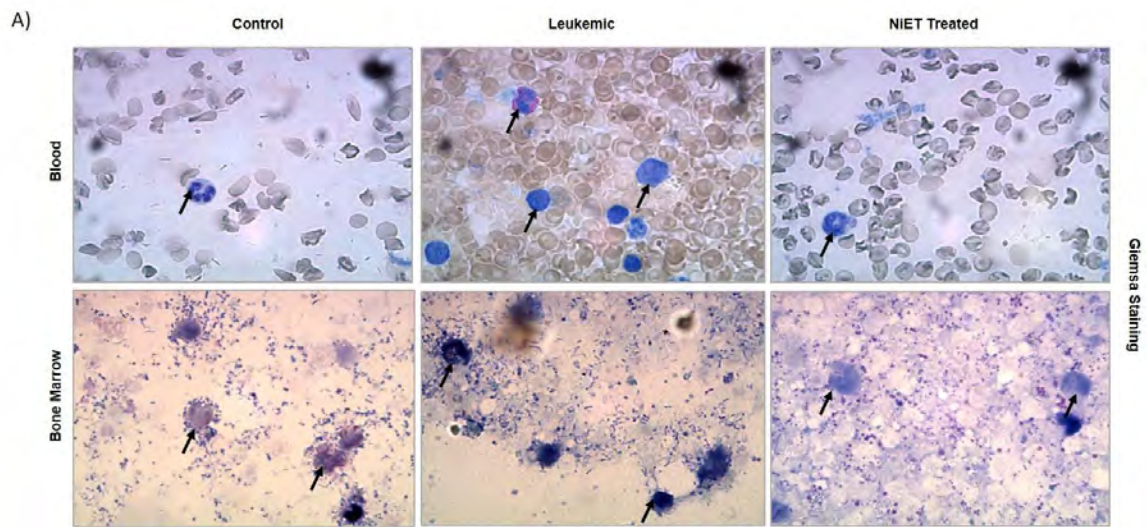


*Figure 4.6: Morphological analysis of blood and bone marrow cells using Giemsa staining dye (10X)*

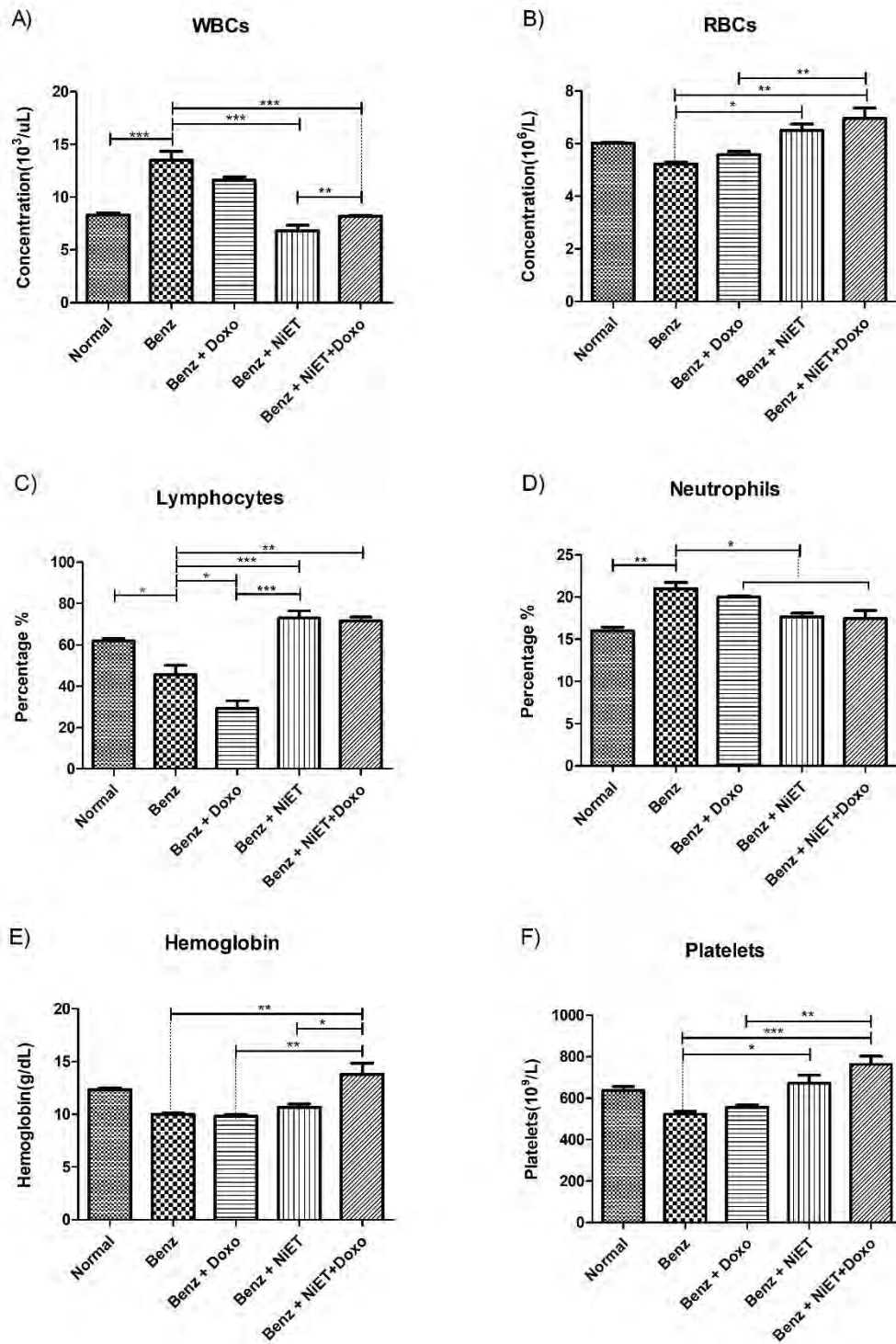


**Figure 4.7: Hematological profile analysis of multiple blood parameters in different experimental groups (n=3).**

#### 4.3.4 NiET's notable antioxidant potential verified by DPPH, TRP, and TAC assays

The DPPH assay exhibited significant ( $p < 0.001$ ) antioxidant potential of NiET at multiple concentrations, however, substantial increase was observed at 0.5 mg/mL dilution (Figure 4.8A). Likewise, the total reducing potential assay exhibited significant ( $p < 0.001$ ) reducing activity at all dilutions. It was observed that the reducing potential of NiET increased substantially when administered at 1 mg/mL concentration as shown in figure 4.8B. The total antioxidant capacity assay also exhibited a similar pattern (Figure 4.8C).

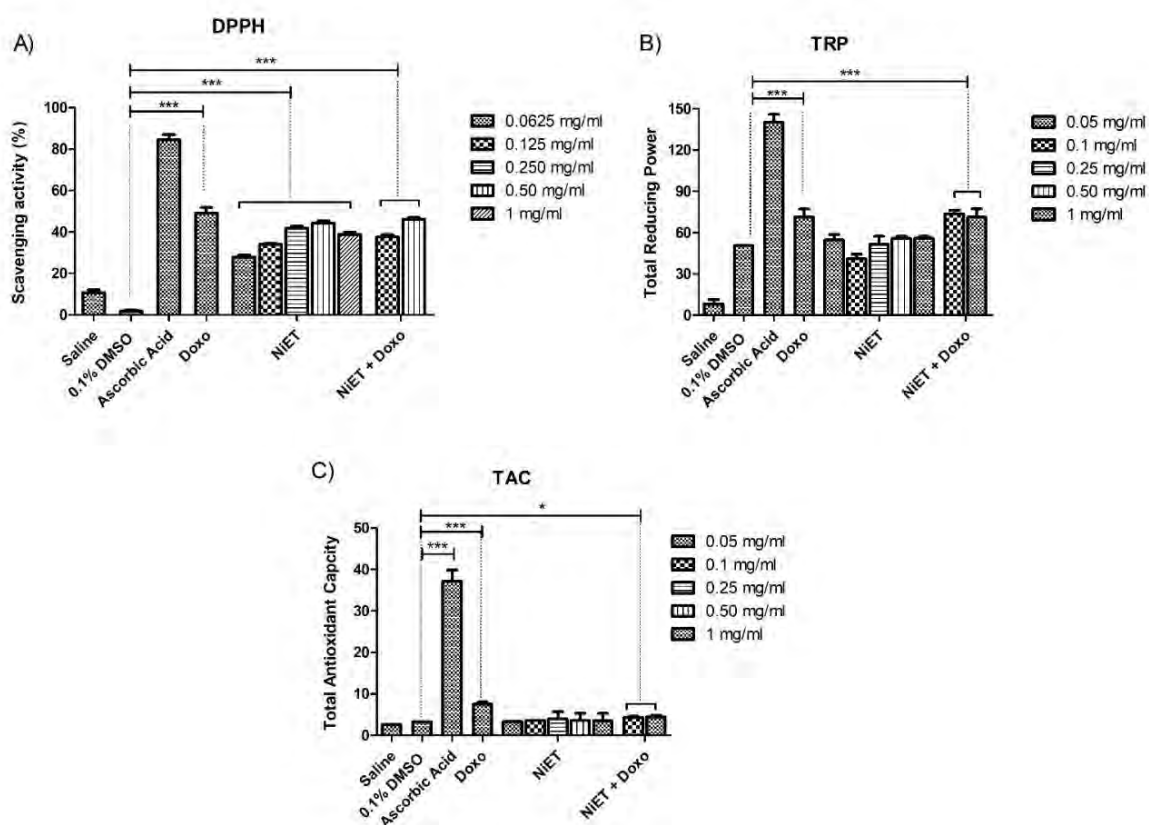
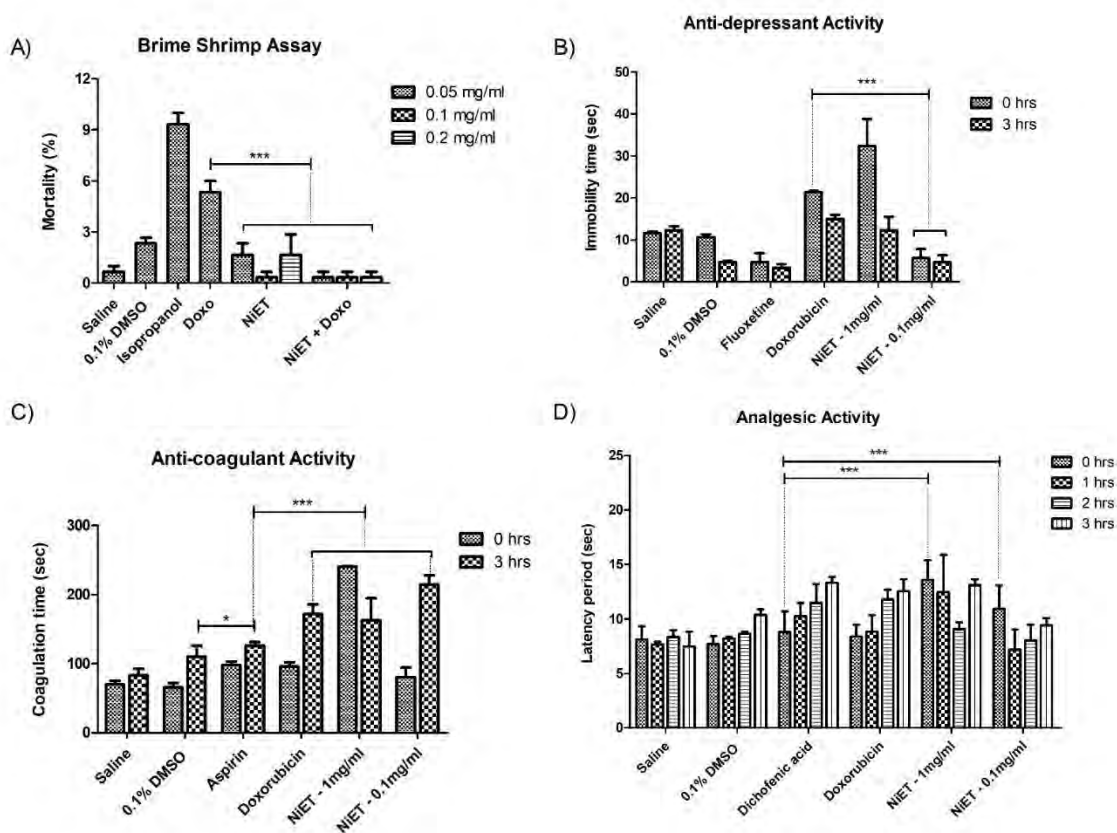


Figure 4.8: Antioxidant potential analysis of NiET at various NiET concentrations

#### 4.3.5 NiET's enhanced biological potential in rat model as an analgesic, anti-depressant, and anti-coagulant

The concurrent administration of NiET with chemotherapy resulted in a substantial decrease ( $p < 0.001$ ) in cytotoxicity, as evidenced by the findings of the brine shrimp assay

(Figure 4.9A). Moreover, the combined therapy demonstrated significant improvements in its anti-depressant ( $p < 0.001$ ), analgesic ( $p < 0.001$ ), and anti-coagulation efficacy ( $p < 0.001$ ) compared to chemotherapy alone, particularly noticeable at a concentration of 1mg/ml (Figure 4.9B–D). Notably, in the assessment of antidepressant, anti-coagulant, and analgesic properties, fluoxetine, aspirin, and diclofenac acid were employed as positive controls, respectively.



**Figure 4.9: Biological potential analysis of NiET via multiple bioassays (n=3).**

#### 4.3.6 Recovery of hepatic enzymes and serum uric acid levels

Hepatic biomarkers including ALT ( $p < 0.01$ ), AST ( $p < 0.001$ ) and ALP ( $p < 0.05$ ) showed significant increase in their serum levels upon benzene treatment. However, both NiET and combination therapy expressed remarkable reduction ( $p < 0.001$ ) in serum levels of all three hepatic markers as shown in figure 4.10A-C. Likewise, significant increase in serum uric

acid levels ( $p < 0.01$ ) was observed in leukemic rats which were reduced back to normal by NiET ( $p < 0.05$ ) and combination therapy ( $p < 0.01$ ) as indicated in figure 4.10D.

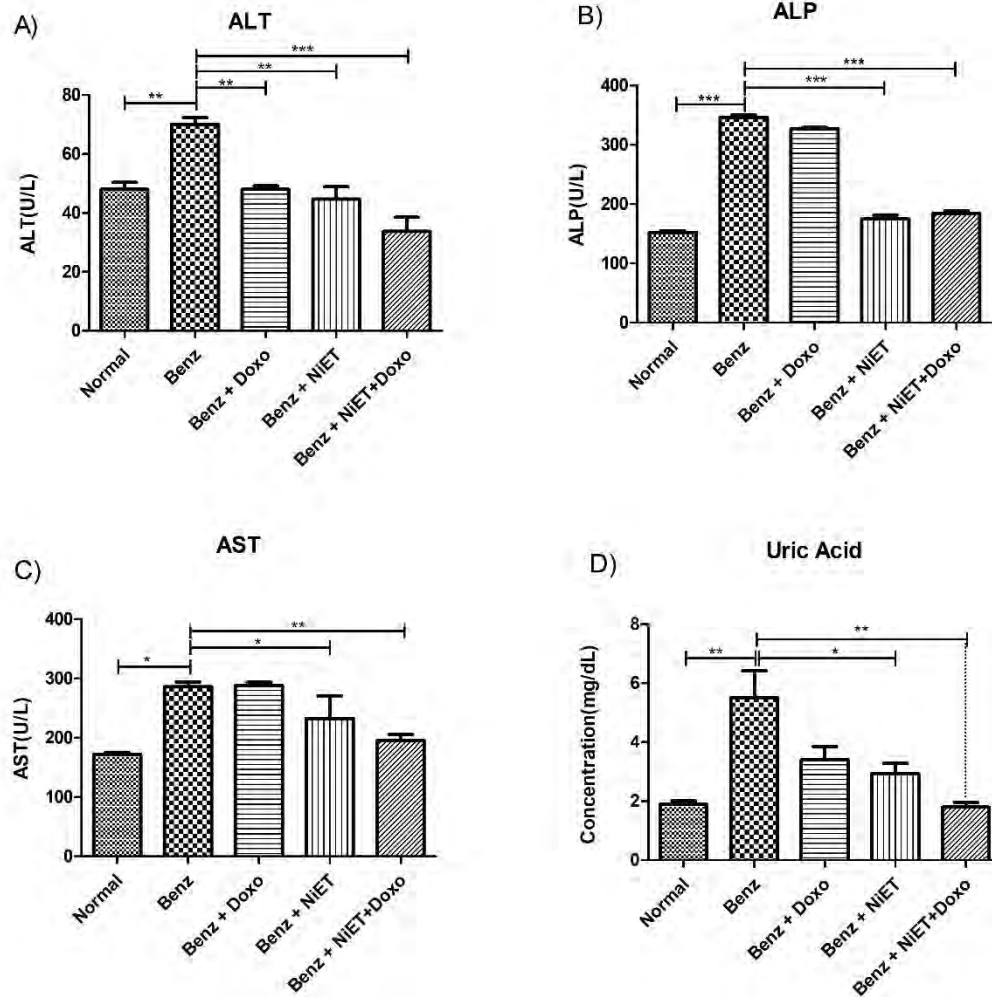


*Figure 4.10: Hepatic and renal biomarkers analysis in multiple treatment groups (n=3).*

#### 4.3.7 AML induction confirmation by dysregulation of STMN1 and S1009A genomic expression

Significant increase ( $p < 0.05$ ) in STMN1 while decrease ( $p < 0.01$ ) in S1009A expressions in benzene treatment group confirmed AML induction. Doxorubicin alone did not exhibit any noticeable recovery in STMN1 expression, whereas substantial ( $p < 0.001$ ) increase was observed in case of S1009A. Likewise, NiET treatment significantly reduced ( $p < 0.001$ )

STMN1 and elevated ( $p < 0.01$ ) S1009A expressions back to normal. Combination regimen remained most effective in decreasing STMN1 expression ( $p < 0.001$ ) indicating the synergy as shown in figure 4.11A, B.

#### **4.3.8 The canonical Wnt signaling pathway exhibited an upregulation of negative regulators**

The expression of Wnt significantly enhanced ( $p < 0.001$ ) in benzene treated group, while its negative regulators, GSK3 $\beta$  ( $p < 0.001$ ) and AXIN ( $p < 0.05$ ), reduced significantly in leukemic rats indicating stimulation of Wnt pathway which gives growth advantage to cancerous cells (Figure 4.11C-F). Doxorubicin and its combination with NiET synergistically reduced the genetic expression of Wnt ( $p < 0.001$ ) along with increased GSK3 $\beta$  expression levels ( $p < 0.001$ ). Individual drug treatment proved to be most effective in restoring expression of AXIN gene ( $p < 0.001$ ) depicting anti-proliferative potential of individual drugs.

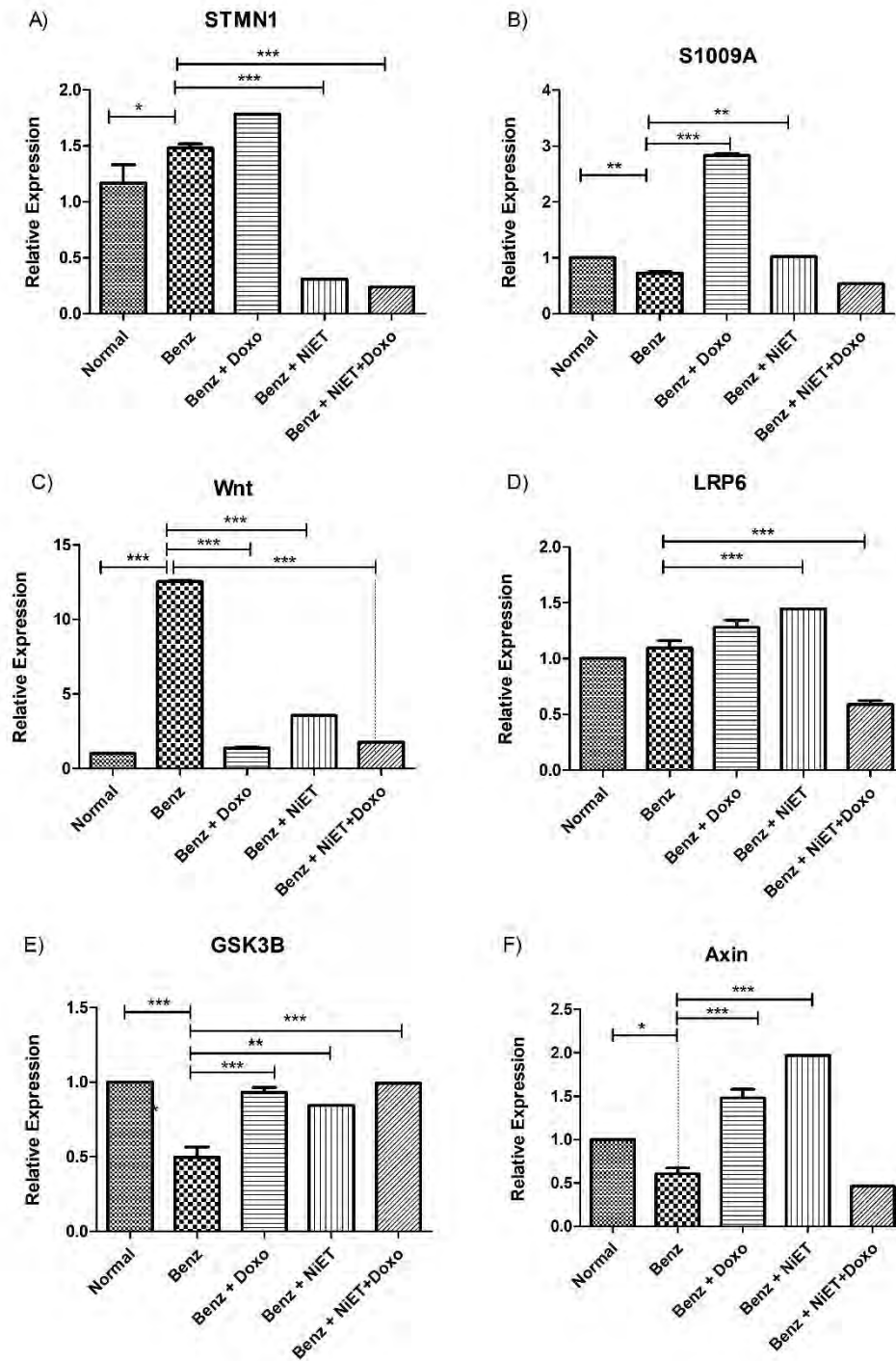


**Figure 4.11: Gene expression analysis of AML genetic markers including A) STMN1 and B) S1009A along with Wnt pathway components including c) Wnt ligand D) LRP6 E) GSK3 $\beta$**

#### **4.3.9 Downregulation of HIF-1 $\alpha$ pathway pro-survival signaling markers**

Benzene induced leukemic rats expressed significantly increased Wnt, Cox-2 and c-MYC expression ( $p < 0.001$ ) which was significantly ( $p < 0.001$ ) reduced by combination therapy. However, standalone doxorubicin treatment was more effective in restoring VHL expression ( $p < 0.001$ ) only indicating promising effects of individual drug treatment in restoring expression of tumor suppressor genes. Both VEGF and PTEN expressions were restored significantly ( $p < 0.001$ ) upon combination treatment as shown in figure 4.12A-F.



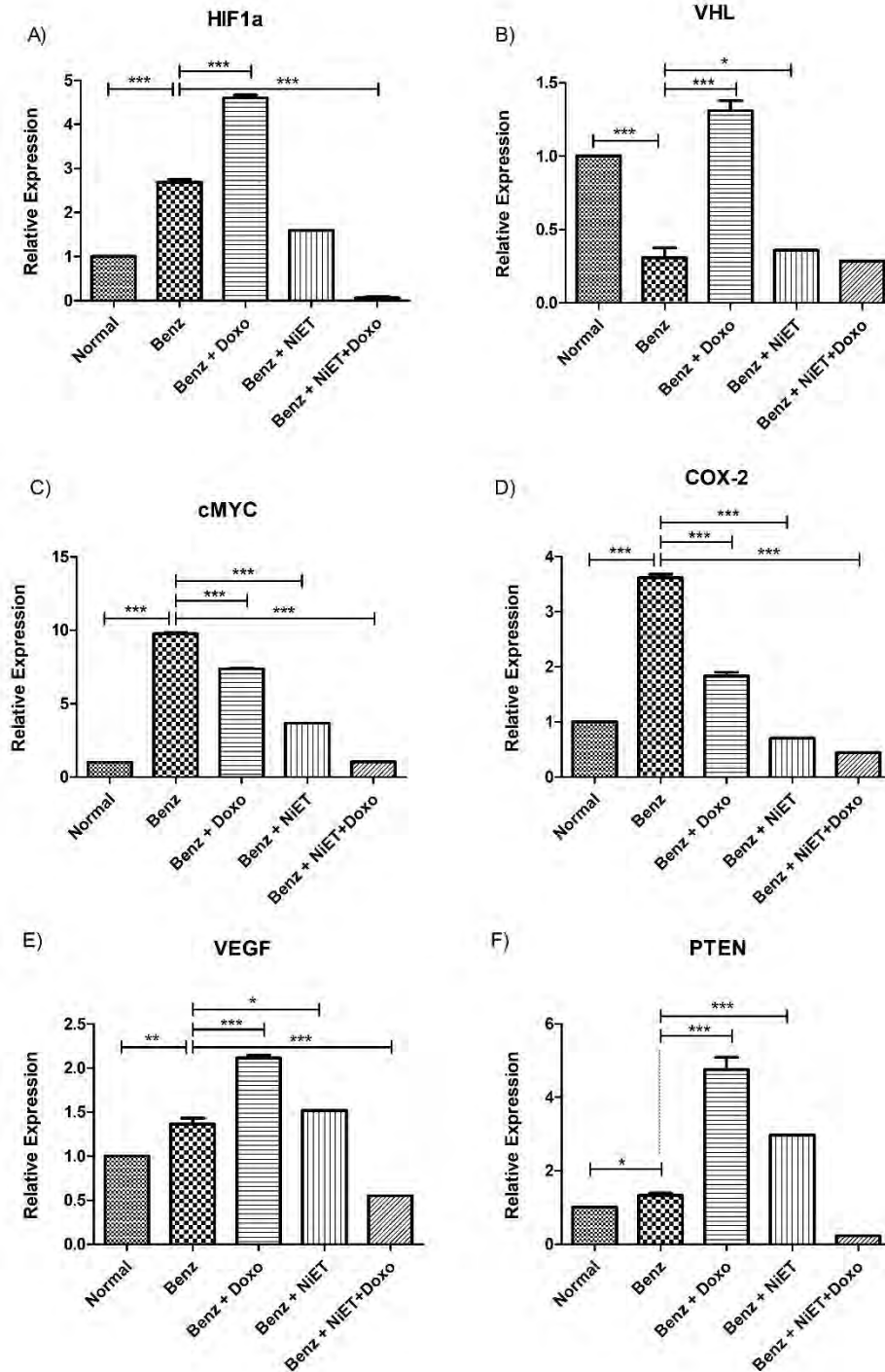


**Figure 4.12: Gene expression analysis of HIF 1 $\alpha$  pathway markers including A) HIF 1 $\alpha$  ligand B) VHL C) cMYC D) COX-2 E) VEGF and F) PTEN in treatment groups (n=3)**

### 4.3.10 The AnnexinV/PI apoptosis test confirms strong synergy of combination treatment

Flow cytometry analysis utilizing annexin V and propidium iodide dyes was employed to evaluate the apoptotic potential of the treatment regimes. The normal group displayed a basal apoptotic cell population of 2.47%, contrasted by a significant increase in leukemic rats i.e. 7.68% due to benzene-induced cell death (Figure 4.13A, B). Doxorubicin treatment increased the apoptotic population to 14.45%, while NiET as a free drug induced 11.53% apoptosis in leukemic cells (Figure 4.13C, D). However, the combination therapy exhibited a substantial enhancement in apoptotic cell population, escalating it to 47.79% in leukemic rats (as shown in figure 4.13E). This remarkable surge in apoptotic cells underscores the synergistic potential of the combined NiET and doxorubicin treatment regimen, presenting a compelling therapeutic advantage.

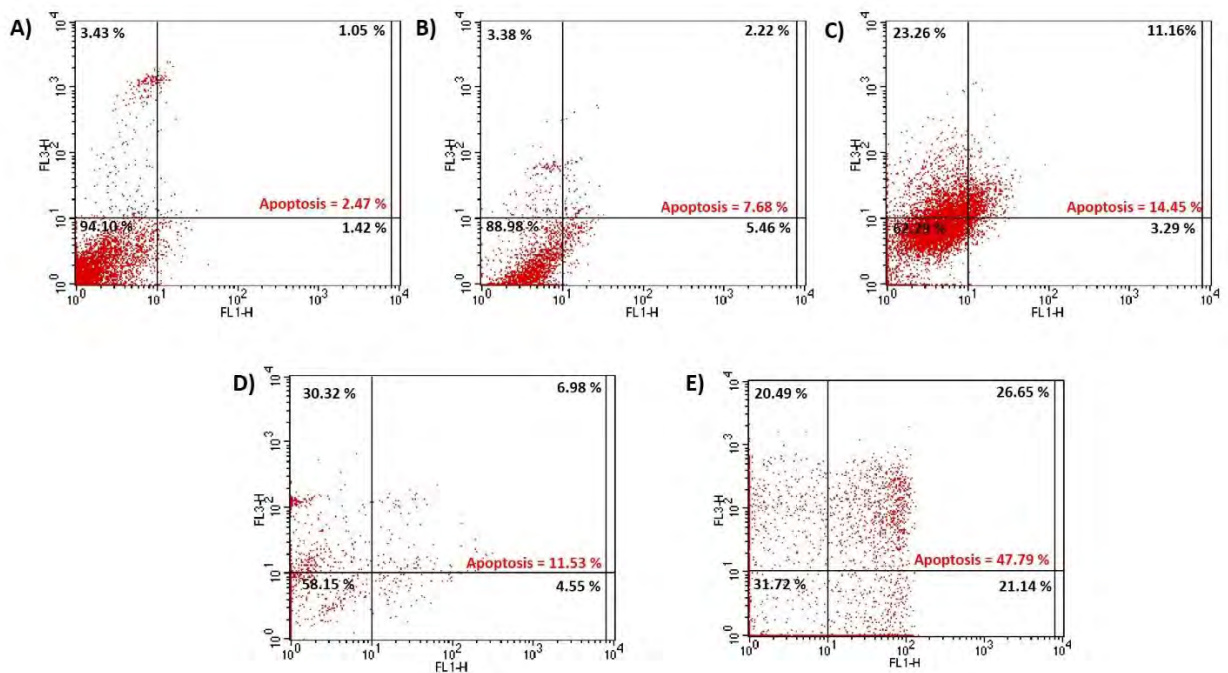


**Figure 4.13: FACS analysis using propidium iodide and annexin V dye in (A) Normal (B) Benzene (C) Doxorubicin (D) NiET and (E) NiET along with Doxorubicin treated groups ( $n=3$ ).**

### 4.3.11. The CD4 viability test

Flow cytometry analysis using CD4 antibody demonstrated the immunomodulatory impact of combination therapy. The control group exhibited 30.95% CD4<sup>+</sup> cells population, which significantly reduced to 7.67% in benzene-induced leukemic rats. However, doxorubicin increased CD4<sup>+</sup> population to 24.25%, whereas 21.54 % CD4<sup>+</sup> population was observed in NiET treated group. Notably, the combination therapy effectively restored CD4<sup>+</sup> population to 27.30%, demonstrating its superior efficacy in reinstating viable cells population in leukemic rats (Figure 4.14A-E).

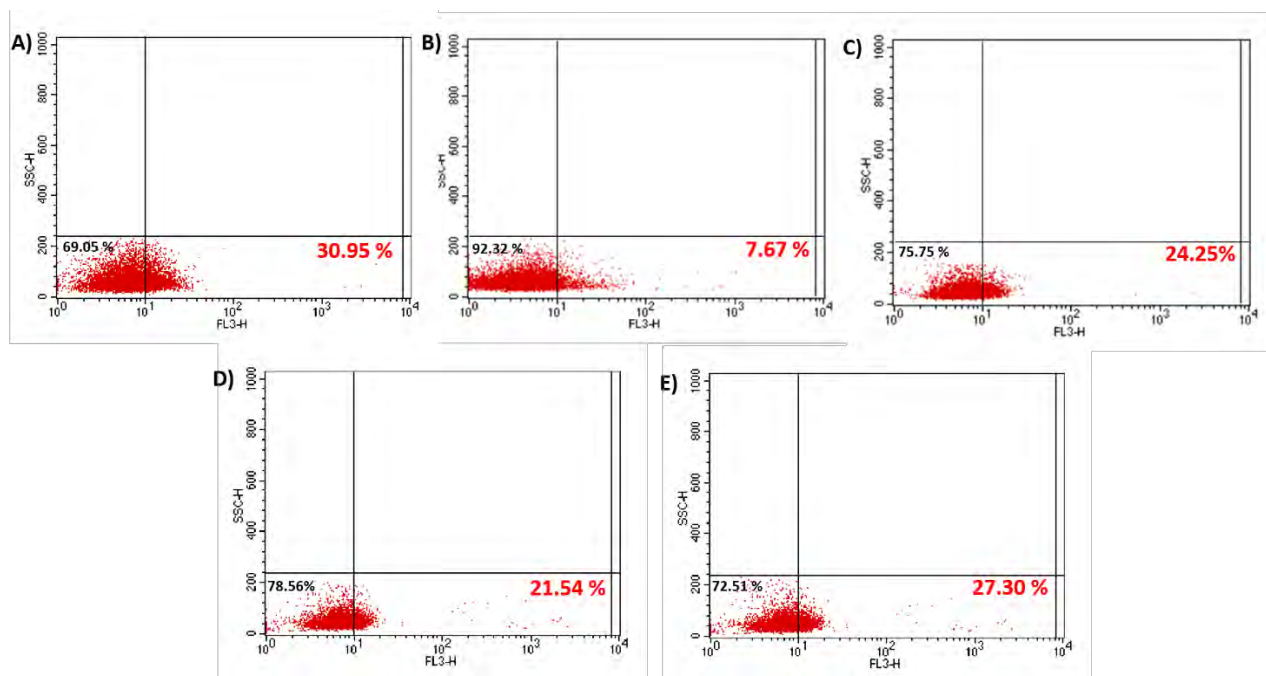


**Figure 4.14:** FACS analysis using CD4 antibody in A) Normal B) Benzene C) Doxorubicin D) NiET and E) NiET along with Doxorubicin treated groups (n=3).

## 4.4. Discussion

Nanoparticles serve as highly effective drug carriers due to their capacity to cross blood-brain barrier and cell membranes, reducing off-target side effects and enabling precise, site-specific delivery (Luo *et al.*, 2020). The NiET nanoparticles were created by combining DTC and Ni<sup>2+</sup> at a specific ratio. These particles had a slightly positive charge due to the presence of Ni<sup>2+</sup> on their surface. This positive charge allowed them to bind with

hyaluronic acid, making modified NiET nanoparticles that could target and damage leukemic cells that express CD33. These nanoparticles could dissolve in acidic environments within cells, releasing drug quickly and causing anti-tumor effects. They were highly effective against leukemic cells in laboratory tests and, when given intravenously, could gather in bone marrow cells, inhibiting the development of acute myeloid leukemia even at very low doses (0.1 mg/kg). This low dosage is significant as it minimizes systemic toxicity and adverse effects while maintaining therapeutic efficacy. The ability to achieve clinical endpoints at such a reduced concentration highlights the potential for improved safety and tolerability in patients, enhancing overall treatment outcomes. Advanced imaging techniques confirmed the structure of these nanoparticles, and analysis confirmed the presence of Nickel within them.

The increase in organ weight observed in our *in vivo* experiments is likely attributable to benzene metabolites directly affecting these organs. This leads to the generation of free radicals, elevated cell turnover, and consequent hypertrophy (Rana & Verma, 2005). Benzene, via its metabolites (phenol, catechol, and hydroquinone), triggers acute myeloid leukemia. Morphological analysis revealed that benzene and these cytotoxic metabolites cause erythrocytopenia, resulting in reduced red blood cell count and related abnormalities like eosinophilia and leukocytosis (Hallenbeck & Cunningham, 1985). Likewise, benzene-induced mutations in bone marrow cells disrupt the typical development of white blood cells, leading to an elevated total white blood cell count and an increased presence of immature leukoblasts in the peripheral bloodstream (Greenwood *et al.*, 2006). In this study, consistent observations were noted. Both standalone NiET and its combination treatment significantly restored a normal blood profile in leukemic rats. This was evidenced by the substantial reduction in eosinophilia and leukocytosis, along with an increase in erythropoiesis (Hallenbeck & Cunningham, 1985). The reduction in platelet levels observed in our study is likely linked to the detrimental effect of benzene exposure on bone marrow cells. However, intriguingly, the combination treatment significantly increased platelet counts by alleviating thrombocytopenia. This presents a promising approach to counteract the reduction in platelet levels (Olsson *et al.*, 2005). NiET functions within tumor cells by binding tightly to nuclear protein localization-4 (NPL4), triggering its aggregation. This interaction disrupts the essential p97-NPL4-UFD1 pathway, causing an

---

accumulation of ubiquitinated proteins and impeding the degradation of cellular waste proteins. As a result, this series of events ultimately leads to cell apoptosis (Peng *et al.*, 2020).

Benzene metabolites disrupt the normal levels of ALP, ALT, and AST by inducing reactive oxygen species (ROS) production through its secondary metabolites. Given that, the liver is a primary target of benzene toxicity, this dysregulation occurs as a consequence of its impact on hepatic functions (Ito *et al.*, 2003). The increased levels of ALP and ALT were possibly a result of abnormal liver cell proliferation, subsequently leading to elevated alanine phosphatase and transaminase levels in leukemic rats (Farrow *et al.*, 1997). Similarly, the elevation in blood serum AST concentration serves as an indicator of hepatocytotoxicity, reflecting the damage inflicted upon liver cells by benzene exposure. Benzene administration also led to increased serum creatinine levels, indicating an impending acute kidney injury in leukemic rats. Remarkably, our combination therapy notably reversed these abnormal levels of hepatic enzymes, owing to its reduced cytotoxicity and an enhanced antioxidant potential (Lahoti *et al.*, 2010).

Genetic expression analysis was performed by homogenizing bone marrow cells since AML originates in myeloid stems cells and NiET is reported to accumulate in bone marrow of leukemia patients. The increased expression of STMN1, one of the most prominently over-expressed genes in AML, was observed in benzene-administered leukemic rats. This elevation confirms leukemia induction, marking a genetic manifestation of the disease (Handschuh *et al.*, 2018). Likewise, The decrease in S1009A expression in AML affirms its role in disease induction, signifying its crucial involvement in leukemia development and progression (Laouedj *et al.*, 2017). The administration of NiET exhibited a mitigating effect on the impact of benzene exposure by downregulating STMN1 expression while concurrently upregulating S1009A expression. This modulation suggests a potential alteration in cellular actin function and microtubule dynamics (Wu *et al.*, 2014).

In benzene induced AML rats, aberrant signaling leads to the upregulation of LRP6, possibly due to enhanced Wnt ligand expression. This upregulation activates Wnt signaling. Conversely, GSK3 $\beta$  and Axin, key components in the destruction complex that usually inhibit Wnt signaling, are downregulated which might result from various mechanisms, including mutations or altered expression patterns, disrupting the inhibitory

function of the destruction complex (Zhan *et al.*, 2017). However, NiET synergistically reversed dysregulated Wnt signaling in leukemic cells by targeting key components of the pathway, when administered with doxorubicin. It intervened by inhibiting the overactive LRP6 receptor and promoting the restoration of GSK3 $\beta$  and Axin expression. NiET's action inhibits aberrant Wnt signaling, thereby restoring the balance and mitigating the abnormal cell proliferation and survival observed in leukemic cells which is in line with previous studies (Hendrych *et al.*, 2022).

Hypoxic environment in AML triggers the stabilization and increased expression of HIF-1 $\alpha$ , promoting its transcriptional activity. Conversely, the downregulation of VHL (Von Hippel-Lindau) in AML contributes to HIF-1 $\alpha$  upregulation as VHL is responsible for targeting HIF-1 $\alpha$  for degradation under normal oxygen levels. The reduced expression or function of VHL leads to the accumulation of HIF-1 $\alpha$ , fostering an environment conducive to leukemic cell survival, proliferation, and angiogenesis within the hypoxic niche of the bone marrow in AML (Magliulo & Bernardi, 2018). NiET as combination regime counteracted hypoxia-driven HIF-1 $\alpha$  upregulation by possibly inhibiting its stabilization, promoting VHL-mediated degradation. This restoration of balanced HIF-1 $\alpha$  and VHL expression levels potentially helps in regulating the hypoxic responses, impeding aberrant survival and proliferation pathways in AML cells. Likewise, benzene exposure induces genetic mutations and epigenetic changes that promote the overexpression of c-myc, a critical regulator of cell proliferation. In contrast to this, NiET's action likely involves inhibiting factors, restoring a more balanced and controlled expression of this oncogene within AML cells (Tang *et al.*, 2021). Additionally, COX-2, an enzyme involved in inflammation and cell signaling, is upregulated, likely due to benzene-induced inflammatory responses (Carter *et al.*, 2019). NiET in combination with doxorubicin may exert its synergy on upstream regulators or signaling cascades influencing COX-2 expression, contributing to its restoration within AML cells. PTEN, a tumor suppressor gene, shows increased expression, potentially as a compensatory response to the heightened proliferation signaling induced by benzene exposure (Peng *et al.*, 2010).

In an Annexin V/PI assay, benzene exposure led to increased apoptosis, indicated by higher levels of Annexin V (marking early apoptosis) and Propidium Iodide (highlighting late

---

apoptosis) (Malovichko *et al.*, 2021). Doxorubicin intercalates into DNA, inhibiting topoisomerase II and leads to DNA damage. This DNA damage triggers cellular stress responses, activating apoptotic pathways resulting in enhanced apoptosis as observed in Annexin V/PI assay (Fujiwara *et al.*, 2006). NiET also induces apoptosis in leukemic population probably by hindering survival pathways, but when combined with doxorubicin, the two compounds act synergistically. NiET's ability to sensitize the cells amplifies doxorubicin's apoptotic effect, leading to a greater induction of programmed cell death than both standalone treatments. The same synergy is observed in CD4 viability assay as when NiET treatment is applied, it potentially targets leukemic cells, depicting high specificity of the combination therapy to spare normal/ healthy cells (Huang *et al.*, 2021). This selective targeting, coupled with the enhanced apoptotic potential of the combination, may result in a higher proportion of viable non-leukemic cells within the leukemic population compared to standalone treatments.

---

## **Conclusion**



## Conclusion

Our collective research underscores the significant therapeutic potential of CcNPs, CuET and NiET nanoparticles, in combination with doxorubicin as promising avenues in the treatment of acute myeloid leukemia. Supported by *in vitro*, *in vivo*, and *in silico* studies, these nanomedicines exhibit unique anti-leukemic properties, inducing the TRAIL-DR5 complex and inhibiting the NF- $\kappa$ B p52/RelB/DNA complex. Moreover, their effectiveness in enhancing the anticancer potential of natural chemicals like caffeine while mitigating the adverse effects of traditional chemotherapy showcases their promise. Comprehensive methodologies, including *in silico* docking studies, antioxidant assays, and *in vivo* experimentation, revealed substantial improvements in hematological parameters, morphological features, and enzymatic markers in CuET and NiET-treated leukemic rats, particularly when combined with doxorubicin. Notably, both nanoparticles demonstrated a noteworthy impact on leukemic genetic markers (STMN1 and S1009A) and the normalization of aberrant Wnt and HIF-1  $\alpha$  pathway gene expression. AV/PI apoptosis and CD4 viability tests further underscored the potent efficacy of these combination therapies against leukemic cells. These findings highlight CuET and NiET nanoparticles, in synergy with doxorubicin, as promising therapeutic approaches for AML, meriting further investigation through clinical trials. Their potential to modulate specific pathways and enhance treatment efficacy while potentially reducing adverse effects signifies a compelling direction in AML therapy.

## Future Directions

The promising results of this study pave the way for several avenues. One crucial next step is to conduct clinical trials to validate the safety and efficacy of CcNPs, CuET, and NiET nanoparticles in combination with doxorubicin in human subjects. These trials should aim to optimize dosing regimens, minimize potential side effects, and assess long-term outcomes to confirm the therapeutic benefits observed in preclinical models. Additionally, further exploration of the molecular mechanisms underlying the nanoparticles' anti-leukemic properties could provide deeper insights into their interactions with cellular pathways.

Expanding the scope of research to include other types of leukemia and solid tumors could also reveal broader applications for these nanomedicines. Comparative studies on the effectiveness of different nanoparticle formulations and their combinations with other chemotherapeutic agents or immunotherapies may identify synergistic effects and novel therapeutic strategies. Moreover, advancements in nanoparticle engineering and functionalization techniques could lead to the development of even more targeted and efficient delivery systems. By incorporating responsive elements that release therapeutic payloads in response to specific tumor microenvironment conditions, we can further enhance the precision and efficacy of AML treatments.

Finally, investigating the potential for personalized medicine approaches, where nanoparticle therapies are tailored based on individual patient profiles and genetic landscapes, could revolutionize AML treatment. This personalized strategy would aim to maximize therapeutic outcomes while minimizing adverse effects, offering a more effective and patient-centric approach to combating this aggressive disease.

## References

---

## References

- Ahn, Y., Lee, S., Park, C.-S., Jang, H. J., Lee, J. H., Park, B.-G., Kwon, D. (2018). Diethylamino-curcumin mimic with trizolyl benzene enhances TRAIL-mediated cell death on human glioblastoma cells. *Molecular & Cellular Toxicology*, *14*(2), 241-245.
- Allen, M., Boyland, E., Dukes, C., Horning, E., & Watson, J. (1957). Cancer of the urinary bladder induced in mice with metabolites of aromatic amines and tryptophan. *British Journal of Cancer*, *11*(2), 212.
- Almasan, A., & Ashkenazi, A. (2003). Apo2L/TRAIL: apoptosis signaling, biology, and potential for cancer therapy. *Cytokine & Growth Factor Reviews*, *14*(3-4), 337-348.
- Amirizadeh, A., Sheikhzadeh, S., & Delirez, N. (2023). Anticancer effects of caffeine nanoemulsions on chronic myeloid leukemia. *Studies in Medical Sciences*, *34*(9), 552-564.
- Anand, P., Kunnumakara, A. B., Sundaram, C., Harikumar, K. B., Tharakan, S. T., Lai, O. S., Aggarwal, B. B. (2008). Cancer is a preventable disease that requires major lifestyle changes. *Pharmaceutical Research*, *25*, 2097-2116.
- Arber, D. A., Orazi, A., Hasserjian, R., Thiele, J., Borowitz, M. J., Le Beau, M. M., Vardiman, J. W. (2016). The 2016 revision to the World Health Organization classification of myeloid neoplasms and acute leukemia. *Blood, The Journal of the American Society of Hematology*, *127*(20), 2391-2405.
- Armstrong, S. A., & Look, A. T. (2005). Molecular genetics of acute lymphoblastic leukemia. *Journal of Clinical Oncology*, *23*(26), 6306-6315.
- Baeuerle, P. A., & Henkel, T. (1994). Function and activation of NF-kappaB in the immune system. *Annual Review of Immunology*, *12*(1), 141-179.
- Bajracharya, R., Baral, K. C., Lee, S. H., Song, J. G., & Han, H.-K. (2023). Organometallic phyllosilicate-gold nanocomplex: an effective oral delivery system of methotrexate for enhanced in vivo efficacy against colorectal cancer. *International Journal of Nanomedicine*, 7257-7266.
- Banti, C. N., & Hadjidakou, S. K. (2021). Evaluation of toxicity with brine shrimp assay. *Bio-protocol*, *11*(2), e3895-e3895.

- Beals, N. (2018). *Evaluation of the delivery and targeting of nucleic acid based nanomaterials for therapeutic application*: Kent State University.
- Belson, M., Kingsley, B., & Holmes, A. (2007). Risk factors for acute leukemia in children: a review. *Environmental Health Perspectives*, *115*(1), 138-145.
- Bennett, H. S., Wyrick, A. D., Lee, S. W., & McNeil, J. H. (1976). Science and art in preparing tissues embedded in plastic for light microscopy, with special reference to glycol methacrylate, glass knives and simple stains. *Stain Technology*, *51*(2), 71-97.
- Bennett, J. M., Catovsky, D., Daniel, M. T., Flandrin, G., Galton, D. A., Gralnick, H. R., & Sultan, C. (1976). Proposals for the classification of the acute leukaemias French-American-British (FAB) co-operative group. *British Journal of Haematology*, *33*(4), 451-458.
- Bhatia, K., & Das, A. (2020). Combinatorial drug therapy in cancer-New insights. *Life Sciences*, *258*, 118134.
- Bobinihi, F. F., Osuntokun, J., & Onwudiwe, D. C. (2018). Syntheses and characterization of nickel (II) dithiocarbamate complexes containing NiS<sub>4</sub> and NiS<sub>2</sub>PN moieties: nickel sulphide nanoparticles from a single source precursor. *Journal of Saudi Chemical Society*, *22*(4), 381-395.
- Bruserud, Gjertsen, B. T., Foss, B., & Huang, T.-S. (2001). New strategies in the treatment of acute myelogenous leukemia (AML): In vitro culture of aml cells—The present use in experimental studies and the possible importance for future therapeutic approaches. *Stem cells*, *19*(1), 1-11.
- Büchner, T., Urbanitz, D., Hiddemann, W., Rühl, H., Ludwig, W., Fischer, J., Zeile, G. (1985). Intensified induction and consolidation with or without maintenance chemotherapy for acute myeloid leukemia (AML): two multicenter studies of the German AML Cooperative Group. *Journal of Clinical Oncology*, *3*(12), 1583-1589.
- Burnett, A. (2005). The treatment of AML: current status and novel approaches. *Hematology*, *10*(sup1), 50-53.
- Burnett, A. K., & Knapper, S. (2007). Targeting treatment in AML. *Education Program Book*, *2007*(1), 429-434.

- 
- Calgarotto, A. K., Longhini, A. L., Pericole de Souza, F. V., Duarte, A. S. S., Ferro, K. P., Santos, I., Torello, C. O. (2021). Immunomodulatory effect of green tea treatment in combination with low-dose chemotherapy in elderly acute myeloid leukemia patients with myelodysplasia-related changes. *Integrative Cancer Therapies*, 20, 1534-7354.
- Calvo, I. A., Gabrielli, N., Iglesias-Baena, I., García-Santamarina, S., Hoe, K.-L., Kim, D. U., Ayté, J. (2009). Genome-wide screen of genes required for caffeine tolerance in fission yeast. *PloS One*, 4(8).
- Care & Animals (1986). *Guide for the care and use of laboratory animals*: US Department of Health and Human Services, *Public Health Service*.
- Carter, B. Z., Mak, P. Y., Wang, X., Tao, W., Ruvolo, V., Mak, D., Andreeff, M. (2019). An ARC-regulated IL1 $\beta$ /Cox-2/PGE2/ $\beta$ -Catenin/ARC circuit controls leukemia–microenvironment interactions and confers drug resistance in AML. *Cancer Research*, 79(6), 1165-1177.
- Chan, J. K. (2014). The wonderful colors of the hematoxylin–eosin stain in diagnostic surgical pathology. *International Journal of Surgical Pathology*, 22(1), 12-32.
- Chang, S.-F., Chang, C. A., Lee, D.-Y., Lee, P.-L., Yeh, Y.-M., Yeh, C.-R., . . . Chiu, J.-J. (2008). Tumor cell cycle arrest induced by shear stress: Roles of integrins and Smad. *Proceedings of the National Academy of Sciences*, 105(10), 3927-3932.
- Chen, C., Xu, W., & Wang, C.-m. (2013). Combination of celecoxib and doxorubicin increases growth inhibition and apoptosis in acute myeloid leukemia cells. *Leukemia & Lymphoma*, 54(11), 2517-2522.
- Chen, K. T., Gilabert-Oriol, R., Bally, M. B., & Leung, A. W. (2019). Recent treatment advances and the role of nanotechnology, combination products, and immunotherapy in changing the therapeutic landscape of acute myeloid leukemia. *Pharmaceutical Research*, 36, 1-20.
- Chomczynski, P. (2010). Reagents and methods for isolation of purified RNA. In: Google Patents. (<https://patents.google.com/patent/US7794932B2/en>)
- Chomczynski, P., Wilfinger, W., Kennedy, A., Rymaszewski, M., & Mackey, K. (2010). RNAzol® RT: a new single-step method for isolation of RNA. In: *Nature Publishing Group US New York*.
-

- 
- Cvek, B., Milacic, V., Taraba, J., & Dou, Q. P. (2008). Ni (II), Cu (II), and Zn (II) diethyldithiocarbamate complexes show various activities against the proteasome in breast cancer cells. *Journal of Medicinal Chemistry*, *51*(20), 6256-6258.
- Das, S., Tripathi, N., Preet, R., Siddharth, S., Nayak, A., Bharatam, P. V., & Kundu, C. N. (2017). Quinacrine induces apoptosis in cancer cells by forming a functional bridge between TRAIL-DR5 complex and modulating the mitochondrial intrinsic cascade. *Oncotarget*, *8*(1), 248-267.
- de Castro, A. A., Soares, F. V., Pereira, A. F., Polisel, D. A., Caetano, M. S., Leal, D. H., . . . Ramalho, T. C. (2019). Non-conventional compounds with potential therapeutic effects against Alzheimer's disease. *Expert Review of Neurotherapeutics*, *19*(5), 375-395.
- Deng, Y., Lin, Y., & Wu, X. (2002). TRAIL-induced apoptosis requires Bax-dependent mitochondrial release of Smac/DIABLO. *Genes & development*, *16*(1), 33-45.
- Dere, E., & Ari, F. (2009). Effect of benzene on liver functions in rats (*Rattus norvegicus*). *Environmental Monitoring and Assessment*, *154*, 23-27.
- Deshantri, A. K., Moreira, A. V., Ecker, V., Mandhane, S. N., Schiffelers, R. M., Buchner, M., & Fens, M. H. (2018). Nanomedicines for the treatment of hematological malignancies. *Journal of Controlled Release*, *287*, 194-215.
- Deshayes, S., & Gref, R. (2014). Synthetic and bioinspired cage nanoparticles for drug delivery. *Nanomedicine*, *9*(10), 1545-1564.
- Devasagayam, T., Kamat, J., Mohan, H., & Kesavan, P. (1996). Caffeine as an antioxidant: inhibition of lipid peroxidation induced by reactive oxygen species. *Bba-Biomembranes*, *1282*(1), 63-70.
- DiNardo, C. D., Pratz, K., Pullarkat, V., Jonas, B. A., Arellano, M., Becker, P. S., Kantarjian, H. M. (2019). Venetoclax combined with decitabine or azacitidine in treatment-naive, elderly patients with acute myeloid leukemia. *Blood, The Journal of the American Society of Hematology*, *133*(1), 7-17.
- Döhner, H., Estey, E., Grimwade, D., Amadori, S., Appelbaum, F. R., Büchner, T., Larson, R. A. (2017). Diagnosis and management of AML in adults: 2017 ELN recommendations from an international expert panel. *Blood, The Journal of the American Society of Hematology*, *129*(4), 424-447.
-

- 
- Dombret, H., & Itzykson, R. (2017). How and when to decide between epigenetic therapy and chemotherapy in patients with AML. *Hematology 2014, the American Society of Hematology Education Program Book, 2017(1)*, 45-53.
- Duchartre, Y., Kim, Y.-M., & Kahn, M. (2016). The Wnt signaling pathway in cancer. *Critical Reviews in Oncology/Hematology, 99*, 141-149.
- Dumut, D. C., DeSanctis, J. B., Mistrik, M., Skrott, Z., Dzubak, P., Bartek, J., Radzioch, D. (2021). Dithiocarb-copper complex, CuET, demonstrates anti-neoplastic activity in mouse model of prostate cancer and prevents recurrence of tumors. *Cancer Research, 81*, 1251-1251.
- Elumalai, P., Gunadharini, D., Senthilkumar, K., Banudevi, S., Arunkumar, R., Benson, C., Arunakaran, J. (2012). Induction of apoptosis in human breast cancer cells by nimbolide through extrinsic and intrinsic pathway. *Toxicology Letters, 215(2)*, 131-142.
- Fahrner, W. R. (2005). Nanotechnology and nanoelectronics: materials, devices, measurement techniques: *Springer*.
- Fang, J. (2006). Nano- or submicron-sized liposomes as carriers for drug delivery. *Chang Gung Medical Journal, 29(4)*, 358.
- Farrow, A. C., Buchanan, G. R., Zwiener, R. J., Bowman, W. P., & Winick, N. J. (1997). Serum aminotransferase elevation during and following treatment of childhood acute lymphoblastic leukemia. *Journal of Clinical Oncology, 15(4)*, 1560-1566.
- Feinberg, A. P. (2004). *The Epigenetics of Cancer Etiology*. Paper presented at the Seminars in cancer biology.
- Ferreira, G., Hernandez-Martinez, A. R., Pool, H., Molina, G., Cruz-Soto, M., Luna-Barcenas, G., & Estevez, M. (2015). Synthesis and functionalization of silica-based nanoparticles with fluorescent biocompounds extracted from *Eysenhardtia polystachya* for biological applications. *Materials Science and Engineering, 57*, 49-57.
- Fruchon, S., Kheirallah, S., Al Saati, T., Ysebaert, L., Laurent, C., Leseux, L., . . . Bezombes, C. (2012). Involvement of the Syk-mTOR pathway in follicular lymphoma cell invasion and angiogenesis. *Leukemia, 26(4)*, 795-805.
-



- Fujiwara, Y., Kawada, K., Takano, D., Tanimura, S., Ozaki, K.-i., & Kohno, M. (2006). Inhibition of the PI3 kinase/Akt pathway enhances doxorubicin-induced apoptotic cell death in tumor cells in a p53-dependent manner. *Biochemical and Biophysical Research Communications*, *340*(2), 560-566.
- Fusco, A. J., Huang, D. B., Miller, D., Wang, V. Y., Vu, D., & Ghosh, G. (2009). NF-kappaB p52:RelB heterodimer recognizes two classes of kappaB sites with two distinct modes. *EMBO Reports*, *10*(2), 152-159.
- Ganten, T., Haas, T. L., Sykora, J., Stahl, H., Sprick, M., Fas, S., Stremmel, W. (2004). Enhanced caspase-8 recruitment to and activation at the DISC is critical for sensitisation of human hepatocellular carcinoma cells to TRAIL-induced apoptosis by chemotherapeutic drugs. *Cell Death & Differentiation*, *11*(1), S86-S96.
- Gao, W., & Zhang, L. (2015). Coating nanoparticles with cell membranes for targeted drug delivery. *Journal of Drug Targeting*, *23*(7-8), 619-626.
- Gibbs, B. F., Silva, I. G., Prokhorov, A., Abooli, M., Yasinska, I. M., Casely-Hayford, M. A., Sumbayev, V. V. (2015). Caffeine affects the biological responses of human hematopoietic cells of myeloid lineage via downregulation of the mTOR pathway and xanthine oxidase activity. *Oncotarget*, *6*(30), 28678.
- Gleissner, B., Maurer, J., Sindram, A., Reinhard, R., & Thiel, E. (2001). Comparison of ethidium bromide-stained agarose gel electrophoresis and automated fragment analysis for evaluation of IgH gene products. *Leukemia Research*, *25*(9), 769-774.
- Greenwood, M., Seftel, M., Richardson, C., Barbaric, D., Barnett, M., Bruyere, H., Song, K. (2006). Leukocyte count as a predictor of death during remission induction in acute myeloid leukemia. *Journal of Leukemia*, *47*(7), 1245-1252.
- Griffith, T. S., Rauch, C. T., Smolak, P. J., Waugh, J. Y., Boiani, N., Lynch, D. H., Kubin, M. Z. (1999). Functional analysis of TRAIL receptors using monoclonal antibodies. *The Journal of Immunology*, *162*(5), 2597-2605.
- Hallenbeck, W. H., & Cunningham-Burns, K. M. (1985). Carbamates. In *Journal of Environmental Science and Health* (pp. 30-32): Springer.
- Hanahan, D., & Weinberg, R. A. (2011). Hallmarks of cancer: the next generation. *Cell*, *144*(5), 646-674.

- 
- Handschuh, L., Kaźmierczak, M., Milewski, M. C., Góralski, M., Łuczak, M., Wojtaszewska, M., Figlerowicz, M. (2018). Gene expression profiling of acute myeloid leukemia samples from adult patients with AML-M1 and-M2 through boutique microarrays, real-time PCR and droplet digital PCR. *International Journal of Oncology*, 52(3), 656-678.
- Hariharan, A., Hakeem, A. R., Radhakrishnan, S., Reddy, M. S., & Rela, M. (2021). The role and therapeutic potential of NF-kappa-B pathway in severe COVID-19 patients. *Inflammopharmacology*, 29, 91-100.
- He, Q., Huang, Y., & Sheikh, M. S. (2004). Proteasome inhibitor MG132 upregulates death receptor 5 and cooperates with Apo2L/TRAIL to induce apoptosis in Bax-proficient and-deficient cells. *Oncogene*, 23(14), 2554-2558.
- Heckman, M. A., Weil, J., & De Mejia, E. G. (2010). Caffeine (1, 3, 7-trimethylxanthine) in foods: a comprehensive review on consumption, functionality, safety, and regulatory matters. *Journal of Food Science*, 75(3), R77-R87.
- Hemmati, S., Joshani, Z., Zangeneh, A., & Zangeneh, M. M. (2020). Green synthesis and chemical characterization of *Thymus vulgaris* leaf aqueous extract conjugated gold nanoparticles for the treatment of acute myeloid leukemia in comparison to doxorubicin in a leukemic mouse model. *Applied Organometallic Chemistry*, 34(2), e5267.
- Hendrych, M., Říhová, K., Adamová, B., Hradil, V., Stiborek, M., Vlček, P., Šmarda, J. (2022). Disulfiram increases the efficacy of 5-fluorouracil in organotypic cultures of colorectal carcinoma. *Biomedicine & Pharmacotherapy*, 153, 113465.
- Hogarth, G. (2012). Metal-dithiocarbamate complexes: chemistry and biological activity. *Mini Reviews in Medicinal Chemistry*, 12(12), 1202-1215.
- Houshmand, M., Garello, F., Circosta, P., Stefania, R., Aime, S., Saglio, G., & Giachino, C. (2020). Nanocarriers as magic bullets in the treatment of leukemia. *Nanomaterials*, 10(2), 276.
- Houwen, B. (2002). Blood film preparation and staining procedures. *Clinics in Laboratory Medicine*, 22(1), 1-14.
-

- 
- Hu, X., Li, F., Xia, F., Wang, Q., Lin, P., Wei, M., Ling, D. (2021). Dynamic nanoassembly-based drug delivery system (DNDDS): learning from nature. *Advanced Drug Delivery Reviews*, 175, 113830.
- Hua, Y., & Yu, J. S. (2019). Broadband near-ultraviolet excited La<sub>2</sub>Mo<sub>2</sub>O<sub>9</sub>: Eu<sup>3+</sup> red-emitting phosphors with high color purity for solid-state lighting. *Journal of Alloys and Compounds*, 783, 969-976.
- Huang, X., Hou, Y., Weng, X., Pang, W., Hou, L., Liang, Y., Yao, M. (2021). Diethyldithiocarbamate-copper complex (CuET) inhibits colorectal cancer progression via miR-16-5p and 15b-5p/ALDH1A3/PKM2 axis-mediated aerobic glycolysis pathway. *Oncogenesis*, 10(1), 4.
- Huelsken, J., & Behrens, J. (2002). The Wnt signalling pathway. *Journal of Cell Science*, 115(21), 3977-3978.
- Islam, T., Rahman, A. S., Hasan, M. K., Jahan, F., Mondal, M. C., Ferdoushi, S., Tohura, S. (2020). Liver function tests in patients of acute leukemia before and after induction chemotherapy. *Journal of Biosciences and Medicines*, 8(2), 110-121.
- Ito, K., Nakazato, T., Miyakawa, Y., Yamato, K., Ikeda, Y., & Kizaki, M. (2003). Caffeine induces G2/M arrest and apoptosis via a novel p53-dependent pathway in NB4 promyelocytic leukemia cells. *Journal of Cellular Physiology*, 196(2), 276-283.
- Jamuna, K., Ramesh, C., Srinivasa, T., & Raghu, K. (2011). Total antioxidant capacity in aqueous extracts of some common fruits. *International Journal of Pharmaceutical Sciences and Research*, 2(2), 448.
- Jang, J. H., Lee, T. J., Sung, E. G., Song, I. H., & Kim, J. Y. (2022). Dapagliflozin induces apoptosis by downregulating cFILP(L) and increasing cFILP(S) instability in Caki-1 cells. *Oncology Letters*, 24(5), 401. doi:10.3892/ol.2022.13521
- Ji, P., Wang, P., Chen, H., Xu, Y., Ge, J., Tian, Z., & Yan, Z. (2023). Potential of Copper and Copper Compounds for Anticancer Applications. *Pharmaceuticals*, 16(2), 234.
- Jiang, G.-J., Wang, K., Miao, D.-Q., Guo, L., Hou, Y., Schatten, H., & Sun, Q.-Y. (2011). Protein profile changes during porcine oocyte aging and effects of caffeine on protein expression patterns. *PloS One*, 6(12).
-

- 
- Jiang, W., Kim, B. Y., Rutka, J. T., & Chan, W. C. (2007). Advances and challenges of nanotechnology-based drug delivery systems. *Expert Opinion on Drug Delivery*, 4(6), 621-633.
- Jiao, Y., Guo, J., Shen, S., Chang, B., Zhang, Y., Jiang, X., & Yang, W. (2012). Synthesis of discrete and dispersible hollow mesoporous silica nanoparticles with tailored shell thickness for controlled drug release. *Journal of Materials Chemistry*, 22(34), 17636-17643.
- Jin, L., Xu, K., Liang, Y., Du, P., Wan, S., & Jiang, C. (2022). Effect of hyaluronic acid on cytokines and immune cells change in patients of knee osteoarthritis. *BMC Musculoskeletal Disorders*, 23(1), 812.
- Johnstone, R. W., Frew, A. J., & Smyth, M. J. (2008). The TRAIL apoptotic pathway in cancer onset, progression and therapy. *Nature Reviews Cancer*, 8(10), 782-798.
- Karalexi, M. A., Dessypris, N., Clavel, J., Metayer, C., Erdmann, F., Orsi, L., Greenop, K. R. (2019). Coffee and tea consumption during pregnancy and risk of childhood acute myeloid leukemia: A Childhood Leukemia International Consortium (CLIC) study. *Cancer Epidemiology*, 62, 101581.
- Khwaja, A., Bjorkholm, M., Gale, R. E., Levine, R. L., Jordan, C. T., Ehninger, G., Cornelissen, J. J. (2016). Acute myeloid leukaemia. *Nature Reviews Disease Primers*, 2(1), 1-22.
- Kim, H. S., Chang, I., Kim, J. Y., Choi, K.-H., & Lee, M.-S. (2005). Caspase-mediated p65 cleavage promotes TRAIL-induced apoptosis. *Cancer Research*, 65(14), 6111-6119.
- Kim, Y. H., & Lee, Y. J. (2007). TRAIL apoptosis is enhanced by quercetin through Akt dephosphorylation. *Journal of Cellular Biochemistry*, 100(4), 998-1009.
- Kimberley, F. C., & Screaton, G. R. (2004). Following a TRAIL: update on a ligand and its five receptors. *Cell Research*, 14(5), 359-372.
- Kingsley, J. D., Dou, H., Morehead, J., Rabinow, B., Gendelman, H. E., & Destache, C. J. (2006). Nanotechnology: a focus on nanoparticles as a drug delivery system. *Journal of Neuroimmune Pharmacology*, 1, 340-350.

- 
- Kolachana, P., Subrahmanyam, V. V., Meyer, K. B., Zhang, L., & Smith, M. T. (1993). Benzene and its phenolic metabolites produce oxidative DNA damage in HL60 cells in vitro and in the bone marrow in vivo. *Cancer Research*, *53*(5), 1023-1026.
- Kondapuram, S., Sarvagalla, S., & Coumar, M. (2021). Docking-based virtual screening using pyrx tool: autophagy target vps34 as a case study. (pp. 463-477).
- Kweon, S. H., Song, J. H., & Kim, T. S. (2010). Resveratrol-mediated reversal of doxorubicin resistance in acute myeloid leukemia cells via downregulation of MRP1 expression. *Biochemical and Biophysical Research Communications*, *395*(1), 104-110.
- Lahoti, A., Kantarjian, H., Salahudeen, A. K., Ravandi, F., Cortes, J. E., Faderl, S., Mattiuzzi, G. N. (2010). Predictors and outcome of acute kidney injury in patients with acute myelogenous leukemia or high-risk myelodysplastic syndrome. *Cancer*, *116*(17), 4063-4068.
- Laouedj, M., Tardif, M. R., Gil, L., Raquil, M.-A., Lachhab, A., Pelletier, M., Barabé, F. (2017). S100A9 induces differentiation of acute myeloid leukemia cells through TLR4. *Blood, The Journal of the American Society of Hematology*, *129*(14), 1980-1990.
- Liang, Y., Zhou, Y., & Shen, P. (2004). NF-kappaB and its regulation on the immune system. *Cellular & Molecular Immunology*, *1*(5), 343-350.
- Lowenberg, B., Downing, J. R., & Burnett, A. (1999). Acute myeloid leukemia. *New England Journal of Medicine*, *341*(14), 1051-1062.
- Lu, Y., Wu, J., Wu, J., Gonit, M., Yang, X., Lee, A., Marcucci, G. (2007). Role of formulation composition in folate receptor-targeted liposomal doxorubicin delivery to acute myelogenous leukemia cells. *Molecular Pharmaceutics*, *4*(5), 707-712.
- Luo, Y., Yang, H., Zhou, Y.-F., & Hu, B. (2020). Dual and multi-targeted nanoparticles for site-specific brain drug delivery. *Journal of Controlled Release*, *317*, 195-215.
- Madhusudanan, P., Yusuff, K. M., & Nair, C. R. (1975). Thermal decomposition kinetics of diethyl dithiocarbamate complexes of copper (II) and nickel (II). *Journal of Thermal Analysis and Calorimetry*, *8*(1), 31-43.
- Magliulo, D., & Bernardi, R. (2018). HIF- $\alpha$  factors as potential therapeutic targets in leukemia. *Expert Opinion on Therapeutic Targets*, *22*(11), 917-928.
-

- 
- Malovichko, M. V., Abplanalp, W. T., McFall, S. A., Taylor, B. S., Wickramasinghe, N. S., Sithu, I. D., Nantz, M. H. (2021). Biomarkers of Cardiovascular Toxicity of Benzene Inhalation in Mice. *BioRxiv*, 2021.2008. 2031.458364.
- Martelli, A., Evangelisti, C., Chappell, W., Abrams, S., Bäsecke, J., Stivala, F., Libra, M. (2011). Targeting the translational apparatus to improve leukemia therapy: roles of the PI3K/PTEN/Akt/mTOR pathway. *Leukemia*, 25(7), 1064-1079.
- Maxwell, P. H., Pugh, C. W., & Ratcliffe, P. J. (2001). Activation of the HIF pathway in cancer. *Current Opinion in Genetics & Development*, 11(3), 293-299.
- Mayengbam, S. S., Singh, A., Pillai, A. D., & Bhat, M. K. (2021). Influence of cholesterol on cancer progression and therapy. *Translational Oncology*, 14(6), 101043.
- McHale, C. M., Zhang, L., & Smith, M. T. (2012). Current understanding of the mechanism of benzene-induced leukemia in humans: implications for risk assessment. *Carcinogenesis*, 33(2), 240-252.
- Meng, X., Wu, J., Hu, Z., & Zheng, X. (2024). Intelligent responsive copper-diethyldithiocarbamate-based multifunctional nanomedicine for photothermal-augmented synergistic cancer therapy. *Journal of Materials Chemistry B*.
- Mérino, D., Lalaoui, N., Morizot, A., Schneider, P., Solary, E., & Micheau, O. (2006). Differential inhibition of TRAIL-mediated DR5-DISC formation by decoy receptors 1 and 2. *Molecular Cell Biology*, 26(19), 7046-7055.
- Merroun, M., Hennig, C., Rossberg, A., Reich, T., & Selenska-Pobell, S. (2003). Characterization of U (VI)-Acidithiobacillus ferrooxidans complexes using EXAFS, transmission electron microscopy, and energy-dispersive X-ray analysis. *Radiochimica Acta*, 91(10), 583-592.
- Mintz, K. J., & Leblanc, R. M. (2021). The use of nanotechnology to combat liver cancer: Progress and perspectives. *Biochimica et Biophysica Acta (BBA)-Reviews on Cancer*, 1876(2), 188621.
- Mirzaei, H., Zarbafian, S., Villar, E. A., Mottarella, S. E., Beglov, D., Vajda, S., computation. (2015). Energy Minimization on Manifolds for Docking Flexible Molecules. 113, 1063-1076.
- Moein, M. R., Moein, S., & Ahmadizadeh, S. (2008). Radical scavenging and reducing power of Salvia mirzayanii subfractions. *Molecules*, 13(11), 2804-2813.
-

- 
- Moein, S., Moein, M., Khoshnoud, M. J., & Kalanteri, T. (2012). In vitro antioxidant properties evaluation of 10 Iranian medicinal plants by different methods. *Iranian Red Crescent Medical Journal*, *14*(12), 771.
- Monteiro, J., Alves, M. G., Oliveira, P. F., & Silva, B. M. (2019). Pharmacological potential of methylxanthines: Retrospective analysis and future expectations. *Critical Reviews in Food Science and Nutrition*, *59*(16), 2597-2625.
- Moon, R. T. (2005). Wnt/ $\beta$ -catenin pathway. *Science's STKE*, *2005*(271).
- Moynagh, P. N. (2005). The NF- $\kappa$ B pathway. *Journal of Cell Science*, *118*(20), 4589-4592.
- Nakamura, K., Yamashita, K., Itoh, Y., Yoshino, K., Nozawa, S., & Kasukawa, H. (2012). Comparative studies of polyethylene glycol-modified liposomes prepared using different PEG-modification methods. *Bba-Biomembranes*, *1818*(11), 2801-2807.
- Nandiyanto, A. B. D., Kim, S.-G., Iskandar, F., & Okuyama, K. (2009). Synthesis of spherical mesoporous silica nanoparticles with nanometer-size controllable pores and outer diameters. *Microporous and Mesoporous Materials*, *120*(3), 447-453.
- Natelson, E. A. (2007). Benzene-induced acute myeloid leukemia: A clinician's perspective. *American Journal of Hematology*, *82*(9), 826-830.
- Nguyen, K. T. (2011). Targeted nanoparticles for cancer therapy: Promises and challenge.
- Olsson, M., Bruhns, P., Frazier, W. A., Ravetch, J. V., & Oldenborg, P.-A. (2005). Platelet homeostasis is regulated by platelet expression of CD47 under normal conditions and in passive immune thrombocytopenia. *Blood*, *105*(9), 3577-3582.
- Ong, Y. C., & Gasser, G. (2020). Organometallic compounds in drug discovery: Past, present and future. *Drug Discovery Today: Technologies*, *37*, 117-124.
- Parmar, R., Mangrola, M., Parmar, B., & Joshi, V. (2012). A software to calculate crystalline size by Debye-Scherrer Formula using VB .NET. *Multi Disciplinary Edu Global Quest*, *1*(1), 33-39.
- Partridge, A. H., Burstein, H. J., & Winer, E. P. (2001). Side effects of chemotherapy and combined chemohormonal therapy in women with early-stage breast cancer. *JNCI Monographs*, *2001*(30), 135-142.
- Paul, A. T., & Jindal, A. (2017). Nano-natural Products as Anticancer Agents. In M. S. Akhtar & M. K. Swamy (Eds.), *Anticancer Plants: Clinical Trials and Nanotechnology: Volume 3* (pp. 27-50). Singapore: Springer Singapore.
-

- 
- Paun, R. A., Dumut, D. C., Centorame, A., Thuraisingam, T., Hajduch, M., Mistrik, M., . . . Tabrizian, M. (2022). One-step synthesis of nanoliposomal copper diethyldithiocarbamate and its assessment for cancer therapy. *Pharmaceutics*, *14*(3), 640.
- Peng, C., Chen, Y., Li, D., & Li, S. (2010). Role of Pten in leukemia stem cells. *Oncotarget*, *1*(2), 156.
- Peng, Y., Liu, P., Meng, Y., Hu, S., Ding, J., & Zhou, W. (2020). Nanoscale copper (II)–diethyldithiocarbamate coordination polymer as a drug self-delivery system for highly robust and specific cancer therapy. *Molecular Pharmaceutics*, *17*(8), 2864–2873.
- Perl, A. E., Altman, J. K., Cortes, J., Smith, C., Litzow, M., Baer, M. R., Goldberg, S. (2017). Selective inhibition of FLT3 by gilteritinib in relapsed or refractory acute myeloid leukaemia: a multicentre, first-in-human, open-label, phase 1–2 study. *The Lancet Oncology*, *18*(8), 1061-1075.
- Phatak, R. S., PRATINIDHI, A. K., & HENDRE, A. S. (2015). Screening of some Indian household spices for comparative studies of antioxidant and antiradical activities by using in-vitro models. *Screening*, *8*(2).
- Poon, E., Harris, A. L., & Ashcroft, M. (2009). Targeting the hypoxia-inducible factor (HIF) pathway in cancer. *Expert Reviews in Molecular Medicine*, *11*, e26.
- Pui, C.-H., & Evans, W. E. (1998). Acute lymphoblastic leukemia. *New England Journal of Medicine*, *339*(9), 605-615.
- Ramdass, B., Chowdhary, A., & Koka, P. S. (2013). Hematological malignancies: disease pathophysiology of leukemic stem cells. *Journal of Stem Cells*, *8*(3/4), 151.
- Rana, S., & Verma, Y. (2005). Biochemical toxicity of benzene. *J Environ Biol*, *26*(2), 157-168.
- Rath, S., Sahu, M. C., Dubey, D., Debata, N. K., & Padhy, R. N. (2011). Which value should be used as the lethal concentration 50 (LC 50) with bacteria? *Interdisciplinary sciences: Computational Life Sciences*, *3*, 138-143.
- Roboz, G. J. (2011). Novel approaches to the treatment of acute myeloid leukemia. *Hematology 2010, the American Society of Hematology Education Program Book*, *2011*(1), 43-50.
-



- 
- Rose-Inman, H., & Kuehl, D. (2017). Acute leukemia. *Hematology/Oncology Clinics*, 31(6), 1011-1028.
- Ross, D. (1996). Metabolic basis of benzene toxicity. *European Journal of Haematology*, 57(S60), 111-118.
- Roy, M., Mukherjee, A., Mukherjee, S., & Biswas, J. (2017). Drug Resistance in Leukemia: Remediation by Natural Means. *Biomedical Research Journal*, 4(1).
- Rubnitz, J. E., Gibson, B., & Smith, F. O. (2008). Acute myeloid leukemia. *Pediatric Clinics of North America*, 55(1), 21-51.
- Sabnis, R. W. (2021). Heterocyclic compounds as dihydroorotate dehydrogenase inhibitors for treating acute myelogenous leukemia (AML). In (Vol. 12, pp. 1641-1642): ACS Publications.
- Safa, A. R., Day, T. W., & Wu, C. H. (2008). Cellular FLICE-like inhibitory protein (C-FLIP): a novel target for cancer therapy. *Cancer Drug Targets*, 8(1), 37-46. doi:10.2174/156800908783497087
- Sahu, B., Laakso, M., Ovaska, K., Mirtti, T., Lundin, J., Rannikko, A., Konsti, J. (2011). Dual role of FoxA1 in androgen receptor binding to chromatin, androgen signalling and prostate cancer. *EMBO Rep.*, 30(19), 3962-3976.
- Samuelson, B. T., Cuker, A., Siegal, D. M., Crowther, M., & Garcia, D. A. (2017). Laboratory assessment of the anticoagulant activity of direct oral anticoagulants: a systematic review. *Chest*, 151(1), 127-138.
- Sarah, Q. S., Anny, F. C., & Misbahuddin, M. (2017). Brine shrimp lethality assay. *Bangladesh Journal of Pharmacology*, 12(2), 186-189.
- Sathpathi, S., Mohanty, A. K., Satpathi, P., Mishra, S. K., Behera, P. K., Patel, G., & Dondorp, A. M. (2014). Comparing Leishman and Giemsa staining for the assessment of peripheral blood smear preparations in a malaria-endemic region in India. *Malaria Journal*, 13(1), 512.
- Sauvage, F., Barratt, G., Herfindal, L., & Vergnaud-Gauduchon, J. (2016). The use of nanocarriers in acute myeloid leukaemia therapy: challenges and current status. *Current Pharmaceutical Biotechnology*, 17(1), 30-41.
-

- 
- Sawyers, C. L., Abate-Shen, C., Anderson, K. C., Barker, A., Baselga, J., Berger, N. A., Li, C. I. (2013). AACR cancer progress report 2013. *Clinical Cancer Research*, *19*, S1-S98.
- Sayers, T. J., Brooks, A. D., Koh, C. Y., Ma, W., Seki, N., Raziuddin, A., Murphy, W. J. (2003). The proteasome inhibitor PS-341 sensitizes neoplastic cells to TRAIL-mediated apoptosis by reducing levels of c-FLIP. *Blood*, *102*(1), 303-310.
- Schmid, C., Labopin, M., Nagler, A., Niederwieser, D., Castagna, L., Tabrizi, R., Vorlicek, J. (2012). Treatment, risk factors, and outcome of adults with relapsed AML after reduced intensity conditioning for allogeneic stem cell transplantation. *Blood, The Journal of the American Society of Hematology*, *119*(6), 1599-1606.
- Seidensticker, M. J., & Behrens, J. (2000). Biochemical interactions in the wnt pathway. *Biochimica et Biophysica Acta (BBA)-Molecular Cell Research*, *1495*(2), 168-182.
- Senftleben, U., & Karin, M. (2002). The Ikk/nf-kb pathway. *Critical Care Medicine*, *30*(1), S18-S26.
- Serasanambati, M., & Chilakapati, S. R. (2016). Function of nuclear factor kappa B (NF- $\kappa$ B) in human diseases-a review. *South Indian Journal of Biological Sciences*, *2*(4), 368-387.
- Shaffer, B. C., Gillet, J.-P., Patel, C., Baer, M. R., Bates, S. E., & Gottesman, M. M. (2012). Drug resistance: still a daunting challenge to the successful treatment of AML. *Drug Resistance Updates*, *15*(1-2), 62-69.
- Shallis, R. M., Weiss, J. J., Deziel, N. C., & Gore, S. D. (2021). A clandestine culprit with critical consequences: Benzene and acute myeloid leukemia. *Blood Reviews*, *47*, 100736.
- Sinha, R., Kim, G. J., Nie, S., & Shin, D. M. (2006). Nanotechnology in cancer therapeutics: bioconjugated nanoparticles for drug delivery. *Molecular Cancer Therapeutics*, *5*(8), 1909-1917.
- Skrott, Z., & Cvek, B. (2012). Diethyldithiocarbamate complex with copper: the mechanism of action in cancer cells. *Mini Reviews in Medicinal Chemistry*, *12*(12), 1184-1192.
- Smith, J. D., Morton, L. D., & Ulery, B. D. (2015). Nanoparticles as synthetic vaccines. *Current Opinion in Biotechnology*, *34*, 217-224.
-

- 
- Smith, M. T., Zhang, L., McHale, C. M., Skibola, C. F., & Rappaport, S. M. (2011). Benzene, the exposome and future investigations of leukemia etiology. *Chemico-biological Interactions*, 192(1-2), 155-159.
- Snyder, R. (2002a). Benzene and leukemia. *Critical Reviews in Toxicology*, 32(3), 155-210.
- Snyder, R. (2002b). Benzene and leukemia. *Critical Reviews in Toxicology*, 32(3), 155.
- Song, J. H., Song, D. K., Pyrzynska, B., Petruk, K. C., Van Meir, E. G., & Hao, C. (2003). TRAIL triggers apoptosis in human malignant glioma cells through extrinsic and intrinsic pathways. *Brain Pathology*, 13(4), 539-553.
- Stellwagen, N. C. (1998). DNA gel electrophoresis. In *Nucleic Acid Electrophoresis* (pp. 1-53): Springer.
- Studio, D. J. A. S. I. (2015). Dassault systemes BIOVIA, Discovery studio modelling environment, Release 4.5. 98-104.
- Suri, S. S., Fenniri, H., & Singh, B. (2007). Nanotechnology-based drug delivery systems. *Journal of Occupational Medicine and Toxicology*, 2, 1-6.
- Szatkowska, P., Koba, M., Koslinski, P., & Szablewski, M. (2013). Molecularly imprinted polymers' applications: A short review. *Mini-Reviews in Organic Chemistry*, 10(4), 400-408.
- Tacar, O., Sriamornsak, P., & Dass, C. R. (2013). Doxorubicin: an update on anticancer molecular action, toxicity and novel drug delivery systems. *Journal of Pharmacy and Pharmacology*, 65(2), 157-170.
- Tang, R., Cheng, A., Guirales, F., Yeh, W., & Tirado, C. A. (2021). c-MYC Amplification in AML. *Journal of the Association of Genetic Technologists*, 47(4).
- Tapia, M. A., González-Navarrete, I., Dalmases, A., Bosch, M., Rodriguez-Fanjul, V., Rolfe, M., Bachs, O. (2007). Inhibition of the canonical IKK/NFκB pathway sensitizes human cancer cells to doxorubicin. *Cell Cycle*, 6(18), 2284-2292.
- Terzibasi-Tozzini, E., Martinez-Nicolas, A., & Lucas-Sanchez, A. (2017). The clock is ticking. Ageing of the circadian system: from physiology to cell cycle. Paper presented at the seminars in cell & developmental biology.
-

- 
- Tita, B., Abdel-Haq, H., Vitalone, A., Mazzanti, G., & Saso, L. (2001). Analgesic properties of *Epilobium angustifolium*, evaluated by the hot plate test and the writhing test. *Farmaco*, *56*(5-7), 341-343.
- Tortora, F., Rendina, A., Angiolillo, A., Di Costanzo, A., Aniello, F., Donizetti, A., Vitale, E. (2022). CD33 rs2455069 SNP: Correlation with Alzheimer's Disease and Hypothesis of Functional Role. *23*(7), 3629.
- Trott, O., & Olson, A. J. (2010). AutoDock Vina: improving the speed and accuracy of docking with a new scoring function, efficient optimization, and multithreading. *Journal of Computational Chemistry*, *31*(2), 455-461. doi:10.1002/jcc.21334
- Ugai, T., Matsuo, K., Sawada, N., Iwasaki, M., Yamaji, T., Shimazu, T., Tsugane, S. (2018). Coffee and green tea consumption and subsequent risk of acute myeloid leukemia and myelodysplastic syndromes in Japan. *International Journal of Cancer*, *142*(6), 1130-1138.
- Vogelstein, B., & Kinzler, K. W. (2004). Cancer genes and the pathways they control. *Nature Medicine*, *10*(8), 789-799.
- Vojoudi, H., Badieli, A., Amiri, A., Banaei, A., Ziarani, G., & Schenk-Joß, K. (2018). Efficient device for the benign removal of organic pollutants from aqueous solutions using modified mesoporous magnetite nanostructures. *Journal of Physics and Chemistry of Solids*, *113*, 210-219.
- Walter, R. B. (2020). Expanding use of CD33-directed immunotherapy. *Expert Opinion on Biological Therapy*, *20*(9), 955-958. doi:10.1080/14712598.2020.1788540
- Wang, J., Wang, H., Zhu, R., Liu, Q., Fei, J., & Wang, S. (2015). Anti-inflammatory activity of curcumin-loaded solid lipid nanoparticles in IL-1 $\beta$  transgenic mice subjected to the lipopolysaccharide-induced sepsis. *Biomaterials*, *53*, 475-483.
- Wang, S., & El-Deiry, W. S. (2003). TRAIL and apoptosis induction by TNF-family death receptors. *Oncogene*, *22*(53), 8628-8633.
- Ward, P. S., & Thompson, C. B. (2012). Metabolic reprogramming: a cancer hallmark even warburg did not anticipate. *Cancer Cell*, *21*(3), 297-308.
- Wu, N., Gao, N., Fan, D., Wei, J., Zhang, J., & An, J. (2014). miR-223 inhibits dengue virus replication by negatively regulating the microtubule-destabilizing protein STMN1 in EAhy926 cells. *Microbes and Infection*, *16*(11), 911-922.
-

- 
- Wu, S.-H., Mou, C.-Y., & Lin, H.-P. (2013). Synthesis of mesoporous silica nanoparticles. *Chemical Society Reviews*, 42(9), 3862-3875.
- Wunderlich, M., Mizukawa, B., Chou, F.-S., Sexton, C., Shrestha, M., Sauntharajah, Y., & Mulloy, J. C. (2013). AML cells are differentially sensitive to chemotherapy treatment in a human xenograft model. *Blood, The Journal of the American Society of Hematology*, 121(12), e90-e97.
- Xu, J., Zhou, P., Wang, W., Sun, A., & Guo, F. (2014). RelB, together with RelA, sustains cell survival and confers proteasome inhibitor sensitivity of chronic lymphocytic leukemia cells from bone marrow. *International Journal of Molecular Medicine*, 92(1), 77-92.
- Yamamoto, T., Nozaki-Taguchi, N., & Chiba, T. (2002). Analgesic effect of intrathecally administered orexin-A in the rat formalin test and in the rat hot plate test. *British Journal of Pharmacology*, 137(2), 170-176.
- Yeung, C. C., & Radich, J. (2017). Predicting chemotherapy resistance in AML. *Current Hematologic Malignancy Reports*, 12, 530-536.
- Zhan, T., Rindtorff, N., & Boutros, M. (2017). Wnt signaling in cancer. *Oncogene*, 36(11), 1461-1473.
- Zhang, Y., Zhi, Z., Jiang, T., Zhang, J., Wang, Z., & Wang, S. (2010). Spherical mesoporous silica nanoparticles for loading and release of the poorly water-soluble drug telmisartan. *Journal of Controlled Release*, 145(3), 257-263.
- Zhou, D., Jin, H., Lin, H.-B., Yang, X.-M., Cheng, Y.-F., Deng, F.-J., & Xu, J.-P. (2010). Antidepressant effect of the extracts from Fructus Akebiae. *Pharmacology Biochemistry and Behavior*, 94(3), 488-495.
- Zidan, A. S. (2001). Nickel (II) complexes containing mixed alkylsalicylaldiminate and alkylxanthate or diethyldithiocarbamate ligands. *Synthesis and Reactivity in Inorganic and Metal-Organic Chemistry*, 31(3), 457-469.
- Zinatizadeh, M. R., Schock, B., Chalbatani, G. M., Zarandi, P. K., Jalali, S. A., & Miri, S. R. (2021). The Nuclear Factor Kappa B (NF- $\kappa$ B) signaling in cancer development and immune diseases. *Genes & diseases*, 8(3), 287-297.
-



# Article

## In Silico, In Vitro, and In Vivo Evaluation of Caffeine-Coated Nanoparticles as a Promising Therapeutic Avenue for AML through NF-Kappa B and TRAIL Pathways Modulation

Muhammad Hamid Siddique <sup>1</sup>, Sidra Bukhari <sup>1</sup>, Inam Ullah Khan <sup>1</sup>, Asiya Essa <sup>1</sup>, Zain Ali <sup>1</sup>, Usama Sabir <sup>1</sup>, Omiya Ayoub <sup>1</sup>, Haleema Saadia <sup>1</sup>, Muhammad Yaseen <sup>2</sup>, Aneesa Sultan <sup>1</sup>, Iram Murtaza <sup>1</sup>, Philip G. Kerr <sup>3</sup>, Mashooq Ahmad Bhat <sup>4</sup> and Mariam Anees <sup>1,\*</sup>

- <sup>1</sup> Department of Biochemistry, Quaid-i-Azam University, Islamabad 45320, Pakistan; hamidsiddique18@gmail.com (M.H.S.); sidrabukhari82@gmail.com (S.B.); iukhan@bs.qau.edu.pk (I.U.K.); asiyaessa78@gmail.com (A.E.); xainsolangee@gmail.com (Z.A.); usamasabir93@gmail.com (U.S.); omiyaayoub1812@gmail.com (O.A.); haleemababar700@gmail.com (H.S.); aneesa@qau.edu.pk (A.S.); irambch@qau.edu.pk (I.M.)
- <sup>2</sup> Institute of Chemical Sciences, University of Swat, Charbagh 19130, Pakistan; muhammadyaseen.my907@gmail.com
- <sup>3</sup> School of Dentistry and Medical Sciences, Charles Sturt University, Sydney, NSW 2678, Australia; philip.kerr@gmail.com
- <sup>4</sup> Department of Pharmaceutical Chemistry, College of Pharmacy, King Saud University, Riyadh 11451, Saudi Arabia; mabhat@ksu.edu.sa
- \* Correspondence: mariam@qau.edu.pk; Tel.: +92-51-9064-3224



**Citation:** Siddique, M.H.; Bukhari, S.; Khan, I.U.; Essa, A.; Ali, Z.; Sabir, U.; Ayoub, O.; Saadia, H.; Yaseen, M.; Sultan, A.; et al. In Silico, In Vitro, and In Vivo Evaluation of Caffeine-Coated Nanoparticles as a Promising Therapeutic Avenue for AML through NF-Kappa B and TRAIL Pathways Modulation. *Pharmaceuticals* 2023, 16, 1742. <https://doi.org/10.3390/ph16121742>

Academic Editors: Muthukumaran Packirisamy and Ahmad Sohrabi Kashani

Received: 12 November 2023  
Revised: 7 December 2023  
Accepted: 13 December 2023  
Published: 18 December 2023



Copyright: © 2023 by the authors. Licensee MDPI, Basel, Switzerland. This article is an open access article distributed under the terms and conditions of the Creative Commons Attribution (CC BY) license (<https://creativecommons.org/licenses/by/4.0/>).

**Abstract:** Background: *Advancements* in nanoscience have led to a profound paradigm shift in the therapeutic applications of traditionally important natural drugs. The goal of this research is to develop a nano-natural product for efficient cancer treatment. Methods and Results: For this purpose, mesoporous silica nanoparticles (MSNPs) were formulated, characterized, and loaded with caffeine to develop a targeted drug delivery system, i.e., caffeine-coated nanoparticles (CcNPs). In silico docking studies were conducted to examine the binding efficiency of the CcNPs with different apoptotic targets followed by in vitro and in vivo bioassays in respective animal models. Caffeine, administered both as a free drug and in nanomedicine form, along with doxorubicin, was delivered intravenously to a benzene-induced AML model. The anti-leukemic potential was assessed through hematological profiling, enzymatic biomarker analysis, and RT-PCR examination of genetic alterations in leukemia markers. Docking studies show strong inter-molecular interactions between CcNPs and apoptotic markers. In vitro analysis exhibits statistically significant antioxidant activity; whereas in vivo analysis exhibits normalization of the genetic expression of leukemia biomarkers STMN1 and S1009A, accompanied by the restoration of the hematological and morphological traits of leukemic blood cells in nanomedicine-treated rats. Likewise, a substantial improvement in hepatic and renal biomarkers is also observed. In addition to these findings, the nanomedicine successfully normalizes the elevated expression of GAPDH and mTOR induced by exposure to benzene. Further, the nanomedicine downregulates pro-survival components of the NF-kappa B pathway and upregulated P53 expression. Additionally, in the TRAIL pathway, it enhances the expression of pro-apoptotic players TRAIL and DR5 and downregulates the anti-apoptotic protein cFLIP. Conclusions: Our data suggest that MSNPs loaded with caffeine, i.e., CcNP/nanomedicine, can potentially inhibit transformed cell proliferation and induce pro-apoptotic TRAIL machinery to counter benzene-induced leukemia. These results render our nanomedicine as a potentially excellent therapeutic agent against AML.

**Keywords:** acute myeloid leukemia; docking; caffeine; MSNPs; nanomedicine; doxorubicin

# Final 21

## ORIGINALITY REPORT

<b>19%</b> SIMILARITY INDEX	<b>16%</b> INTERNET SOURCES	<b>15%</b> PUBLICATIONS	<b>3%</b> STUDENT PAPERS
--------------------------------	--------------------------------	----------------------------	-----------------------------

## PRIMARY SOURCES

<b>1</b>	<a href="http://www.mdpi.com">www.mdpi.com</a> Internet Source	<b>6%</b>
<b>2</b>	Muhammad Hamid Siddique, Sidra Bukhari, Inam Ullah Khan, Asiya Essa et al. "In Silico, In Vitro, and In Vivo Evaluation of Caffeine-Coated Nanoparticles as a Promising Therapeutic Avenue for AML through NF-Kappa B and TRAIL Pathways Modulation", Pharmaceuticals, 2023 Publication	<b>1%</b>
<b>3</b>	<a href="http://link.springer.com">link.springer.com</a> Internet Source	<b>1%</b>
<b>4</b>	Submitted to Nottingham Trent University Student Paper	<b>1%</b>
<b>5</b>	Submitted to Higher Education Commission Pakistan Student Paper	<b>&lt;1%</b>
<b>6</b>	<a href="http://archive.org">archive.org</a> Internet Source	<b>&lt;1%</b>